VNiVERSiDAD Ð SALAMANCA

FACULTAD DE FARMACIA

DEPARTAMENTO DE QUÍMICA ANALÍTICA, NUTRICIÓN Y BROMATOLOGÍA

Development of cosmeceutical formulations based on mushroom extracts and their individual compounds

DOCTORAL THESIS

Taofiq Ayodele Oludemi

Supervisors

Dr. Isabel Cristina Fernandes Rodrigues Ferreira

Dr. Maria Filomena Barreiro

Dr. Ana María González Paramás

Salamanca, 2019

ACKNOWLEDGEMENTS

First and foremost, I would like to extend my heartfelt gratitude to my supervisor **Prof. Isabel C.F.R Ferreira** for giving me the opportunity to be part of this amazing team. You have been very influential in my development as a researcher and as an individual. It is an honour to have the opportunity to learn from you and I will be forever grateful for all your efforts, unending support and continuous encouragement throughout my years of study. Your passion and enthusiasm towards science has been an inspiration to me.

My sincere gratitude also goes to my co-supervisor **Prof. Maria Filomena Barreiro** for your advices and encouragement. I greatly benefited from your keen scientific insight, vast knowledge and scientific curiosity. You have been helpful and gave all necessary information towards the successful completion of this project.

My profound gratitude also goes out to my co-supervisor **Prof. Ana Maria González-Paramás** for your guidance and support all through these years. Thank you so much for always finding the time to provide valuable comments and contributions towards the successful completion of this project.

My gratitude also goes out to **Dr. Lillian Barros** for your continuous support, motivation and patience. Your work ethics have been a continuous source of inspiration to me and I am sincerely thankful for all your time and advices over the years.

My sincere appreciation also goes out to **Prof. Celestino Santos-Buelga**, from Unidad de Nutrición y Bromatología, Faculty of Pharmacy, University of Salamanca, I want to thank you for your advices and continuous support.

I would also like to appreciate the effort of **Dr. Sandrina Heleno** and **Dr. Ricardo Calhelha**. You both have contributed immensely towards achieving this goal. You have been patient and continue to offer advices whenever the need arises. Thank you so much for everything.

My profound gratitude also goes out to all members of **Biochemcore research group**. Thank you so much for your friendship, assistance and scientific discussions. You have provided a wonderful environment for me to learn and this has really helped me.

My gratitude also goes out to members of the **Laboratory of Separation and Reaction Engineering (LSRE)** especially **Dr. Isabel Fernandes**. You have been very helpful towards the course of this project. My gratitude also goes out to members of the **REQUIMTE/LAQV**,

ABSTRACT

The cosmetic industry is constantly in search of ingredients from natural sources because of their multifunctional properties, competitive effectiveness, and lower toxicity effects. Otherwise, mushrooms have been an important part of our diet for years due to their rich nutritional and abundant content in biomolecules; however, their cosmeceutical and nutricosmetic potential have not been fully exploited. This study aimed at optimizing the extraction of bioactive compounds from *Ganoderma lucidum* and *Agaricus blazei* by Response Surface Methodology (RSM) and comparing conventional extraction techniques with more sustainable methods. Further studies regarding their nutritional and chemical composition (e.g., sugars, organic acids, tocopherols, and fatty acids), were conducted. Also, extracts obtained from those mushrooms, but also from *Agaricus bisporus*, *Pleurotus ostreatus* and *Lentinula edodes* extracts, using the Soxhlet extraction system, were analysed in terms of anti-inflammatory, anti-tyrosinase, antioxidant, and antimicrobial activities followed by their characterization in terms of phenolic acids and related compounds, ergosterol, and triterpenoids. Furthermore, the obtained extracts were incorporated in a base cosmetic cream to ascertain bioactive properties sustainment. Moreover, to evaluate the individual cosmeceutical contribution of *p*-hydroxybenzoic acid, *p*-coumaric acid, protocatechuic acid, cinnamic acid and ergosterol, their anti-inflammatory, anti-tyrosinase, and antimicrobial activities were studied, followed by incorporation of these compounds in a base cosmetic cream. Because of the possibility of the extracts and the individual compounds to lose their potency over time either due to oxidation or degradation, microparticles were prepared using the atomization/coagulation technique. The microparticles were characterized in terms of morphology, particle size distribution, and encapsulation efficiency. This is followed by incorporation of the produced microparticles into a base cosmetic cream and comparison of their performance with the free forms (formulations containing free extracts/individual compounds). The most promising extracts and their corresponding formulations were submitted to *in vitro* safety evaluation using the MTT and LDH assays in keratinocyte (HaCaT) and fibroblast (HFF-1) cell lines. Moreover, they were submitted to *ex vivo* skin permeation studies using a Franz diffusion apparatus with pig ear skin as permeation membrane to determine topical bioavailability of the bioactive compounds present in the extracts.

The optimization study on bioactive compounds recovery from *G. lucidum* and *A. blazei* using RSM showed that the values predicted by the models were in close agreement with

experimental observations. Furthermore, it was concluded that the extraction yield of bioactive compounds from the studied mushrooms was highly dependent on the extraction variables (time, temperature, solvent proportion, solid-liquid ratio, and power). *A. blazei* and *G. ludidum* also showed high nutritional contribution. α-Tocopherol, oxalic acid and twenty-one fatty acids (mainly PUFA) were quantified in *A. blazei*. *G. lucidum* showed a similar fatty acids' profile (PUFA>SFA>MUFA) and with the presence of α-tocopherol and δ-tocopherol. Comparatively, *A. blazei* revealed lower fat content, but higher energy contribution. The cell viability effect of the extract prepared from *A. blazei* on Caco-2 and HT29-MTX cells was found to be maintained in a concentration-dependent manner.

The ethanolic extracts obtained from the studied mushrooms showed antioxidant, anti-inflammatory, anti-tyrosinase and antimicrobial activities, and after incorporation into the base cosmetic cream, the final cosmeceutical formulations preserved some of these bioactivities. *G. lucidum* extract was found to be a rich source of triterpenoids mainly due to the high contribution of ganoderic acid A, C2, and H, while phenolic acids (*p*-hydroxybenzoic acid, *p*-coumaric acid and protocatechuic acid), the related compound cinnamic acid, and ergosterol were identified in *A. bisporus, P. ostreatus, L. edodes* and *A. blazei* extracts. Each one of these compounds also showed anti-inflammatory, anti-tyrosinase and antimicrobial activities. Furthermore, microparticles were successfully used to encapsulate extract/individual compounds with high encapsulation efficiency and yield. After incorporation of the free extracts/individual compounds and the produced microparticles into the base cosmetic cream, the encapsulated forms allowed for a controlled release leading to bioactivity preservation when compared with the free forms.

Because they presented the most interesting cosmeceutical potential, *P. ostreatus* and *G. lucidum* extracts were submitted to toxicological studies, revealing no toxicity in keratinocytes and fibroblast cell lines, which is indicative of their potential safety to be used as cosmeceutical ingredients. Protocatechuic acid and syringic acid were the only compounds permeating from the *G. lucidum* extract, while very low detection was observed for compounds present in the *P. ostreatus* extract. Similar results were also obtained for the formulation prepared using both extracts. The results showed that tritepenoids in *G. lucidum* might be natural permeation enhancers and these results pointed out for the suitability of using these mushroom extracts as skin care ingredients. Overall, the results showed that skin care products can be formulated using mushroom extracts and that these extracts have the potential to be utilised at large scale

use. Hence, integration of wastes generated by the mushroom processing industry, which can serve as raw materials for the obtainment of bioactive extracts, can be intensified.

RESUMEN

La industria cosmética está constantemente en busca de ingredientes de origen natural debido a sus propiedades multifuncionales, su eficacia competitiva, y su menor toxicidad. Por otra parte, los hongos han sido una parte importante de nuestra dieta durante años debido a su riqueza nutricional y su abundante contenido en biomoléculas; sin embargo, su potencial cosmecéutico y nutricosmético no ha sido plenamente explotado. Este estudio tuvo como objetivo la optimización, utilizando la metodología de superficie de respuesta (RSM), de la extracción de compuestos bioactivos a partir de *Ganoderma lucidum* y *Agaricus blazei* y la comparación de técnicas de extracción convencionales con métodos más sostenibles. Se llevaron a cabo estudios adicionales relacionados con su composición química y valor nutricional (por ejemplo, azúcares, ácidos orgánicos, tocoferoles, y ácidos grasos). Además, extractos obtenidos, utilizando el sistema de extracción de Soxhlet, a partir de esos hongos junto con otros procedentes de *Agaricus bisporus*, *Pleurotus ostreatus* y extractos de *Lentinula edodes*, se analizaron en términos de actividad anti-inflamatoria, anti-tirosinasa, antioxidante, y antimicrobiana seguido de su caracterización en términos de ácidos fenólicos y compuestos relacionados, ergosterol, y triterpenoides. Además, los extractos obtenidos fueron incorporados en una crema cosmética base para evaluar propiedades bioactivas de soporte. Además, para evaluar la contribución individual como cosmecéuticos del ácido p-hidroxibenzoico, ácido p-cumárico, ácido protocatéquico, ácido cinámico y ergosterol, fueron estudiadas sus propiedades anti-inflamatorias, anti-tirosinasa, y actividades antimicrobianas, seguido de la incorporación de estos compuestos en una crema cosmética base. Debido a la posibilidad de que los extractos y los compuestos individuales puedan perder su potencia con el tiempo, ya sea debido a la oxidación o la degradación, se prepararon en forma de micropartículas usando la técnica de atomización/coagulación. Las micropartículas se caracterizaron en términos de morfología, distribución de tamaño de partícula, y la eficiencia de encapsulación. A continuación, dichas micropartículas se incorporaron en una crema cosmético de base y se comparó su comportamiento frente a las formas libres (formulaciones que contienen extractos libres/compuestos individuales). Los extractos más prometedores y sus correspondientes formulaciones fueron sometidos a test de evaluación *in vitro* de su seguridad utilizando los ensayos de MTT y LDH en líneas celulares de queratinocitos humanos (HaCaT) y fibroblastos (HFF-1). Además, los extractos fueron sometidos a estudios *ex vivo* de permeabilidad de la piel utilizando una celda de Franz provista con una membrana natural obtenida a partir de la piel

de oreja de cerdo para determinar la biodisponibilidad tópica de los compuestos bioactivos presentes en los extractos.

El estudio de optimización en la recuperación de compuestos bioactivos de *Ganoderma lucidum* y *A. blazei* mediante RSM mostró que los valores predichos por los modelos estaban muy de acuerdo con las observaciones experimentales. Además, se concluyó que el rendimiento de extracción de compuestos bioactivos a partir de los hongos estudiados era altamente dependiente de las variables de extracción (tiempo, temperatura, proporción de disolvente, la relación sólido-líquido, y potencia). *A. blazei* y *G. ludidum* también mostraron un elevado valor nutricional. Se cuantificaron α-tocoferol, ácido oxálico y veintiún ácidos grasos (principalmente PUFA) en *A. blazei*. G. lucidum, por su parte, mostró un perfil de ácidos grasos similares (PUFA>SFA>MUFA) y con la presencia de α-tocoferol y δ-tocoferol. Comparativamente, *A. blazei* reveló un menor contenido de grasa, pero mayor aporte de energía. Se observó que el efecto sobre la viabilidad celular del extracto preparado a partir de *A. blazei* en líneas celulares Caco-2 y HT29-MTX se mantenía de una manera concentración-dependiente.

Los extractos etanólicos obtenidos a partir de los hongos estudiados mostraron actividad antioxidante, anti-inflamatoria, anti-tirosinasa y antimicrobiana, y después de la incorporación en la crema cosmético base, las formulaciones cosmecéuticas finales conservaron algunas de estas bioactividades. El extracto de *G. lucidum* se encontró que era una fuente rica de triterpenoides debido principalmente a la alta contribución de ácidos ganodéricos A, C2, y H, mientras que los ácidos fenólicos (ácido p-hidroxibenzoico, p-cumárico, ácido protocatéquico y ácido cinámico) y ergosterol se identificaron en *A. bisporus*, *P. ostreatus*, *L. edodes* y extractos de *A. blazei*. Cada uno de estos compuestos también mostraron efectos anti-inflamatorios, anti-tirosinasa y actividades antimicrobianas. Además, se utilizaron con éxito micropartículas para encapsular los extractos/compuestos individuales con alta eficiencia de encapsulación y rendimiento. Después de la incorporación en la crema cosmética base de los extractos/compuestos individuales libres y las micropartículas producidas a partir de ellas, las formas encapsuladas permitieron una liberación controlada que conduce a una mayor preservación de la bioactividad cuando se compara con las formas libres.

Debido a que presentaban el potencial cosmecéutico más interesante, los extractos de *P. ostreatus* y *G. lucidum* fueron sometidos a estudios toxicológicos, que revelaron ausencia de toxicidad en líneas celulares de queratinocitos y fibroblastos, lo cual es indicativo de su

potencial seguridad para ser utilizados como ingredientes cosmecéuticos. Los ácidos protocatequico y siríngico fueron los únicos compuestos que permeaban a partir del extracto de *G. lucidum*, mientras que se observó una muy baja permeación para los compuestos presentes en el extracto de *P. ostreatus*. También se obtuvieron resultados similares para la formulación preparada usando ambos extractos. Los resultados mostraron que los triterpenoides presentes en *G. lucidum* podrían ser potenciadores de la permeabilidad natural, lo que corrobora la idoneidad del uso de estos extractos de hongos como ingredientes para el cuidado de la piel. En general, los resultados mostraron que los productos para el cuidado de la piel se pueden formular usando extractos de hongos y que estos extractos tienen el potencial de ser utilizados a gran escala. Por lo tanto, la integración de los residuos generados por la industria de transformación de hongos, que pueden servir como materia prima para la obtención de extractos bioactivos, puede intensificarse.

LIST OF PUBLICATIONS

The studies developed within this Ph.D. thesis led to the following articles, copies of which are included as annexes:

1. Taofiq, O., Heleno, S.A., Calhelha, R.C., Alves, M.J., Barros, L., Barreiro, M.F., González-paramás, A.M., Ferreira, I.C.F.R. Development of mushroom-based cosmeceutical formulations with anti-inflammatory, anti-tyrosinase, antioxidant, and antibacterial properties. *Molecules*, 2016, 21, 1-12.

2. Taofiq, O., Heleno, S.A., Calhelha, R.C., Alves, M.J., Barros, L., González-Paramás, A.M., Barreiro, M.F., Ferreira, I.C.F.R. The potential of *Ganoderma lucidum* extracts as bioactive ingredients in topical formulations, beyond its nutritional benefits. *Food and Chemical Toxicology*, 2017, 108, 139–147.

3. Taofiq, O., Barros, L., Prieto, M.A., Heleno, S.A., Barreiro, M.F., Ferreira, I.C.F.R. Extraction of triterpenoids and phenolic compounds from *Ganoderma lucidum*: optimization study using the response surface methodology. *Food & Function*, 2018, 9, 209-226.

4. Taofiq, O., Heleno, S.A., Calhelha, R.C., Fernandes, I.P., Alves, M.J., Barros, L., González-Paramás, A.M., Ferreira, I.C.F.R., Barreiro, M.F. Mushroom-based cosmeceutical ingredients: Microencapsulation and *in vitro* release profile. *Industrial Crops and Products*, 2018, 124, 44–52.

5. Taofiq, O., Rodrigues, F., Barros, L., Barreiro, M.F., Oliveira, M.B.P.P., Ferreira, I.C.F.R. *Agaricus blazei* Murrill from Brazil- a potential ingredient for nutraceutical and cosmeceutical applications: preliminary studies. *Food and Function*, 2019,10, 565-572.

6. Taofiq, O., Heleno, S.A., Calhelha, R.C., Fernandes, I.P., Alves, M.J., Barros, L., González-Paramás, A.M., Ferreira, I.C.F.R., Barreiro, M.F. Phenolic acids, cinnamic acid, and ergosterol as cosmeceutical ingredients: stabilization by microencapsulation to ensure sustained bioactivity. *Microchemical Journal*, 2019, 147, 469-477.

7. Taofiq, O., Rodrigues, F., Barros, L., Barreiro, M.F., Oliveira, M.B.P.P., Ferreira, I.C.F.R. Mushroom ethanolic extracts as cosmeceuticals ingredients: safety and *ex vivo* skin permeation studies. *Food and chemical toxicology*, 2019, 127, 228-236.

8. Taofiq, O., Corrêa, R.C.G., Barros, L., Prieto M.A., Bracht, A., Peralta, R.M., González-Paramás, A.M., Barreiro, M.F., Ferreira, I.C.F.R. A comparative study

between conventional and non-conventional extraction techniques for the recovery of ergosterol bioactive compound from Agaricus *blazei* Murrill using response surface methodology. *Food research international*, Submitted.

The topic of this Ph. D thesis was also subject of the following review articles and book chapters, copies of which are also included as annexes:

1. Taofiq, O., Martins, A., Barreiro, M.F., Ferreira, I.C.F.R. Anti-inflammatory potential of mushroom extracts and isolated metabolites. *Trends in Food Science and Technology*, 2016, 50, 193–210.

2. Taofiq, O., González-paramás-Paramas, A.M., Martins, A., Barreiro, M.F., Ferreira, I.C.F.R. Mushrooms extracts and compounds in cosmetics, cosmeceuticals and nutricosmetics-A review. *Industrial Crops and Products*, 2016, 90, 38-48.

3. Taofiq, O., González-paramás, A.M., Barreiro, M.F., Ferreira, I.C.F.R. Hydroxycinnamic Acids and Their Derivatives: Cosmeceutical Significance, Challenges, and Future Perspectives, a Review. *Molecules*, 2017, 22, 1–24.

4. Taofiq, O., Fernandes, Â., Barros, L., Barreiro, M.F., Ferreira, I.C.F.R. UV-irradiated mushrooms as a source of vitamin D2: A review. *Trends in Food Science and Technology*, 2017, 70, 82–94.

5. Taofiq, O., Barreiro, M.F., Ferreira, I.C.F.R. Role of bioactive compounds and other metabolites from mushrooms against skin disorders- a systematic review assessing their cosmeceutical and nutricosmetic outcomes. *Current Medicinal Chemistry*, Submitted.

TABLE OF CONTENTS

LIST OF FIGURES

LIST OF TABLES

ABBREVIATIONS AND ACRONYMS

AD	Atopic dermatitis
ANOVA	Analysis of variance
ANVISA	National Sanitary Surveillance Agency
AP-1	Activator protein-1
ATCC	American Type Culture Collection
CA-SFM	Committee of L'Antibiogramme de la Société Française de Microbiologie
cAMP	Cyclic adenosine monophosphate
CFU	Colony forming unit
CREB	cAMP-response element binding protein
CLS	Cell Lines Service
CLSI	Clinical and Laboratory Standards Institute
COX-2	Cyclooxygenase-2
DCs	Dendritic cells
DMEM	Dulbecco's Modified Eagle Medium
DMSO	Dimethyl sulfoxide
DNA	Deoxyribonucleic acid
DPPH	2,2-Diphenyl-1-picrylhydrazyl
DOPA	Dihydroxyphenylalanine
ECM	Extracellular matrix
EDTA	Ethylenediamine tetraacetic acid
EE	Encapsulation efficiency
EL	Encapsulation load
ESBL	Escherichia coli spectrum extended producer of β-lactamases
ESI-MS	Electrospray ionization mass spectrometry
EU	European Union
EY	Encapsulation yield
FAME	Fatty acids methyl ester
FBS	Foetal bovine serum
FD&C Act	Food, Drug and Cosmetic Act
FDA	Food and Drug Administration
FPLA	Fair Packaging and Labelling Act
GA	Gallic acid
GAG	Glycosaminoglycan
GIT	Gastrointestinal tract

GP	Glutathione peroxidase
H_2O_2	Hydrogen peroxide
HAE	Heat-assisted extraction
HBSS	Hank's balanced salt solution
HeLa	Cervical carcinoma
HepG2	Hepatocellular carcinoma)
HPLC	High-performance liquid chromatography
HPLC-DAD	High-performance liquid chromatography with diode-array detection
HPLC-UV	High-performance liquid chromatography with an ultraviolet detector
IκB	Inhibitor of kappa B
IL	Interleukin
iNOS	inducible Nitric oxide synthase
INT	p-Iodonitrotetrazolium chloride
LDH	Lactate dehydrogenase
LPS	Lipopolysaccharides
MAAs	Mycosporine-like amino acids
MAE	Microwave-assisted extraction
MAPKs	Mitogen-activated protein kinase
MCF-7	Breast adenocarcinoma)
MHB	Mueller Hinton Broth
MIC	Minimal inhibitory concentration
MITF	Microphthalmia-associated transcription factor
MMPs	Matrix metalloproteinases
mRNA	Messenger Ribonucleic acid
MRSA	Methicillin-resistant Staphylococcus aureus
MS	Mass spectrometry
MSSA	Methicillin-sensitive Staphylococcus aureus
MyD88	Myeloid differentiation protein 88
MTT	3-(4,5-dimethylthiazol-2-yl)-2,5-diphenyltetrazolium
NCI-H460	Non-small cell lung cancer
NED	N-(1-naphthyl) ethylenediamine hydrochloride
NF-κB	Nuclear factor kappa-light-chain-enhancer of activated B cells
NK	Natural killer cells
NO	Nitric oxide
NSAIDs	Non-steroidal anti-inflammatory drugs
O_2^-	Superoxide anion

$O_2{}^{2-}$	Peroxide anion
OH^-	Hydroxyl ion
$OH^{\bullet}$	Hydroxyl radical
OM	Optical microscopy
$ONOO^-$	Peroxynitrite
PAMPs	Pathogen-associated molecular patterns
PBS	Phosphate buffered saline
pH	Potential of Hydrogen
PG	Prostaglandins
PKA	Protein kinase A
PUFA	Polyunsaturated fatty acids
REACH	Registration, evaluation, authorization and restriction of chemicals
RNS	Reactive nitrogen species
ROS	Reactive oxygen species
RPMI	Roswell Park Memorial Institute
RSS	Reactive sulfur species
S/L	Solid/liquid ratio
SB	Stratum basale
SC	Stratum corneum
SD	Standard deviation
SG	Stratum granulosum
SOD	Superoxide dismutase
SRB	Sulforhodamine B
SS	Stratum spinosum
TCA	Trichloroacetic acid
TGF-β	Transforming growth factor β
TLRs	Toll-like receptors
TNF-α	Tumor necrosis factor- α
TNFR	Tumor necrosis factor receptors
TRP	Tyrosinase-related protein
TSB	Tryptic soy broth
TX	Thromboxane
UAE	Ultrasound-assisted extraction
UFLC	Ultra-fast liquid chromatography
UV	Ultraviolet

CHAPTER 1: Background

1.1. Skin biology, skin ageing, and common skin disorders

The skin is the largest organ in the human body accounting for about 15% of total body weight. It acts as a barrier between the external environment providing protection against foreign bodies (Kamble, Sadarani, Majumdar & Bhullar, 2017). The skin structure is divided into three functional layers: epidermis (the outermost layer); dermis (structural support and mechanical barrier) and hypodermis (deepest layer) (Mota, Rijo, Molpeceres, & Reis, 2017), as shown in **Figure 1**. The epidermis is divided into *Stratum corneum* (SC), *Stratum granulosum* (SG), *Stratum spinosum* (SS) and *Stratum basale* (SB), from the exterior to the interior with the cells comprising 95% of keratinocytes and 5% of other cells (Langerhans cells, melanocytes and Merkel cells) (Mota et al., 2017).
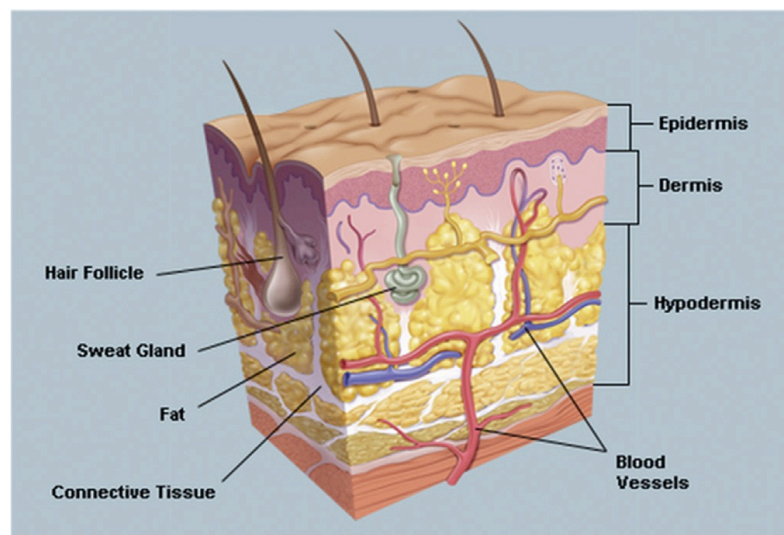
Figure 1. Structure of the skin showing the three functional layers (Kamble et al., 2017).

Keratinocytes cells continue to undergo differentiation (i.e. keratinization), forming the dead superficial layer referred to as the "cornified layer", which is considered to be the first line of defence against an environmental threat (Hirobe, 2014). The major proteins found in keratinocytes are keratin and filaggrin, which together with ceramides and fatty acids, regulate the barrier function of the skin and prevent water loss (Juráňová, Franková, & Ulrichová, 2017). The dermis is the layer of the skin that offers support and mechanical barrier, being mainly comprised by fibroblasts, dendritic, mast cells, blood and lymphatic vessels, sensory nerve endings, hair follicles, sweat and sebaceous glands. This layer contains structural

components such as collagen, elastin and extracellular fibres that maintain the tensile strength and elasticity of the skin. The fibroblasts are the principal cell type within the dermis and are primarily responsible for production, deposition, and remodelling of the extracellular matrix (ECM) components thereby contributing significantly to the wound healing process of the skin (Li, Zhao, Hao, Han, & Fu, 2017). The hypodermis is the deepest layer of the skin also known as the subcutaneous layer, composed of areolar and adipose tissues that anchor the skin to the underlying structures (muscles or bones). This layer serves as energy storage in the form of fat (triglycerides and cholesterol), as well as assuring thermoregulatory functions (Mota et al., 2017).

Bioactive compounds can effectively scavenge free radicals when they are applied topically to protect the skin if they reach deeper cutaneous layers. Despite the skin possessing a strong barrier, there are several routes in which the active ingredient can penetrate and permeate the skin (Costa & Santos, 2017). The absorption of bioactive ingredient into the skin takes place by dissolution and molecular diffusion through the skin membrane, via three different penetration pathways namely, intracellular pathway, intercellular pathway and appendageal pathway (through sweat gland and hair follicles) as shown in **Figure 2** (Bolzinger, Briançon, Pelletier, & Chevalier, 2012). Bioactive ingredients from various natural sources are becoming the major focus of recent developments in skin care products and it is important that these ingredients penetrate the *stratum corneum* and reach other skin layers. Penetration through the intercellular pathway occurs through the intercellular spaces and this penetration method predominates over the other two penetration pathways. The contribution of the appendageal route is negligible considering only 0.1% of the total surface area of human skin is covered by sweat glands and hair follicles (Lane, 2013).
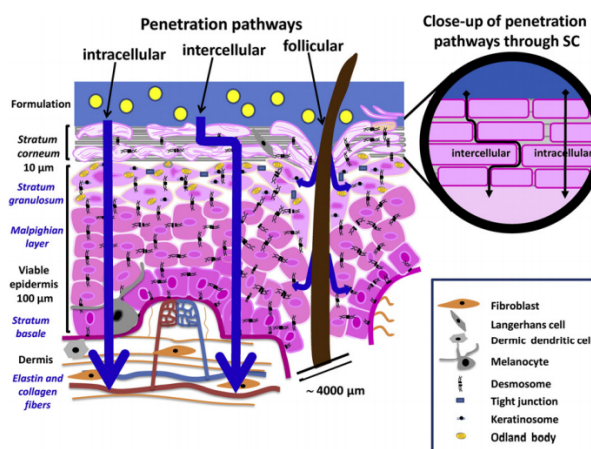
Figure 2. Different penetration pathways (Bolzinger et al. 2012).

Studies have shown that skin diseases account for nearly 34% of all the diseases encountered worldwide with skin ageing being the most prominent problem that tends to worsen over time (Xie et al., 2018). The aetiology of skin diseases varies from environmental factors such as UV radiation, pollution, pathogens, genetic factors and autoimmune disorders (Działo et al., 2016). Some of the most common skin diseases will be discussed below.

***Skin ageing*:** The extracellular matrix (ECM) of the skin is the structural support network made up of diverse proteins, sugars, and other components. These structural components include collagen, elastin, fibronectin, laminin, tenascin, hyaluronic acid and collectively, they are responsible for maintaining the tensile strength, cell adhesion, cell migration and wound healing of the skin (Kular, Basu, & Sharma, 2014). The breakdown of the ECM is carried out by a group of calcium-dependent zinc-containing endopeptidases called "matrix metalloproteinases (MMPs)". The activities of these enzymes result in enzymatic degradation and reduced de novo synthesis of collagen and elastin, while also causing changes in hyaluronic acid content, resulting in skin laxity and ageing (Taofiq, González-Paramás, Martins, Barreiro, & Ferreira, 2016). The mechanism behind the ageing process can either be intrinsic or extrinsic, with the intrinsic mechanism being a natural or cellular based process in the skin and other organs as a consequence of physiological changes that occur over time (Lorencini, Brohem, Dieamant, Zanchin, & Maibach, 2014). The skin is equipped with intrinsic enzymatic antioxidants, such as superoxide dismutase (SOD), catalase and glutathione peroxidase (GP), which collectively neutralize free radicals and repair oxidative damage. Continuous oxidative and repair processes in the body generate free radicals that often cause low activity of these antioxidants thereby promoting the ageing process (Taofiq, González-paramás, Barreiro, & Ferreira, 2017). UV radiation from sun exposure is the major environmental insult to skin and this tends to trigger the extrinsic ageing mechanism that results in the generation of free radical species (Kammeyer & Luiten, 2015). Subsequently, the free radicals induce activator protein-1 (AP-1), a transcription factor that promotes collagen breakdown by up-regulating the MMPs. Overexpression of these MMPs leads to elevated levels of degraded collagen and a photoaged skin (Taofiq et al., 2016). Another similar extrinsic pathway responsible for an ageing skin is the downregulation of transforming growth factor (TGF-β), a cytokine that promotes pro-collagen production by UV radiation, thus causing low levels of collagen synthesis (**Figure 3**) (Taofiq et al., 2016). With increasing age, collagen synthesis becomes lower and MMPs activities becomes higher resulting in skin wrinkling and loss of elasticity (Hui, Pin-ru, Shen, & Xiang-dong, 2010).
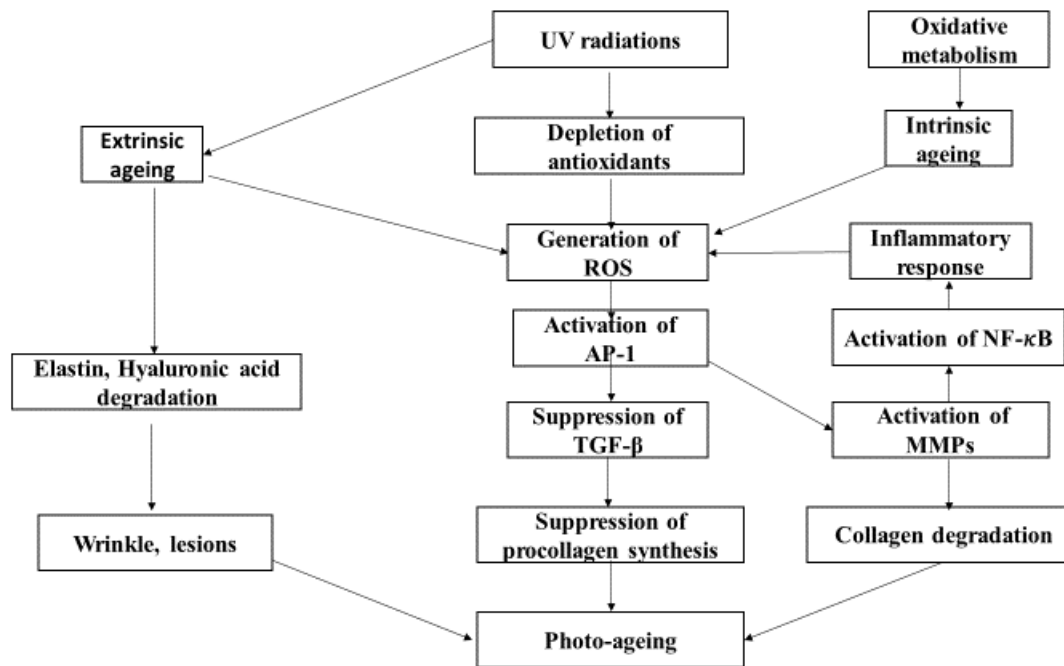
Figure 3. An overview of the skin ageing process (UV: ultraviolet radiation; AP-1: activator factor protein; ROS: reactive oxygen species; MMPs: matrix metalloproteinases; NF-κB: nuclear factor κB; TGF-β: transforming growth factor β).

Atopic dermatitis: Atopic dermatitis (AD) is a chronic inflammatory skin disease characterized by eczematous lesions, intense itch, swollen and severely dry skin, making the skin susceptible to cutaneous infections (Akdis, Akdis, Trautmann, & Blaser, 2000). Uncontrolled production of inflammatory mediators has been known to cause several cell damages and initiate the inflammation process, with many therapeutic trials already performed to find potent treatments to suppress AD (Choi et al., 2011). Some glucocorticoids and other steroids have been utilised as anti-AD treatment. Nevertheless, prolonged use at high doses of these treatments has been reported to cause a variety of side effects, motivating the desire to find new promising alternatives of natural origin (Choi et al., 2011; Taofiq, Martins, Barreiro, & Ferreira, 2016).

Hyperpigmentation: Hyperpigmentation is a common skin problem in middle-aged and elderly people. It is caused by overproduction of melanin, the pigment that is responsible for the colour of hair and skin either because of excessive exposure to UV light or as a manifestation of an ageing skin (Ali, Choudhary, Naaz, & S Ali, 2015). Tyrosinase is the key enzyme in melanin production and over-activity of this enzyme leads to uncontrolled production of melanin, causing hyperpigmentation of the skin. Hyperpigmentation disorders manifest either in the form of brown spots, melasma, freckles or solar lentigines (Fisk, Agbai, Lev-Tov, & Sivamani,

2014). Formulations containing ingredients such as hydroquinone, kojic acid, and retinoids have been utilised in the past to suppress the severity of hyperpigmentation, however, long term exposure to them have been reported to present cytotoxic, irritating and mutagenic effects on the skin (Chaowattanapanit, Silpa-archa, Kohli, Lim, & Hamzavi, 2017). Hence the need to find safe and effective alternatives from bio-based sources.

***Skin cancer*:** Skin cancers are the most dangerous skin diseases, and are often manifested as basal cell carcinoma, squamous cell carcinoma and malignant melanoma suggesting that the cells affected in each case are the basal cells, the squamous cells and the melanocytes, respectively (Działo et al., 2016). Studies have shown an increase in the reported cases of skin cancer, and if untreated they can spread to nearby areas, colonizing bones, other connective tissues, lymph nodes and other parts of the body (Epstein, 2009). One of the most common risk factors responsible for skin cancer development is the overexposure to UV light. Other causes include immunosuppression, exposure to certain chemicals, ageing and genetically inherited skin disorders (Chen, Hu, & Wang, 2012).

***Acne vulgaris*:** Acne vulgaris, occurs during adolescence due to the over stimulation of sebaceous glands, which causes an increased secretion of sebum (Choi et al., 2011). Another common cause is colonization of the skin with the bacterium *Propionibacterium acnes* and inflammation (Działo et al., 2016). *Staphylococcus aureus*, *Staphylococcus epidermidis* and *P. acnes* are the most common bacterial species that colonize the skin in acne patients. An investigation into the prevalence of skin colonization by these bacteria in acne patients showed the presence of strains resistant to one or more commonly used anti-acne antibiotics (Agrawal, Adholeya, Barrow, & Deshmukh, 2018). New therapy includes the use of topical formulations with bioactive extracts, or individual compounds, having a broad antimicrobial spectrum, antioxidant and anti-inflammatory properties (Tamrakar et al., 2017).

Wound healing: Would healing includes a series of complex biological processes involving interaction between several inflammatory mediators, platelets, extracellular matrix molecules, fibroblasts, and other inflammatory cells (Yahaya, Cordier, Steenkamp, & Steenkamp, 2018). The proliferation and cellular differentiation of fibroblasts, stimulated by growth factors released by platelets and monocytes, are the most important key factors during wound healing. Even though conventional wound treatment has been practiced across the world, natural extracts, which possess important biological properties, mainly those related with anti-inflammatory and antioxidative stress activities, can act as alternatives (Pitz et al., 2016).

1.2. Cosmetics, Cosmeceuticals and Nutricosmetics

1.2.1. Cosmetics

A "cosmetic product" is any substance with soft action that is either rubbed or sprinkled on the various parts of the human body (epidermis, hair, nails, lips, external genitals, the teeth or mucous membranes of the oral cavity) with the sole aim to clean, beautify, increase the attractiveness, protect and keep them in good condition (Luque de Castro, 2011). The world's cosmetic industry is worth tens of billions of US dollars and is in a constant search for new and improved natural products to serve as suitable raw-materials, able to compete with the artificial synthetic counterparts or add new bioactivities (Hyde, Bahkali, & Moslem, 2010; Ramli, 2015). While there are several cosmetic products available on the market, they can be categorized into 5 groups as follows:

Skin care products: These are products designed to cleanse, sooth, restore, reinforce and protect the skin, thereby improving the appearance and feel of skin. This skin care category of cosmetic products corresponds to the largest market, accounting for about 30% of all cosmetics sold. It is difficult to subcategorize these products accordingly, but they include cleansers, exfoliants, conditioners, sunscreens and anti-ageing products (Surber & Kottner, 2017). According to the "Euromonitor International" anti-ageing skincare covers over 22% of the global skincare market, and their worth is expected to reach US$ 216 billion by 2021 (Agrawal et al., 2018).

Hair care products: These cosmetic products are intended to be placed on the hair and scalp with the sole purpose of cleansing, promoting attractiveness and changing hair appearance. They account for about 25% of all cosmetics sold in the market and generally include products like tints, bleaches, lotions, conditioners, styling products, powders, shampoos, brilliantines and lacquers (Guerra-Tapia & Gonzalez-Guerra, 2014).

Colour cosmetics: The colour category of cosmetics accounts for about 20% of all commercial cosmetics and are the most regulated cosmetic category. They are products intended to be applied on the skin to confer changes in colour and appearance. It includes products for the face like foundations, lipsticks, blushes, eye shadow, eyeliner, and mascara. These cosmetic products contain mixtures of multiple colouring ingredients, either from natural sources or of synthetic origin. The synthetic colorants are quite common due to their low cost and higher stability in formulations when compared to their natural counterparts (Chen et al., 2019).

Perfume and fragrances: This category account for about 10% of commercial cosmetics. They are products intended to change natural body odour. These products have been utilised since ancient times and the proportion of women's to men's fragrances is approximately two to one in most European countries, with France having the highest contribution in annual fragrance sales in Europe (Lenochová et al., 2012).

Personal care products: They account for up to 15% of total cosmetics sold in the market. They include oral care products such as toothpaste, mouthwash and teeth whitening products as well as products as diverse as deodorant, hand soap, facial cleanser, body wash, pomade, perfumes, shaving cream, and toilet paper. It is important to note that these categories of cosmetic are complementary and have been able to satisfy user's needs over the years (Surber & Kottner, 2017).
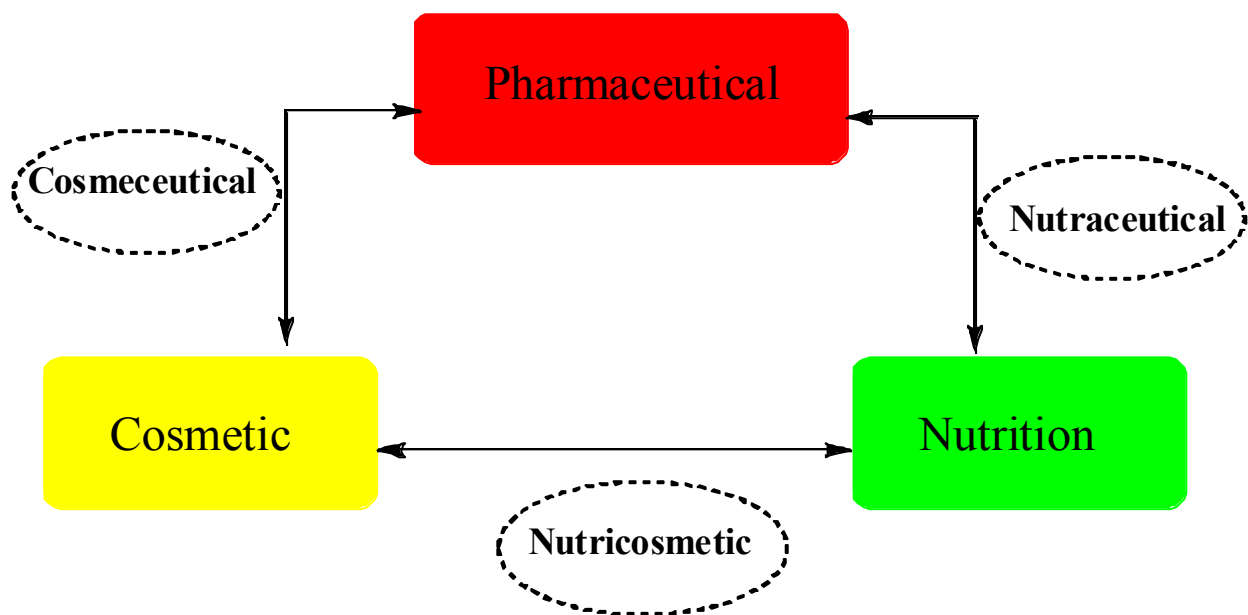
Figure 4. The emergence of new trends in the food, pharmaceutical, and cosmetic industries.

As the global cosmetic market continues to grow steadily, there is a continuous demand for product diversification resulting in the emergence of products with different claims and functional properties. Because of the rising consciousness and awareness among consumers about the origin, safety and environmental implications of some of the ingredients used in cosmetic formulations, there is an increasing demand for the use of green and more sustainable raw materials during product formulation (Luque de Castro, 2011). Over the years, the

pharmaceutical, cosmetics, and food industries have converged, giving rise to new categories such as cosmeceuticals, nutraceuticals, and nutricosmetics (**Figure 4**).

1.2.2. Cosmeceuticals

Cosmeceuticals are products in the interphase between cosmetics and pharmaceuticals. They consist of products in the forms of creams, ointments or lotions with biologically active compounds, which are applied topically on the skin with a medical drug-like benefit (Sharma, 2011). The term "cosmeceutical" was first coined by Raymond Reed, a founding member of the United States Society of Cosmetic Chemists, but not until 1971 when the term was popularized by Dr. Albert Kligman, when he developed a formula to improve the appearance of UV damaged and wrinkled skin using retinoic acid (Amer & Maged, 2009). In the United States and Europe, cosmeceuticals are commercialized as cosmetics, although in Japan this category is termed as "quasi-drugs", "controlled cosmetics" in Thailand and "cosmetic-type drugs" in Hong Kong. The regulations of cosmeceuticals have not been harmonized between the USA, Europe, Asia, and other countries (Ramos-e-Silva, Celem, Ramos-e-Silva, & Fucci-da-Costa, 2013). These products are known to contain ingredients that influence the biological function of the skin by supplying the needed nutrients for healthy skin, while improving the appearance, the radiance, texture and anti-ageing activity (Hyde et al., 2010). The application of natural ingredients such as phytonutrients, microbial metabolites, dairy products (Haruta-Ono et al., 2012; Keller et al., 2014), minerals and animal protein components (Rodrigues, Pimentel, & Oliveira, 2015) for skin care is very popular today. The Asia Pacific is the largest cosmeceutical market and is also expected to witness the highest growth, while North America, Europe, Latin America, and the Middle East are growing at a modest rate with the development of novel and innovative products in these markets (Brandt, Cazzaniga, & Hann, 2011). There are more than 400 cosmeceutical manufacturers, in the U.S. market with the most well-known being Procter & Gamble, Johnson & Johnson, L'Oréal, Estée Lauder and Avon and Allergan, among others (Brandt, Cazzaniga, & Hann, 2011; Lohani et al., 2014).

Plant-derived compounds have been used extensively for cosmeceutical applications and more recently, attention has been directed to the waste and residue produced during their processing, resulting in some of their derived bio-products, which may have the potential to be applied as cosmetic ingredients (Barbulova, Colucci, & Apone, 2015). Bio-products of plant species, such

as citrus, tomato, and olives, contain compounds like limonene, lycopene, unsaturated fatty acids and phenolic compounds that have shown biological properties, such as antioxidant, anti-inflammatory and anti-tyrosinase activity. Rodrigues et al. (2015) reported that different bio-products of the olive oil processing industry (leaves, stones, wastewater and pomace) displayed high antioxidant activity and contained minerals and fatty acids, with functional roles compatible with cosmetic ingredients. Hydroxy acids, such as glycolic, hydroxybutanoic, malic, citric, salicylic and lactic acids, isolated from several natural sources have been highlighted in the skin care sector for anti-wrinkling benefits, radical-scavenging effects, and treatment of several hyperpigmentation disorders (Tang & Yang, 2018). Their safety is constantly evaluated, and among them, glycolic and salicylic acids are becoming very popular in skin care products (Kornhauser, Coelho, & Hearing, 2012).

Also, in the context of cosmetic ingredients, Wang, Chen, Huynh, & Chang (2015) reviewed the bioactive properties of marine algae. The authors highlighted the presence of alginate and mycosporine-like amino acids (MAAs) imparting anti-oxidative properties and the ability to act as reactive oxygen species (ROS) scavengers. Some algae extracts were also reported to inhibit activator protein (AP-1) and nuclear factor kappa B (NF-κB), both transcription factors associated with the expression of enzymes, like matrix metalloproteinase and inducible nitric oxide synthase responsible for collagen degradation, and to increase the release of inflammatory mediators causing skin wrinkling and inflammation, respectively. The authors also mentioned the potential of fucoxanthin (carotenoid), phlorotannins and phloroglucinol (phenol derivative), to inhibit the tyrosinase enzyme and prevent melanin biosynthesis. These multiple properties displayed by marine algae and their bioactive components have demonstrated that they can be exploited as new and powerful cosmeceutical ingredients.

Animal processing for human consumption also generates a handful of residues and raw materials, such as collagen, elastin and keratin, ingredients that are slowly finding their way into the cosmetic industry. Collagen is often recovered from the hides, skin, and bones of cows and pigs, while elastin can be recovered from the ligaments of cow, pork, fish and chicken. They are both important components of the extracellular matrix, being responsible for both skin elasticity and flexibility maintenance (Theocharis, Skandalis, Gialeli, & Karamanos, 2016). Keratin, on the other hand, can be recovered from poultry feathers and porcine hairs. In combination, elastin and collagen offer the mechanical resistance necessary for an intact skin (Ferraro, Anton, & Santé-Lhoutellier, 2016).

Marine animals, such as starfish, sponges, and jellyfish, are other raw material sources with growing importance in the cosmetic industry due to their richness in phenolics and carotenoids (Lee et al., 2015). The mentioned authors conducted comprehensive studies to evaluate the antioxidant, anti-collagenase, anti-elastase and anti-hyaluronidase activity of stalked sea squirt (*Styela clava* Herdman) extract. The results revealed that the obtained extract inhibited collagenase, elastase and hyaluronidase enzymes, highlighting its potential to be utilised as an ingredient to maintain the flexibility and elasticity of the skin, as well as preserve the moisture content and tension of the skin. The compounds responsible for the shown activity were not identified or isolated. Earthworm (*Lumbricus terrestris* L.) has also been reported to show cosmeceutical significance even though very few studies have been reported so far (Azmi, Hashim, Hashim, Halimoon, & Majid, 2014). These authors described elastase, tyrosinase and collagenase inhibitory activities, suggesting that the extract contains useful anti-wrinkling and depigmenting ingredients. All these interesting reports have shown that extracts and compounds obtained from diverse natural sources have high potential to be used as cosmetic ingredients and thus should be investigated for this purpose. Very few studies have been carried out to determine the mechanism of action of the relevant extracts, as well as to identify the individual bioactive metabolites responsible for the ascribed bioactivities.

1.2.3. Nutricosmetics

Nutricosmetics are the newest trend in skin care and involve combining food, cosmetic and pharmaceuticals being still unknown to some dermatologists and consumers. This involves the consumption of dietary and nutritional supplements to produce a visual appearance benefit and improve the health of the skin (Luque de Castro, 2011). The focused primary action areas are skin, hair, and wellbeing. Healthy skin is a manifestation of overall health and as such can be influenced by the consumption of bioactive substances (Royer, Prado, García-Pérez, Diouf, & Stevanovic, 2013). This is regarded as the "inside out" approach because ingestion of bioactive ingredients and topical application of cosmeceuticals can synergistically combine together to maintain a positive skin appearance (Draelos, 2010). Many micronutrients can provide these effects (e.g. vitamin C has an antioxidant potential and tends to reduce free radical generation when the skin is exposed to UV radiation) (Royer et al., 2013). Following these trends, cosmetic industries are now putting more efforts to develop nutricosmetics with high contents

of several ingredients, such as collagen, hyaluronic acid, elastin and ceramide, known to maintain skin structure and function (Haruta-Ono et al., 2012). These authors reported that oral ingestion of dietary products improved the water-holding capacity of the skin and the barrier function. Hong, Jung, Noh, & Suh, (2014) also reported the beneficial effect of green tea ingestion due to the presence of numerous phenolic compounds responsible for significant inhibition of enzymes such as collagenase, elastase, and tyrosinase, thereby maintaining the structural stability, elasticity and blocking melanogenesis, respectively. Nutricosmetic formulations containing vitamin C, in the form of L-ascorbic acid, vitamin E and carotenoids such as astaxanthin, lutein, and lycopene all act as antioxidants and tend to quench free radicals (Draelos, 2010). To the best of our knowledge, the nutricosmetics area is still without enough scientific references as most available data are based on assumptions and some of the manifestations can be over-ambitious. Studies to confirm these claims are difficult to conduct as each control will be devoid of one essential nutrient or the other to be able to observe the progressive effects of deficiency of some of these bioactive ingredients on the skin and general health.

1.3. Mushrooms: mycological classifications, bioactive and chemical compositions

Mushrooms belong to the kingdom Fungi and are often referred to as the "Forgotten Kingdom" or the "unnoticeable Kingdom" but in fact, they have inhabited different ecological niches and carried out important ecosystem roles (de Mattos-Shipley et al., 2016). Basidiomycota together with Ascomycota are the two phyla to which most mushrooms belong, but in what concern their utilisation as food and medicine, the basidiomycetes are the most common (Landi et al., 2017). Mushrooms have been an important part of our diet, consumed for years because of their attractive nutritional composition being an excellent source of nutrients, low in calories and fats and free of cholesterol. They are also an important source of proteins, vitamins, fibre and minerals as well as presenting multiple functional properties (Heleno et al., 2013; Money, 2016; Oliveira et al., 2014; Taofiq et al., 2015). The consumption of mushrooms dates back to ancient times where they are referred to as "divine food" (de Mattos-Shipley et al., 2016). Generally, based on the different usages, mushrooms can be classified as edible species such as *Pleurotus ostreatus* (Jacq. ex Fr.) P. Kumm., *Lentinula edodes* (Berk.) Pegler, *Agaricus bisporus* (J.E. Lange) Imbach, *Flammulina velutipes* (Curtis) Singer and *Auricularia auricular*

(Bull.) J.Schröt., and medicinal species such as *Ganoderma lucidum* (Curtis) P. Karst., *Cordyceps sinensis* (Berk.) Sacc*., Agaricus blazei* Murrill (ABM) and *Poria Cocos* F.A. Wolf, among others. Knowledge about the bioactive composition and nutritional value of different mushrooms is extensive and already present for several years. In fact, they are considered as functional foods because of the presence of a wide range of bioactive metabolites, e.g. phenolic compounds, terpenoids, polysaccharides, lectins, steroids, glycoproteins and several lipid components (Barreira, Oliveira, & Ferreira, 2014; Ferreira et al., 2015; Oliveira et al., 2014; Reis, Martins, Vasconcelos, Morales, & Ferreira, 2017).

1.3.1. Mycological characteristics of some selected mushroom species

Agaricus bisporus is well known for its taste and aroma and is one of the most widely cultivated mushrooms in the world, produced on the scale of millions of tons yearly (de Mattos-Shipley et al., 2016). They are popularly referred to as white mushrooms, button mushrooms and portobello mushrooms (Leiva, Saenz-Díez, Martínez, Jiménez, & Blanco, 2015). It is an edible mushroom belonging to the phylum Basidiomycota, a litter-decomposing saprotroph that grows in a wide range of environment, native to North America, Asia and Europe (de Mattos-Shipley et al., 2016). It typically bears a white cap (**Figure 5**) with dark brown gills, but the earliest forms growing wild had brownish cap and gills. The cultivation of this mushroom for commercial purposes dates back to the 16th century, and continues, nowadays, to grow significantly providing food with a high nutritional value in an environmentally sustainable way because of the use of organic waste and other low-value substrates (Leiva et al., 2015).

| *Agaricus bisporus* | *Agaricus blazei* | *Ganoderma lucidum* | *Lentinula edodes* | *Pleurotus ostreatus* |

Figure 5. Selected mushroom species studied in the present work.

Agaricus blazei is a medicinal mushroom, identical to *Agaricus brasiliensis* and *Agaricus subrufescens*, popularly referred to as 'Cogumelo do Sol' in Brazil, 'Himematsutake' in Japan, and 'Ji Song Rong' in China. It is rich in polysaccharides, phenolic acids, and ergosterol (Yue et al., 2012). *A. blazei* was first cultivated and consumed in the Atlantic states of the United States in the late 19th century, however, it was later discovered in Brazil, and called the ''Piedade mushroom'' by Takatoshi Furumoto, who then sent it to Japan in 1965 to study their medicinal properties (Wisitrassameewong et al., 2012). Since then, *A. blazei* have become one of the most important mushroom exports from Brazil. In recent years, its extracts have become increasingly popular because of its long history of applications in treatments of diseases, mainly due to its immunomodulatory, anti-inflammatory, antitumor, antioxidant and antiviral properties (Lima, Gris, & Karnikowski, 2016; Zhai, Wang, & Han, 2015).

Ganoderma lucidum is a large, dark, woody, Basidiomycota mushroom popularly referred to as reishi in Japan and lingzhi in China (Ferreira et al., 2015). It has been utilised as a functional food, and in traditional medicines in Korea and other Asian countries to promote longevity and better health (de Mattos-Shipley et al., 2016). It could be parasitic, living on hardwoods (especially oaks) or saprobic, living on the deadwood of hardwoods (Heleno et al., 2012). Some pharmacological and nutraceutical properties have been related to its capacity to act as immune suppressors, hypocholesterolemic agents or as coadjutant treatments in diseases such as cancer, hypertension, insomnia, anorexia, dizziness and chronic hepatitis (Baby, Johnson, & Govindan, 2015; Zhao et al., 2016). These beneficial health properties are attributed to a wide variety of bioactive components such as polysaccharides, polyphenols, triterpenes, sterols, and proteins (Bishop et al., 2015; Heleno et al., 2012).

Lentinula edodes popularly referred to as shiitake, is one of the most cultivated edible mushrooms in the world, being second only to *A. bisporus* (Hearst et al., 2009). Medicinal use of the shiitake mushroom, dates to the Ming dynasty (1368-1644), where reports refer that shiitake increased human vigour and energy, and it was used to suppress aches, pains, and fatigue associated with ageing (Sasaki, Linhares, Nozawa, Montalván, & Paccola-Meirelles, 2001). Research interest on this mushroom has increased due to its content in functional bioactive compounds (Hearst et al., 2009). Its polysaccharide content seems to be one of the most interesting biomolecule's fractions being reported to contribute to immunomodulatory, antimicrobial and antitumor activities (Villares, Mateo-Vivaracho, & Guillamón, 2012, Wu, Choi, Li, Yang, & Shin, 2016).

Pleurotus ostreatus commonly known as oyster mushroom, is an important edible mushroom widely cultivated all over the world. *P. ostreatus* was initially named as *Agaricus ostreatus* but later placed in the *Pleurotus* genus by the German mycologist Paul Kummer. It is a saprotroph which acts as a primary decomposer on wood growing in a wide range of temperatures, and utilising various lignocelluloses (Hearst et al., 2009). *P. ostreatus* is typically found growing out from trees in shelf-like clusters, widely distributed in North America, Asia, Britain, Ireland, and most mainland Europe. Commercial cultivation of *P. ostreatus*, unlike *A. bisporus*, commenced in the 19th century and ever since, its cultivation has rapidly become a worldwide phenomenon (de Mattos-Shipley et al., 2016). It has well-reported health-promoting benefits and is becoming very popular throughout the world as a good source of dietary fibre and other valuable nutrients (Alam et al., 2010).

1.3.2. Bioactive compounds present in mushroom extracts

There is an increasing interest in mushrooms because of their biologically active compounds, which presents medicinal and health-promoting benefits. Some of these secondary metabolites will be discussed below.

1.3.2.1. Polyphenols and related compounds

Phenolic compounds are a major class of secondary metabolites, with structural diversity, found in plant and fungi (Vieira da Silva, Barreira, & Oliveira, 2016). They are not needed for growth or reproduction but are secreted for protection against UV, competitive warfare against other plants, insects, viruses and bacteria. They are also responsible for plant smell, colour, and flavour (Heleno, Martins, Queiroz, & Ferreira, 2015). According to their carbon chain, phenolic compounds can be divided into 16 major classes namely: simple phenols (C_6), benzoquinones (C_6), hydroxybenzoic acids (C_6-C_1), acetophenones (C_6-C_2), phenylacetic acids (C_6-C_2), hydroxycinnamic acids (C_6-C_3), phenylpropenes (C_6-C_3), coumarins (C_6-C_3), chromones (C_6-C_3), naphthoquinones (C_6-C_4), xanthones (C_6-C_1-C_6), stilbenes (C_6-C_2-C_6), anthraquinones (C_6-C_2-C_6), flavonoids (C_6-C_3-C_6), lignans (C_6-C_3)$_2$ and ellagitannins (C_6-C_3)$_n$ (Vieira da Silva et al., 2016).

Phenolic acids are derived from the shikimate pathway (**Figure 6**) involving several enzymatic steps responsible for converting intermediates of the pentose phosphate pathway and glycolysis to form three crucial aromatic amino acids (phenylalanine, tyrosine, and tryptophan) (Dias, Sousa, Alves, & Ferreira, 2016; Heleno, Martins, et al., 2015). They have a benzene ring, a

carboxylic group and one or more hydroxyl and/or methoxy groups and are divided into two groups: i) hydroxybenzoic acids; ii) hydroxycinnamic acids.
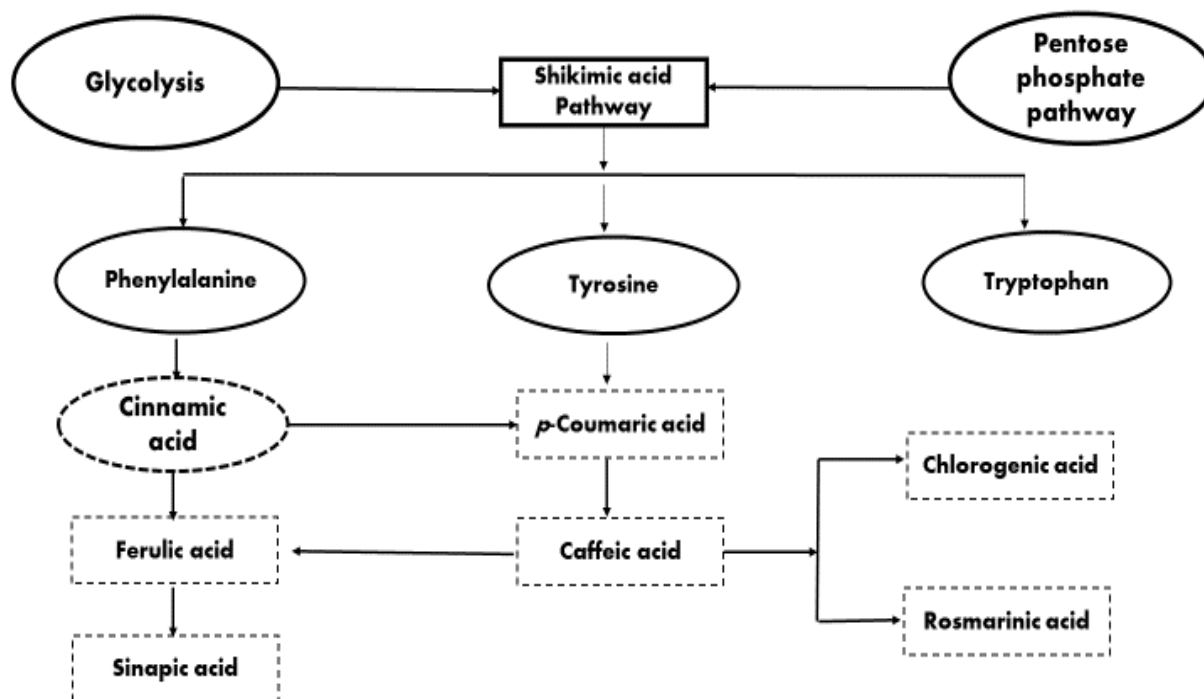
Figure 6. Schematic representation of the hydroxycinnamic acids synthesis.

The hydroxycinnamic acids group, the largest class (**Figure 7**), has nine carbon atoms (C_6–C_3); examples include caffeic, ferulic, *p*-coumaric and sinapic acids; (ii) the hydroxybenzoic acids group have seven carbon atoms (C_6–C_1); it includes gallic, *p*-hydroxybenzoic, protocatechuic, vanillic and syringic acids (**Figure 7**) (Pereira, Valentão, Pereira, & Andrade, 2009). Some of these phenolic acids can also be found in form of derivatives, such as amides (combination with amino acids or peptides) and esters (combination with hydroxyl acids or glycosides). These forms have also been reported to present interesting biological properties (Pei, Ou, Huang, & Ou, 2016; Pragasam & Rasool, 2013), but very few data are available to support their application as cosmeceutical ingredients. They exhibit multiple physiological functions, such as antioxidant, anti-inflammatory, anti-microbial, anti-collagenase, anti-melanogenic and anti-cancer (Amirullah, Zainal Abidin, & Abdullah, 2018; Carocho & Ferreira, 2013b; Ferreira, Barros, & Abreu, 2009; Moro et al., 2012) properties that are the basis behind their increased

use as cosmeceutical and nutricosmetic ingredients. The pharmacological potential displayed by these phenolic acids and derivatives has been largely attributed to the presence of multiple hydroxyl groups in their chemical structure, making them suitable free radical scavengers (Zhang & Tsao, 2016). Extensive work has been done on the role of these compounds in disease prevention and their fate *in vivo* after metabolism (Heleno, Martins, et al., 2015). However, their utilisation as skin care ingredient is gradually gaining attention.
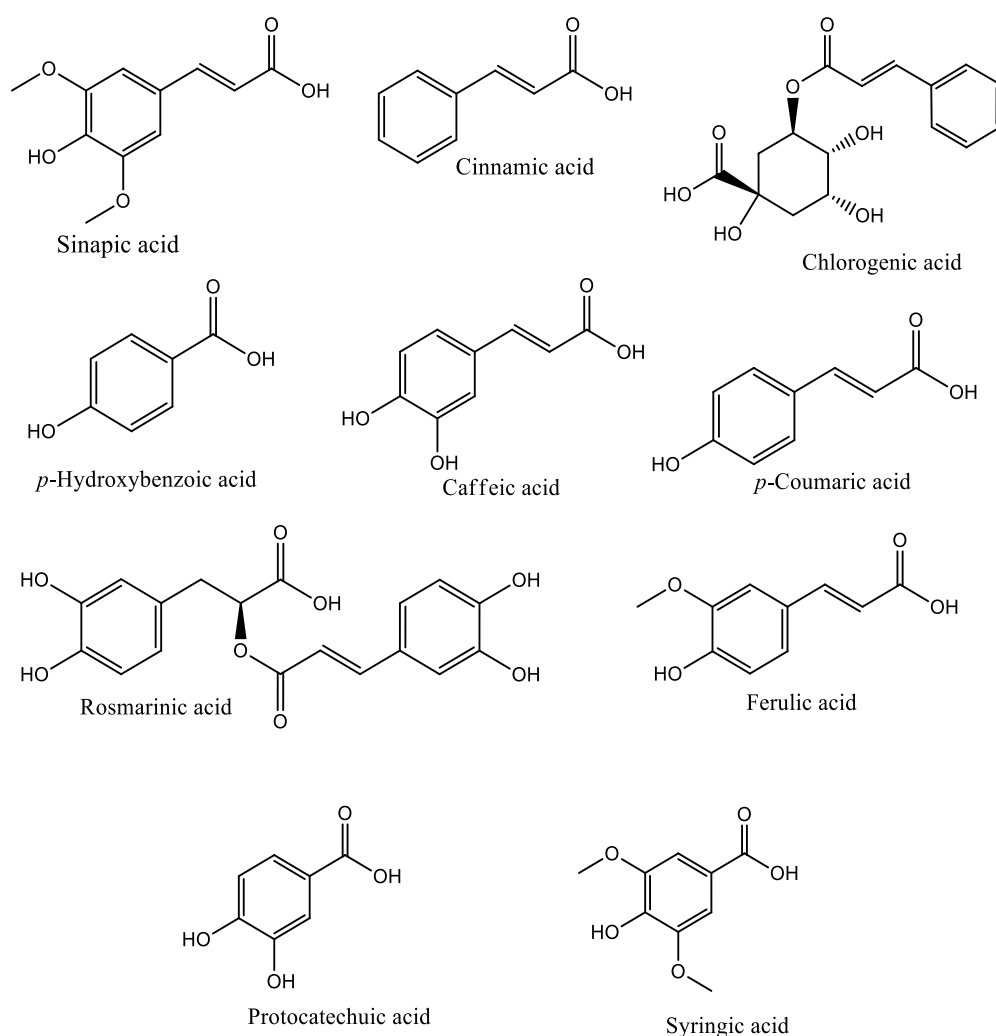
Figure 7. Common phenolic compounds found in mushrooms.

1.3.2.2. Polysaccharides

Polysaccharides are the major class of bioactive compounds found in mushroom and they are present either as glucan polysaccharides or as polysaccharide-protein complexes (Milhorini et

al., 2018). They generally differ in their primary structure, type of linkage, the degree of branching and molecular weight. They occur mostly as glucans (**Figure 8**), linked by β-(1-3), (1-6) and α-(1-3) glycosidic bonds. Some common polysaccharides found in mushrooms include pleuran (*P. ostreatus*), lentinan (*L. edodes*), glucomannan (*A. blazei*), β-D-glucan (*Agaricus brasiliensis, Collybia dryophila*), α-1,6, α-1,4-glucan (*A. blazei*), heteroglycan (*Lentinus squarrosulus, Pleurotus florida, Volvariella volvace*), (1-3), (1-6)-β-D-glucan (*G. lucidum*), coriolan (*Coriolus versicolour*), agaritine (*A. bisporus*), calocyban (*Calocybe indica*), α-fucoglucomannan (*Inonotus obliquus*), ganoderan (*G. lucidium*), β-pachyman (*Wolfiporia extensa*), schizophyllan (*Schizophyllum commune*), acidic glucuronoxylomannan (*Tremella fuciformis*) (Rathore, Prasad, & Sharma, 2017; Singdevsachan et al., 2016). These compounds are either intracellular as reserve material or extracellular as structural components of the fungal cell wall, playing vital roles in immunomodulatory and anticancer activities.
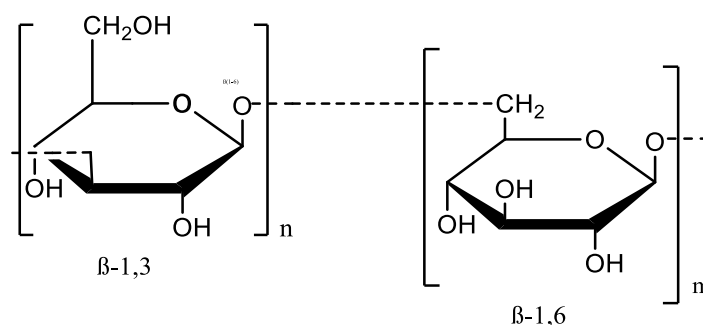
Figure 8. The molecular structure of β-D-glucan (1→3), (1→6).

They generally act as immuno-enhancers stimulating inflammatory cells such as lymphocytes, macrophages, hematopoietic stem cells, T cells, dendritic cells (DCs) and natural killer (NK) cells, that are important in the innate and adaptive immune system (Meng, Liang, & Luo, 2016).

1.3.2.3. Terpenoids, triterpenes and steroidal compounds

Terpenes are a group of organic compounds in plants, animals and macrofungi consisting of five carbon isoprene unit $(C_5H_8)_n$ as their building block, where *n* represents the number of units involved. They are classified as monoterpenes: 2 isoprene units, 10 carbon atoms, sesquiterpenes: 3 isoprene units, 15 carbon atoms, diterpenes: 4 isoprene units, 20 carbon atoms, triterpenes: 6 isoprene units, 30 carbon atoms, tetraterpenes: 8 isoprene units, 40 carbon atoms (Taofiq, Martins, et al., 2016). Some common terpenoids and their derivatives (**Figure 9**) found in mushrooms include pleurospiroketal (*Pleurotus cornucopiae*), enokipodin J, 2,5-

cuparadiene-1,4-dione, flammulinolide, enokipodin (*F. velutipes*), eryngiolide A (*Pleurotus eryngii*), erinacine A (*Hericium erinaceum*), tricholomalide A-C (*Tricholoma sp.*) and ganoderic acid, elfvingic acid A, ganoderenic acid (*G. lucidum*) (Rathore, Prasad, & Sharma, 2017). These compounds have well recognized medicinal properties namely cytotoxic, antioxidant, anti-inflammatory and antimicrobial properties and are considered suitable in maintaining the overall wellbeing of the body (Ma, Chen, Dong, & Lu, 2013; Van Nguyen et al., 2015). The fruiting body of mushrooms, either in their fresh or processed forms, are also rich in sterols, mainly ergosterol, a form that can be converted into vitamin D2 by UV-radiation. This conversion occurs due to series of ring rearrangement forming previtamin D and, lastly, the active form of Vitamin D2 (Slawinska et al., 2016). Among others, vitamin D has an impact on bone and muscle health, cancer, cardiovascular diseases, liver function, atopic dermatitis, obesity, depression, and diabetes. The amount of vitamin D varies among mushroom species, and within the same species. Among them, mushrooms belonging to the genera *Agaricus*, *Lentiula* and *Pleurotus* have been reported to contain interesting amounts of vitamin D after exposure to UV (Edward et al., 2015; Jasinghe & Perera, 2006; Slawinska et al., 2016). Ergosterol has been reported to play several biological functions such as cytotoxic, antioxidant, anti-inflammatory and immunomodulatory functions (Duarte, Ferreira1, Martins, Viveiros, & Amaral, 2007; Shimizu et al., 2016).
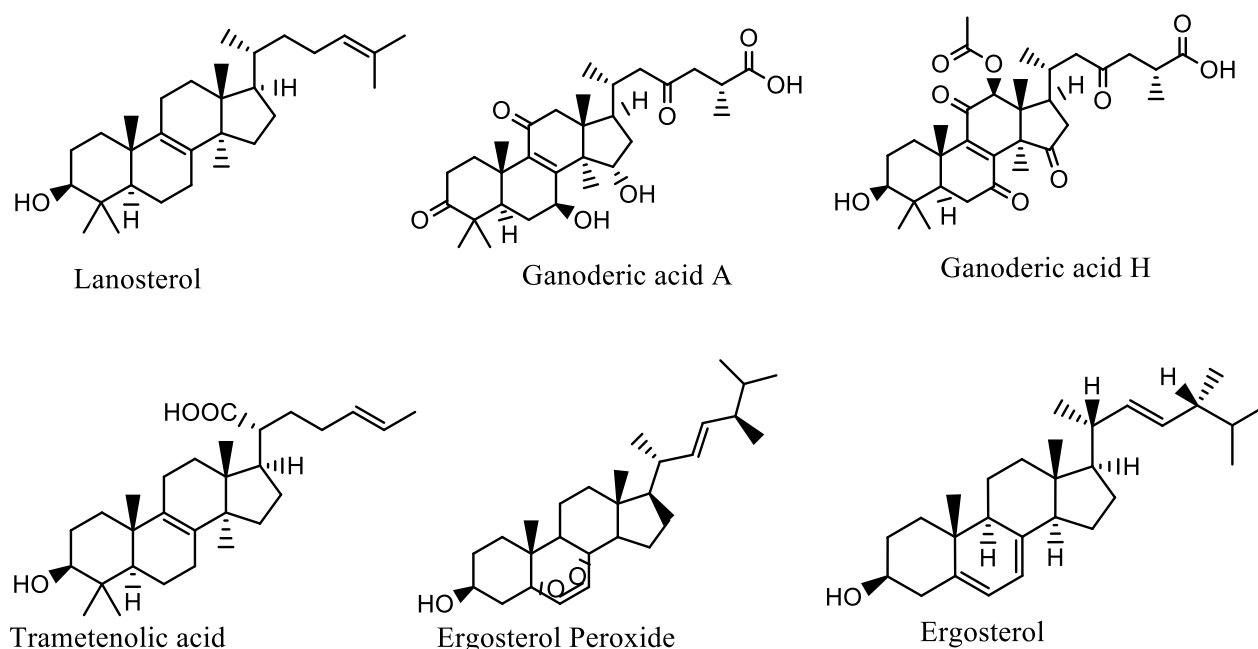
Figure 9. Common terpenoids and steroidal compounds in mushroom.

1.3.2.4. Other bioactive metabolites

While the above-mentioned bioactive compounds are the most abundant, other compounds have also been identified in different mushroom extracts. Bioactive metabolites such as organic acids, fatty acids, succinic and maleic derivatives, adenosine, cordycepin, and glycopeptides (**Figure 10**) have been reported to display important beneficial health properties (Imamura et al., 2015; Tuli, Sharma, Sandhu, & Kashyap, 2013). Lectins are glycoproteins reported to show physiological activity in the gastrointestinal tract (GIT) by enhancing nutrient absorption, inhibiting enzymes, and modulating the immune system to defend against foreign pathogens (Rathore et al., 2017). Cordycepin, an adenosine analog, initially extracted from the fungus *Cordyceps militaris* and *Cordyceps sinensis* can be utilised for several preliminary studies. This compound has been reported to suppress lung infections, display hypoglycaemic activity, act as an antidepressant and suppress the severity of inflammation (Choi, Kim, & Lee, 2014; Jeong et al., 2010; Rathore et al., 2017).
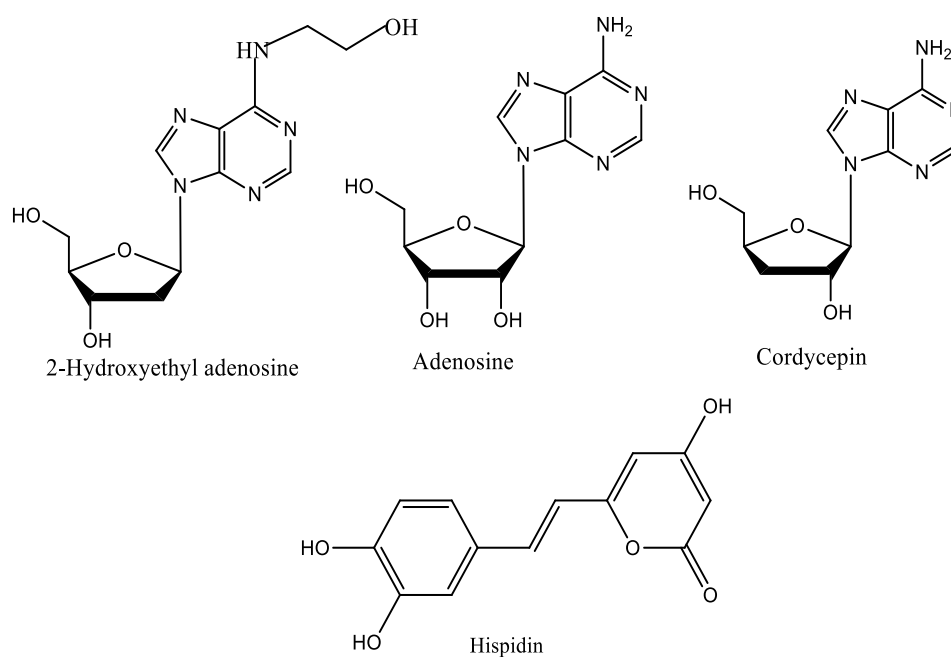
Figure 10. Other bioactive metabolites found in mushrooms.

1.4. The case of mushroom extracts and their individual metabolites as cosmeceutical ingredients

Mushroom extract and their individual metabolites are slowly gaining attention as cosmeceutical ingredients because of the numerous beneficial effect they exert to the skin (Wu, Choi, Li, Yang, & Shin, 2016). The compounds that they contain show excellent antioxidant, anti-ageing, anti-inflammatory and moisturizing effects, which make them ideal ingredients in the development of cosmeceutical and nutricosmetic formulations (Ferreira et al., 2015; Hyde et al., 2010; Taofiq et al., 2015). Despite this, only a small percentage of mushroom species and their individual metabolites have been explored for cosmeceutical purposes. A detailed description of species that have been fully explored scientifically with their active ingredient identified; types of bioactive properties associated with the mushroom extracts and their metabolites in relation to skin care; pharmacological activity of mushroom extracts and the bioactive compounds for skin care; mushroom ingredients that have successfully penetrated the *stratum corneum* with specific biochemical mechanism of action and proven safety in epidermal and dermal cells; and future trends and challenges in their use as cosmeceutical and nutricosmetic ingredients will be discussed below.

1.4.1. Anti-tyrosinase activity of mushroom extracts and their associated metabolites

Melanin is a natural pigment produced by specialized cells called melanocyte, responsible for the skin colour. Tyrosinase is the rate-limiting enzyme in melanin biosynthesis pathway, where it converts tyrosine to dihydroxyphenylalanine (DOPA) and then oxidizes it to dopaquinone (Meng, 2012). Subsequently, dopaquinone is converted to dopachrome through auto-oxidation, and finally to eumelanin (brown-black pigment) in the presence of dopachrome tautomerase (**Figure 11**). Alternatively, dopaquinone can also be converted to cysteinyl DOPA in the presence of cysteine or glutathione to form pheomelanin (yellow-red pigment). The synthesis of melanin is regulated by several signal transducers responsible for regulating the expression of tyrosinase and tyrosinase-related protein (TRP1 and TRP2), which in turn promotes the expression of microphthalmia-associated transcription factor (MITF) a melanocyte-specific transcription factor that is responsible for differentiation of melanocytes (Jang et al., 2017). Hence, most tyrosinase inhibiting compounds tend to target down-regulation of MITF

expression, inhibiting the whole process of melanogenesis (Działo et al., 2016). Melanin biosynthesis is initiated by several hormonal and chemical mediators and the most common is the cAMP-mediated pathway. The cAMP is known to increase the expression of MITF via activation of the cAMP-dependent protein kinase A (PKA) and the cAMP-response element binding protein (CREB) transcription factor (Park, Jin, Kim, Kim, & Lee, 2011). The complex process of melanogenesis is regulated by MITF through binding to the promoter region of TRP-1, and TRP-2 thereby causing increase expression of tyrosinase enzyme responsible for melanin biosynthesis (Meng, 2012). Hence, compounds that tend to cause inhibition of MITF expression will be an inhibitor to the whole process of melanogenesis. Hyperpigmentation disorders, the result of increase melanin biosynthesis are unfavourable abnormalities usually characterized by darker skin appearance, light to dark brown spots, irregular grey patches on the face, neck, and trunk, and pale brown to dark brown spots on the skin, motivating researchers to find new ingredients or combinations of ingredients; among them the ones of natural origin can be effective solutions (Ali, Choudhary, Naaz, & S Ali, 2015).
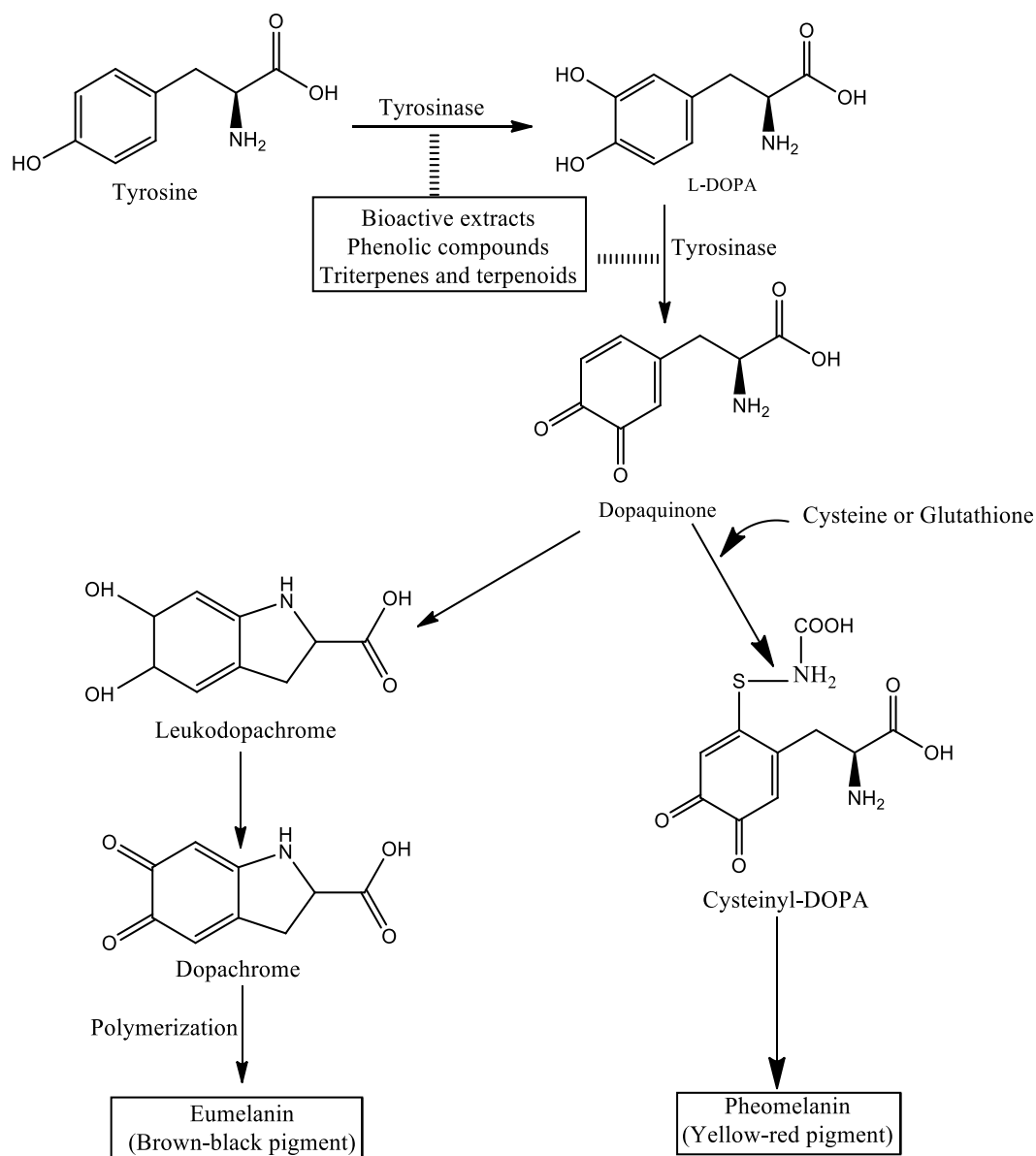
Figure 11. The melanin biosynthesis pathway.

The mechanism of depigmentation involves the inhibition of one or more steps in the melanogenic pathway or melanosome transfer resulting in lower melanin release and finally combating melanogenesis (Ali et al., 2015). Studies conducted have shown that bioactive compounds obtained from natural sources have the potential to suppress melanin synthesis and correct hyperpigmentation (Agrawal et al., 2018; Hapsari, Elya, & Amin, 2012; Maack & Pegard, 2016; Sanjeewa, Kim, Son, & Jeon, 2016). The most widely found compounds in formulations used to correct hyperpigmentation include hydroquinone, mequinol, retinoic acid, azelaic acid and arbutin/deoxyarbutin among others (Ali et al., 2015). The mechanism behind

their hyperpigmentation correcting effect include tyrosinase enzyme inhibition, melanosome transfer inhibition, increased epidermal turnover, antioxidation, melanosome maturation inhibition, inhibition of UV-induced plasmin activity in keratinocytes and direct destruction of melanin (Chaowattanapanit et al., 2017). Some of the above-mentioned compounds used to treat hyperpigmentation over the years have raised safety concerns, namely the reported carcinogenic potential, exogenous ochronotic effect, cell irritants and exudation of offensive fish odour from the skin (Tse, 2010). Others consider the use of corticosteroids and kojic acid that, nevertheless their high effectiveness, have been reported to cause a local or systemic negative effect upon long term exposure (Ali et al., 2015). Because of the negative effect associated with the above depigmenting agents, the search for alternative natural products rich in bioactive molecules with the ability to treat these disorders, such as the ones obtained from plants, mushrooms, rhizomes or marine algae, have become important fields of research. Several compounds especially phenolics such as arbutin, resveratrol, ellagic acid, and gentisic acid have been isolated from plants and reported to inhibit one or more steps in the melanogenic pathway (Ali et al., 2015). These phytochemicals do not only combat melanogenesis but also play additional functions such as acting as moisturizers, provide support and stability to the skin and have anti-ageing effect, thereby preserving the skin health (Działo et al., 2016; Svobodová, Psotová, & Walterová, 2003). Studies reporting the anti-tyrosinase inhibitory activity of mushroom extracts and individual bioactive metabolites are described in **Table 1**.

Pleurotus species are among the most exploited mushroom species presenting an anti-tyrosinase potential. Meng et al. (2011) reported that treatment of B16 melanoma cells with various fractions of *P. citrinopileatus* were able to inhibit tyrosinase activity up to 40% without any cytotoxic effect on the cells, while acetonic, methanolic, and hot water extracts prepared from the fruiting bodies of *P. ferulae* (0.125–1.0 mg/mL), were reported by Alam et al. (2012) to inhibit tyrosinase activity up to 60.10%. Similar tyrosinase activity was reported for *P. nebrodensis* with the most potent inhibition obtained for its methanolic extract (up to 50%) (Nuhu, Ki, & Tae, 2011). *P. ostreatus* being one of the most extensively studied mushroom has also shown anti-tyrosinase activity; ethanolic and aqueous extracts (EC_{50} 1.13 and 2.35 mg/mL respectively) (Hapsari et al., 2012). However, none of these studies have been able to identify the most important compounds contributing to these tyrosinase inhibition activities or further determine the mechanism behind the anti-tyrosinase activity of these extracts. Extract from *Inonotus obliquus* presented tyrosinase repression, predominantly due to the contribution

of betulin (5.13 μM) and trametenolic acid (7.25 μM) displaying an activity that is comparable to kojic acid (6.43 μM) (Yan et al., 2014).

A potent suppressive impact on tyrosinase was also shown by Miyake et al. (2010). The authors reported that 2-amino-3*H*-phenoxazin-3-one (APO), a phenoxazinone isolated from extracts of *A. bisporus* showed melanin inhibitory activity. After exposure of murine B16 melanoma cells to the isolated compound, cell viability was not suppressed, while melanin accumulation was significantly inhibited up to 80%. To determine the mechanism behind inhibition of the melanogenesis process, MITF expression was monitored in a dose-dependent manner with APO showing a significant decrease in its expression without affecting TRP-2 and TRP-1 proteins. Hu et al., (2017) studied the tyrosinase inhibition effects of a triterpene rich extract obtained from *Poria cocos*, and poricoic acid A (PAA) isolated from its fruiting body, in B16F1 melanoma cells. PAA had the best inhibitory effect up to 45.24% when its concentration reached 166.67 μg/mL. Different volatile constituents were obtained from *Tricholoma magnivelare* (Peck) Redhead, and their tyrosinase inhibitory activities in B16-F10 mouse melanoma cells were as follows α-pinene (40%), 3,5-dichloro-4-methoxybenzaldehyde (37%) and methyl cinnamate (24.2%) (Satooka, Cerda, Kim, Wood, & Kubo, 2017). However, the authors found enhanced cytotoxicity in the first two tested compounds making methyl cinnamate a novel potential melanogenesis inhibitor.

The search for tyrosinase inhibiting compounds have been conducted in different mushroom species, however, phenolic compounds have been well reported as being the most important contributors to this phenomenon (Yoon, Atom, Lee, Lee, & Lee, 2011). In what concerns *p*-coumaric acid as a tyrosinase inhibitor, interesting studies have been reported when compared to other phenolic acids (An, Koh, & Boo, 2010; Jun et al., 2012). Seo et al., (2011) reported the effects of a formulation containing *p*-coumaric acid on UV induced erythema and hyperpigmentation in human skin. The formulation was applied on volunteers twice daily for seven days. Afterward, the site of application was monitored, and the result showed that there was suppression of erythema formation up to 77% and subsequent skin pigmentation was also reduced. Recent studies reported that phenolic acids such as caffeic acid (IC_{50}, 43.09 ± 2.3 μM) and ferulic acid (IC_{50}, 51.85 ± 1.7 μM) (Chaiprasongsuk, Onkoksoong, Pluemsamran, Limsaengurai, & Panich, 2016; Thangboonjit, Limsaeng-u-rai, & Panich, 2014) exhibit melanin biosynthesis inhibition.

Cinnamic acid is one of the most common phenolic acid derivatives found in mushrooms. Because of their relative hydrophilicity, which hinders its absorption on the skin. Ullah et al. (2019) synthesized fifteen amide derivatives and evaluated their tyrosinase inhibition potential in B16F10 melanoma cells. At 25 µM, the cell viability was maintained, and four of the compounds were able to exhibit strong inhibition of tyrosinase, which was found to be three-fold greater than kojic acid. Also, four synthesized nicotinic acid derivatives, namely, nicotinamide, methyl nicotinate, nicotinic acid hydroxamate (NAH), and N-methyl nicotinic acid hydroxamate (NAH-M), were studied by Lin et al. (2012). The tyrosinase inhibitory activity was found to follow the following order: NAH > NAH-M > methyl nicotinate > nicotinamide. These results showed that nicotinamides, the water-soluble amide of nicotinic acid, a component of the two most important coenzymes (nicotinamide adenine dinucleotide (NAD) and nicotinamide adenine dinucleotide phosphate (NADP)) can be used in cosmetic products to suppress melanogenesis coupled with their potential as antioxidant and anti-inflammatory agents (Otte, Borelli, & Korting, 2005).

Chlorogenic acid (CGA) is another interesting phenolic acid with an anti-tyrosinase capacity. B16 melanoma cells exposed to chlorogenic acid were found to sustain their cell viability up to 80% and at 500 µM, tyrosinase activity was reduced significantly (Li, Habasi, Xie, & Aisa, 2014). In the work conducted by Kwak et al. (2015), two hybrid compounds, ascorbyl-3-*p*-coumarate, and ascorbyl-2-*p*-coumarate (A-3-*p*-C and A-2-*p*-C) were generated from *p*-coumaric acid and ascorbic acid. Both compounds were found not to reduce cell viability of murine melanoma B16/F10 cells and at 100 µM, they decreased melanin content up to 65 and 59% for A-3-*p*-C and A-2-*p*-C respectively. It is interesting to note that these bioactive compounds, when utilised in cosmetic formulations, do not only combat melanogenesis, but can also cause skin cell revival, stimulate collagen and elastin synthesis and slow down the ageing process. These additional functions tend to further provide support and stability to the skin. One major drawback in the use of these compounds especially the phenolic compounds is their sensitivity to oxidation thus contributing to their instability in cosmetic formulations.

Table 1. Previous studies on the anti-tyrosinase activity of different mushroom species and their individual metabolites

Mushroom species	Pharmaceutical form	Effects	Reference
A. bisporus	2-Amino-3*H*-phenoxazin-3-one	At 0.5 µM, 1 µM and 2 µM, melanin production was inhibited by 80%, 54.1% and 39.4%, respectively.	(Miyake et al., 2010)
Agaricus brasiliensis Fr.	Methanolic extract	Methanolic extract at 10 mg/mL inhibited tyrosinase activity up to 49.82±0.51% relative to 48.95±0.35% for kojic acid.	(H. Huang et al., 2014)
Coriolus versicolour (L.: Fr.) Quél.	Ethanolic extract	At 10 mg/mL, tyrosinase activity was inhibited up to 26.3±8.3%.	(K. M. Park, Kwon, & Lee, 2015)
Ganoderma lucidum (Curtis) P. Karst.	Ethanolic extract	At 1 mg/mL, the extract inhibited tyrosinase activity up to 80%.	(C. C. Chien et al. 2008)
Grifola frondosa (Dicks.) Gray	Mycelia extract (GF-M), Exopolysaccharide (EPS)	At 100 µg/mL, EPS and GFM inhibited melanogenesis by 25 and 17% respectively.	(S. W. Kim et al. 2007)
Inonotus mikadoi (Lloyd) Gilb. & Ryvarden	Extracts	At 10 mg/mL, it showed tyrosinase inhibitory activity up to $46.0 \pm 7.5\%$.	(K. M. Park et al., 2015)
Inonotus obliquus (Ach. Ex. Pers.) Pilát	Extracts	At 10 μg/mL, petroleum ether and n-butanol extract showed tyrosinase inhibitory activity with IC_{50} value of 3.81 and 6.32 μg/mL respectively.	(Yan et al., 2014)
	Betulin and trametenolic acid	Betulin tyrosinase activity showed an IC_{50} of 5.13 μM, trametenolic acid 7.25 μM while kojic acid (6.43 μM) was used as a control.	(Yan et al., 2014)
Lentinus lepideus (Fr.) Redhead & Ginns	Extracts	Acetonic, methanolic, and hot water extracts at 0.125–1.0 mg/mL inhibited tyrosinase enzyme by 9.71–58.84, 11.23–56.22 and6.97–51.52% respectively.	(K. N. Yoon et al., 2011)
Metarhizium anisopliae (Metschn.) Sorokīn	2-Hydroxytyrosol (2-HT)	2-HT inhibited tyrosinase activity with an IC_{50} value of 13.0 mmol/L compared to 14.8 mmol/L for kojic acid.	(R. Uchida, Ishikawa, & Tomoda, 2014)
Pleurotus citrinopileatus Singe*r*	Extracts	At 100 µg/mL, *n*-butanol soluble, *n*-hexane soluble and ethyl acetate soluble extract caused 41.0, 27.4 and 28.8% tyrosinase inhibition respectively.	(T. X. Meng et al., 2011)

Pleurotus ferulae (Lanzi) X.L. Mao	Extracts	At 0.125–1.0 mg/mL, acetonic, methanolic, and hot water extracts inhibited tyrosinase enzyme by 19.81–60.10%, 13.12–59.87% and 15.92–55.07% respectively.	(Alam et al., 2012)
Pleurotus nebrodensis (Inzenga) Quél.	Extracts	At 0.125-1.0 mg/mL, acetonic, methanolic and hot water extracts showed 2.57-55.76, 11.54-51.54 and 6.52-50.96% tyrosinase inhibition activity respectively.	(Nuhu et al., 2011)
Pleurotus ostreatus (Jacq. ex Fr.) P. Kumm.	Extracts	At 0.125-1.0 mg/mL, acetone, methanol, and hot water extracts inhibited tyrosinase activity by 11.37-52.05%, 11.36-59.56%, and 9.60-49.60% respectively.	(Alam et al., 2010)
	Extracts	Ethanolic and aqueous extracts inhibited tyrosinase activity with an EC_{50} value of 1.125 mg/mL and 2.350 mg/mL respectively.	(Hapsari et al., 2012)
Poria cocos F.A. Wolf	Poricoic acid A	At 166.67 µg/mL, tyrosinase activity was inhibited up to 45.24%, with no reduction in cell viability of B16F1 melanoma cells.	(S. Hu et al., 2017)
Rugiboletus extremiorientalis (Lj.N. Vassiljeva)	Methanolic extract	The tyrosinase inhibition was inhibited up to 50% at 0.17 mg KAE/g DW.	(Kaewnarin, Suwannarach, Kumla, & Lumyong, 2016)
Russula emetica (Schaeff.) Pers.	Methanolic extract	The tyrosinase inhibition was inhibited up to 50% at 0.066 KAE/g DW.	(Kaewnarin et al., 2016)
Tricholoma magnivelare (Peck) Redhead	Methyl cinnamate	Tyrosinase was inhibited up to 24.2% in B16-F10 mouse melanoma cells without presenting cytotoxicity.	(Satooka et al., 2017)
Bioactive compounds	**Type**	**Bioactive Effects**	**Reference**
Ascorbyl-3-*p*-coumarate (A-3-*p*-C), Ascorbyl-2-*p*-coumarate (A-2-*p*-C)	Synthesized	A-3-*p*-C and A-2-*p*-C at 1.0 mM were found to be nontoxic to murine melanoma B16/F10 cells and at 100 µM, both hybrid compounds decreased melanin content by 65 and 59%, respectively.	(Kwak et al., 2015)
Caffeic acid	Commercial	At 43.09 ± 2.3 µM, UVA-mediated increased melanogenesis in G361 melanoma cells was suppressed.	(Thangboonjit et al., 2014)
	Commercial	The test compound inhibited UVA-induced melanin content, as well as tyrosinase activity in B16F10 mouse melanoma cells presenting IC_{30} (µM), values of 17.54±4.8 and 24.1±6.2 respectively.	(Chaiprasongsuk, et al 2016)
Chlorogenic acid	Commercial	At 100 µM, cell viability of B16 melanoma cells were maintained and at 500 µM after 48-h exposure to B16 melanoma cells, melanin levels were suppressed.	(H. R. Li et al., 2014)

Cinnamic amides	Synthesized	At 25 μM, four cinnamic amide derivatives maintained B16F10 melanoma cell viability and significantly inhibited tyrosinase activity.	(Ullah et al., 2019)
2-chlorcinnamic and 2,4-dichlorocinnamic acid	Synthesized	Tyrosinase was inhibited up to 50% at 0.765 mM and 0.295 mM, for 2-chlorcinnamic acid and 2,4-dichlorocinnamic acid respectively.	(Y. H. Hu et al., 2014)
Ferulic acid	Commercial	At 51.85 ± 1.7 μM, UVA-mediated increased melanogenesis in G361 melanoma cells was suppressed.	(Thangboonjit et al., 2014)
	Commercial	At 30 μM, ferulic acid was not able to suppress UVA-induced melanin content and tyrosinase activity in B16F10 mouse melanoma cells.	(Chaiprasongsuk et al., 2016)
Gallic acid	Commercial	Gallic acid at 12.5-100 μM was able to maintain cell viability of B16 melanoma cells, suppressed melanin content and tyrosinase activity with IC_{50} values of 18.3 μM and 24.8 μM respectively.	(Kumar et al., 2013)
	Commercial	At 200 μM maintained cell viability of B16F10 melanoma cells and reduces melanin synthesis via down-regulation of MITF, CREB, tyrosinase and TRP-1 expression.	(Su et al., 2013)
Gallic acid	Commercial	At 200 μM inhibited tyrosinase activity up to 85% and suppress melanin content in B16 melanoma cells.	(Y.-J. Kim, 2007)
Hispolon	Commercial	Test compound at 2 μM was able to suppress the expression of tyrosinase and MITF and subsequent reduction in melanin production up to 58.9-61.7%.	(Y. S. Chen, Lee, Lin, & Liu, 2014)
p-Coumaric acid	Commercial	At 10 μg/mL showed a higher tyrosinase activity inhibition than arbutin, but comparable to kojic acid.	(An et al., 2010)
	Commercial	Reduced MITF and tyrosinase mRNA expression by 73 and 82%, respectively.	(Jun et al., 2012)
	Commercial	Inhibited hyperpigmentation up to 77% in human skin.	(Seo et al., 2011)
	Commercial	At 22.86 ± 2.1 μM, UVA-mediated increased melanogenesis in G361 melanoma cells was suppressed.	(Thangboonjit et al., 2014)
p-Coumaric acid, methyl p-coumarate	Synthesized	Inhibited tyrosinase activity with an IC_{50} of 3 mM compared to methyl p-coumarate IC_{50} 30 mM.	(Song, An, Kim, Koh, & Boo, 2011)
Vanillin and vanillin derivatives	Synthesized	Cell viability in fibroblast (L929) and keratinocyte (HaCaT) cell lines were maintained in a dose-dependent manner. Compound A, B, and C displayed tyrosinase inhibin with IC_{50}, 21.60 μM, 16.13 μM and 30.85 μM comparable to kojic acid 16.69 μM.	(Ashraf, Rafiq, Seo, Babar, & Zaidi, 2015)

1.4.2. Anti-inflammatory activity of mushroom extracts and their associated metabolites

Inflammation is one of the most important biological responses to remove harmful toxins or pathogens from the body (Bellik et al., 2013). Macrophages are large specialized cells that are the first line of defense against invading pathogens (cellular debris, microbes, and cancer cells), by engulfing and digesting in a process called phagocytosis (Francisco et al., 2013). They play important roles in non-specific host defense mechanism and help to initiate other defense mechanisms. Beyond stimulating the immune system, macrophages play a crucial role in the inflammatory response through the release of a variety of factors. During inflammation, macrophages, monocytes and other inflammatory cells secrete excess inflammatory mediators, among them nitric oxide (NO). Production of these mediators in inflammatory cells increases following exposure to immune stimulants including bacterial endotoxin lipopolysaccharide (LPS) or viral proteins (Hseu et al., 2005). This bacteria component initiates several signal transduction pathways that are central to the pathogenesis of inflammation (Jeong et al., 2010).

NO is a short-lived free radical and a signaling molecule produced from L-arginine by the inducible nitric oxide synthase (iNOS) enzyme (Castro et al., 2014; Hämäläinen, Nieminen, Vuorela, Heinonen, & Moilanen, 2007). NO, known to induce vasodilation in the cardiovascular system through a Ca^{2+}-dependent pathway, play an important function in the immune and nervous systems as well as in cell death (Hseu et al., 2005; Sharma, Al-Omran, & Parvathy, 2007). It gives an anti-inflammatory effect under normal physiological conditions, is also involved in many pathological diseases in the body (Cirino, Distrutti, & Wallace, 2006; Joo et al., 2014). Reactive oxygen species (ROS) production play an important role in the modulation of inflammation. Major ROS produced within the cell are superoxide anion (O_2^-), hydrogen peroxide (H_2O_2), peroxide anion (O_2^{2-}), hydroxyl ion (OH^-) and hydroxyl radical ($^\cdot OH$). Nitric oxide is less reactive but can attack superoxide ion (O_2^-) to form peroxynitrite $ONOO^-$ (Castro et al., 2014). This peroxynitrite and several oxidative products can accumulate in the cells causing oxidative damages and increased cytotoxicity leading to tumor development, DNA damage and cell proliferation (Fangkrathok, Junlatat, & Sripanidkulchai, 2013; Quang, Harinantenaina, et al., 2006). The inhibition of NO and other inflammatory mediator's overproduction in cells may prevent the occurrence of inflammatory diseases and cancer.

Another class of important pro-inflammatory mediator is the tumor necrosis factor-α (TNF-α) secreted by activated macrophages, T-lymphocytes, mast cells, natural killer cells, monocytes and other defense cells (Habtemariam, 2013). TNF-α is one of the important pro-inflammatory mediators involved in the inflammatory process. When there is an immune stimulant, TNF-α attaches to some specific transmembrane receptors that tend to activate several signal transduction pathways responsible for the production of more TNF-α to the site of infection (Siqian Li & Shah, 2016). As TNF-α continues to accumulate, it causes a wide range of human diseases, apoptosis, excess pain, and cell damage. Regulation of the transcription factor NF-κB is the key component of TNF-α regulation (Habtemariam, 2013). The inhibition of TNF-α in LPS activated THP-1 monocytic cells, or RAW 264.7 macrophage cells, is generally used as *in vitro* models for evaluating the anti-inflammatory effects of various materials including mushroom extracts (S.-J. Wu, Lu, Lai, & Ng, 2013). Some of the studied mushrooms whose mechanism of action is the inhibition of TNF-α release are described in **Table 2**.

NF-κB is a transcription factor that regulates the expression of several pro-inflammatory cytokines and enzymes such as IL-1β, TNF-α, iNOS, and COX-2 that play vital roles in apoptosis, immunity, and inflammation (Hseu, Huang, & Hsiang, 2010). When there is an immune stimulant (i.e lipopolysaccharide, viral proteins or cytokines), the NF-κB becomes activated (K. M. Kim et al., 2003). Toll-like receptors (TLRs) and tumor necrosis factor receptor (TNFr) localized in the macrophages membrane can detect these pathogen-associated molecular patterns (PAMPs) necessary for activation of several signaling cascade (**Figure 12**). After ligand binding, these receptors activate the myeloid differentiation protein 88 (MyD88) responsible for the activation of mitogen-activated protein kinase (MAPKs). This MAPKs further activate the IKK kinases (IKKα, IKKβ, IKKγ) leading to phosphorylation of the IκB proteins complex (Hasnat, Pervin, Cha, Kim, & Lim, 2015). Cytosolic IκB forms a complex with NF-κB and the IκB proteins become degraded allowing NF-κB to translocate to the nucleus where it triggers the transcription of several chemokines and cytokine genes involved in the innate and adaptive immune response (K. M. Kim et al., 2003). Some polyphenols have been known to inhibit specific steps in the pathway leading to NF-κB release (Ruiz & Haller, 2006). These authors investigated the anti-inflammatory mechanism of flavonoids that were able to inhibit the phosphorylation of IκB preventing translocation of NF-κB to the nucleus. Hence, finding natural inhibitors of NF-κB for treatment and prevention of various inflammatory diseases have been the target of several scientists.
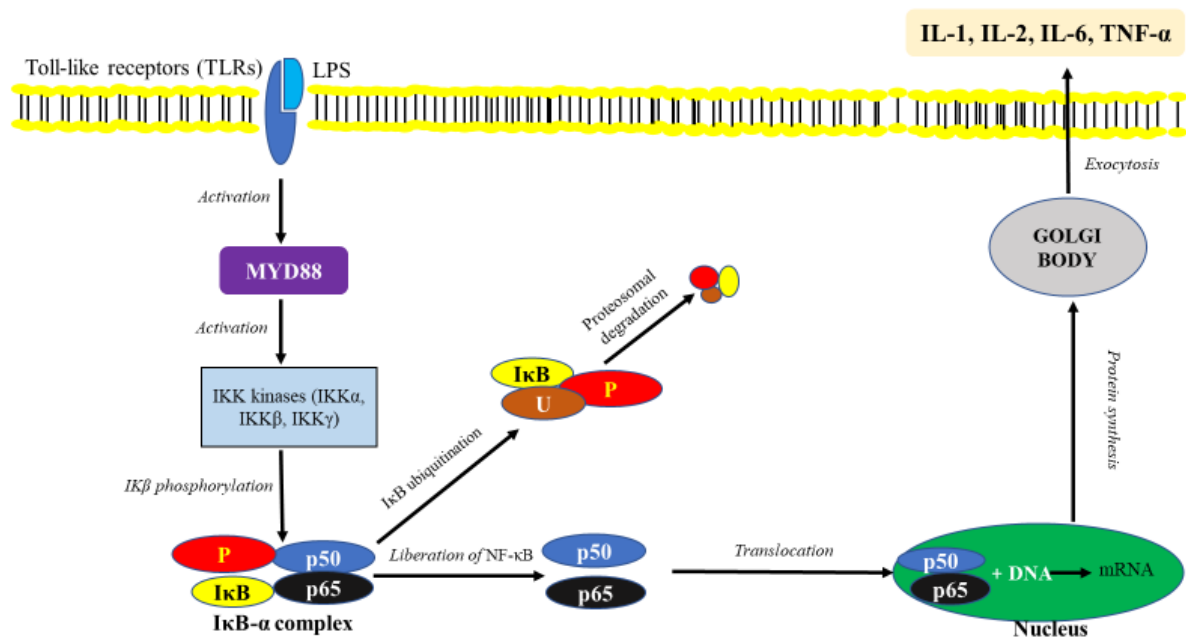
Figure 12. Schematic diagram of nuclear factor-κB (NF-κB) pathway. Macrophage cells express membrane receptors such as toll-like receptors (TLRs) and tumor necrosis factor receptors (TNFR). These receptors recognize pro-inflammatory stimuli such as lipopolysaccharides and viral proteins. Attachment of these pathogen-associated molecular patterns (PAMPs) to membrane receptors activates the myeloid differentiation protein 88 (MyD88). MyD88 activates specific protein kinases that are responsible for activation of IKK kinase (IKKα, IKKβ, IKKγ). This kinase further phosphorylates IκB-α complex leading to dissociation of the complex, and its proteasomal degradation, allowing NF-κB to translocate to the nucleus, where it binds to specific DNA sequences encoding the pro-inflammatory cytokines (e.g., IL-1, IL-2, IL-6, TNF-α as well as cyclooxygenase-2 (Cox-2) and inducible nitric oxide synthase (iNOS).

The nonsteroidal anti-inflammatory drugs (NSAIDs) are a group of medications commonly administered to manage pain and inflammation (Moro et al., 2012). Most of them are available over the counter in the United States while the rest needs a prescription (Meek, van de Laar, & Vonkeman, 2010). Several side effects have been associated with frequent administration of NSAIDs particularly in the GIT where they cause bleeding, intestinal perforation and peptic ulcer. Other less pronounce side effects include renal dysfunction, high blood pressure and cardiovascular toxicity (Elsayed, El Enshasy, Wadaan, & Aziz, 2014). NSAIDs act by inhibiting the intracellular cyclo-oxygenase enzymes which have two isoforms (COX-1 and COX-2). Cyclooxygenases are enzymes involved in the process of inflammation. They catalyze the rate-limiting step in the biosynthesis of prostaglandins, prostacyclin's, and thromboxane's from arachidonic acid (Diyabalanage, Mulabagal, Mills, DeWitt, & Nair, 2008; Noreen, Ringbom, Perera, Danielson, & Bohlin, 1998; Stanikunaite, Khan, Trappe, & Ross, 2009). Prostaglandins (PG) are hormone-like chemicals in the body that perform ''housekeeping'' functions required for normal physiological activities. They are structurally related and have

regulatory roles as well as a pathological implication (Silveira et al., 2014). Cyclooxygenase enzymes catalyze the conversion of arachidonic acid to PGH2, which is converted to other prostanoid species including PGD2, PGE2, prostacyclin (PGI2), and thromboxane (TXA2) by the action of specific synthases (**Figure 13**) (M. Joo & Sadikot, 2012). COX-1 is primarily involved in the regulation of homeostatic functions and is constitutively expressed in a wide variety of cells, promoting physiological functions, such as gastric mucosal protection, control of renal blood flow, hemostasis, autoimmune responses, lungs, central nervous system, cardiovascular system and reproductive functions (Grosser, Fries, & FitzGerald, 2006). On the other hand, COX-2 is an inducible isoform of prostaglandin synthase in activated macrophages, fibroblasts, and endothelial cells that are responsible for inflammation. They are expressed significantly due to stimuli such as cytokines, endotoxins, viral proteins, and growth factors. COX-2 originates inducing prostaglandins, which contributes to the development of the four cardinal signs of inflammation: pain, heat, redness, and swelling, thus being considered as the main target for the anti-inflammatory action (FitzGerald, 2004). The search for selective inhibitors of COX-2 is considered important, based on the theory that the side effects, such as gastric lesions, that occurred from inhibition of COX-1 activity, were observed with some non-selective nonsteroidal anti-inflammatory drugs (NSAIDs) such as dexamethasone, diclofenac, and indomethacin (Lu et al., 2013). Until now, very few compounds of natural origin have been reported to possess COX-2 inhibitory effects. (Yoshikawa et al., 2005) were the first to report the potential of lanostane triterpenoids and their glycosides as selective inhibitors of the COX-2 enzyme.

Usually, NSAIDs inhibit both isoforms of the cyclooxygenase enzyme but the recently discovered selective COX-2 inhibitors are specific for the COX-2 isoform, thus exerting the anti-inflammatory property of COX-2 inhibition while theoretically evading the adverse effect associated with COX-1 isoform inhibition (Nowak, 2012). Considerable resources have thus been invested in the pharmaceutical industries for development and design of drugs that act through selective inhibition of COX-2 to control inflammation with improved tolerability, less adverse effects, and without affecting normal metabolic processes.
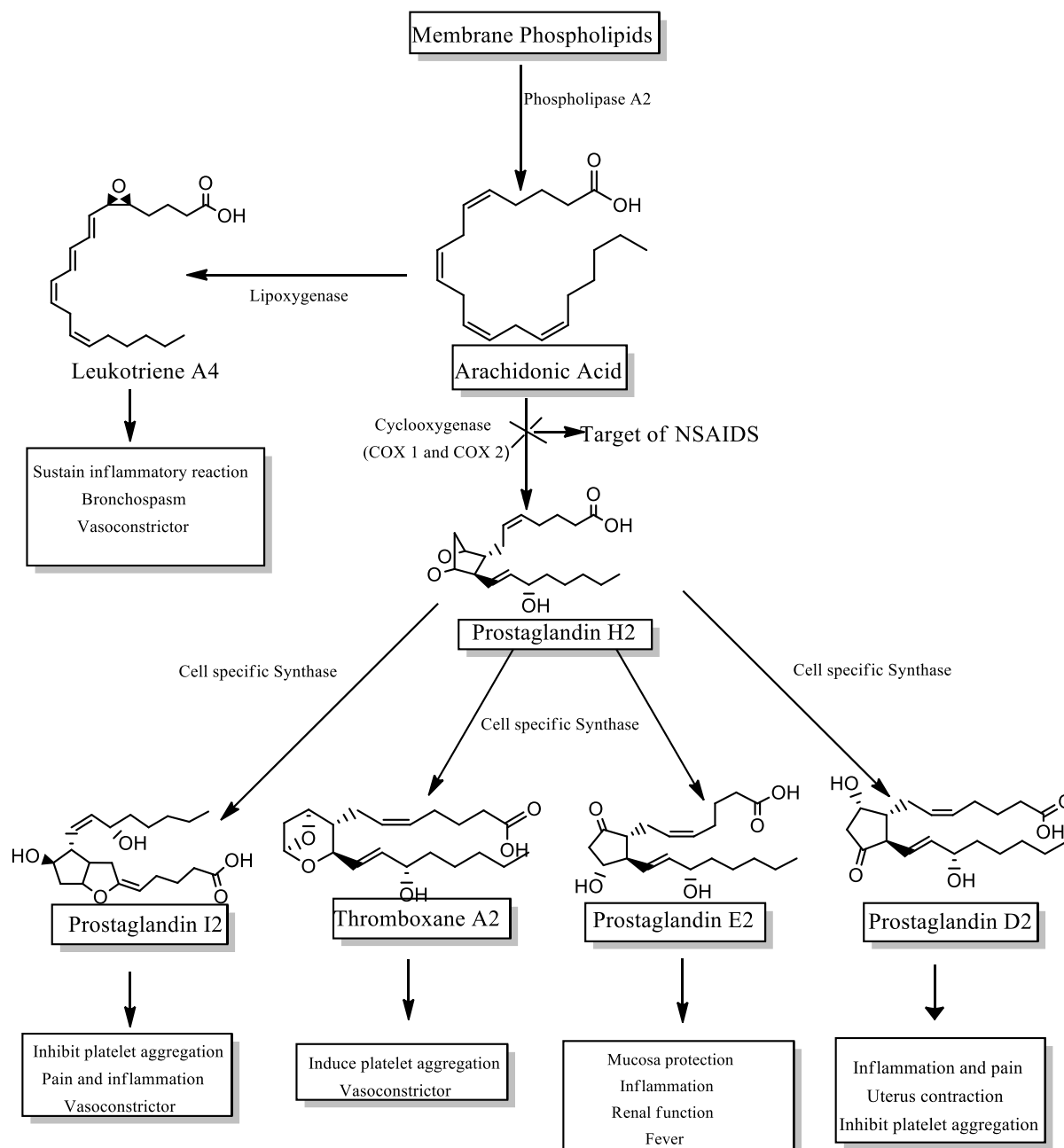
Figure 13. Schematic diagram of the biosynthetic pathway of common prostaglandins.

Numerous investigations have suggested that several mushroom species and their individual metabolites can exhibit anti-inflammatory potential based on their ability to reduce the production of inflammatory mediators. *Antrodia camphorata* (M. Zang & C.H. Su) Sheng H. Wu, Ryvarden & T.T. Chang also known as "Taiwanofungus *camphoratus*" is a well-known medicinal mushroom with a lot of pharmacological potentials (antioxidant, hepatoprotective, anti-inflammatory and immunomodulatory properties) (Geethangili & Tzeng, 2011). Hseu et

al., (2010) reported the anti-inflammatory effect of fermented culture broth of *A. camphorata* by measuring the level of pro-inflammatory cytokine IL-1β and TNF-α expression in different organs using ELISA kits. The extract was found to inhibit the LPS-induced production of cytokines and suppressed LPS-induced NF-κB activation in transgenic mice. The same researchers also studied fermentation culture of *A. camphorata* and examined its effect in LPS stimulated RAW 264.7 cells for NO, PGE2, iNOS and COX-2 protein expression. The results indicate inhibition of the production of TNF-α, IL-1β, NO and PGE2, as well as suppressing iNOS and COX-2 expression by blocking activation of NF-κB transcription factor. Gunawardena et al., (2014) studied the anti-inflammatory potential of five commercial mushroom species (*A. bisporus*, *A. bisporus* Portobello, *F. velutipe*, *L. edodes*, and *P. ostreatus*) in LPS activated RAW 264.7 macrophages cells for NO production and detection of TNF-α level using ELISA kit. Three mushroom species showed the highest activity with the result expressed in terms of IC_{50} for NO production and TNF-α release respectively: *P. ostreatus* (0.077 mg/mL and 0.035 mg/mL), *L. edodes* (0.027 mg/mL and 0.047 mg/mL) and *F. velutipes* (0.024 mg/mL and 0.099 mg/mL). Ethanolic extract of *G. lucidum* was studied for its anti-inflammatory potential by stimulating murine BV2 cell line with LPS, and the amount of NO, PGE2 and Cytokine (IL-1β and TNF-α) in culture supernatants quantified as reported by H. M. Yoon et al. (2013). Treatment of cell line with extract up to 1 mg/mL significantly repressed the production of NO due to the inhibition of iNOS mRNA protein expression. The amount of cytokine released was measured by ELISA and a significant reduction in the level of cytokines after treatment with extract was observed. Methanolic extract of *G. lucidum* was also evaluated by C. Chu, Ye, Wu, & Chiu, (2015), RAW 264.7 monocytic cells were stimulated with LPS and treated with extract at different concentrations. From the result, 100 mg/mL of extract significantly inhibited NO production in the culture medium up to 85%.

Moro et al. (2012) analysed six mushroom species from Spain (*Boletus edulis*, *Cantharellus cibarius*, *Craterellus cornucopioides*, *Lactarius deliciosus*, *A. Bisporus* and *P. ostreatus*) in what concerns the anti-inflammatory activity of their methanolic extracts through NO production in LPS stimulated RAW 264.7 cells. At 0.5 mg/mL, *A. bisporus*, *Cratarellus cornucopioides*, *C. cibarius* and *L. deliciosus* showed 35%, 65%, 80% and 40% of NO production inhibition, respectively. The release of TNF-α production was estimated by ELISA kits, but methanolic extracts showed no reduction of TNF-α production in the macrophages. Rao, Fang, & Tzeng, (2007), studied anti-inflammatory activity using methanolic extracts from the fruiting body of *Cordyceps sinensis* by stimulating macrophages cells with LPS and NO

production later quantified. The amount of TNF-α level and IL-12 were quantified by the ELISA test. From the results, 100 mg/mL of *C. sinensis* extract inhibited NO production by 70%. E. S. Han, Oh, & Park, (2011) also studied the anti-inflammatory effect of hot water extract of *Cordyceps militaris* (L.) Fr. *in vivo* by inducing inflammation in mice. The extracts were known to inhibit inflammation as well as iNOS and TNF-α expression in colon tissue of Dextran sulfate sodium (DSS) induced colitis and in LPS-stimulated RAW 264.7 cells. K. M. Kim et al. (2003) also described the anti-inflammatory activity of another *Cordyceps* species. Methanolic extracts of *Cordyceps pruinose* (L.) Fr. were tested *in vitro* for inhibition of pro-inflammatory cytokines production by using ELISA kit as well as NO production in LPS stimulated RAW 264.7 macrophages. The extracts suppressed gene expression of IL-1β, TNF-α, iNOS, and COX-2.

Silveira et al. (2014) isolated a 1,3 β-glucan from the fruiting body of *Pleurotus sajor-caju* and tested its anti-inflammatory effect in a monocytic cell line (THP-1) after LPS induction, for inhibition of proinflammatory genes production. Monocyte cells showed a significant decrease in TNF-α expression (61.8% inhibition) while IL-1β and COX-2 mRNAs were also significantly inhibited (37.0% and 63.6%, respectively). Silveira et al. (2015) isolated a mannogalactan from *P. sajor-caju* by submerged fermentation. The purified polysaccharide was chemically characterized, and its anti-inflammatory potential evaluated *in vivo* for reduction of carrageenan-induced paw edema in mice. The group treated with purified mannogalactan was able to reduce edema after 5-6 h of exposure to 1% carrageenan, with 69-71% edema reduction observed and was quite as effective as dexamethasone used as a control. Therefore, mushroom polysaccharides have shown to be lead compounds for the development of anti-inflammatory agents. Andrea C. Ruthes et al. (2013) isolated and purified a fucogalactan from *A. bisporus* fruiting bodies, and its anti-inflammatory effect was evaluated *in vivo* by formalin-induced pain in mice and detection of iNOS and COX-2 protein expression. Fucogalactan significantly decreased both iNOS and COX-2 expression by 53% and 54%, respectively, in relation to dexamethasone used as a control, which also affected both iNOS and COX-2 expression by 74.5% and 71.4%, respectively. The results showed significant inhibition of inflammatory pain and strongly confirm the anti-inflammatory potential of fucogalactan.

Table 2. Previous studies on anti-inflammatory activity of different mushroom extracts and their isolated metabolites

Mushroom species	Pharmaceutical form	Main Findings	Reference
Agaricus bisporus J.E.Lange	Methanolic extract	At 0.5 mg/mL, cell viability of RAW 264.7 macrophage cells was not inhibited and NO and TNF-α levels were reduced.	(Moro et al., 2012)
	Fucogalactan	Fucogalactan at 100 mg kg−1 decreased both iNOS and COX-2 expression by 53 and 54%, respectively.	(Andrea C. Ruthes et al., 2013)
	2-amino-3*H*-phenoxazin-3-one	NO production was inhibited and iNOS protein expression suppressed at 1.5 μM while PGE2 production was inhibited at 0.27 μM.	(Kohno et al., 2008)
	Extract	Cell viability was not affected up to 2 mg/mL, NO and TNF-α production was inhibited at 0.032 mg/mL and 1.88 mg/mL respectively.	(Gunawardena et al., 2014)
A. bisporus Portobello J. E. Lange	Extract	Cell viability was not affected up to 2 mg/mL, NO production was inhibited at 0.063 mg/mL.	(Gunawardena et al., 2014)
Agrocybe chaxingu Huaag	β-Glucan	Up to 100 μg/mL, RAW 264.7 macrophage cell viability was not affected and at 50 μg/mL, COX-2 and iNOS protein expression were inhibited. Topical application of β-Glucan to mice ears suppressed TPA-induced edema formation.	(B. R. Lee et al., 2009)
Amanita muscaria (L.) Lam.	Fucomannogalactan and β-Glucan	Formalin-induced inflammation was suppressed up to 91 ± 8% at a dose of 30 mg kg−1 and 88 ± 7% and 10 mg kg−1 for β-Glucan and Fucomannogalactan respectively.	(Andrea Caroline Ruthes et al., 2013)
Albatrellus caeruleoporus (Peck) Pouzar	Grifolin dervatives	Grifolinones A and B, grifolin, and neogrifolin inhibited NO production with IC50 values of 23.4, 22.9, 29.0, and 23.3 μM, respectively.	(Quang, Hashimoto, et al., 2006)
Antrodia camphorata (M. Zang & C. H. Su) Sheng H. Wu, Ryvarden & T.T. Chang	Eburicoic acid Dehydroeburicoic acid	TNF-α, IL-1β and NO levels were significantly suppressed and at 10 mg/kg acetic acid and formalin-induced inflammation was significantly suppressed.	(J. S. Deng et al., 2013)
	Antrocamphin A (Benzenoids)	After exposure of antrocamphin A (1, 5, 10, 20 μg/mL) to LPS induced Male rats, NO, COX-2 and PGE2 production were significantly reduced.	(Hsieh et al., 2010)
	Ergostatrien-3β-ol	Acetic acid induced paw edema was significantly suppressed coupled with decreased IL-1β, NO and TNF-α levels.	(G. J. Huang et al., 2010)

	Antrocamphin A and its analogue	At 20 mg/mL, cell viability of RAW 264.7 macrophage cells was maintained up to 99.71% while NO production was significantly inhibited up to 98.10%.	(C.-L. Lee et al., 2011)
	Zhankuic acid C	At 12.5 100 μg/mL, TNF-α, IL-6, and IL-12 release were significantly inhibited in mouse bone marrow-derived dendritic cells.	(M. K. Lin et al., 2015)
	Benzocamphorin	Isolated benzocamphorin (8.6 ± 2.7 μM) suppressed LPS-induced NO production in murine microglial cells (BV2) cells.	(Liao, Kuo, Liang, Shen, & Wu, 2012)
	Succinic and maleic derivatives	Six compounds were found to suppress IL-1β and TNF-α release (10-25 μg/mL) in LPS-stimulated RAW264.7 cells.	(S. C. Chien et al., 2008)
Antrodia cinnamomea Chang & Chou	Maleimide and Maleic Anhydride	Antrocinnamomins A, B, C and D extracted from the mycelium inhibited NO Production (IC$_{50}$ 12.5 - 21.8 μM) with no decrease in cell viability.	(M. Der Wu et al., 2008)
	Maleimide Derivatives	Four new maleimide derivatives, antrocinnamomins E, F, G and H extracted from the mycelium inhibited NO Production (IC$_{50}$, 29 - 45 μM) and compounds did not cause cytotoxicity in RAW 264.7 macrophage cells.	(M. Der Wu, Cheng, Yech, Yuan, & Chen, 2013)
Armillariella mellea (Vahl) P. Kumm	Polysaccharides and sulfated polysaccharides	At 500 μg/mL TNF-α and IL-6 were inhibited up to 31.17% and 62.74% with subsequent suppression of NF-κB activation.	(C. W. Chang, Lur, Lu, & Cheng, 2013)
	Phenolic compounds	At 300 μg/mL, NO production was significantly suppressed and nuclear translocation of NF- κB/p65subunit was prevented.	(Geng et al., 2017)
Caripia montagnei (Berk.) Kuntze	β-Glucan	The β-glucans rich extract was found to show no reduction in cell viability of peripheral blood mononuclear cells and *in vivo* administration in male Swiss mice showed a significant reduction in NO, IL-10 and IFN-γ levels.	(Queiroz et al., 2010)
Cordyceps cicadae	N^6-(2-Hydroxyethyl) adenosine	At 0.5-10μg/mL, cell viability of RAW264.7 macrophage cells was maintained, while NF-κB pathway was activated leading to decrease levels of IL-1β, TNF-α, and PGE2.	(M. Y. Lu, et al. 2015)
Cordyceps militaris (L.) Fr.	Cordycepin	At 7.5 μg/mL, levels of NO, TNF-α and IL-12 levels were suppressed up to 50%.	(Rao, Fang, Wu, & Tzeng, 2010)
	Cordycepin	Up to 7.5 μg/mL, cell viability of murine BV2 cell line was maintained and there was a significant reduction in NO, PGE2, IL-1β and TNF-α levels. At 0.5-7.5μg/mL, NF-κB translocation was suppressed by blocking IkappaB-α (IκB-α).	(Jeong et al., 2010)

	Extract	Up to 500 μg/mL, aqueous extract suppressed NO, TNF-α and iNOS levels up to 50% in RAW264.7 macrophages cells.	(E. S. Han et al., 2011)
Cordyceps pruinosa (L.) Fr.	Extract	Methanolic extract between 10-100 μg/mL reduced IL-1, TNF-α, NO and PGE2 levels and suppressed NF-κB activation in LPS-stimulated RAW264.7 cells.	(K. M. Kim et al., 2003)
Cordyceps sinensis (Berk.) Sacc.	Extract	Methanolic extract between 25-100 μg/mL, TNF-α and IL-12 levels in murine peritoneal macrophages were significantly inhibited.	(Rao et al., 2007)
Coriolus versicolour (L.) Lloyd	Extract	Hydroethanolic extract at 400 μg/mL reduced IL-2, IL-4, IL-6, IL-12, IL-18 and IFN- γ levels in murine splenic lymphocytes with no reduction in cell viability.	(Ho et al., 2004)
Cyathus africanus H. J. Brodie	Diterpenoid	Diterpene rich extract reduced NO level in RAW264.7 macrophage cells.	(J. Han et al., 2013)
Cyathus hookeri Berk.	Cyathane diterpenoid	Three diterpenes isolated from ethyl acetate extract suppressed NO level with IC_{50} between 15.5-52.3 μM.	(Z. Xu et al., 2013)
Daedalea gibbosa (Pers.)	Extract	Ethyl acetate extract suppressed NO, TNF-α and PGE2 levels with significant suppression of iNOS promoter activity.	(Nili Ruimi, et al., 2010)
*Daedalea quercina (*L.) Pers.	Quercinol	Isolated quercinol significantly suppressed COX-1 and COX-2 activity.	(Gebhardt et al., 2007)
Daldinia childcare Ces. & De Not.	Benzophenone derivatives	Daldinals A, B, and C suppressed NO and iNOS activity in RAW 264.7 cells with IC_{50} values of 15.2, 4.6 and 6.4 μM.	(Quang, Harinantenaina, et al., 2006)
Elaphomyces granulatus Fr.	Extract, syringaldehyde and syringic acid	Ethanolic extract inhibited COX-2 activity up to 68% at 50 μg/mL, while isolated syringaldehyde and syringic acid reduced COX-2 activity with an IC_{50} of 3.5 and 0.4 μg/mL respectively.	(Stanikunaite et al., 2009)
Flammulina velutipes (Curtis) Singer	Extract	Cell viability was not affected up to 2 mg/mL, NO and TNF-α production was inhibited at 0.024 mg/mL and 0.099 mg/mL respectively.	(Gunawardena et al., 2014)
Fomes fomentarius (L.) Fr.	Methyl 9-Oxo-(10E,12E) octadecadienoate	Isolated compound reduced NO PGE2, TNF-α, IL-6, iNOS and COX-2 levels in peritoneal macrophages.	(Choe et al., 2015)
Fomitella fraxinea (Bull.) Imazeki	Exttracts, fomitellanols, cryptoporic acids,	Ethyl acetate extract suppressed COX 1 and COX 2 activity at 10 μg/mL up to 96 and 59% respectively. Also, its four isolated fomitellanols suppressed COX 1 and COX 2 with inhibitory activity up to 90.5%.	(Yoshikawa et al., 2013)

Fomitopsis nigra (Berk.) Imaz.	Pachymic acid	The isolated compound (15 μM) maintained cell viability of Human dental pulp cells and significantly suppressed expression of ICAM-1, VCAM-1, iNOS, and COX-2.	(Y. H. Lee et al., 2013)
Fomitopsis pinicola (Sw. Fr.) P. Karst.	Lanostane triterpenoids, triterpene glycosides	Isolated compounds, fomitopinic acid, formitoside E and Formitoside F showed significant Inhibition of COX-2 activity (IC$_{50}$, 0.15-1.15 μM) corresponding to indomethacin (IC$_{50}$, 0.60 μM).	(Yoshikawa et al., 2005)
Ganoderma capense (Lloyd) Teng	Glycopeptide	At 100 μg/mL, NO production and iNOS expression were significantly suppressed in RAW264.7 mouse macrophage cell line.	(Zhou, Chen, Ding, Yao, & Gao, 2014)
*Ganoderma lucidum (*Curtis) P. Karst	Lanostane triterpenes	Twelve lanostane triterpenes were isolated and up to 50 μM cell viability of RAW264.7 cells were not affected and there was significant suppression of NO, TNF-α, and IL-6 levels.	(S. Choi et al., 2014)
	Triterpene extract	Up to 100 μg/mL, cell viability of RAW264.7 cells was maintained and between 3–50 μg/mL exposure to triterpene rich extract, NO, TNF-α and IL-6 levels were suppressed.	(Dudhgaonkar, et al. 2009)
	Triterpenic acids	Nine lucidenic acids and four ganoderic acids were found to inhibit TPA-induced inflammation (1 μg/ear) in mice.	(Akihisa et al., 2007)
	Triterpene butyl esters	Isolated lanostane triterpenes suppressed NO levels and reduced iNOS and COX-2 protein expressions in RAW 264.7 cells with IC$_{50}$ values between 4.3-9.4 μM.	(Tung et al., 2013)
	Aqueous extract, Ganoderic acid C1 (GAC1)	At 100 μg/mL exposure to aqueous extract, cell viability of RAW 264.7 macrophage cells was maintained and TNF-α levels were suppressed with IC$_{50}$ value 33.8, μg/mL. GAC1 suppressed TNF-α levels and <10 μg/mL was sufficient to account for 50% inhibition.	(C. Liu et al., 2015)
Geastrum saccatum Fr.	β-Glucan	Isolated glucan suppressed croton oil-induced edema (60.4% at 10 mg/kg) comparable to diclofenac (89.2% at 5 mg/kg) or L-NAME (86.23% at 60 mg/kg). Expression of iNOS and COX were suppressed.	(Guerra Dore et al., 2007)
Grifola frondosa (Dicks.) Gray	Agaricoglycerides	At 500 mg, the levels of IL-1β, TNF-α, NF-κB, ICAM-1, COX-2, and iNOS were significantly reduced.	(C. Han & Cui, 2012)
	Fatty acid fraction, steroidal compounds	The fatty acid fraction and isolated compounds up to 250 μg/mL displayed COX-1 and COX-2 enzyme inhibition	(Y. Zhang, Mills, & Nair, 2002)
Hericium erinaceum (Bull.) Persoon	Hericirine (ergosterol)	Up to 40μM, the isolated compound inhibits the expression of iNOS and COX-2, and reduced the levels of NO, PGE2, TNF-α, IL-6 and IL-1β in RAW264.7 cells.	(W. Li et al., 2014)
	Hericenone C, D, F,	At 200 μg/mL, cell viability of RAW264.7 cells was maintained, and NO production was suppressed	(D. G. Lee, Kang, et al., 2016)

Inonotus obliquus (Ach. ex Pers.) Pilát	Extract fractions, steroidal compounds	Ethanol extract, petroleum ether fraction, ethyl acetate fraction and *n*-butyl alcohol fraction showed 50% reduction in NO levels at 40 μg/mL. Trametenolic acid and ergosterol peroxide suppressed NO levels by 50.04% and 36.88% respectively.	(Ma et al., 2013)
Inonotus xeranticus (Berk.) Imazeki & Aoshima	Davallialactone	Cell viability of RAW264.7 cells was maintained between 3.12-50 μg/mL and NO and PGE2 release were suppressed. Following treatment with the isolated compound, the signaling cascade that activates NF-kB was blocked up to 40%.	(Y. G. Lee et al., 2008)
Lactarius deliciosus (L. ex Fr.) S.F. Gray	Extract	At 0.5 mg/mL, cell viability of RAW 264.7 macrophage cells was not inhibited and NO and TNF-α levels were reduced.	(Moro et al., 2012)
Laetiporus sulphureus (Bull.) Murrill	Acetyl Eburicoic Acid	At 100 μg/mL, cell viability of RAW 264.7 cells were maintained and identified compound dose-dependently inhibited the NO production and suppressed iNOS, COX-2, IL-1β, IL-6, and TNF-α expression.	(Saba et al., 2015)
Lentinus edodes (Berk.) Pegler	β-Glucan	At 200 μg/mL, NO and TNF-α levels were significantly reduced due to suppression of JNK1/2 and ERK1/2 kinases.	(X. Xu, Yasuda, et al. 2012)
	Fucoidan and Lentinan	At 500 μg/mL, both polysaccharides down-regulated IL-8 mRNA expression and suppressed TNF-α release from RAW264.	(Mizuno, et al., 2009)
Lentinus polychrous (L.) Fr.	Mycelia extract	At 100 μg/mL, cell viability of RAW 264.7 cells were not affected and expressions of iNOS, IL-1β, IL-6, TNF-α, and COX-2 were significantly suppressed.	(Fangkrathok et al., 2013)
Lignosus rhinocerotis (Cooke) Ryvarden	Extract fractions, Protein complexes	Cold water extract, hot water extract, and methanol extract reduced carrageenan-induced edema. Its protein component inhibited of TNF-α production with an IC_{50} of 0.76 μg/mL.	(S. S. Lee et al., 2014)
Neolentinus lepideus (Fr.) Redhead & Ginns	Benzoquinone, cinnamic acid derivatives	5-methoxyisobenzofuran- 4,7(1H,3H)-dione (6.2μM) one of the isolated compounds showed strong NO inhibitory activity even better than hydrocortisone (53.78μM) used as the positive control.	(Yongxia Li et al., 2013)
Phellinus linteus (Berk. & M. A. Curtis) Teng	Inotilone	Cell Viability of RAW264.7 cells was maintained after exposure to inotilone (25μM), NO and iNOS expression were inhibited due to suppression of MAPK and NF-κB expressions.	(G. J. Huang, Huang, & Deng, 2012)
	Hispolon	Cell viability RAW264.7 cells was maintained after exposure to hispolon rich mycelial extract (50-400 μg/mL) and levels of NO, iNOS, TNF-α, and NF-κB expressions were significantly decreased.	(C. J. Lin et al., 2014)
	n-Butanol fraction	At 0.1- 1 mg/mL, iNOS promoter activity were suppressed.	(B. C. Kim et al., 2006)

Piptoporus betulinus (Bull. ex Fr.) P. Karst.	Lanostanoids, polyporenic acid C	Both compounds inhibited COX-1 activity with IC_{50} values of 8.5μM and 4 μM even comparable to indomethacin (6.5 μM).	(Wangun, et al., 2004)
	Lanostane-type triterpene	Polyporenic acids A, C, and its derivatives were found to suppress TPA (12-O-tetradecanoylphorbol-13-acetate) induced edema up to 49-86% with a 400 nmol/ear application.	(Kamo, et al., 2003)
Pleurotus citrinopileatus Singer	nonlectin glycoprotein	Isolated compound up to 6.25 μg/mL, maintained cell viability and suppressed iNOS, COX-2, and NF-kB expressions in RAW264.7 cells.	(J.-N. Chen, et al. 2011)
*Pleurotus pulmonarius (*Fr.) Quél.	Mycelia extracts and β-Glucan rich fraction	TNF-α, IL-1β, and IL-10 mRNA expression were suppressed.	(Lavi et al., 2010)
Pleurotus sajor-caju (Fr.) Singer	β-Glucan	At 250 μg/mL, expression of TNF-α, IL-1β, and COX-2 were significantly suppressed.	(Silveira et al., 2014)
Poria cocos F.A. Wolf	Triterpenes	Five of the isolated compounds suppressed NO secretion in RAW264.7 cells with IC_{50} values between 16.8-44.9 μM even comparable to L-NMMA (28.4 μM).	(Cai & Cai, 2011)
Scleroderma nitidum Berk.	β-Glucan	The polysaccharide reduced edema formation up to 73% at 50 mg/kg, NO, IFN-γ, IL-2, IL-10 levels were significantly suppressed.	(Nascimento et al., 2011)
Termitomyces albuminosus (Berk.) R. Heim	Crude polysaccharide, crude saponin extract	Acetic acid-induced inflammation was reduced by 61.8%, 79.0% and 81.6% after treatment with crude saponin extract (200 mg/kg) and crude polysaccharide extract (200 mg/kg) respectively.	(Y. Y. Lu et al., 2008)
Tremella fuciformis Berk	Polysaccharide	At 300 μg/mL, cell viability RAW264.7 cells were maintained, TNF-α and IL-6 expression were suppressed due to inactivation of NFκB.	(Y. Ruan, Li, Pu, Shen, & Jin, 2018)
Bioactive compounds	**Type**	**Main findings**	**Reference**
3,4,5-Trihydroxycinnamic acid	Commercial	At 100 μM, it suppressed NO production up to 70% and reduced Iκβ degradation.	(J. W. Lee et al., 2013)
Caffeic acid	Commercial	At 10–200 μg/mL, IL-8, IL-1β, IL-6, and TNF-α levels were suppressed, IκB-α degradation and p65 phosphorylation inhibited.	(M. Liu et al., 2014)
	Commercial	At 10 μg/mL, it suppressed NO levels, blocked NF-κB translocation and prevented IκB-α degradation.	(Búfalo et al., 2013)
Caffeic acid phenethyl ester (CAPE)	Commercial	At 1 μM, COX-1 and IL-1β expression was suppressed.	(Nagasaka et al., 2007)

Caffeic acid derivatives (methyl, ethyl, butyl)	Synthesized	At 21.4, 11.9 and 8.4 μM, the derivatives inhibited NO levels up to 50%.	(da Cunha et al., 2004)
Chlorogenic acid	Commercial	0.5–100 μmol/L of CGA suppressed the expression of NF-κB, p50, and IKKα/β.	(L. Lou et al., 2016)
	Synthesized	Intraperitoneally at 2.5–50 mg/kg, it suppressed TNF-α, IL-1β, and IL-6 release by inhibiting the TLR4-mediated NF-κB signalling pathway.	(Ruifeng et al., 2014)
	Commercial	At 20 μM, levels NO, IL-1β, TNF-α, and IL-6 were suppressed and the expression of COX-2 and iNOS reduced.	(Hwang, Kim, Park, Lee, & Kim, 2014)
	Commercial	At 20 μM, expression of IL-1β and COX-2 was significantly suppressed.	(W.-P. Chen & Wu, 2014)
Cinnamic aid	Commercial	At 182 ± 1 μM, NO secretion was suppressed by 50% in RAW264.7 cells.	(Taofiq et al., 2015)
Cordycepin	Commercial	At 5 μM, NO production suppressed by 50% in RAW264.7 cells.	(Imamura et al., 2015)
Ferulic acid	Commercial	FA topically and intraperitoneally inhibited the expression of TNF-α and IL-6.	(Ambothi, Prasad, & Balupillai, 2015)
p-Coumaric acid	Commercial	Suppressed TNF-α levels *in vivo* at 100 mg/kg body weight in arthritis-induced rats.	(Pragasam & Rasool, 2013)
	Commercial	At 442 ± 33 μM, NO secretion was suppressed by 50% in RAW264.7 cells.	(Taofiq et al., 2015)
p-Hydroxybenzoic	Commercial	At 239 ± 29 μM, NO secretion was suppressed by 50% in RAW264.7 cells.	(Taofiq et al., 2015)
Rosmarinic acid	Commercial	At 2.75 μM, the expression of IL-6 and IL-8 were inhibited.	(Lembo et al., 2014)
	Commercial	At 1 μg/mL, TNF-α levels were reduced and iNOS expression suppressed.	(Zdařilová et al., 2009)
	Commercial	TNF- α, IL-6 and IL-1β levels were suppressed after administration of 5, 10 and 20 mg/kg of rosmarinic acid/mice weight.	(X. Chu et al., 2012)

X. Xu, Yasuda, Nakamura-Tsuruta, Mizuno, & Ashida, (2012) isolated a β-glucan (lentinan) from the fruiting bodies of *L. edodes* and investigated its effects on NO and TNF-α production in LPS stimulated murine RAW 264.7 macrophages. Lentinan, at a concentration of 200 mg/mL, was found to significantly inhibit NO production (70%) and was dose-dependent. Also, the amount of TNF-α released from RAW 264.7 cells was quantified and found to be suppressed up to 75% at 200 mg/mL. Furthermore, the protein expression of iNOS and the gene expression of iNOS mRNA and TNF-α mRNA were suppressed by lentinan suggesting its usefulness as an anti-inflammatory agent.

S. Choi et al. (2014) isolated 12 triterpenes from the fruiting body of *G. lucidum* and the anti-inflammatory activity was evaluated in LPS induced RAW 264.7 cells. Seven triterpenes; butyl lucidenate E2 (GT-1), butyl lucidenate D2 (GT-2), butyl lucidenate P (GT-3), butyl lucidenate Q (GT-4), Ganoderiol F (GT-5), methyl ganodenate J (GT-7) and butyl lucidenate N (GT-12), out of the studied twelve triterpenes, showed significant decrease in NO production. 20 mM of GT-2 showed up to 70% inhibition of NO production relative to the control. Dudhgaonkar, Thyagarajan, & Sliva (2009) also studied triterpene rich ethanolic extracts from *G. lucidum* in LPS stimulated RAW 264.7 macrophage cells. The extract at 10-50 mg/mL suppressed TNF-α production in RAW 264.7 cells ($IC_{50,}$ 15.1 mg/mL), reduced IL-6 production (IC_{50} 14.4 mg/mL) and decreased the secretion of PGE2 and NO in a dose-dependent manner with IC_{50} values of 28.2 mg/mL and 11.4 mg/mL, respectively.

Cyathus africanus H. J. Brodie, also known as "bird nest fungi", usually grows on animal dungs, woody debris, and soil rich in humus. J. Han et al. (2013) isolated diterpenes from its fruiting body and the anti-inflammatory activity was evaluated regarding NO production in LPS induced macrophages. Five diterpenes showed potent NO inhibition with IC_{50} values of 2.57, 1.45, 12.06, 10.73, and 9.45 µM, compared to hydrocortisone 53.78 (µM) used as the control. *Albatrellus caeruleoporus* (Peck) Pouzar is an edible mushroom that grows on woody debris as well as on the ground, common in North America. Quang, Hashimoto, et al. (2006) chemically characterized its methanolic extracts in terms of phenolic acids and evaluated their anti-inflammatory potential in LPS induced RAW 264.7 cells regarding NO production. All four identified grifolin derivatives showed a significant reduction in NO production with IC_{50} values of 23.4, 22.9, 29.0, and 23.3 µM compared to 88.4 µM of NG-methyl-L-arginine (L-NMMA), a potent inhibitor of NO production used as the control.

Elaphomyces granulatus Fr. is an inedible mushroom known as "false truffle" in the United Kingdom and widely distributed in Europe and North America. Stanikunaite et al. (2009) studied the ethanolic extracts of *E. granulatus* and isolated syringaldehyde and syringic acid from its fruiting body. Extracts and phenolic acids were evaluated for their anti-inflammatory activity in RAW 264.7 macrophages cells by the COX-1 and COX-2-catalysed prostaglandin biosynthesis assay. The extracts caused a 68% inhibition of COX-2 activity at 50 mg/mL. Syringaldehyde and syringic acid moderately inhibited COX-2 activity with IC_{50} values of 3.5 mg/mL and 0.4 mg/mL, respectively. NS-398, a specific inhibitor of COX-2, was used as a positive control and had IC_{50} 0.2 mg/mL.

P. linteus is a medicinal mushroom used for centuries in oriental countries to prevent several diseases (G. J. Huang et al., 2012; S. H. Kim et al., 2004). C. J. Lin et al., (2014) isolated hispolon from the fermentation broth of *P. linteus* and its anti-inflammatory activity was evaluated in LPS induced RAW 264.7 cells regarding inhibition of NO production. Hispolon at 10 mg/mL inhibited NO production by 72.1% and suppressed the expression levels of iNOS. Hence this compound has useful therapeutic potential, and additional research studies are needed to understand its mechanism of action. G. J. Huang et al. (2012) isolated inotilone, from the fruiting body of *P. linteus* and tested the anti-inflammatory effects *in vivo* in carrageenan-induced hind mouse paw edema model as well as *in vitro* for inhibition of NO production and iNOS expression. Carrageenan-induced mouse paw edema volume was significantly decreased to 56.2%, NO production was inhibited up to 26.2-59.7%, TNF-α release was inhibited up to 10.6-40.3%, while iNOS expression was significantly inhibited in a dose-dependent manner. Inhibition of NF-κB and MAPK activation was also observed. Ma, Chen, Dong, & Lu, (2013) isolated six main constituents from *P. linteus* fruiting body and their anti-inflammatory activity was evaluated for NO production in RAW 264.7 cell lines. Among the isolated compounds, ergosterol peroxide and trametenolic acid had the highest anti-inflammatory potential and significantly inhibited NO production by 36.88% and 50.04%, respectively. Other steroidal compounds isolated from mushrooms (e.g. lanosterol, 3b-hydroxy8, 24-dien-21-al, ergosterol, and inotodiol) had relatively low percentages of NO production inhibition.

Liu et al. (2014) reported the anti-inflammatory activity of ethanolic extract from mycelia of *P. tuber-regium* produced by submerged fermentation broth in LPS induced murine macrophage cell line RAW 264.7. Two compounds, cerevisterol (CE) and ergosta-4, 6, 8(14), 22-tetraen-3-one, were isolated, characterized and their anti-inflammatory activity evaluated. From the result, both compounds at 10 μM inhibited NO production in a dose-dependent

manner, very similar to the control. They also significantly inhibited TNF-α, IL-6, and PGE2 release from the cell culture supernatant. The anti-inflammatory activity was reported to be due to down-regulation of iNOS and COX-2 mRNA protein expression.

Fomes fomentarius is an inedible mushroom species common in Europe, Asia and North America, known for its large fruiting body and decomposing property. Its fruiting body was extracted with methanol and methyl 9-oxo-(10E, 12E)-octadecadienoate isolated (Choe et al., 2015). The anti-inflammatory activity was evaluated in peritoneal macrophages for NO, PGE2 production, TNF-α, and IL-6 release. At 20 mg/mL, the compound significantly inhibited NO and PGE2 by 65% and 50%, respectively, while TNF-α and IL-6 levels were inhibited up to 35% and 13%, respectively. Finally, the mechanism of action of the compound was found to be due to inhibition of iNOS and COX-2 protein expression and due to a slight inhibition of phosphorylation of ERK1/2 kinase.

Armillaria mellea P. Kumm., popularly referred to as honey fungus is a medicinal and edible mushroom widely distributed in North America, Europe, and Northern Asia. The anti-inflammatory activity of its ethyl acetate extract showed maintenance of cell viability in BV-2 mouse microglia cell line. At 300 μg/mL, NO production was significantly suppressed and nuclear translocation of NF-κB/p65subunit was prevented. The authors went on to identify the most import contributors to the anti-inflammatory activity as 5-hydroxymethylfurfural, 2-furoic acid, 4-hydroxybenzoic acid, vanillic acid, syringate, daidzein, genistein (Geng et al., 2017).

The anti-inflammatory activity of a glycopeptide from *Ganoderma capense* (Lloyd) Teng was evaluated in RAW 264.7 cells for NO production and for iNOS enzyme activity (Zhou et al., 2014). It was found that LPS-induced NO production and iNOS expression were significantly inhibited in a dose-dependent manner. Jeong et al. (2010) studied the anti-inflammatory activity of commercial cordycepin in LPS stimulated murine BV2 microglia cells for inhibition of NO production as well as PGE2, and pro-inflammatory cytokine release. Cordycepin at 7.5 mg/mL, decreased levels of NO production up to 65%, while the PGE2 concentration measured using ELISA kit was also repressed up to 60%. This anti-inflammatory mechanism was found to be due to the inhibition of iNOS and COX-2 protein expression. Y. H. Choi, Kim, & Lee, (2014) also studied the anti-inflammatory potential of cordycepin in LPS stimulated RAW 264.7 macrophage cell line for NO production, cytokine (TNF-α and IL-1β) levels, and PGE2

production. At 30 mg/mL exposure of induced cells to cordycepin, there was a significant decrease in NO, TNF-α, IL-1β and PGE2 levels.

Several publications have reported the medicinal properties of Cordyceps mushroom, including the anti-inflammatory activity (E. S. Han et al., 2011; K. M. Kim et al., 2003; Rao et al., 2007, 2010; Won & Park, 2005). This mushroom contains a lot of bioactive compounds and "Cordycepin" an adenosine analog is one of the most important one. Jeong et al. (2010) studied the anti-inflammatory activity of commercial cordycepin in LPS stimulated murine BV2 microglia cells for inhibition of NO production as well as PGE2, and pro-inflammatory cytokine release. Cordycepin at 7.5 µg/mL, decreased levels of NO production up to 65% while the PGE2 concentration measured using ELISA kit was also repressed up to 60%. This anti-inflammatory mechanism was found to be due to the inhibition of iNOS and COX-2 protein expression. The mechanism of inhibition was further confirmed by decreased levels of LPS-induced NF-kB/p65 levels in the nucleus and inhibition of phosphorylation of IκB-α complex.

Researchers have attempted to synthesize compounds with improved properties as drug candidates with the potential to inhibit production of NO and other inflammatory mediators such as interleukins (IL 1β, IL-6, IL-8), TNF-α and PGE2. Some synthesized and commercial compounds with positive anti-inflammatory potential have been reported (**Table 2**). Taofiq et al. (2015) studied the anti-inflammatory activity of commercial phenolic acids (*p*-hydroxybenzoic and *p*-coumaric acids) and cinnamic acid, and of their synthesised metabolites (glucuronated *p*-coumaric acid, methylated *p*-coumaric acid, glucuronated cinnamic acid, methylated cinnamic acid, methylated *p*-hydroxybenzoic acid, glucuronated *p*-hydroxybenzoic acid) (Heleno et al., 2014). All compounds were then tested for their potential to inhibit NO production in LPS stimulated RAW 264.7 cells. Cinnamic acid had the highest activity (IC_{50} value 182 µM), followed by *p*-hydroxybenzoic (239 µM) and *p*-coumaric (442 µM) acids, in comparison with dexamethasone (40 µM) used as a control. Among the synthesized metabolites, CoA-GP (glucuronated derivative of *p*-coumaric acid) and CoA-M1 (methylated derivative with the methoxy group at the para position) presented strong anti-inflammatory activity with IC_{50} values of 58 µM and 35 µM respectively.

1.4.3. Anti-ageing and UV protective effects of mushroom extracts and their associated metabolites

Several biological reactions, required for normal functioning of the organism, take place in body cells and tissues. These reactions often cause generation of species with unpaired electrons called free radicals. These free radicals include ROS, reactive nitrogen species (RNS) and reactive sulfur species (RSS) (Carocho & Ferreira, 2013a, H. Zhao et al., 2017). The body has mechanisms to balance ROS production and neutralization by means of its intrinsic antioxidant pool (glutathione peroxidase, catalase, and superoxide dismutase), but most of the times it can become depleted due to excessive ROS production allowing the body cells to suffer from oxidative stress (Carocho & Ferreira, 2013a). Subsequently, endogenous sources are needed to fulfill the antioxidant requirements and mushrooms, used as a dietary source, can help to surpass this lack since they contain high amounts of bioactive compounds displaying antioxidant activity (Hui et al., 2010). These dietary sources of antioxidants such as vitamin C (ascorbic acid), vitamin E (tocopherol), carotene, vitamin K, flavonoids, phenolic acids, selenium, and zinc tend to maintain a balance to control oxidative stress (Carocho & Ferreira, 2013a). Skin exposure to high UV radiation causes ROS generation, which usually leads to a combined effect of DNA damage, skin inflammation, hyperpigmentation and stimulation of dermal fibroblast for expression of matrix metalloproteinase 1 (MMP-1). The results are collagen degradation and a decrease in collagen synthesis, thus resulting into a photo-aged skin (Masaki, 2010). The important role of antioxidants in skin health drives the continuous search for compounds of natural origin capable of scavenging ROS, inhibiting tyrosinase enzyme as well as suppressing MMP-1 expression. Ascorbic acid is usually used in skin care products but controversy in its efficacy has been raised due to its inability to penetrate the skin together with its poor stability in cosmetic formulations (Spagnol et al., 2016). α-Tocopherol is also an important antioxidant that is reported to downregulate MMP-1 expression by suppressing AP-1 and also inhibiting tyrosinase enzyme, making it an important anti-wrinkle and hyperpigmentation correcting agent (Miyake et al., 2010). Several publications have reported the antioxidant activity of mushroom extracts mainly as radical scavengers (DPPH 2,2-diphenyl-1-picrylhydrazyl; ABTS 2,20-azinobis 3- ethylbenzothiazoline-6-sulfonic acid; H_2O_2 and O_2 scavenging activity), reducing power (FRAP ferric reducing antioxidant power) and lipid peroxidation inhibitors (TBARS thiobarbituric acid reactive substances; Heme degradation of peroxides and FOX ferrous oxidation-xylenol) (Carocho & Ferreira, 2013a, Hui et al., 2010).

Antioxidant compounds are a key ingredient in preventing an ageing skin. These compounds act on several cell signal transduction pathways related to ageing, inflammation, hyperpigmentation and extracellular matrix degradation. As mentioned earlier, free radicals produced because of different cell functions are the most important contributors to an ageing skin and as such, compounds with antioxidant capacity have been described as the most important cosmetic and cosmeceutical ingredients against exogenous oxidative stress that occurs in our daily life. Some studies (**Table 3**) that have so far been reported on the anti-ageing potential of mushroom extracts or their individual compounds will be discussed.

A. bisporus is one of the most widely consumed mushrooms in the world. It contains high amount of dietary fibres, phenolic compounds and polysaccharides. Polysaccharide fraction obtained from *A. bisporus* at the dose of 400 mg/kg was able to significantly decrease the activities of SOD, GSH-Px and CAT, in an ageing mice (Shangshang Li, Liu, Zhang, et al., 2018). An exopolysaccharide was isolated from *Grifola frondosa*, the extract was submitted to cell viability assay in human dermal fibroblasts by the MTT (3-(4,5-dimethylthiazol-2-yl)-2,5-diphenyltetrazolium bromide) method. The extracts (5-200 µg/mL) were found to significantly reduce expression of MMP-1 up to 61% and no reduction in cell viability was observed (J. T. Bae et al., 2005). Kim et al. (2007) also reported the contribution of both mycelia extract (GF-M) and exopolysaccharide fraction (EPS) obtained from *G. frondosa* on the expression of MMP-1 and collagen synthesis. The samples were found not to cause any morphological change in human dermal fibroblast cell lines, while also reducing the expression of MMP-1 by 20 and 40% for GF-M and EPS respectively. Another interesting finding regarding the contribution of a polysaccharide as an anti-ageing ingredient was reported by Hui et al. (2010), where mice were exposed to a polysaccharide-rich diet from *H. erinaceum* and the activities of SOD, CAT and GSH-Px were compared with a placebo group. The samples exposed to the bioactive fraction were found to have high MMP-1 and antioxidant enzyme activity and resulted in an enhanced collagen level. Polysaccharide-rich extract from *Volvariella volvacea* was also submitted to cell viability assessment (0.001-10 mg/mL) on human fibroblasts cell lines and up to 80% cell viability was achieved. The authors went further to report that the extract was able to stimulate collagen biosynthesis up to 146.77±13.20% (Ruksiriwanich, et al., 2014). Beside been able to act as anti-ageing ingredients, polysaccharides especially those from botanical and algae origin have been reported to have interesting skin hydrating and moisturizing effects because of their high water holding capacity (Z. S. Zhang, Wang, Han, Zhao, & Yin, 2012). Significant studies are still needed to be conducted to determine the

mechanism behind the anti-ageing potential of these class of compounds. Anti-ageing effects of exopolysaccharides (EPS) from *Agrocybe cylindracea* was conducted in mice and the authors reported an increase in serum activities of SOD, GSH-Px and total antioxidant capacity (H. Zhao et al., 2017). Similar studies were also reported for acidic-extractable polysaccharides from *A. bisporus* (Shangshang Li, Liu, Wang, et al., 2018), crude polysaccharides from *Calocybe indica* Purkay. & A. Chandra (Govindan et al., 2016), and acidic- and alkalic-extractable mycelium polysaccharides from *Agrocybe aegerita* (Brig.) Sing (Jing et al., 2018). All extract fractions provided enhanced enzymatic (SOD, GSH-Px and CAT) and non-enzymatic (MDA) free radical-scavenging defense. Polysaccharide fractions were prepared from the mycelium extract of *G. frondosa* and their cosmeceutical potential was evaluated in human dermal fibroblasts, showing no inhibition of cell growth and maintenance of cell viability. Also, biosynthesis of collagen was quantified and up to 80% was achieved at a concentration of 0.05% (*w/v*) (B. C. Lee et al., 2003).

Besides the contribution of compounds that tend to elevate collagen synthesis, decrease the activities of intrinsic antioxidant enzymes and suppress collagen inhibitors, compounds that inhibit the activity of hyaluronidase have drawn increased attention in preventing an ageing skin (Meng et al., 2011). Hyaluronic acid is a glycosaminoglycan (GAG), a key component of the ECM that promotes dermal cell proliferation, suppresses cell differentiation and retains skin moisture, thereby preventing an ageing skin (Stern, 2004). To our best of knowledge, even though inhibitor of these molecules has been described in the past, very little is known or reported about them. Different extract fractions prepared from *P. citrinopileatus* were reported by Meng et al. (2011) to show antioxidant activity, and their potential to inhibit hyaluronidase was evaluated using hyaluronic acid potassium salt as substrate. The results showed that the *n*-butanol, aqueous and methanol extract showed hyaluronidase inhibition up to 9.7%, 10.8%, and 25.4% respectively. Hyaluronidase inhibition activity was also reported for aqueous and acetonic extract prepared from *Trametes lactinea* and they were found to inhibit hyaluronidase activity by $88.6 \pm 0.11\%$ and $88.3 \pm 0.14\%$ respectively (Y. A. Yahaya & Don, 2012). To our best of knowledge, only these two reports are available on the hyaluronidase inhibition activity of mushroom extracts or their individual metabolite. Research studies in this area are still lacking. Commercial extracts prepared from the mycelium of *Tricholoma matsutake* was submitted to cytotoxicity assay in fibroblast cell lines and the anti-elastase was determined using the peptide N-Succinyl-tri-L-alanine 4-nitroanilide (STANA) as substrate. The extract at 100 µg/mL did not cause any decrease in cell viability, while expression of MMP-3 was

significantly suppressed (Kim et al., 2014). Also, the extract at 100 μg/mL was found to inhibit elastase activity by 81.4 ± 3.92%. The authors suggested that the extract can be utilised as a potential anti-wrinkle agent. *G. frondosa* has interesting potential as a skin care ingredient. Its polysaccharide fraction isolated from its fruiting body was evaluated for cosmeceutical potential. At 100 μg/mL, it was found to suppress MMP-1 activity by 40% even more potent than trans-retinoic acid (tRA), a common MMP-1 inhibitor (S. W. Kim et al., 2007). The extracts were found to stimulate an increase of 53% in the biosynthesis of collagen without presenting any cytotoxicity. Finally, its polysaccharide fraction was found to present tyrosinase inhibition activity in B16 mouse melanoma cells up to 20%. These results showed that *G. frondosa* can be an efficient multifunctional cosmeceutical ingredient offering photoprotection and suppressing melanogenesis.

Wound healing is a natural restorative response characterized by several complex cascades of cellular events associated with inflammation, fibroplasia, neovascularization, collagen deposition, epithelialization and wound contraction (Kimura, Hashimoto, Yamada, & Nishikawa, 2013). A β-glucan rich extract prepared from *Sparassis crispa* (Wulfen) Fr., an edible and medicinal mushroom commonly consumed in China and Japan, was investigated for its *in vivo* wound healing potential. The results showed histologically that there was an increased epithelialization and a rapid wound healing in the β-glucan treated wounds when compared to the placebo group. Also, collagen levels were elevated in normal adult human dermal fibroblasts (NHDF) exposed to β-glucan (100 μg/mL) fraction (Kwon, Qiu, Hashimoto, Yamamoto, & Kimura, 2009). More so, regarding *S. crispa*, orally and topically applied β-glucan rich extract, improved wound healing *in vivo* (K. Yamamoto & Kimura, 2013), and oral administration also improved *stratum corneum* turn over and accelerated collagen synthesis (Kimura, Hashimoto, Yamada, & Nishikawa, 2013).

A topical formulation containing 10% (*w/w*) of *G. lucidum* extract was compared with intrasite gel, an amorphous hydrogel which gently re-hydrates necrotic tissue, facilitating its healing. The former showed signs of dermal healing with the shortest re-epithelisation period (12.37 ± 0.49 days). Intrasite-gel wound closure was 136.86 ± 22.8 mm^2 (55%), while *G. lucidum* formulation was 242.08 ± 7.8 mm^2 (97%). Serum activities of antioxidant enzymes were also enhanced *in vivo* (Cheng et al., 2013). Similarly, the wound healing potential of *Antrodia camphorata* was evaluated by Amin, Ali, Alshawsh, Darvish, & Abdulla, (2015). Cell viability of fibroblast cells was maintained at 100 μg/mL, and a topical formulation based on this mushroom was prepared. Wound closure was 33.67 ± 4.81mm^2 (90.21%), comparable to

intrasite-gel ($36.67 \pm 7.45mm^2$; 89.29%). Aqueous extract from *G. lucidum* and *Crinipellis schevczenkovi* Bukhalo topically applied also showed wound healing activity (Krupodourova et al., 2015). The authors were not able to determine the mechanism behind the wound healing process and the most important bioactive compounds contributing to the observed effect. *Agaricus blazei* polysaccharides has an effective wound healing properties by suppressing IL-1β release by macrophages (Sui et al., 2010). These findings showed that extracts and individual compounds from mushrooms have wound healing properties and can be explored as cosmeceutical ingredients to accelerate the wound healing process.

The most widespread organic acids found in mushrooms include oxalic acid, quinic acid, malic acid, citric acid, and fumaric acid (Barros, Pereira, & Ferreira, 2013). These acids have been reported to normalize the rate of desquamation in the skin by increasing epidermal thickness, stimulate cellular renewal, increase dermal firmness and skin smoothness (Sams et al., 2001). They have been clinically proven to suppress photoageing, improve wrinkles, maintain skin elasticity, and promote skin hydration (Green, Yu, & Van Scott, 2009; Moghimipour, 2012). Alpha hydroxy acid (AHA) and beta hydroxy acid (BHA) are two main classes of hydroxy acids, both differing in the position of the hydroxyl group (Kornhauser et al., 2012). Citric acid, and its salts and esters are reported to have multifunctional properties in cosmetics as chelating agents, pH adjusters, skin-conditioning agents, fragrance ingredient and as plasticizers (Fiume et al., 2014). A 20% citric acid lotion, topically applied to photodamaged skin was found to increase skinfold thickness, viable epidermis thickness, and GAG content in a statistically significant manner (Bernstein et al., 1997). Both citric and malic acid presented photoprotective properties in UVB-irradiated keratinocytes (Tang & Yang, 2018). These organic acids can, therefore, enhance and improve the therapeutic effects of certain bioactive compounds, through a synergistic interaction that will result in the skin health improvement. Despite the multifunctional properties of these organic acids, caution should be exercised due to some adverse reactions associated with them.

Ultraviolet (UV) radiation has been responsible for several skin damages, ranging from precancerous and cancerous skin lesions and accelerated skin ageing. Topical formulations containing sunscreen and antioxidant resources have been utilised to absorb UV rays and reduce the risk of oxidative damages (Maske, Lokapure, Nimbalkar, Malavi, & D'souza, 2013; Saija et al., 1999). Phenolic compounds such as flavonoids, stilbenes, and hydroxycinnamic acid derivatives are the most utilised compounds as photoprotectors. Several studies have mentioned that polyphenolic rich extracts have high sun protection factor offering protection

to UV-irradiated cells (A. S. Fernandes et al., 2018, Tang & Yang, 2018). To our best of knowledge, Saija et al. (1999) were the first to report a potential UV protective effect for ferulic and caffeic acid. The authors mentioned that the compounds were able to suppress UV induced peroxidation. They conducted a skin permeation assay using human skin samples as membrane and ferulic acid (19.94%) was found to permeate more than caffeic acid (11.14%). These interesting findings let the authors to conduct further *in vivo* studies, to evaluate the potential of the studied compounds to reduce the severity of UVB-induced skin erythema. The level of erythema of volunteers was accessed by means of reflectance spectrophotometry, generating skin reflectance spectral values that can be utilised as reliable parameters to evaluate skin erythema. The results showed that both compounds were able to display significant protection to the skin against UVB-induced erythema (Saija et al., 2000). Pluemsamran et al. (2012) accessed the UV protective effect of caffeic and ferulic acid. The authors reported that exposure of human keratinocyte cell line (HaCaT) to UV radiation at a dose of 4 Jcm^{-2} significantly reduced cell viability up to 30%. After exposure of the compounds to the cells, cell viability was markedly enhanced in a concentration-dependent manner. Both compounds (3.75–30 µM) were found to also suppress MMP-1 activity. Another interesting method to suppress the severity of UV induced skin damages is the combination strategy where different compounds with antioxidant and UV protective capacity are formulated together in order to deliver the desired effect. Kwak et al. (2015) reported that ascorbic acid and *p*-coumaric acid were utilised to generate two hybrid compounds, Ascorbyl-3-*p*-coumarate, and Ascorbyl-2-*p*-coumarate (A-3-*p*-C and A-2-*p*-C). The effects of these compounds on collagen synthesis were examined and at 100–300 µM, A-3-*p*-C and A-2-*p*-C promote collagen release up to 120–144% and 125–191%, respectively. Both compounds were also found to decrease MMP-1 activity in a concentration-dependent manner. Phenolic compounds rich serum was applied topically in ten female volunteers, aged 38-52 years. There was a significant increase in epidermal and dermal thickness, increased fibroblast density and enhanced activity of antioxidant enzymes up to 32% (Freedman, 2009). Besides being able to protect the skin against UV induced damages, long term effects of these extracts and/or individual compounds have not yet been well reported clinically. Even though more progress has been made in the use of natural extracts as anti-ageing ingredients, their safety and efficacy are not well regulated, and this challenge makes it difficult for consumers to know if these claims are true.

Table 3. Previous studies on anti-ageing and UV protective effects of different mushroom species.

Mushroom	Pharmaceutical form	Main findings	Reference
Agaricus bisporus J.E.Lange	Polysaccharide fraction	Superoxide dismutase (SOD), catalase (CAT) and glutathione peroxidase (GSH-Px) activity were effectively improved after oral exposure to extract fraction.	(Shangshang Li, Liu, Zhang, et al., 2018)
	acidic-extractable polysaccharides	Serum activities of SOD, GSH-Px and total antioxidant capacity were enhanced *in vivo*.	(Shangshang Li, Liu, Wang, et al., 2018)
Agrocybe aegerita (Brig.) Sing	acidic- and alkalic-extractable mycelium polysaccharides	Extract displayed enhanced enzymatic (SOD, GSH-Px and CAT) and non-enzymatic (Malondialdehyde) free radical-scavenging defense.	(Jing et al., 2018)
Agrocybe cylindracea (V. Brig.) Vizzini	exopolysaccharides	Serum activities of SOD, GSH-Px and total antioxidant capacity were enhanced *in vivo*.	(H. Zhao et al., 2017)
Calocybe indica Purkay. & A. Chandra	crude polysaccharides	Serum activities of SOD, GSH-Px and total antioxidant capacity were enhanced *in vivo*.	(Govindan et al., 2016)
Grifola frondosa (Dicks.) Gray	Exopolysaccharide	At 100μg/mL, cell viability of fibroblast cells was not inhibited and expression of MMP-1 mRNA was significantly suppressed up to 61.1%.	(J. T. Bae et al., 2005)
	Mycelia extract (GF-M), Exopolysaccharide (EPS)	At 100 μg/mL EPS and GF-M inhibit expression of MMP-1 by 20 and 40%, GF-M caused a 53% increase in collagen synthesis.	(S. W. Kim et al., 2007)
Hericium erinaceum (Bull.) Persoon	Polysaccharides	Bioactive fraction significantly enhanced skin antioxidant enzymes (SOD, CAT, GSH-Px), MMP-1 activities and collagen protein levels in a dose-dependent manner.	(Hui et al., 2010)
Pleurotus citrinopileatus Singer	Extract	At 2.0, 1.1, and 4.1 mg/mL, extract inhibited hyaluronidase activity by 9.7%, 10.8%, and 25.4% respectively.	(T. X. Meng et al., 2011)
Tremella fuciformis Berk	Polysaccharides	Oral administration enhanced SOD, GSH-Px, and CAT activity after UV exposure. Collagen content in the UV-induced animal skin was enhanced up to 26%.	(Wen et al., 2016)
	Polysaccharides	After exposure to 400 μg/mL, H_2O_2-induced oxidative stress and apoptosis in human Dermal Fibroblast cells were significantly suppressed.	(T. Shen et al., 2017)
Trametes lactinea (Berk.) Sacc.	Extract	Aqueous and acetonic extract inhibited hyaluronidase activity by 88.6 ± 0.11% and 88.3 ± 0.14% inhibition for respectively.	(Y. A. Yahaya & Don, 2012)

Tricholoma matsutake (S. Ito & S. Imai) Singer	Extract	At 100 μg/mL, it decreased the expression of MMP-3 and inhibited elastase activity by 81.4 ± 3.92%.	(S. Y. Kim et al., 2014)
Volvariella volvacea (Bulliard ex Fries) Singer	Phenolic compounds and polysaccharide-rich extract	Aqueous extracts stimulate collagen biosynthesis up to 146.77±13.20%.	(Ruksiriwanich et al., 2014)
Individual compounds	**Type**	**Main findings**	**Reference**
Ascorbyl-3-*p*-coumarate, Ascorbyl-2-*p*-coumarate	Synthesized	At 100–300 μM, A-3-*p*-C, and A-2-*p*-C promote collagen release by 120–144% and 125–191%, respectively.	(Kwak et al., 2015)
Caffeic acid	Commercial	Cell viability of UV exposed HaCaT cell were maintained (3.75–30 μM) and MMP-1 activity was enhanced up to 70% at 30 μM. Serum activities of SOD, GSH-Px and total antioxidant capacity were enhanced *in vivo*.	(Pluemsamran et al., 2012)
Ellagic acid	Commercial	At 5μM suppressed the expression of MMP-1 and at 1-10μM up-regulated collagen levels.	(J. Y. Bae et al., 2010)
Ferulic acid	Commercial	Cell viability of UV exposed HaCaT cell were maintained (3.75–30 μM) and MMP-1 activity was enhanced up to 90% at 30 μM. Serum activities of SOD, GSH-Px and total antioxidant capacity were enhanced *in vivo*.	(Pluemsamran et al., 2012)
	Commercial	FA applied topically at 0.01, 0.05–1 mg/site/mouse, significantly suppressed the expression of MMP-2 and MMP-9.	(Staniforth, et al., 2012)
Ferulic and caffeic acids	Commercial	Both compounds at 200 μL offered a protective activity to UVB-induced skin erythema.	(Saija et al., 2000)
Hispidin	Commercial	Expression of heme oxygenase-1 and catalase was enhanced.	(D. E. Kim, et al., 2014)
Lentinan	Commercial	Up to 6 μg/mL, lentinan protect H_2O_2-damaged Keratinocytes (HaCaT) cells and enhanced SOD activity.	(Zi et al., 2018)
p-Coumaric acid	Commercial	At 30 μg/mL inhibited MMP-1 expression from dermal fibroblasts.	(Seok & Boo, 2015)

1.4.4. Antimicrobial activity of mushroom extracts and their associated metabolites

The skin is constantly colonized by non-pathogenic microorganisms such as *Staphylococcus aureus*, *Candida albicans* and *Streptococcus* species. The distribution and density of the skin microflora depend on the individual's age and environmental factors such as sebum secretion, temperature, and humidity (Elsner, 2006). The presence of these microorganisms is known to cause inflammatory skin diseases like atopic dermatitis, seborrheic dermatitis, cellulitis, erysipelas, impetigo, folliculitis, furuncle, carbuncle abscess and psoriasis (Alsterholm, Karami, & Faergemann, 2010). Among the common skin diseases mentioned above, atopic dermatitis and acne vulgaris have been known to be associated with increased colonization of the skin by microbes such as *S. aureus* and *P. acne* and these organisms tend to worsen the state of the diseases (Salah & Faergemann, 2015). Cosmetic industries are constantly searching for interesting bioactive compounds from natural origin to replace synthetic anti-microbial agents coupled with the fact that these microorganisms also develop resistance against conventional topical antimicrobials (Ribeiro, Estanqueiro, Oliveira, & Sousa Lobo, 2015). External application of medicinal plants in the form of paste and infusions for the treatment of skin inflammatory diseases has been practiced for many decades (Nesy & Mathew, 2014). Parabens are synthetic alkyl esters of *p*-hydroxybenzoic acid that are common preservatives in personal care products and pharmaceuticals, preventing the growth of bacteria, thanks to their broad-spectrum antimicrobial activity (Kerdudo et al 2016). However, some of their butyl and propyl esters have been discovered to cause reproductive defects (Heffernan et al., 2015). Their use is now facing some constraints, with the cosmetic industry starting to exclude this ingredient from their products (Velegraki, Hapeshi, Fatta-Kassinos, & Poulios, 2015). In this context, bioactive compounds from natural sources can become viable alternatives based on their antimicrobial activity. Phenolic acids, such as ferulic, caffeic acids and their derivatives, are known to cause disruption of bacterial and fungal cell membrane, allowing the leakage of the cytoplasmic membrane and, finally, cell death (Teodouro, Ellepola, Seneviratne, & Koga-Ito, 2015). Numerous research studies have reported the anti-microbial potential of mushrooms as well as their bioactive compounds. Alves et al. (2012) reviewed the anti-microbial activity of mushroom extracts as well as their bioactive compounds and reported that both, edible and non-edible mushroom, displayed activity against pathogenic microorganisms. *L. edodes* was indicated to be the most interesting species against both gram-positive and gram-negative bacteria followed by species from the genera *Boletus*, *Ganoderma*, and *Lepista*. Phenolic compounds have been reported to display antibacterial activity by interfering with the cell

membrane and cell wall of invading pathogen and subsequently leading to the death of the pathogen (Ribeiro et al., 2015). Alves et al., (2013) revealed that phenolic acids such as 2,4-dihydroxybenzoic, protocatechuic, vanillic and *p*-coumaric acids showed higher antimicrobial potential against both Gram-positive and Gram-negative bacteria, while ferulic, caffeic, syringic, ellagic and chlorogenic acids also displayed interesting results. These authors went on to conclude that despite the recognized antimicrobial activity of some of the enumerated compounds, their mechanism of action needs to be fully understood and before the problem of the multiple resistance of bacteria to antibiotics is solved. Some interesting antimicrobial activity reported for some individual metabolites found in mushrooms is presented in **Table 4**.

Table 4. Antimicrobial activity reported for some individual metabolites found in mushrooms.

Compound	Source	Microorganisms	Effect	Reference
2-Coumaric acid	Synthesized	*Mycobacterium tuberculosis.*	MIC value of 122 μM	(Guzman et al., 2014)
3,4-Dialkoxy caffeic acids	Synthesized	*Staphylococcus aureus, Corynebacterium diphtheria, Escherichia coli, Klebsiella pneumonia, Salmonella typhi.*	GI 100 μg/mL	(Gangan et al., 2014)
5-*O*-caffeoylquinic acid	Commercial	*Escherichia coli, Staphylococcus aureus, Enterococcus faecium, Proteus vulgaris, Pseudomonas aeruginosa, Klebsiella pneumoniae and Candida albicans.*	MIC 5–10 mg/mL	(Bajko, et al., 2016)
Caffeic and cinnamic acid ester	Synthesized	*Candida albicans* biofilm.	MIC 32 μg/mL	(De Vita et al., 2014)
Caffeic, chlorogenic, *o*-coumaric, *p*-coumaric acid	Commercial	*E. coli, S. aureus, Salmonella typhimurium, Lactobacillus rhamnosus.*	MIC 125–1000 μg/mL	(Parkar, Stevenson, & Skinner, 2008)
Chlorogenic acid	Synthesized	*S. aureus, Streptococcus pneumoniae, Bacillus subtilis, E. coli, Shigella dysenteriae Salmonella Typhimurium.*	MIC 20–80 μg/mL.	(Z. Lou, Wang, Zhu, Ma, & Wang, 2011)
Chlorogenic, rosmarinic, sinapic and ferulic acid	Commercial	*Campylobacter jejuni, Campylobacter coli.*	MIC 4.9–313 μg/mL	(Klančnik, Možina, & Zhang, 2012)
Ferulic acid	Commercial	*P. aeruginosa, E. coli, L. monocytogenes, S. aureus* biofilm formation.	MBC 500–5000 μg/mL	(Borges, Saavedra, & Simões, 2012)
	Commercial	*Bacillus cereus and Pseudomonas fluorescens* single- and dual-species biofilms.	MIC 500 μg/mL	(Lemos et al., 2014)
Ferulic acid esters	Synthesized	*Escherichia coli, Klebsiella pneumoniae, Staphylococcus aureus, Enterococcus faecalis, Candida albicans, Candida krusei, Candida parapsilosis.*	MIC 8–1024 μg/mL	(Ergün, Çoban, Onurdag, & Banoglu, 2011)
Ferulic acid, *p*-coumaric acid	Commercial	*Bacillus cereus, Micrococcus flavus, S. aureus, Listeria monocytogenes, E. coli, Enterobacter cloacae, P. aeruginosa, S. typhimurium, C. albicans.*	MIC 0.01–0.04 mg/mL	(Šiler et al., 2014)
o-Coumaric, *m*-coumaric, *p*-coumaric acid	Commercial	*C. albicans, Candida parapsilosis, Candida glabrata, Candida tropicalis, Candida krusei, Candida lusitaniae, Cryptococcus neoformans.*	GI 5.9%–99.9%	(Faria et al., 2011)
p-Coumaric acid	Commercial	*S. aureus, Streptococcus pneumoniae, B. subtilis, E. coli, Shigella dysenteriae, S. typhimurium.*	MIC 10–80 μg/mL	(Z. Lou et al., 2012)

p-Coumaric acid derivatives	Synthesized	*S. aureus*, *B. subtilis*, *E. coli C. albicans*, *Aspergillus niger*.	MIC 0.68–1.93 µM/mL	(Khatkar, Nanda, Kumar, & Narasimhan, 2017)
Trans-cinnamaldehyde, *p*-coumaric, ferulic acid.	Commercial	*E. coli* biofilm.	0.25%–0.5% concentration	(Kot, Wicha, Piechota, Wolska, & Grużewska, 2015)

GI: growth inhibitory activity, MBC: minimal bactericidal concentrations, MIC: minimum inhibitory concentration.

Some of the studies reported above have shown that mushrooms are important sources of natural bioactive compounds with the potential to be used as cosmetic ingredients to treat several disorders associated with the skin. Among the reviewed mushroom species, *Pleurotus* species seem to be the most reported even though the bioactive compounds responsible for some of the bioactive properties have not been identified yet. Other interesting mushrooms are *Agaricus* species, *Inonotus* species, *Lentinula* species, and *Ganoderma* species. Different classes of bioactive compounds were also reported to show promising cosmeceutical benefits. *p*-Coumaric acid seems to be a very interesting cosmetic ingredient because of its reported anti-collagenase, anti-tyrosinase, and anti-inflammatory activity. Some mushroom species such as *Lyophyllum decastes*, were reported to combat atopic dermatitis by oral ingestion of their fruiting bodies, resulting in the disease improvement. The results suggest that oral ingestion of mushroom can also exert a positive appearance benefit (Ukawa et al., 2007). These studies have shown that cosmeceutical and nutricosmetics formulations developed with mushroom extracts or their individual metabolites have the potential to successfully protect and defend the skin against free radicals, reduce production of inflammatory mediators, inhibit collagenase, elastase, and tyrosinase associated with inflammatory diseases, wrinkle, ageing, and hyperpigmentation. However, studies regarding the safety, topical bioavailability and clinical studies on the potential of these mushroom extracts and their associated metabolites as a cosmetic material are still lacking.

1.5. Commercially available cosmeceutical and nutricosmetic formulations with mushroom-based ingredients

Mushroom extracts and their individual metabolites have been formulated either in the form of lotions and creams for topical application or as supplements for oral ingestion. Some of them are formulated either alone or in combination with other botanical extract and are commercially available, with the sole aim of maintaining skin health. Dr. Andrew weil for Origins™ mega-mushroom (www.origins.com/dr-weil-mega-mushroom) was among the first premium western brands to exploit fungi in skin care. Launched in 2006, the product is a skin relief face mask used to calm, soothe, and defend skin against visible signs of ageing. In its formulation, it includes *Hypsizygus ulmarius* mycelium, *G. lucidum* and *Cordyceps sinensis* extracts. Recently added by Dr. Weil for Origins product catalog is Plantidote mega-mushroom body cream, a moisturizing cream containing the three mushrooms complex as well as other ingredients like

ginger, turmeric and holy basil (*Ocimum sanctum* L.). Menard is a brand of cosmetic product with mushroom ingredients (www.menard-cosmetic.com). It employs the use of *G. lucidum* extract in its Embellir range, not only to give an appearance benefit but to eliminate toxins and help repair skin damage associated with overexposure to UV radiation and free radicals. Estée Lauder developed a formulation with *G. lucidum,* wolfberry and ginseng along with other antioxidants, moisturizers, some cell-communicating ingredients and mixtures of common skin ingredients in its new Re-Nutriv sun care product (www.esteelauder.com). This product claims to defend, revive the skin radiance, and help reduce the ageing effects of everyday exposure to UV radiation, including the formation of age spots, uneven skin tone, and other imperfections. Aveeno positively ageless is a moisturizing eye cream that contains natural shiitake complex, a clinically proven antioxidant that works with the skins natural renewal process (www.aveeno.com). This formula intends to brighten the appearance of the skin around the eyes and reduce the appearance of dark circles. Positively ageless collection launched in October 2007 has been developed to improve the appearance of skin and fight the signs of ageing. Dr. Patricia Wexler owns Wexler Dermatology in New York City. The Instant De-Puff Eye Gel was reformulated with *A. bisporus* and other important ingredients (www.wexlerdermatology.com). This anti-ageing product contains ingredients that improve the skin surface and boost elastin level in the skin necessary for preventing wrinkling. One Love Organics Vitamin D Moisture Mist (www.oneloveorganics.com), formulated with different botanical extract and *L. edodes* extract is used to tone, hydrate and protect the skin against environmental stress. Body Repair Lotion from CV Skinlabs (www.cvskinlabs.com), free from synthetic fragrances, parabens, and hydroquinone, formulated with *G. lucidum* extract and other botanical extracts (*Aloe Barbadensis* leaf juice, *Calendula Officinalis* flower extract, *Curcuma Longa* (Turmeric) root extract, *Hypericum Perforatum* flower/leaf/stem extract (St. John's Wort) and *Rosa Canina* fruit oil (Rose Hip)), is used to accelerate wound healing and suppress skin inflammation. Osmia facial brightening serum is formulated with botanical extracts (broccoli, papaya, pumpkin seed oils), algae extract (*Spirulina platensis*) and mushroom extract (*L. edodes*) (https://osmiaorganics.com). This serum facilitates healthy cell turnover and improves the elasticity of the skin resulting in a more luminous and more moisturized skin appearance.

1.6. Challenges associated with the use of mushroom extracts and their associated metabolites as cosmeceutical ingredients

1.6.1. Extraction process

The emergence of bioactive compounds as value-added ingredients with potential applications in the pharmaceutical, cosmeceutical and nutraceutical industries, has drawn significant attention over the last couple of years (Chanioti & Tzia, 2018; Heleno, Martins, et al., 2015; Santos et al., 2013). Considering all the health promoting benefits associated with these compounds, their recovery is becoming a very hot topic in the multidisciplinary area of applied chemistry, biology and technology. Among several techniques of extraction, the conventional extraction methods such as maceration and heat-assisted extraction in their simplest form basically involve mixing the matrix and the solvent allowing for interaction and subsequent release of bioactive compounds. These processes require long extraction times, high solvent and energy consumption with a resulting lower extraction yield. Bearing in mind these constraints, several non-conventional extraction techniques have been utilized to successfully maximize extraction of phenolic compounds such as microwave assisted (MAE), hydrostatic pressure (HPAE), pulsed electric field (PEF), supercritical fluid extraction (SFE) and ultrasound-assisted extraction (UAE), offering advantages of short extraction time, lower solvent consumption and maximum extraction yield (Albuquerque et al., 2016; Heleno, Prieto, et al., 2016).

UAE is based on the principle of acoustic cavitation, which can disrupt the cell walls thereby allowing the release of bioactive compounds (Heleno et al., 2016; Medina-Torres et al., 2017). MAE, also an effective extraction method, maximizes extraction yield at shorter times, using moderate energy and a low solvent amount, while also offering protection to thermo-labile bioactive compounds. It is based on using microwave energy to heat up samples, causing reduction in the moisture present in the matrices, and further generates a high pressure on the cell wall, allowing the leaching out of the bioactive compounds (Heleno, Prieto, et al., 2016; Medina-Torres et al., 2017; Vieira et al., 2017). HPAE is a faster, effective, non-thermal and environment-friendly extraction process that operates under very high pressure. In this method, higher pressure favours solvent penetration into the solid cells increasing compounds release (Briones-Labarca, Giovagnoli-Vicuña, & Cañas-Sarazúa, 2018; Chanioti & Tzia, 2018; Haining & Yongkun, 2017). SFE is a sustainable extraction process that utilises supercritical fluids such as CO_2, ethane, butane, pentane, nitrous oxide, ammonia, trifluoromethane and water (Cong-cong, Bing, Yi-qiong, Jian-sheng, & Tong, 2017). This technique requires high capital investment but it is environment-friendly, safe,

non-toxic, non-carcinogenic and non-flammable (Ghafoor, AL-Juhaimi, & Choi, 2012; Santos, Villaverde, Silva, Neto, & Silvestre, 2012). PEF technology is an emerging non-thermal extraction technique that involves the exposure of solid samples to short duration electric field pulses of high intensity, causing a transmembrane potential difference across the cell membrane. When the potential difference reaches a critical value, the cell membrane starts to collapse allowing for increased intracellular metabolite extraction (Barba, Zhu, Koubaa, Sant'Ana, & Orlien, 2016; López-Giral et al., 2015; López, Puértolas, Condón, Álvarez, & Raso, 2008).

Obtaining an enhanced compound rich extract from different matrices depends on the extraction method utilised as well as the range of the experimental domain used. Different extraction variables such as solvent type and proportion, temperature, time, the molecular affinity between solvent and solute, liquid-to-solid ratio, and particle size have been reported to influence the extraction yield (Azmir et al., 2013, Heleno, Prieto, et al., 2016). Therefore, it is essential to define the main variables and relevant response criteria prior to the optimization process to determine the values corresponding to response maximization according to the defined objectives (e.g. using minimum time, energy and solvent to achieve a cost-effective and profitable extraction system). To effectively carry out an optimization, the influence of each defined variable should be independently assessed. Nevertheless, the application of mathematical models such as the response surface methodology (RSM) is gaining visibility among the scientific community. Through RSM design, the optimization of possible interactions between experimental variables is allowed simultaneously with the prediction of the most efficient conditions (Albuquerque et al., 2016; Heleno, Prieto, et al., 2016; Jiménez et al., 2018; Oludemi et al., 2018; Pinela, Prieto, Carvalho, et al., 2016; Vieira et al., 2017).

1.6.2. Use of extract vs individual compound

Extracts possess an array of structurally diverse bioactive compounds, with either similar, overlapping, different or complementary biological capacities. When these extracts are utilised, either as nutraceutical or cosmeceutical ingredients, the total biological capacity of the individual bioactive may be modified via synergistic, additive, or antagonistic interactions with other components, which may in turn change their physiological impacts (Phan, Paterson, Bucknall, & Arcot, 2018; S. Wang, Meckling, Marcone, Kakuda, & Tsao, 2011). In additive phytochemical interactions, the combined effect is equal to the sum of the individual effects of the biomolecules present in the mixture. In synergistic interaction, the combined effect produces a response greater than the arithmetical sum of their individual effects, while if an antagonistic interaction occurs, the

combined effect resulted to be less potent (Phan et al., 2018). Extracts are a combination of hydrophilic and lipophilic antioxidants, such as polyphenols, carotenoids, organic acids, and tocopherols. When these compounds coexist in a mixture, they present advantages, possibly leading to synergistic effects, but exerting health promoting benefits associated with the diverse array of bioactive molecules.

When an individual compound with a target biological property is to be utilised, large doses are often needed. The possibility to use extracts may lower the required doses due to the cumulative effect of the individual compounds present in the extract. This helps to prevent some side effects associated with the use of large amounts of the individual compounds. Significant antioxidant synergism between β-carotene paired with puerarin, quercetin and rutin were reported with an increase antioxidant activity up to 50% (R. M. Han et al., 2011). Rosmarinic acid was shown to have a strong antioxidant capacity due to its synergistic interaction with α-tocopherol, which resulted in caffeic acid generation (Panya et al., 2012). These results showed that synergistic antioxidant response of extract combinations may not necessarily be due to the interaction among polyphenols but possibly from interactions with other bioactive molecules. A synergistic interaction between chlorogenic, gallic, protocatechuic and vanillic acid was also reported (Hugo et al., 2012). On the contrary, Pinelo et al. (2004) found an antagonistic effect when catechin, resveratrol, and quercetin interacted at three different temperatures using the DPPH method. Antagonistic interactions were also reported in myricetin/naringenin combinations in terms of Oxygen radical absorbance capacity (Freeman, Eggett, & Parker, 2010). The mechanisms underlying the combined biological effects of these phytochemicals are still unknown imposing further studies to assist the future design, standardization, and optimization of extract mixtures preparation based on their synergistic or antagonist interactions. However, despite all the mentioned benefits for extracts use, they may also present some limitations. These limitations are mostly resulting from the presence of several anti-nutritional or toxic compounds such as alkaloids, tannins, saponins and mycotoxins, which at higher amounts could result in numerous health-related implications in humans (Malongane, McGaw, & Mudau, 2017). These naturally occurring compounds, when ingested can affect nutrient utilisation in the human body, especially proteins, vitamins, and minerals, which reduce their absorption, inhibit enzyme activities and reduce their bioavailability in the gastrointestinal tract (Nikmaram et al., 2017). Based on the various interactive mechanisms among these bioactive compounds, and nutritional components affecting their bioavailability, further studies must be conducted to balance extract intake. This must be based on their content in

biomolecules to maximize the supplementation process to improve the nutritional quality and health-promoting benefits of the extract.

1.6.3. Safety and Efficacy

Cosmetic users often believe that cosmeceutical claims are valid and properly regulated. Even though cosmetics are regulated by the Federal Food, Drug, and Cosmetic Act (FD&C Act) and the Fair Packaging and Labelling Act (FPLA), the term cosmeceuticals still have no meaning under the FD&C Act because of the claims stated that they have "medical drug-like effects" (Newburger, 2009). The U.S. Food and Drug Administration, Centre for Food Safety and Applied Nutrition, Office of Cosmetics and Colours, however, says, "The FD&C Act does not recognize 'cosmeceuticals' and they reiterated that a product can be a drug, a cosmetic, or a combination of both, but the term 'cosmeceutical' has no meaning under the law" (Lintner, Mas-Chamberlin, Mondon, Peschard, & Lamy, 2009). Thus, cosmeceuticals are a category of cosmetic dermatology that is still undefined, unclassified, unregulated and is still in its early years of exploitation. Advertising claims made by cosmeceutical manufacturers are investigated for efficacy by the Federal Trade Commission (FTC) and the claims suggesting that the products have a positive effect on the structure or function of the human body must be substantiated by scientific evidence. These limitations faced by the cosmeceutical firms is based on the overestimation of the efficacy and safety claims of the products, which would remove them from the cosmetic category to place them into the drug category since they are stated to improve skin function (Draelos, 2009). Most of the products introduced in the market by cosmeceutical manufacturers undergo self-policing as no regulations for cosmeceutical are in place at present times. Some of these ingredients can cause several allergies, hence the need to set up approaches and regulations to identify allergens in some of these products (Draelos, 2009). Some of the common unwanted skin irritation encountered with topical cosmeceuticals include contact dermatitis, photosensitivity, hair and nail damage, hyperpigmentation, hypopigmentation and systemic effects (Gao, Zhang, Wei, & Chen, 2008).

The Scientific Committee on Cosmetic Products and Non-Food Products intended for consumers (SCCNFP) and its successor, the Scientific Committee on Consumer Products (SCCP) is the scientific advisory body to the European Commission in matters of consumer protection with respect to cosmetic ingredients and non-food products (Pauwels et al., 2009). Safety data leading to a positive opinion include characterisation and physicochemical

properties; acute oral toxicity; skin/eye irritation; skin sensitization; *in vitro* dermal absorption; oral toxicity; mutagenicity/genotoxicity and reproductive toxicity (Vinardell and Mitjans, 2017). Over the years the body has also supported the development of alternative methods to replace animal testing. According to the Cosmetics Regulation, it is prohibited in the EU to market any cosmetic products and ingredients that have been tested on animals (Pauwels et al., 2009). It is expected that more sophisticated formulations will be developed in the future and if regulations are not continuously adhered to, more bioactive molecules with no proper safety assessment will get into the market and this might result in health implications.

Assessing the toxicological profile of cosmeceutical ingredients is a regulatory requirement and this evaluation should take the route of administration into consideration. Considering that cosmeceuticals are ingredients for topical use, studies need to be conducted in skin cell lines, in particular with keratinocytes and fibroblasts. The determination of cytotoxicity is crucial to identify toxic effects elicited by these cosmetic ingredients before they are available in the market, and over the years several *in vitro* assays have been developed to measure cell viability or toxicity (Rampersad, 2012). One of the most widely used methods is the assessment of cell membrane integrity by measuring lactate dehydrogenase (LDH) leakage. LDH is a cytosolic enzyme released into the extracellular medium when the cell membrane is compromised because of apoptosis or necrosis. Even though other cellular enzymes such as adenylate kinase and glucose-6-phosphate dehydrogenase are released during cell death, LDH is found to be stable with no significant loss of activity (Fotakis & Timbrell, 2006). Another common assay to determine cell cytotoxicity is the measurement of viable cells after exposure to an active ingredient. This is conducted by measuring the metabolic activity of the viable cells based on tetrazolium reduction (Rodrigues et al. 2013).

Like challenges in the area of safety, it is also difficult to ascertain the efficacy of some of these cosmeceuticals since the required clinical studies have, ideally, to go through several steps. Cosmeceutical development involves several steps, like extraction to identify the chemical compounds, extract purification and fractionation to isolate compounds of interest, *in vitro* studies to assess bioactive properties, studies to understand the mechanism behind the upregulation or downregulation of key cellular bioactivities, formulation in a vehicle for topical delivery, clinical trials to determine if bioactive compounds show cosmeceutical claims, and finally patenting and licencing for the product to enter the market (Draelos, 2009). Most reputable cosmeceutical formulators tend to test only the active ingredient with very few testing on the final formulation. Even when *in vivo* trials are conducted, they are often few and rarely

subjected to peer review, making physicians and dermatologists question the benefits of these cosmeceutical products (Baumann, 2012). Presently, cosmetic scientists and researchers have conducted interesting studies regarding formulation development with bioactive ingredients and, certainly, some of these cosmeceutical formulations affect the function of the skin and as such the FDA, should put in strict amendment of laws to authorize evaluation of such cosmeceuticals claims from their safety, efficacy and labelling (Newburger, 2009).

The debate whether to classify active cosmeceuticals as cosmetic or drugs is also down to the fact that the average time for drug development ranges from 7 to 15 years, because it must go through strict safety and efficacy studies (toxicology, pharmacokinetics, pharmacology, and drug-drug interaction) (Norman, 2016), while the time for cosmetic development with significant breakthrough technology can occur in less than 5 years (Newburger, 2009). Hence, time and financial resources, strict regulations and long efforts are the main reason why cosmeceutical manufacturers prefer to avoid drug classification. Although many trusted manufacturers have emerged in the cosmeceutical world, and some of the active ingredients and the final formulations have been subjected to clinical testing with proven efficacy, the lack of official oversight leaves room for doubt both from consumers, physicians, and dermatologists.

1.6.4. Stability and Degradation

Bioactive compounds from natural sources have interesting properties that can support the design of innovative cosmeceutical formulations. Despite these promising bioactive properties, the efficacy and usage of mushroom extract and their individual metabolites in topical formulations are still affected by their poor stability, increased oxidation, degradation and poor permeability across biological membranes (Casanova, Estevinho, & Santos, 2016). To overcome such constraints, new strategies have been developed in the form of nano- and micro- technologies that employ the use of coating material, either as pure compounds or a mixture of components (sugars, gums, proteins, natural and modified polysaccharides, lipids and synthetic polymers) to protect active principles, conferring protection, improving stability, and/or provide their gradual release over time, assuring therapeutic treatments at correct concentrations at the target sites (Carvalho, Estevinho, & Santos, 2016; Dias, Ferreira, & Barreiro, 2015). The encapsulation process can be performed using different methods such as coacervation, extrusion-based processes, spray-based processes, emulsion-based processes, liposomes, supercritical fluid-based processes, ultrasound-based processes and fluid bed

coating among others (Dias et al., 2015). The choice of the encapsulation technique is driven by the desired application in the product, and selected methods should be capable to produce particles with homogeneous size distribution, with high encapsulation efficiency, high loading capacity, and be able to ensure a release (Vincekovi et al., 2017). Controlled release is one of the main goals of microencapsulation, i.e. release phenomenon can be modulated, including maintained during the time (sustained release) or suppressed until the right time or site (Aguiar, Estevinho, & Santos, 2016). The mechanism behind the controlled release of the active ingredient is partly due to the physico-chemical properties of the wall materials and the type of active ingredient itself. Most release mechanisms comprise diffusion, dissolution, erosion, digestion, mechanical disruption, and triggered release due to environmental changes (i.e temperature, pH, pressure, and ionic force) (Vincekovi et al., 2017).

To develop cosmeceutical formulations using microencapsulation processes, it is vital to utilise non-toxic and biodegradable raw materials and be in accordance with the legal regulations. Additionally, evaluating the performance of the microencapsulated ingredients, after incorporation on the final products, is of high relevance and can often range from months to even years. Attention is now focused on finding effective microencapsulation methods that will optimally encapsulate the bioactive materials ensuring their sustained release. Casanova et al. (2016) prepared microparticles containing rosmarinic acid (RA) using chitosan and modified chitosan as the encapsulating materials. RA has vital biological properties, being an interesting ingredient for cosmetic formulations, but its use is limited due to its poor stability, degradation, and slow transport across biological membranes. The authors employed a spray drying technique to produce the microcapsules, and their release profile was analysed in aqueous and coconut oil media. Encapsulation yield and particle sizes were 42.6% and 39.8% and 4.2 μm and 7.7 μm for chitosan and modified chitosan particles, respectively, and the results showed that the chitosan particles displayed a slower release in water, while those in oil were more sustained. On the other hand, Biswick, Park, & Choy, (2012), due to the poor stability of caffeic acid towards solar radiation and oxidation, prepared microcapsules using zinc hydroxide nitrate as a matrix to prevent degradation and ensure a sustainable release compatible with cosmeceutical applications. The prepared microparticles were able to withstand both UVA and UVB radiation, indicating that this technology can be applied in the design of sunscreen cosmetic formulations. Due to the unique properties exhibited by chitosan, it was selected by Lee, Woo, Ahn, & Je, (2014) for encapsulating hydroxycinnamic acids (caffeic acid, ferulic acid, and sinapic acid). The idea was to develop a conjugate made up of chitosan and the

phenolic acids to evaluate and compare their bioactive properties. The antioxidant activity was screened by DPPH and ABTS assays, and the results indicated that chitosan conjugated with hydroxycinnamic acids displayed higher radical-scavenging activity than the unmodified form. The results also showed that the conjugated chitosan inhibited bacterial growth, suggesting that this application can be useful in formulations preventing bacterial growth, thus, increasing shelf life. *Candida*, a common skin microflora, was studied by Panwar, Pemmaraju, Sharma, & Pruthi (2016), who reported the potential of encapsulated ferulic acid against *C. albicans*. Ferulic acid was encapsulated into chitosan with an encapsulation efficiency and particle size diameter of 56.45% ± 2.47% and 52.54 ± 0.22 nm, respectively. The stability and integrity of the phenolic acid after encapsulation were also studied; the nanoparticles showed activity against *C. albicans* biofilm formation, confirming the integrity of ferulic acid in the microencapsulated form. The results showed that microencapsulation procedures can be efficient in the development of cosmetic formulations against fungal infection. Several technologies can be used for the encapsulation of bioactive compounds (Dias et al., 2015). Ignatova et al., (2016) encapsulated caffeic acid using poly (3-hydroxybutyrate) (PHB) and polyethylene glycol (PEG). The nanoparticles prepared by electrospinning were evaluated for antibacterial activity against *S. aureus* and *E. coli*, as well as for their release profile. The results showed that after 24 h 95.4% and 97.0% of caffeic acid were released from PHB and PEG, respectively. Free and nanoencapsulated CA displayed antibactericidal activity against *S. aureus* after 24 h exposure at 1800 µg/mL. Ouimet, Faig, Yu and Uhrich (2015) showed that encapsulated ferulic acid presented a slow release over time, so it is necessary to work on alternative methods to ensure a quicker release adapted to topical delivery. These authors reported that the incorporation of ethylene glycol with the encapsulating material could allow a faster degradation of the polymeric matrix and, therefore, a faster release. Complete release of ferulic acid was achieved after a few days, and the antioxidant activity was also found to be higher. Furthermore, Vashisth, Kumar, Sharma and Pruthi (2015) isolated and characterized ferulic acid from the *Parthenium hysterophorus* L. plant, further nanoencapsulated by electrospinning. Polylactic-co-glycolic acid (PLGA) and polyethylene oxide (PEO) were employed as encapsulating materials at a PLGA:PEO ratio of 1:1 using dichloromethane/dimethylformamide (4:1, *v/v*) as the solubilizing medium. The free and encapsulated ferulic acid were evaluated for DPPH radical scavenging activity. The antioxidant activity of the encapsulated ferulic acid was found to be 59%, while the isolated compound gave 41%, thus suggesting that encapsulated ferulic acid preserved the antioxidant activity. Even though the active ingredient can be efficiently encapsulated, there is still a continuous

search for new methods to overcome some of the limitations associated with the process of microencapsulation (Casanova & Santos, 2016). Another major drawback in the use of the microencapsulation system in personal care products involves properly evaluating the release profile of the active ingredient from the encapsulating material, as well as skin permeation studies. Furthermore, the behaviour of the microparticles produced needs to be further studied to be able to understand the mechanism of diffusion and how the microparticles interact with the lipid component of the *stratum corneum*. Hence, conducting more studies will further allow for a better understanding of the choice of encapsulating system and the polymeric material.

1.6.5. Skin permeation

The barrier properties of the SC of the skin have made it difficult for transdermal penetration of some ingredient in the cosmetic formulation. The SC offers a barrier against the entry of foreign materials, pathogens and loss of moisture (Kubota, Shibata, & Yamaguchi, 2016). Physico-chemical parameters, such as the molecular weight and lipophilic/hydrophilic balance, have been reported to affect the permeability of compounds in cosmetic formulation through the skin (T. Uchida et al., 2015). Conducting *in vitro* permeation studies is important to fully understand the permeation profile of these topically-applied chemicals. However, using human samples is very expensive and is subject to ethical evaluation, and that has led to the increased search for alternative artificial skin diffusion apparatus (T. Uchida et al., 2015, 2016). Strat-M™ (Merck Millipore, Billerica, MA, USA) is the most utilised to mimic the skin in a Franz-type diffusion cell, while epidermal full thickness (EFT) human skin cultures (MatTek, Ashland, MA, USA) can also be used to validate the penetration through skin for various bioactive metabolites. The skin permeation studies of mushroom extracts and their individual metabolites have not been fully studied, but among the ones available in the literature, only ferulic acid seems to be the most widely reported. *In vitro* experiments were conducted by Thitilertdecha, Guy, & Rowan, (2014) using a pigskin model with a cosmetic formulation containing phenolic compounds, but none of the hydroxycinnamic acids were able to penetrate the skin in an amount that could be quantified after 3 h of exposure. The authors suggested that the use of a potential skin penetration enhancer, like propylene glycol, can increase skin penetration of these compounds, but the use of penetration enhancers is subject to controversies and still lacks regulatory approval (Mujica Ascencio et al., 2016). *In vitro* skin permeation studies of a gel containing coumaric, caffeic and ferulic acids were conducted by Žilius,

Ramanauskiene, & Briedis, (2013) using Bronaugh-type diffusion cells. The results showed that after 24h exposure of the gel to the skin cells, the epidermis was found to contain 5% coumaric and ferulic acids and 4% coumaric and 6% ferulic acid in the dermis, while no traces of caffeic acid were found. The authors report that the differences in penetration might be associated with the variation in the lipophilicity of the tested compounds, as well as the composition of the cosmetic vehicle used. After 8 h of *in vitro* skin permeation experiments, over 90% phenolic compounds were released from hydrophilic gel and only up to 5% and 22% of phenolic compounds were released from ointment and w/o cream respectively. Another author prepared an aqueous vehicle with ferulic acid (FA) and its skin permeation potential was evaluated using porcine skin because of its physiological similarity to human skin (L. W. Zhang, Al-Suwayeh, Hsieh, & Fang, 2010). Ferulic acid was found to permeate the skin with the flux; a term used to denote the amount of compound that traverses across a unit area of the skin per unit time reported to be between 0.48 ± 0.10 and 1.16 ± 0.30 nmol/cm^2/h at pH 6 and pH 9, respectively. The result suggests that this compound exhibits penetration ability across the skin, and the pH of the vehicle does not significantly affect the penetration profile of this compound. The release of phenolic compounds from semisolid vehicles is influenced not only by the physiochemical properties of the bioactive ingredient but also by the properties of the vehicle and concentration of the bioactive in the formulation. L. W. Zhang et al. (2010) reported the potential of FA and its derivative ferulic acid ethyl ether (FAEE) to be utilised as an antioxidant to prevent damage from ultraviolet (UV) radiation and skin carcinogenesis. The above authors conducted a skin permeation analysis to determine transdermal bioavailability of the studied compounds using porcine skin. The results showed that FA and FAEE were able to permeate the skin and there was no significant difference in skin deposition between pH 6 and 9.9 buffers. Further studies on the compounds were evaluated by transepidermal water loss (TEWL), erythema and pH value. The result showed that topical application of FA and related compounds for up to 24 h did not cause skin irritation. Cutaneous permeation of FA into the skin layers, from different cosmetic vehicles, an O/W emulsion (pH 6.0) and two gel-type formulations (A and B at pH 6.0 and 7.4, containing FA alone and with α-cyclodextrin respectively) were conducted by Monti et al. (2011). *In vitro* permeation studies were conducted using hairless rat excised skin. The results showed that FA fluxes were 8.48±2.31, 8.38±0.89 and 5.72±0.50 μg/cm^2 h, for O/W emulsion, gels A and B, respectively, suggesting that the pH significantly influenced FA permeation. Overall, ferulic acid seem to be one of the phenolic acids with the most *in vitro* permeation studies reported (Bai et al., 2014; Harwansh, Mukherjee, Bahadur, & Biswas, 2015; Monti et al., 2011; Nazaré et al., 2014; L. W. Zhang et

al., 2010). Hence, more studies need to be conducted on more mushroom extract and their individual metabolites.

1.7. Objectives and Working Plan

The cosmetic industry is constantly in search of ingredients from natural sources because of their competitive effectiveness and lower toxicity effects. Mushrooms, for years, have been an important part of our diet because of the essential biomolecules they contain. Nowadays it is perceived that they can be interesting sources of cosmeceutical or nutricosmetic ingredients. In the present thesis, five mushroom species *Agaricus bisporus*, *Agaricus blazei*, *Ganoderma lucidum*, *Lentinula edodes,* and *Pleurotus ostreatus* were selected to evaluate their potential to be used as ingredients in cosmeceutical and nutricosmetic formulations. The specific objectives of this work were:

1. Extraction optimization to maximize the recovery of phenolic compounds and triterpenic acids from *Ganoderma lucidum* as well as ergosterol from *A. blazei*, using response surface methodology. Conventional techniques (Soxhlet and maceration) were compared with more sustainable methods (microwave and ultrasound assisted extraction).

2. Chemical and nutritional characterization of the previously mentioned species, including macronutrients, energetic contribution, hydrophilic (sugars and organic acids) and lipophilic (tocopherols and fatty acids) components. Preliminary safety tests for nutraceutical applications were conducted.

3. Preparation of ethanolic extracts from the previously mentioned species, but also from *A. bisporus*, *Lentinula edodes* and *Pleurotus ostreatus* using the Soxhlet extraction system, followed by chemical characterization in terms of phenolic acids and related compounds and ergosterol. Screening of the bioactivity of the extracts considering antioxidant, anti-tyrosinase, anti-inflammatory, antimicrobial and cytotoxic properties, and further incorporation into base cosmetic cream to provide cosmeceutical properties.

4. Evaluation of the contribution of individual phenolic acids and their related compounds (*p*-hydroxybenzoic, *p*-coumaric, protocatechuic and cinnamic acids), and ergosterol as cosmeceutical ingredients (anti-inflammatory, anti-tyrosinase and antimicrobial activity), followed by incorporation into base cosmetic creams to provide cosmeceutical properties.

5. Encapsulation of the bioactive ingredients (extracts and individual compounds) using the atomization/coagulation technique, to avoid loss of potency over time due to degradation or oxidation (confer protection). Characterization of the microparticles (morphology evaluation, particle size distribution and encapsulation efficiency), and incorporation into base cosmetic creams. Comparison of their performance in relation to free forms and physico-chemical evaluation (colour and pH) of the final formulations until 6 months of storage.

6. *In vitro* safety evaluation of the most promising extracts and their corresponding formulations, using MTT and LDH assays in keratinocyte (HaCaT) and fibroblast (HFF-1) cell lines.

7. *Ex vivo* skin permeation studies with the most promising extracts and their corresponding formulations, using a Franz diffusion apparatus with pig ear skin as permeation membrane.

CHAPTER 2: Material and Methods

2.1. Standards and reagents

For chemical analysis: Acetonitrile 99.9%, *n*-hexane 95% and ethyl acetate 99.8% were of HPLC grade from Fisher Scientific (Lisbon, Portugal). Formic acid was purchased from Prolabo (VWR International, Fontenay-sous-Bois, France). Fatty acids methyl ester (FAME) reference standard mixture 37 (standard 47885-U), ergosterol (98%), ganoderic acid A, α and δ-tocopherols and sugar standards as well as phenolic standards (*p*-hydroxybenzoic, *p*-coumaric, syringic acid, protocatechuic and cinnamic acids) were all purchased from Sigma (St. Louis, MO, USA). Tocol, β- and γ-tocopherols were purchased from Matreya (Pleasant Gap, PA, USA). Perchloric acid 70%, glacial acetic acid, and sulphuric acid were purchased from Fischer chemicals (Loughborough, UK). Vanillin from Labkem (Barcelona, Spain) and ursolic acid from Acros Organics (New Jersey, USA). Water was treated in a Milli-Q water purification system (TGI Pure Water Systems, Greenville, SC, USA).

For antioxidant activity evaluation: 2,2-Diphenyl-1-picrylhydrazyl (DPPH) was obtained from Alfa Aesar (Ward Hill, MA, USA). Trolox (6-hydroxy-2,5,7,8-tetramethylchroman-2-carboxylic acid) was from Sigma (St. Louis, MO, USA).

For cytotoxicity in human tumor and non-tumor cells: Ellipticine, phosphate buffered saline (PBS), acetic acid, sulforhodamine B (SRB), trichloroacetic acid (TCA) and Tris were purchased from Sigma (St. Louis, MO, USA). Foetal bovine serum (FBS), L-glutamine, Hank's balanced salt solution (HBSS), trypsin-EDTA (ethylenediaminetetraacetic acid), nonessential amino acids solution (2 mM), penicillin/streptomycin solution (100 U/mL and 100 mg/mL, respectively) and DMEM (Dulbecco's Modified Eagle Medium) were from Hyclone (Logan, Utah, USA).

For anti-inflammatory activity: Griess reagent system (Promega), Dimethyl sulfoxide (DMSO) and lipopolysaccharide (LPS) were obtained from Sigma-Aldrich Co. (Saint Louis, MO, USA).

For anti-tyrosinase activity: 3,4-dihydroxy-L-phenylalanine (L-DOPA) and tyrosinase enzyme were obtained from Sigma-Aldrich Co. (Saint Louis, MO, USA).

For antimicrobial activity evaluation: The culture media Mueller Hinton broth (MHB) and tryptic soy broth (TSB) were from Biomerieux (Marcy l'Etoile, France). The dye *p*-

iodonitrotetrazolium chloride (INT) was purchased from Sigma-Aldrich (St Louis, MO, USA) to be used as a microbial growth indicator.

For MTT and LDH assays: Deionized water was obtained using the Mili-Q water purification system (TGI Pure Water Systems, Carrollton, TX). Dulbecco's modified Eagle's medium (DMEM) with GlutaMAX-I, fetal bovine serum (FBS), streptomycin, penicillin, and amphotericin B were from Invitrogen (Carlsbad, CA). 3-(4,5-dimethylthiazol-2-yl)-2,5-diphenyltetrazolium (MTT) assay kit (CellTiter 96 Aqueous One Solution Cell Proliferation Assay) was purchased from Promega (Madison, WI). Lactate dehydrogenase (LDH) colorimetric cytotoxicity assay kit (LDH Cytotoxicity Detection Kit) was purchased from Takara Bio Inc. (Shiga, Japan). Human immortalized non-tumorigenic keratinocyte cell line HaCaT (Ethnicity, Caucasian; age, 62 years; gender, male and tissue, skin) was supplied by CLS cell lines service, Germany. Human foreskin fibroblasts (HFF-1) were purchased from ATCC (ATCC Number: SCRC-1041; ATCC, Manassas, VA). Caco-2 cells were obtained from American Type Culture Collection (ATCC, USA) and HT29-MTX cell line was kindly provided by Dr. T. Lesuffleur (INSERMU178, Villejuif, France). Culture flasks were from OrangeScientific, (Belgium) and Triton X-100 was purchased from Boehringer, Mannheim.

For Microencapsulation: Sodium alginate was provided by Fluka Chemie (USA), calcium chloride and Tween 80 by Panreac (Spain).

For skin permeation assays: Franz cells assembly, 9 mm with 5 mL receptor volume (PermeGear, Inc. Pennsylvania USA) and pig ear skin obtained from a slaughterhouse (Porto).

2.2. Mushroom Samples

The fruiting bodies (basidiocarps) of *A. blazei* used in the present work were donated by a local producer in Maringá, Paraná, Brazil. They were dried in a circulation oven at 40 °C and milled to a fine powder (40 mesh). Finally, the samples were vacuum packed and stored at room temperature until analysis. Fresh samples of *Pleurotus ostreatus, Agaricus bisporus* and *Lentinula edodes* were purchased from a local supermarket in the Northeast of Portugal. The fruiting bodies were dried at 30 °C in an oven, reduced to a fine powder (20 mesh) and were stored at room temperature until analysis. The fruiting bodies of *Ganoderma lucidum* were provided by Bioreishi - Agricultura Biologica, Lda, Portugal (Reishi producers; Batalha,

Portugal) as dry material. The specimens were reduced to powder (20 mesh) and mixed to obtain homogeneous samples.

2.3. Extraction methodologies

2.3.1. Heat-assisted extraction (HAE)

The samples of dry powdered mushroom (600 mg) were placed in a vial with 20 mL of solvent maintaining the solid/liquid ratio (S/L) at 30 g/L. The beaker was then placed in a thermostatic water bath under continuous electromagnetic stirring for the required time. The variables tested were: time (t, min), temperature (T, ºC) and solvent content (S, %). The powdered samples were extracted using different t, T, and S as defined by the RSM design. After extraction, samples are filtered, supernatant is carefully collected, and the dry weight obtained to deduce the extraction yield.

2.3.2. Soxhlet extraction (SE)

Soxhlet extraction is also an HAE. The powdered samples (3.0 g) were extracted with 100 mL of ethanol by refluxing in a Soxhlet apparatus. Finally, the solvent was evaporated under reduced pressure (rotary evaporator Büchi R-210, Flawil, Switzerland) to obtain the dried ethanolic extracts. To compare the efficiency of the extraction system, the number of cycles in the Soxhlet system was taken into consideration and up to seven cycles were analysed.

2.3.3. Microwave-assisted extraction (MAE)

The MAE process was performed with a Biotage Initiator Microwave (Biotage® Initiator+, Uppsala, Sweden) using closed vessels. The samples mushroom powder (300 mg) were extracted with 10 mL of solvent maintaining the solid/liquid ratio (S/L) at 30 g/L. The variables and ranges tested were: time (t, min) and temperature (T, ºC). During processing, the fixed hold-time and cooling options were "off", samples were stirred at 600 rpm using a magnetic stirring bar, power variable was set to 400W as previous studies have shown that microwave power has nearly no influence on the extraction process (Pinela, Prieto, Carvalho, et al., 2016). After extraction, samples are filtered, supernatant is carefully collected, and the dry weight obtained to deduce the extraction yield.

2.3.4. Ultrasound-assisted extraction (UAE)

The UAE was carried out using an ultrasonic probe device (QSonica sonicators, model CL-334, Newtown, CT, USA). The dried mushroom powder (3 g) were extracted with 100 mL (solvent at different %) maintaining the solid/liquid ratio (S/L) at 30 g/L using different times (t, min) and ultrasound power ranges (P, W), while the temperature was constantly maintained at 30-35 ºC using an ice bath (Heleno, Diz, et al., 2016). The obtained extraction solutions were filtered through a Whatman paper nº 4 and then evaporated under reduced pressure to remove the solvent, and the dry weight obtained to deduce the extraction yield.

2.4. Analysis of the chemical composition

2.4.1. Total phenolics

Total phenolics (Ph) in the mushroom extract was estimated based on the procedure reported previously (Heleno et al., 2012). In brief, the extract solution (0.5 mL, 1 mg/mL) was mixed with the Folin–Ciocalteu reagent (2.5 mL, previously diluted in water 1:10, v/v) and sodium carbonate (Na_2CO_3; 2 mL, 75 g/L). The tubes containing the solutions were then vortexed for 15 s and allowed to stand for 30 min at 40 °C for colour development. The absorbance was then measured at 765 nm against a blank (methanol). Gallic acid (chosen as the standard) was used to obtain the calibration curve (0.0094–0.15 mg/mL), and the results were expressed as mg of gallic acid equivalents (mg equiv. GA).

2.4.2. Total terpenoids

Mushroom material (800 mg) was extracted with methanol (10 mL) for 1 h and subsequently filtered. Shortly, 1 mL of the supernatant was mixed with chloroform (0.4 mL) and sulphuric acid (0.6 mL). The sample solution absorbance was measured at 538 nm against a blank containing methanol, using a UV-visible-light spectrophotometer (UV-160A; Shimadzu Corporation, Kyoto, Japan). Linalool (0.1875–6 mg/mL in methanol) was used as a standard and results were expressed in mg of linalool per g of dw.

2.4.3. Total triterpenes

The triterpene content was evaluated according to the protocol described by Chang, Lin, & Lai, (2012). Shortly, 10 mg of the previously obtained mushroom extract was dissolved in 1 mL methanol, 100 μL of this solution was mixed with a vanillin-glacial acetic acid solution (150 μL, 5% w/v) and perchloric acid solution (500 μL, 70%) in triplicate. Sample solutions are further heated for 45 min at 60 °C and then cooled in an ice-water bath followed by addition of glacial acetic acid (2.25 mL). The absorbance of the sample solution was measured at 548 nm against a blank containing methanol, using a UV-visible-light spectrophotometer (UV-160A; Shimadzu Corporation, Kyoto, Japan). Ursolic acid (0.0078–0.5 mg/mL in methanol) was used as a standard. Results were expressed as milligram ursolic acid equivalent (mg ursolic acid equivalent/g extract).

2.4.4. Individual phenolic acids

Dried extracts were re-dissolved in a water/ethanol mixture (80:20, v/v) and filtered through a 0.22 μm nylon disposable filter. The Shimadzu 20A series ultra-fast liquid chromatograph (UFLC, Shimadzu Corporation, Kyoto, Japan), operating at 0.5 mL/min and equipped with a Waters Spherisorb S3 ODS2 C18 column (3 μm, 150 × 4.6 mm) thermostatted at 35 °C, was used for phenolic acids identification and quantification. A binary solvent mixture consisting of 0.1 % formic acid in water (A) and acetonitrile (B) was used. The detection was performed using a photodiode array detector (PDA) at 280 nm as the preferred wavelength. The phenolic acids were quantified using calibration curves obtained from commercial standards, namely: protocatechuic acid (y = 164741x; R^2 = 0.999), p-hydroxybenzoic acid (y = 113523x; R^2 = 0.999), p-coumaric acid (y = 433521x; R^2 = 0.998), syringic acid (y = 376056x; R^2 = 0.998) and cinnamic acid (y = 583527x; R^2 = 0.998). The results were expressed as μg per g of extract.

2.4.5. Individual triterpenes

For the individual triterpenoid compounds characterization, the obtained extracts were dissolved in ethanol (5.5 mg/mL), filtered through a 0.22 mm nylon syringe filter and analysed by HPLC-DAD-ESI/MSn in a Dionex Ultimate 3000 UPLC system (ThermoScientific, San Jose, CA, USA). The equipment consisted of a diode array detector coupled to an electrospray

ionization mass detector, a quaternary pump, an auto-sampler (kept at 5˚C), a degasser and an automated thermostated column section (kept at 35 ˚C). Waters Spherisorb S3 ODS-2 C_{18} (3 mm, 4.6 × 150 mm, Waters, Milford, MA, USA) column was used. The solvents used were (A) 0.1% formic acid in water and (B) acetonitrile. The gradient elution applied was: 15% B (0-5 min), 15% B to 20% B (5-10 min), 20-25% B (10-20 min), 25-35% B (20-30 min), 35-50% B (30-40 min), the column was then re-equilibrated, using a flow rate of 0.5 mL/min. Data were collected simultaneously with DAD (280 nm) and in negative mode detection on a Linear Ion Trap LTQ XL mass spectrometer (ThermoScientific, San Jose, CA, USA), following a procedure previously described by Bessada, Barreira, Barros, Ferreira, & Oliveira, (2016). Xcalibur® data system (ThermoScientific, San Jose, CA, USA) was used in data acquisition. To perform quantitative analysis, the calibration curves of the available triterpenoid standards were constructed based on the UV signal (ganoderic acid A: y = 2539.7x, R^2 = 0.999). Compounds with unavailable commercial standards were quantified using the calibration curve of the most similar available standard. The results were expressed as mg/g of extract.

2.4.6. Ergosterol

Each dried mushroom extract was re-dissolved in ethanol and filtered through a 0.22 µm nylon disposable filter. The ergosterol identification and quantification was performed in HPLC-UV equipment, an integrated system composed by a pump (Knauer, Smartline system 1000, Berlin, Germany), a degasser system (Smartline manager 5000), an auto-sampler (AS-2057 Jasco, Easton, MD, USA), and a UV detector (Knauer Smartline 2500) according to a procedure previously described by Barreira, Oliveira, & Ferreira, (2014). Chromatographic separation was achieved with an Inertsil 100A ODS-3 reversed-phase column (5 µm, 4.6 × 150 mm, BGB Analytik AG, Boeckten, Switzerland) operating at 35 °C (7971R Grace oven). The mobile phase was acetonitrile/methanol (70:30, v/v) and detection was performed at 280 nm. The results were expressed as mg per g of extract.

2.5. Analysis of the nutritional composition

2.5.1. Crude composition

The samples were analysed for its crude composition (proteins, fat, carbohydrates and ash) using the standard AOAC procedures (Latimer 2016). The sample crude protein content (N

4.38) was estimated by the Kjeldahl method; the crude fat was determined using a Soxhlet apparatus by extracting a known weight of sample with petroleum ether; the ash content was determined by incineration at 600 ± 15 °C. The amount of available carbohydrate present in the given sample was determined by using Anthrone method. The total carbohydrates were calculated by difference and the energy content estimated using the following equation:

Energy (kcal) = 4 (g protein) + 4 (g carbohydrate) + 9 (g fat).

2.5.2. Sugars

Free sugars were identified and quantified using the high-performance liquid chromatography coupled to a refraction index detector (HPLC-RI) after an extraction procedure previously described by Fernandes et al. (2016). The equipment consists of an integrated system with a pump (Knauer, Smartline system 1000, Berlin, Germany), a degasser system (Smartline manager 5000), an autosampler (AS-2057 Jasco) and an RI detector (Knauer Smartline 2300), operating at 30 °C (7971 R Grace oven). The chromatographic separation was achieved with a Eurospher 100-5 NH_2 column (5 µm, 4.6 mm x 250 mm, Knauer). Quantification was achieved based on refraction signal response of each standard, using the internal standard (IS, raffinose) method and by using calibration curves obtained from commercial standards of each compound: fructose (y=0.864x; R^2=0.999); glucose (y=0.909x; R^2=0.999); mannitol (y=0.892x; R^2=0.999) and trehalose (y=0.953x; R^2=0.999). The results were recorded and processed using Clarity 2.4 software (DataApex, Prague, Czech Republic), Sugar contents of the samples were further expressed in g per 100 g of dw.

2.5.3. Fatty acids

Samples (1.5 g) were extracted using the Soxhlet apparatus with petroleum ether as recycling solvent. The samples undergo transesterification using a derivatization reagent in the presence of anhydrous sodium sulfate as a catalyst (Fernandes et al., 2016). The analysis was carried out using a gas chromatography equipment (DANI 1000, Contone, Switzerland), with a split/splitless injector and a flame ionization detector (FID at 260 °C). Separation was achieved with a Macherey-Nagel (Duren, Germany) column (50% cyanopropyl-methyl- 50% phenylmethyl polysiloxane, 30 m×0.32 mm ID×0.25 µm df). The oven temperature program was as follows: the initial temperature of the column was 50 ºC, held for 2 min, then a 30

ºC/min ramp to 125 ºC, 5 ºC/min ramp to 160 ºC, 20 ºC/ min ramp to 180 ºC, 3 ºC/min ramp to 200 ºC, 20 ºC/min ramp to 220 ºC and held for 15 min. The carrier gas (hydrogen) flow-rate was 4.0 mL/min (0.61 bar), measured at 50 ºC. Split injection (1:40) was carried out at 250 ºC. Fatty acids identification was made by comparing the relative retention times of FAME peaks from samples with standards. The results were recorded and processed using CSW 1.7 software (DataApex 1.7, Prague, Czech Republic), and expressed in relative percentage (%) of each fatty acid.

2.5.4. Tocopherols

Tocopherols were determined similarly to a procedure previously described by Fernandes et al. (2016). Samples (500 mg) were extracted in the presence of BHT (butylhydroxytoluene) solution in hexane (10 mg/mL; 100 ml) and internal standard (IS) solution in hexane (tocol; 2.0 mg/mL; 250 mL). The samples were homogenized with methanol (4 mL) by vortex mixing (1 min), followed by addition of hexane (4 mL), NaCl aqueous solution (2 mL) and homogenizing the mixture (1 min). The samples were centrifuged (Centurion K24OR-2003 refrigerated centrifuge) 5 min and the clear upper layer were carefully transferred to a vial. The sample was re-extracted twice with hexane. The combined extracts were taken to dryness under a nitrogen stream, re-dissolved in 1 mL of hexane, dehydrated with anhydrous sodium sulfate, filtered through a 0.22 µm nylon disposable filter, transferred into a dark injection vial and analysed by HPLC coupled to a fluorescence detector (FP-2020; Jasco, Easton, MD, USA) programmed for excitation at 290 nm and emission at 330 nm. The chromatographic separation was achieved with a Polyamide II (5 µm, 250 mm x 4.6 mm) normal-phase column from YMC Waters (Dinslaken, Germany) operating at 30 °C. Quantification was based on calibration curves obtained from commercial standards of each compound: α-tocopherol (y=1.295x; R^2=0.991); β-tocopherol (y=0.396x; R^2=0.992); γ-tocopherol (y=0.567x; R^2=0.991); δ-tocopherol (y=0.678x; R^2=0.992). The results were expressed in µg per 100 g of dw.

2.5.5. Organic acids

Organic acids were determined following a procedure previously optimized and described by the authors Barros, Pereira, & Ferreira, (2013). Samples (1.5 g) were extracted by stirring with 25 mL of meta-phosphoric acid (25 °C at 150 rpm) for 45 min and subsequently filtered through Whatman no. 4 paper. The resulting solution was filtered through 0.2 µm nylon filters and

analysis was performed by ultra-fast liquid chromatograph (UFLC) coupled to photodiode array detector (PDA), using a Shimadzu 20A series UFLC (Shimadzu Cooperation). Detection was carried out in a PDA, using 215 and 245 nm as preferred wavelengths. The organic acids were quantified by comparison of the area of their peaks recorded at 215 nm with calibration curves obtained from commercial standards of each compound: oxalic acid, ($y=9\times10^6 x$; $R^2=0.99$); malic acid ($y=912441 x$; $R^2=0.99$) and citric acid ($y=1\times10^6 x$; $R^2=0.99$). The results were expressed in mg per 100 g of dry weight.

2.6. Bioactive properties evaluation

2.6.1. Antioxidant activity

2.6.1.1. Reducing Power

The extracts were dissolved in ethanol at 10 mg/mL and further diluted to achieve several concentration ranges (25 mg/mL to 0.078 mg/mL). The extract solutions (0.5 mL) were mixed with sodium phosphate buffer (200 mmol/L, pH 6.6, 0.5 mL) and potassium ferricyanide (1% *w/v*, 0.5 mL). The mixture was incubated at 50 ˚C for 20 min and trichloroacetic acid (10% *w/v*, 0.5 mL) was added. Then, 0.8 mL of the mixture was transferred to a 48-well plate, followed by addition of deionized water (0.8 mL), ferric chloride (0.1% *w/v*, 0.16 mL) and the absorbance measured at 690 nm in the Microplate Reader (ELX800 Bio-Tek Instruments, Inc.). Trolox was used as a positive control.

2.6.1.2. DPPH scavenging activity

The reaction mixture in each 96-wells consist of 30 µL of each different concentration of ethanolic extract solution and 270 µL of methanol containing DPPH radicals (6×10^{-5} mol/L). The mixture was allowed to stand in the dark for 1 h. The absorbance was measured at 515 nm in the Microplate Reader mentioned above. The radical scavenging activity (RSA) was calculated using the equation: $\%RSA = [(A_{DPPH} - A_S)/A_{DPPH}] \times 100$, where A_S is the absorbance of the sample solution with the sample and A_{DPPH} is the absorbance of the DPPH solution. The concentrations responsible for 50% of RSA (EC_{50} values) were calculated from the graphs of RSA percentages versus extract concentrations.

2.6.2. Anti-tyrosinase activity

Tyrosinase inhibition assay was performed using L-DOPA as substrate according to the procedure described by Yoon et al. (2011). The ethanolic extract was dissolved in 50% DMSO at 10 mg/mL and submitted to successive dilutions (10 to 0.10 mg/mL). The assays were carried out in a 96-well microplate with each well containing 40 µL of the sample, 80 µL of phosphate buffer (0.1 M, pH 6.8), 40 µL of tyrosinase enzyme (60 units/mL) and 40 µL of L-DOPA (3.5 mM). The mixture was incubated for 10 min at 37 °C and the absorbance measured at 475 nm using a microplate reader (ELX800 Bio-Tek Instruments, Inc.). L-ascorbic acid was used as the positive control and the results were compared with a control comprising 50% DMSO instead of the sample. The percentage of tyrosinase inhibition was calculated as follows: $[(A_{control} - A_{sample})/A_{control}] \times 100$. EC_{50} values were calculated from the calibration curve of tyrosinase inhibition percentage versus extract concentration.

2.6.3. Anti-inflammatory activity

The anti-inflammatory activity was carried out according to the procedure reported by Moro et al. (2012). The mouse macrophage-like cell line RAW 264.7 cultured in DMEM medium was supplemented with 10% heat-inactivated fetal bovine serum, glutamine and antibiotics at 37 °C under 5% CO_2, in humidified air. A cell density of 5×10^5 cells/mL was used followed by seeding cells in a 96-well plate at 150,000 cells/well and allowed to stand for attachment overnight. The cells were treated with different concentration of extract (400 to 50 µg/mL) in order to determine effective concentration necessary to evaluate the anti-inflammatory activity, followed by stimulation with LPS (1 µg/mL) for 18 h. The effect of all the tested samples in the absence of LPS was also evaluated, in order to observe if they induced changes in nitric oxide (NO) basal levels. In negative controls, no LPS was added. Both extracts and LPS were dissolved in supplemented DMEM. Nitric oxide was evaluated using Griess Reagent System kit which contains sulphanilamide, *N*-(1-napthyl) ethylenediamine hydrochloride (NED) and nitrite solutions. A reference curve of the nitrite (sodium nitrite 100 µM to 1.6 µM; y = 0.0066x + 0.1349; R^2 = 0.9986) was prepared in a 96-well plate. The cell culture supernatant (100 µL) was transferred to the plate and mixed with sulphanilamide and NED solutions, 5–10 min each, at room temperature. The nitric oxide produced was determined by measuring the absorbance at 540 nm (microplate reader ELX800 Biotek), and by comparison with the standard calibration curve.

2.6.4. Antimicrobial activity

The microbial strains used in the present work are clinical isolates obtained from patients hospitalized in various departments at the Hospital Centre of Trás-os-Montes and Alto Douro (Vila Real, Portugal). Six Gram-negative bacteria (*Escherichia coli*, *E. coli* ESBL, *Klebsiella pneumoniae*, *K. Pneumoniae* ESBL, *Proteus mirabilis* and *Morganella morgani* (all isolated from urine), *Pseudomonas aeruginosa* (isolated from expectoration)) as well as four Gram-positive bacteria (*Enterococcus faecalis* (isolated from urine), methicillin-sensitive *Staphylococcus aureus* (MSSA) (isolated from wound exudate), *Listeria monocytogenes* and methicillin-resistant *Staphylococcus aureus* (MRSA) (isolated from expectoration)), and *Candida albicans* (isolated from urine) were tested . All microbial strains were cultured in the appropriate fresh medium for 24 h and kept in the oven at 37 ˚C before analysis in order to maintain the exponential growth phase.

The minimal inhibitory concentration (MIC) was determined by the microdilution method using *p*-iodonitrotetrazolium chloride (INT) dye as a microbial growth indicator. Initially, 50 µL of the extract solution at different concentrations were added to 450 µL of medium TSB or MHB, according to the bacteria requirements. Then, 190 µL of this extract solution was added to each well of the 96-well microplate and therefore submitted to successive dilutions over the wells containing 90 µL of MHB or TSB media, starting by taking 100 µL of the higher concentration to the right below one and thus repeating this procedure sequentially. Afterward, 10 µL of inoculum (1.5×10^8 CFU/mL) was added to all the microplate wells. Three negative controls were prepared (one with MHB/TSB 5% DMSO, another one with the extract, and the third one with medium and antibiotic). Colistin and vancomycin were used for Gram-negative and Gram-positive bacteria's respectively. Positive control was also performed with MHB/TSB medium at 5% DMSO and the inoculum. The plates were then incubated at 37 ˚C, for 24 h, in an oven (Jouan, Berlin, Germany) and the MIC determined after adding INT (0.2 mg/mL, 40 µL) and incubating at 37 ˚C for 30 min. Viable microorganisms reduced the yellow dye to a pink colour. MIC was defined as the extract concentration that prevented colour change thus showing complete inhibition of microbial growth (Kuete et al., 2011).

2.6.5. Cytotoxic activity

2.6.5.1. Cytotoxicity in human tumor cell lines

The antitumor potential of the extract was evaluated in four human tumor cell lines MCF-7 (breast adenocarcinoma), NCI-H460 (non-small cell lung cancer), HeLa (cervical carcinoma) and HepG2 (hepatocellular carcinoma) according to the procedure previously reported by Abreu et al. (2011). Cells were routinely maintained as adherent cell cultures in RPMI-1640 medium supplemented with 10% heat-inactivated FBS and 2 mM glutamine, at 37 °C, under 5% CO_2, in humidified air. Each cell line was plated at an appropriate density (7.5×10^3 cells/well for MCF-7 and NCI-H460 or 1.0×10^4 cells/well for HeLa and HepG2) in 96-well plates. The sulforhodamine B assay was performed and ellipticine an antitumor agent was used as positive control. Extract concentrations (1.56–400 µg/mL) were added to the cells and incubated for 48 h. After that, prechilled trichloroacetic acid (TCA 10%, 100 µL) was added and incubated for 60 min at 4 °C to improve the adherence of the cells. The plates were washed with deionized water, dried and after the addition of a sulforhodamine B solution (SRB 0.1% in 1% acetic acid, 100 µL), the mixture was incubated for 30 min at room temperature. Subsequently, the plates were washed with acetic acid (1%) to remove the unbound SRB and dried. The bounded SRB was solubilized with Tris (10 mM, 200 µL) and the absorbance measured at 540 nm using an ELX800 microplate reader (Bio-Tek Instruments, Inc.; Winooski, VT, USA). The results were expressed as GI_{50} values in µg/mL which correspond to sample concentration that inhibited 50% of the net cell growth.

2.6.5.2. Cytotoxicity in non-tumor liver cells primary culture

Cell culture from a freshly harvested porcine liver obtained from a local slaughterhouse was prepared and designated as PLP2. The cell culture was constantly monitored every two to three days using a phase contrast microscope. Before confluence was reached, cells were sub-cultured and plated in 96-well plates at a density of 1.0×10^4 cells/well in DMEM medium supplemented with 10% FBS, 100 U/mL penicillin and 100 µg/mL streptomycin. The results were expressed as GI_{50} values in µg/mL as described above.

2.6.6. MTT assay

MTT assay was used to assess cell integrity of the extract and the final cosmetic formulation by monitoring the uptake of the vital mitochondrial dye, 3–(4,5-dimethylthiazol-2-yl)-5-(3-

carboxymethoxyphenyl)-2–(4-sulfophenyl)-2H-tetrazolium (MTT) by cell mitochondria. For the cell treatment, samples were dissolved in DMEM and subsequent dilutions were prepared from 1μg/mL to 10 mg/mL. HaCaT, HFF-1, Caco-2, and HT29-MTX cell lines were grown separately in tissue culture flasks (Orange Scientific, Belgium). Cell lines were grown in DMEM medium fortified with L-glutamine, 10% inactivated fetal calf serum (FBS), antibiotic–antimitotic mixture (final concentration of 100 U/mL penicillin, 100 μg/mL streptomycin and 0.25 μg/mL amphotericin B) maintained in 5% CO_2 incubator (Cell Culture$^®$ CO_2 Incubator, ESCO GB Ltd., UK). At 90–95% confluence, cells were trypsinized and plated in microtiter dishes. The viable cells were counted using trypan blue dye (Gibco) in a hemocytometer. Cell viability was assessed using the (MTT) conversion assay. Cells were cultured in 96-well micro titter plate at a density of $25×10^3$ cells per mL culture medium for 24 h. Then, cells were incubated with 1 μg/mL–10 mg/mL of both extracts and its corresponding formulation, for 24 h at 37 ˚C. After the removal of samples from the wells, cells were washed in phosphate-buffered saline, followed by addition of fresh medium. The micro titer plates were then incubated in a humidified atmosphere of 5% CO_2 at 37 ºC for 24 h. To evaluate the number of viable cells, 100 μL of MTT solution was added into each well and incubated for 4 h at 37 ˚C in the dark. Afterward, the medium was removed, the intracellular formazan crystals were solubilized and extracted with 100 μL dimethylsulfoxide (DMSO). After 15 min in continuous stirring at room temperature, the absorbance was measured at 490 nm with background subtraction at 630 nm in a Synergy HT Microplate Reader (BioTek Instruments, Inc., Winooski, VT) (Rodrigues et al., 2013).

2.6.7. LDH assay

To access cell integrity and cytotoxicity of the extracts and final cosmetic formulations leakage of the cytosolic enzyme, lactate dehydrogenase (LDH) into the cell medium (LDH assay) was measured. For the cell treatment, samples were dissolved in DMEM and subsequent dilutions were prepared from 1 μg/mL to 10 mg/mL. In both tests, triplicate wells were incubated with fresh medium in the absence or presence of samples. Briefly, cell lines were seeded in 96-well plates and cultured for 48 h. Ethanolic extract at different concentrations was prepared in the appropriate medium and added to the cells. After incubation (37 C/5% CO_2), cells were washed twice with PBS (pH 7.4) and the kits were used according to the instructions of the manufacturers (Rodrigues et al., 2013). To determine maximum LDH release (high control),

some cells were solubilized with a final concentration of 1% (w/v) Triton X-100. Absorbance was measured at 490 nm with background subtraction at 690 nm in a Synergy HT Microplate Reader (BioTek Instruments, Inc., Winooski, VT). Each concentration was tested in triplicate in three independent experiments.

2.7. *Ex vivo* skin permeation studies

Skin model. Porcine ear skin was freshly obtained from a slaughterhouse in Porto, Portugal. Preparation of the porcine skin samples consisted of cleaning with water to remove debris and drying them with paper towels. The prepared skin was protected with aluminum foil and frozen at -20 °C until required. Before each test, the skin was placed in a 0.9 % NaCl solution at room temperature for rehydration.

Franz diffusion cells. The Franz diffusion cell system was used to test the penetration of compounds present in the ethanolic extract of *P. ostreatus* and *G. lucidum* and their corresponding formulations. A Franz cell assembly (9 mm unjacketed Franz Diffusion Cell) comprising a 5-mL receptor volume and a diffusion area of 0.8 cm^2 (PermeGear, Inc. Pennsylvania USA) was used. The skin cells were placed between the donor and the receptor phase with the *stratum corneum* side facing upward into the donor compartment. The donor medium consisted of 300 µL (500 µg/mL) in the case of ethanolic extracts and 100 mg of formulation accurately spread on the skin membrane with the help of a spatula. The receptor (5 mL) was filled with PBS buffer. The stirring rate and temperature of the receptor solution were, respectively, kept at 600 rpm and 37 °C. At appropriate intervals (15 min, 30 min, 45 min, 1 h, 2 h, 4 h, 6 h and 8 h) 600 µL aliquots of the receptor medium were withdrawn with a syringe and immediately replaced with equal volumes of fresh receptor phase (Casiraghi et al., 2017). The cumulative quantity of compounds was determined by HPLC.

2.8. Microencapsulation procedure

The atomization/coagulation technique was employed to microencapsulate mushroom extracts and individual metabolites, similarly to the protocol reported by Caleja et al. (2016) with slight modifications. Sodium alginate, in combination with calcium chloride (CaCl$_2$), was used. The

microspheres were produced as follows: 100 mg in the case of extracts and 50 mg for individual compounds were suspended in 20 mL of distilled water in the presence of 100 mg of tween 80 as a surfactant. The mixture was then homogenized for 20 min using a Unidrive X100 homogenizer (Ingenieurbüro CAT, Germany). Afterward, 400 mg of sodium alginate was added to the suspension, keeping this mixture under stirring until complete dissolution of alginate. The produced solution was atomized in the NISCO Var J30 system (Zurich, Switzerland) at a flow rate of 0.3 mL/min and a nitrogen pressure of 100 mbar (**Figure 14**).
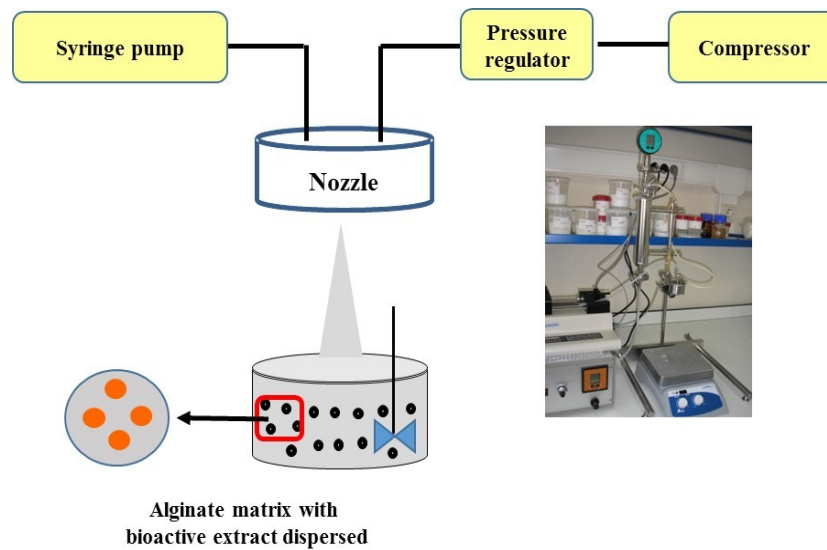
Figure 14. Nisco Var J30 microencapsulation unit used for microparticles preparation.

The atomized droplets were coagulated by contacting with the aqueous solution of $CaCl_2$ (250 mL, concentration of 4% (w/v)) over a time period of 4 h. The produced microspheres were then recovered by filtration under reduced pressure, washed twice with distilled water, and finally lyophilized and stored in the dark conditions at 4 °C.

2.8.1. Microspheres characterization

Microspheres were analysed by optical microscopy (OM) using a Nikon Eclipse 50i microscope (Tokyo, Japan) equipped with a Nikon Digital Sight camera and NIS Elements software for data acquisition. OM analysis was applied to assess the size and morphology of the microspheres after the atomization and coagulation stages.

2.8.2. Microparticle yield, loading and encapsulation efficiency

*Encapsulation efficiency (*EE %*)*

This parameter measures the ability of the encapsulating material to properly encapsulate the bioactive ingredient and can be achieved by analysing the amount of compounds presents in the coagulation solution and in the first washing solution by using the HPLC system. The encapsulation efficiency is calculated using the following expression:

$$\text{EE (\%)} = \frac{mass\ of\ encapsulated\ bioactive}{total\ mass\ of\ bioactive} \times 100$$

*Encapsulation yield (*EY %*)*

This parameter compares the total mass of microcapsules obtained after encapsulation and the total mass of material before encapsulation. It is calculated using the following expression:

$$\text{EY (\%)} = \frac{mass\ of\ microphere\ produced}{mass\ of\ polymeric\ material + mass\ of\ bioactive\ ingredient} \times 100$$

*Encapsulation load (*EL %*)*

This parameter measures the mass fraction of encapsulated bioactive ingredient per unit mass of the encapsulating material and is expressed using the relation:

$$\text{EL (\%)} = \frac{mass\ of\ encapsulated\ bioactive}{mass\ of\ microphere\ produced} \times 100$$

2.8.3. Particle size measurement

The particle size distribution of the microspheres was analysed using a Malvern Mastersizer 3000 laser diffraction equipment, equipped with a Hydro MV dispersion unit (Malvern, UK). Data were obtained and treated with Mastersizer software version 3.10. Water was used as a sample dispersion medium. Five measurements were made to ensure reproducibility, and the results were expressed in volume distributions, being the mean particle size results expressed as the percentiles of 10%, 50%, and 90%. All the residual values were less than 1%. The number distribution was calculated based on the volume distribution, and the corresponding

percentiles were also obtained. The span of the particle size distribution in terms of volume was also determined using the expression $(Dv_{90}-Dv_{10})/Dv_{50}$.

2.9. Incorporation of the extracts in a base cosmetic cream

In the present work, a base cosmetic cream Versatile™, with a light colour, free from fragrances, colourants, parabens, mineral oils, sodium lauryl sulfate (SLS), propylene glycol, and ethoxylates purchased from Fagron Iberica S.A.U. (Barcelona, Spain) was used. According to the supplied technical data available, this formulation has been certified to be safe by the US Food and Drug Administration (FDA), Regulation (EC) No 1907/2006—REACH and the National Health Surveillance Agency (ANVISA) of Brazil. Example of active pharmaceutical ingredients (APIs) and Dermaceutical ingredients (DIs) compatible with Versatile™ cream base is described in **Table 5**.

To cover all the bioactive properties evaluated, the base cosmetic creams were incorporated with 2.5 times EC_{50} and MIC values which correspond to a scale of 25 mg of extract and 125 mg of microspheres per gram of base cream. For the compounds, 7 mg of individual compound and 63 mg of microspheres were incorporated per gram of base cream. The formulations were continuously mixed until sample homogenization is fully achieved. The samples were stored at 5 °C for chemical characterization, evaluation of bioactive properties and its physico-chemical properties. The final cream formulations were extracted with methanol for 30 min, filtered, dried in a rotary evaporator, and re-dissolved in a water:methanol mixture (80:20, *v/v*) for phenolic acids analysis; in methanol for ergosterol analysis; in 50% DMSO for anti-inflammatory activity evaluation; in 50% DMSO for anti-tyrosinase activity evaluation; in 100% DMSO for antioxidant activity evaluation; and in 5% DMSO for antibacterial activity evaluation.

Table 5. List of active pharmaceutical ingredients (APIs) and Dermaceutical ingredients (DIs) usual intervals for dermatological application.

Ingredients	Topical intervals	Versatile™
Alpha-bisabolol	0.5-5	0.5-5
Aloe vera	0.5-10	0.5-10
Ascorbic, acid	5-15	5-15
Azelaic, acid	10-20	10-20
Sulfur	5-10	5-10
Benzoyl peroxide	2.5-10	2.5-10
Benzyl Benzoate	25	25
Caffeine	1-2	1-2
Ciclopirox olamine	1	1
Clindamycin HCl	1-3	1-3
Clotrimazole	1-2	1-2
Coaltar saponinado	5-20	10
Diclofenac sodium	3	3
Glycerol	0.5-20	0.5-20
Glycolic, acid	5-15	5-15
Sodium hyaluronate	1	1
Ketoconazole	2	2
Lactic, acid	1-20	1-20
Lidocaine HCl	0.5-10	0.5-10
Shea butter	1-20	1-20
Menthol	1-3	1-3
Metronidazole	0.5-3	0.5-3
Nicotinamide (Vit. B3)	2-5	2-5
Salicylic, acid	0.5-20	10
Tetracycline HCl	2-3	2-3
Tocopherol alfa, acetate (vit. E)	0.5-20	0.5-20
Urea	5-40	5-40
Zinc oxide	1-40	10
Zinc sulfate	1-10	1-10

2.10. Physico-chemical parameters

2.10.1. Colour measurement

The colour of each cosmeceutical formulation was measured using a colourimeter (model CR-400, Konica Minolta Sensing Inc., Tokyo, Japan) that has been calibrated against a standard white tile (Caleja, Barros, Antonio, Oliveira, & Ferreira, 2017). The colour was measured using the *L*a*b** system where *L** is a measure of the lightness, *a** is a measure of the (greenness/redness) while *b** is a measure of the (blueness/yellowness). The colour of each sample was measured in three different points, and the average considered the true colour value. Colour space values were registered using the data software "Spectra Magic Nx" (version CM-S100W 2.03.0006).

2.10.2. pH measurement

The pH of each cosmeceutical formulation was measured directly in triplicate with an HI 99161 pH-meter (Hanna Instruments, Woonsocket, Rhode Island, USA).

2.11. Statistical analysis

For all the experiments three samples were analysed and all the assays were carried out in triplicate. The results are expressed as mean values ± standard deviation (SD). The differences between the different samples were analysed using one-way analysis of variance (ANOVA) followed by Tukey's honestly significant difference post hoc test with $\alpha = 0.05$, coupled with Welch's statistic. This treatment was carried out using SPSS v. 23.0 program (IBM Corp., Armonk, New York, USA).

CHAPTER 3: Results and Discussion

3.1. Optimization of bioactive compounds extraction

Generally, solid-liquid extraction by conventional techniques such as Soxhlet extraction (SE) and heat-assisted extraction (HAE) require the consumption of large solvent amounts and are time-consuming processes. In this context, several non-conventional extraction techniques are being successively proposed and applied to maximally extract valuable compounds from natural matrices using much more amiable conditions. Among them, ultrasound-assisted extraction (UAE) and microwave-assisted extraction (MAE) are among the most widely used alternative extraction methods, offering the advantage of reaching interesting results using, for example, hydroalcoholic mixtures. Moreover, some other advantages over other conventional systems include the use of lower extraction times and lower solvent consumption (Chemat, Zill-E-Huma, & Khan, 2011; Garcia-Salas, Morales-Soto, Segura-Carretero, & Fernández-Gutiérrez, 2010; L. Wang & Weller, 2006).

Independently of the employed system, the extraction of target compounds is often influenced by several variables, which require individual analysis due to their intrinsic nature and stability. Therefore, it is essential to define the main variables and relevant responses prior to the optimization process in order to determine the values conducting to the response maximization according to the defined objectives (e.g. using minimum time, energy and solvent and achieve a cost-effective and profitable extraction system) (Dai & Mumper, 2010). To effectively carry out an optimization, the influence of each defined variable should be independently assessed. Nevertheless, the application of mathematical models such as the response surface methodology (RSM) is gaining visibility among the scientific community. Through RSM design the optimization of possible interactions between experimental variables is allowed simultaneously with the prediction of the most efficient conditions. This is achieved by using second order polynomial models with interactions able to describe and maximize the selected response criteria, based on the tested experimental range (Albuquerque et al., 2016).

3.1.1. Extraction of triterpenoids and phenolic compounds from *Ganoderma lucidum*: optimization study using the response surface methodology.

The purpose of this part of the work was to optimize and compare the extraction of phenolic compounds and triterpenes from *G. lucidum* for food, pharmaceutical and cosmetic application by SE, HAE, and UAE. For that, the extraction yield and their content in triterpenes and total phenolics were maximized by RSM using as independent variables, ethanol solvent proportion (hydroethanolic mixtures), temperature and ultrasonic power (in the case of UAE). The extracts corresponding to the optimal conditions were fully characterized in terms of individual phenolic compounds and triterpenoids by HPLC-DAD-ESI/MS analysis.

The influence of the various independent variables, defined for HAE and UAE techniques, was studied using one-factor-at-a-time to select the significant ones and to determine their preliminary range. Based on previous experimental results (data not shown), the variables X_1 (time in min), X_2 (temperature in ºC or power in W) and X_3 (ethanol content in %) were selected for the RSM design. Therefore, the combined effect of these three variables on the achieved extraction yield (Y_1) and content on Tr and Ph present in *G. lucidum* (maximizing responses individually or globally), was studied using *circumscribed central composite design* (*CCCD*) as proposed formerly (Box & Hunter, 1957). The responses were solved using 20 independent combinations including 6 replicates at the centre of the experimental domain. In this design, the experimental points are generated on a sphere around the centre point. It is supposed that the centre point is close to an optimum position for the response, so it is repeated to maximize the prediction (Box, Hunter, & Hunter, 2005). 5 Levels of each factor were also necessary for this design. Experimental runs were randomized to minimize the effects of unexpected variability in the observed responses. A detailed description of the mathematical expressions used to calculate the design distribution and to decode and code the tested variable's ranges can be found in **Table 6**. Once the optimal conditions (X_1, X_2, and X_3) were found, the next step was to optimize the solid/liquid ratio (*S/L* or X_4, expressed in g/L), in order to scale-up processes and maximize the extraction efficiency

Table 6. Experimental design and responses achieved. Variable values of the RSM experimental design applied in HAE and UAE are presented in coded and natural values. Extraction time (X_1: t), temperature or power (X_2: T or P); and solvent proportion (X_3: S) are combined in five levels experimental design of 14 independent variable combinations and 6 replicates at the centre of the experimental domain (20 data points). Results of the response surface experimental plan for the HAE and UAE optimization process of independent variables comprising the following: 1) % extraction yield of the R; 2) Tr content in the format values Y_1 and Y_2; and 3) Ph content in the format values Y_1 and Y_2.

| | EXPERIMENTAL DESIGN | | | | | | | | | HAE RESPONSES | | | | | UAE RESPONSES | | | | |
| | CODED VALUES | | | HAE CONDITIONS | | | UAE CONDITIONS | | | RESIDUE | TRITERPENE CONTENT | | PHENOLIC CONTENT | | RESIDUE | TRITERPENE CONTENT | | PHENOLIC CONTENT | |
	X_1	X_2	X_3	X_1: t min	X_2: T °C	X_3: S %	X_1: t min	X_2: P W	X_3: S %	Yield %	Y_1 mg/g dw	Y_2 mg/g R	Y_1 mg/g dw	Y_2 mg/g R	Yield %	Y_1 mg/g dw	Y_2 mg/g R	Y_1 mg/g dw	Y_2 mg/g R
1	-1	-1	-1	40	35	20.3	13.5	180	20.3	3.83	3.60	93.81	2.54	66.17	4.30	7.02	163.25	3.02	70.25
2	1	-1	-1	130	35	20.3	33.5	180	20.3	3.86	3.67	95.51	2.71	68.93	4.62	7.54	162.89	3.20	66.31
3	-1	1	-1	40	75	20.3	13.5	420	20.3	6.99	3.51	50.27	3.61	56.10	3.64	6.12	167.79	2.96	85.32
4	1	1	-1	130	75	20.3	33.5	420	20.3	3.35	3.46	103.56	3.17	90.08	4.56	6.89	152.82	4.46	102.08
5	-1	-1	1	40	35	79.7	13.5	180	79.7	15.51	7.49	48.23	5.93	39.03	7.02	17.10	245.65	6.28	88.60
6	1	-1	1	130	35	79.7	33.5	180	79.7	10.84	13.02	120.14	5.82	49.16	5.77	21.62	374.96	6.67	110.81
7	-1	1	1	40	75	79.7	13.5	420	79.7	8.14	13.52	166.27	6.00	73.68	5.58	18.68	336.73	6.22	112.65
8	1	1	1	130	75	79.7	33.5	420	79.7	11.64	12.91	112.18	5.79	52.18	5.10	16.00	314.30	6.13	123.25
9	-1.68	0	0	9	55	50	6.7	300	50	5.11	11.07	219.19	5.41	105.77	8.55	13.06	152.92	7.56	93.81
10	1.68	0	0	160	55	50	40.3	300	50	8.50	15.21	181.41	6.21	72.92	6.04	11.43	189.26	5.93	96.17
11	0	-1.68	0	85	20	50	23.5	100	50	6.02	11.44	189.85	5.86	100.62	6.09	14.35	235.76	6.28	100.93
12	0	1.68	0	85	90	50	23.5	500	50	4.50	14.66	325.37	7.38	160.39	8.48	10.92	128.66	6.80	84.99
13	0	0	-1.68	85	55	0	23.5	300	0	4.97	4.67	94.41	3.27	78.27	7.19	4.75	65.07	3.43	48.74
14	0	0	1.68	85	55	100	23.5	300	100	5.74	12.34	214.20	3.61	59.34	3.71	15.24	410.68	4.90	126.09
15	0	0	0	85	55	50	23.5	300	50	5.52	12.29	222.66	5.28	100.74	6.59	11.01	166.99	6.04	100.37
16	0	0	0	85	55	50	23.5	300	50	5.14	11.52	224.43	5.29	103.52	6.08	10.46	172.13	6.84	114.00
17	0	0	0	85	55	50	23.5	300	50	4.84	11.73	242.70	5.36	110.75	6.42	10.94	170.70	6.44	97.82
18	0	0	0	85	55	50	23.5	300	50	5.26	11.83	225.40	5.49	105.00	6.63	10.58	159.78	6.39	96.54
19	0	0	0	85	55	50	23.5	300	50	4.74	10.77	228.07	5.04	104.53	6.54	10.01	153.68	6.44	99.14
20	0	0	0	85	55	50	23.5	300	50	4.81	11.78	245.84	5.10	106.53	8.04	11.27	140.07	7.32	91.96

Mathematical model

The response surface models were fitted by means of least-squares calculation using the following second-order polynomial equation:

$$Y = b_0 + \sum_{i=1}^{n} b_i X_i + \sum_{\substack{i=1 \\ j>i}}^{n-1} \sum_{j=2}^{n} b_{ij} X_i X_j + \sum_{i=1}^{n} b_{ii} X_i^2 \tag{1}$$

where Y is the dependent variable (response variable) to be modeled, X_i and X_j define the independent variables, b_0 is the constant coefficient, b_i is the coefficient of linear effect, b_{ij} is the coefficient of an interaction effect, b_{ii} the coefficients of quadratic effect and n is the number of variables. As dependent variables, for each extraction technique, the following responses were used: the extraction yield and the two format values (Y_1 and Y_2) defined for Tr and Ph, reflecting, respectively, the content of Tr or Ph in the dry material and in the extract (5 genuine responses for each extraction technique) were used.

Procedure to optimize the variables to a maximum response

A maximization process of the model produced responses was achieved, using a simple method tool to solve non-linear problems (Heleno, Diz, et al., 2016; Pinela, Prieto, Barreiro, et al., 2016). Limitations were made to the variable coded values to avoid unnatural conditions (*i.e.*, times lower than 0).

Fitting procedures and statistical analysis

The experimental results statistical analysis and fitting were built according to the equations for the responses obtained using a Microsoft Excel spreadsheet in three phases:

1) Coefficients measurement was achieved using the nonlinear least-square (quasi-Newton) method provided by the macro '*Solver*' in *Microsoft Office Excel* (Prieto, Vázquez, & Murado, 2015), by minimization of the sum of quadratic differences between observed and model-predicted values.

2) Coefficients significance was obtained via '*SolverAid*' macro in *Microsoft Office Excel* (Prieto, Curran, Gowen, & Vázquez, 2015) to determine the parametric confidence intervals. The terms that were not statistically significant (*p*-value > 0.05) were dropped to simplify the model.

3) Model reliability was confirmed by applying the following standards: a) the Fisher *F*-test (α=0.05) was used to determine the consistency of the constructed models to describe the obtained data (Pinela, Prieto, Antonio, et al., 2017); b) the '*SolverStat*' macro in *Microsoft Office Excel* was used to make assessment of parameter and model prediction uncertainties (Comuzzi, Polese, Melchior, Portanova, & Tolazzi, 2003); c) R^2 was determined to explain the proportion variability of the dependent variable obtained by the model.

Extraction efficiency by Soxhlet technique

The used extraction conditions with SE technique were selected by applying 7 cycles that correspond to a total extraction time of 4 h. The used solvent was ethanol and the extraction was performed at its boiling point (80 °C). However, depending on the compounds to be extracted, the number of time-cycles can influence the recovered quantity. For the studied target compounds (Tr and Ph) there are many scientific references suggesting a significant degradation rate at ethanol's boiling point as the time-cycles are prolonged (Sathishkumar et al., 2013). Therefore, to optimize the number of cycles, and consequently measure the total content of Tr and Ph at its maximum, the time-cycle (note that each cycle account approximately for a 30-min period) of the SE for *G. lucidum* was monitored.

A) Triterpene content
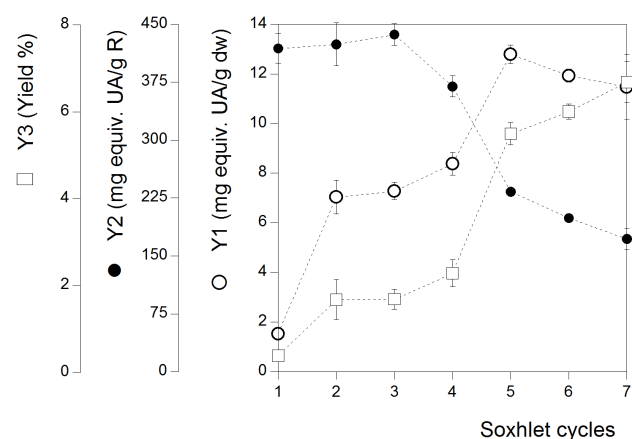
B) Phenolic content
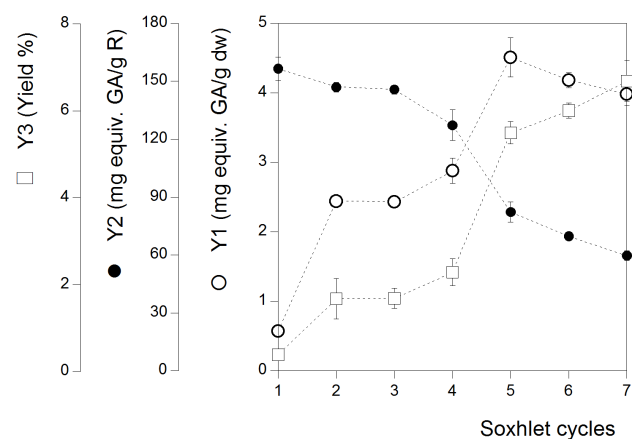
Figure 15. Results obtained for the cycles optimization of the conventional Soxhlet extraction using the responses extraction yield and the two format values (Y_1 and Y_2) of the Tr and Ph content.

Figure 15 shows the effect of the time-cycles number on Tr (part A) and Ph (part B) contents. The results were performed in triplicate for each considered time-cycle and confidence intervals were calculated ($\alpha=0.05$). For Tr content (**Figure 15**, part A), a positive linear dependency was achieved for the responses Y_3 and Y_1. At the final number of performed time-cycles, the response Y_1 shows an asymptotic-decreasing extraction stage (likely to be related to Tr maximum extraction level combined with Tr slight degradation). However, the increase in Y_3 is more prominent than the one observed for Y_1, suggesting that other compounds of the sample start to be extracted at higher rates than the Tr. This intensifies the decrease of Y_2, causing a sharp decrease of Tr content in the R, which is reflected by the decreasing patterns

of Y_2 (from 410 to 150 mg Equiv. UA/g R). Although the Tr content in the R is lower, the overall number of optimal time-cycles for Tr extraction was determined as 5-6 time-cycles in which ~14 mg Equiv. UA/g dw were obtained. These claims have been supported by other authors Y. Gao et al. (2011), who reported that the extraction of Tr from *G. lucidum* is largely influenced in the *T* range between 80 to 100 °C and if prolonged time-cycles of 2 h (~4 cycles) are used.

In what concerns Ph from *G. lucidum*, a nearly identical pattern to the one described for Tr was observed. The Ph content expressed in terms of Y_1 was found to increase significantly up to 5 time-cycles (~5 mg Equiv. GA/g dw) reaching a maximum value before a gradual decrease starts to be observed (likely attributed to degradation rates of Ph). The Y_3 response increases linearly with increasing number of cycles, presenting also a higher slope when compared with Y_1 response, finishing with a sharp decrease in Ph content in the dry material. In terms of Ph content in the extract (Y_2 format value) the number of time-cycle maximizing its value was achieved at the early stages of the process (1-3 time-cycles with ~160 mg Equiv. GA/g R), thereafter decreasing significantly as the extraction process is extended. This behaviour is similar to the one reported for flavonoids extraction from flowers of *Tabernaemontana heyneana* Wall (Sathishkumar et al., 2013). To the authors' best knowledge, the effect of the applied time-cycles number on the extraction efficiency of Tr and Ph from *G. lucidum*, through SE, have not been previously reported.

The extraction efficiency of HAE and UAE optimized by RSM

Theoretical response surface models

The selected variables for the techniques HAE (*t*, *T* and *S* variables) and UAE (*t*, *P* and *S* variables) of the applied *CCCD* experimental design (**Table 6**) were based on preliminary tests and information collected from bibliographic data (Albuquerque et al., 2016; Thabit et al., 2014; Wei et al., 2015).

The obtained results, according to the proposed RSM design (based in a *CCCD*), are shown in **Table 6** for the optimization of HAE and UAE techniques using as responses the extraction yield (%) and Tr and Ph in the format values Y_1 and Y_2. Therefore, by using a non-linear least-squares procedure to fit Eq. (1) to the response results, the estimated parametric values of the equation, the parametric confidence intervals (α=0.05) and relevant statistical values to assess the goodness of fit were presented in the first part of **Table 7**.

Those coefficients, which showed effects with coefficient interval values higher than the parameter value, were considered as non-significant (ns) and were not considered for the model development.

Consequently, non-linear equations were built based in the second-order polynomial model of Eq. (1). Then, for HAE system:

$$Ph_{Y1}^{HAE} = 5.3 + 0.16t + 0.01T + 1.2S + 0.05T^2 - 1.1S^2 \tag{2}$$

$$Tr_{Y1}^{HAE} = 11.6 + 2.1t + 0.5T + 3.7S - 0.28t^2 - 1.7S^2 - 0.11tS + 1.3TS \tag{3}$$

$$Yield^{HAE} = 5.3 - 0.46T + 3.2S + 1.1t^2 + 0.96S^2 - 1.4TS \tag{4}$$

$$Ph_{Y2}^{HAE} = 108.1 + 10.4T - 7.9S - 12.6t^2 - 20.1S^2 \tag{5}$$

$$Tr_{Y2}^{HAE} = 220.1 - 14.1t + 38.4T - 23.4t^2 - 37.4S^2 - 39.4tT + 20.6TS \tag{6}$$

and for UAE process:

$$Ph_{Y1}^{UAE} = 6.45 + 1.22S - 0.23t^2 - 1.17S^2 + 0.21tP - 0.23tS - 0.19PS \tag{7}$$

$$Tr_{Y1}^{UAE} = 11.2 - 0.62P + 4.41S + 0.55P^2 - 0.54S^2 - 0.58tS \tag{8}$$

$$Yield^{UAE} = 6.64 - 0.35t + 0.73S - 1.4S^2 - 0.27tS - 0.41PS \tag{9}$$

$$Ph_{Y2}^{UAE} = 96.7 + 1.9t + 3.7P + 18.4S - 2.5S^2 + 4.5tP - 2.5PS \tag{10}$$

$$Tr_{Y2}^{UAE} = 178.9 + 89.5S + 30.5S^2 - 19.3tP \tag{11}$$

These equations translate the patterns for individual measurement of the assessed response (Eqs. (2) to (6) for HAE and Eqs. (7) to (11) for UAE). Note that not all the parameters of Eq. (1) were used for building the model since some coefficients were rejected (**Table 7**).
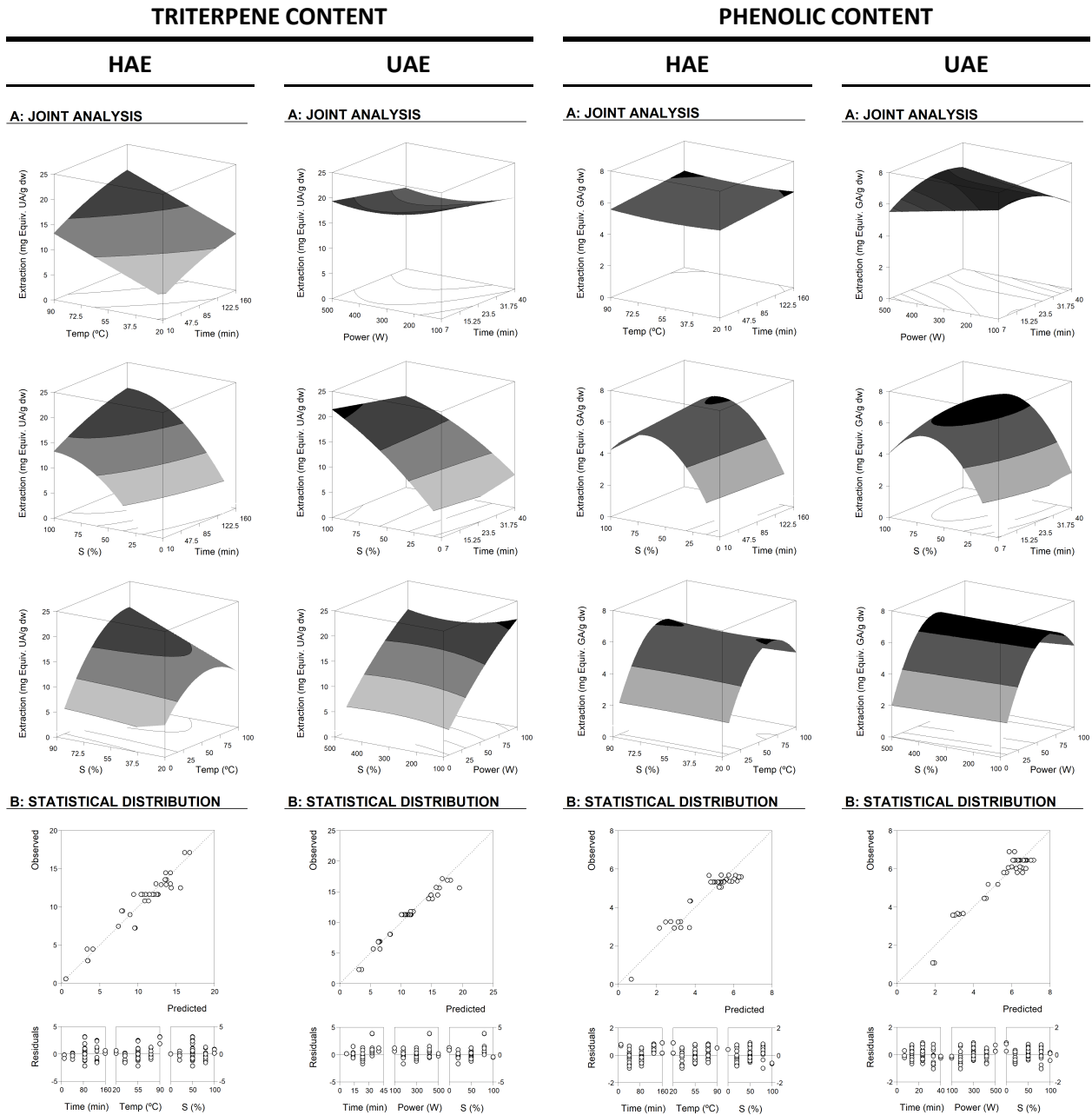
Figure 16. Shows the graphical results in terms of the response surfaces of the format value of Y_1 (mg/g dw) of Tr and Ph from the developed equations for the HAE and UAE system optimizations. _Part A_: Shows the joint graphical 3D analysis as a function of each of the variables involved. Each of the net surfaces represents the theoretical three-dimensional response surface predicted with the second order polynomial Eq. (1) as a function of each one of the involved variables and described by Eqs. (2) and (3) for HAE and Eqs. (7) and (8) for UAE. The statistical design and results are described in **Table 6**. Estimated parametric values are shown in **Table 7**. The binary actions between variables are presented when the excluded variable is positioned at the centre of the experimental domain (**Table 6**). _Part B_: To illustrate the goodness of fit, two basic graphical statistic criteria are used. The first one, the ability to simulate the changes of the response between the predicted and observed data; and the second one, the residual distribution as a function of each of the variables. Note all the differences in the axes scales.

The profile patterns derived from the parametric values of these mathematical models on the assessed response criteria can also be depicted by graphical representation. **Figure 16** and **Figure 17** represent a 3D graphical analysis of the results concerning the extraction yield and Ph and Tr (expressed as Y_1 and Y_2) for the studied techniques (HAE and UAE).

Regarding the interactive effects for HAE system in terms of Tr-Y_1, there was no significant interaction between t & T but a positive correlation for the pairs t & S and T & S was observed. In terms of Tr-Y_2, a negative correlation for t & T and a positive for t & S, and no interaction for T & S was detected. In the case of HAE system in terms of Ph-Y_1 and Ph-Y_2 no interaction was found between the variables t, T and S. For the UAE system in terms of Tr-Y_1, there was no significant interaction between t & S, and P & S while a negative interaction for t & P was observed. In terms of Tr-Y_2, a negative correlation for t & P, a positive for t & S, and no interaction for P & S was observed. Also, in the Ph-Y_1, the correlation was negative for t & S, and P & S. No significant interaction was observed in terms of Ph-Y_1 and Ph-Y_2 between t & P, while for P & S it was negative for Ph-Y_1 and not significant for Ph-Y_2.

HEAT ASSISTED EXTRACTION

ULTRASOUND ASSISTED EXTRACTION
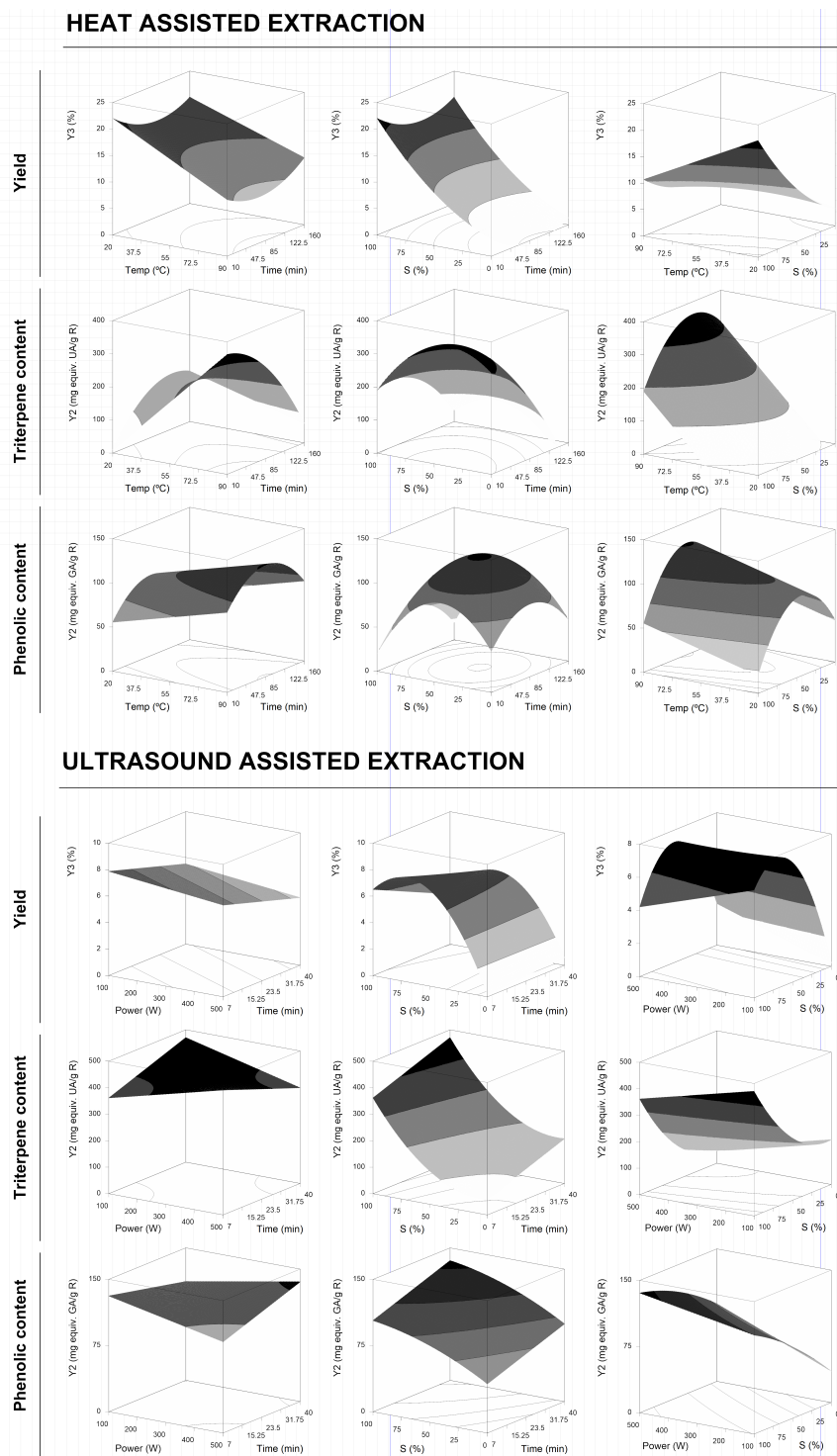
Figure 17. Shows the joint graphical 3D analysis as a function of each variable involved for HAE and UAE systems for the extraction yield and the response content of Tr and Ph in the format value of Y_2 (mg/g R). Each of the net surfaces represents the theoretical three-dimensional response surface predicted with the second order polynomial Eq. (1) as a function of each one of the involved variables and described by Eqs. (4), (5) and (6) for HAE and Eqs. (9), (10) and (11) for UAE. The statistical design and results are described in **Table 6**. Estimated parametric values are shown in **Table 7**. The binary actions between variables are presented when the excluded variable is positioned at the centre of the experimental domain (**Table 6**).

Table 7. Estimated coefficient values obtained from the second-order polynomial model, parametric intervals and numerical statistical criteria for each parametric response criteria of the extractions systems tested (HAE and UAE). Response criteria comprise the following: 1) % extraction yield; 2) Tr content in the format values Y_1 and Y_2; and 3) Ph content in the format values Y_1 and Y_2.

PARAMETERS		RESIDUE	TRITERPENE CONTENT		PHENOLIC CONTENT	
		Yield	Y_1	Y_2	Y_1	Y_2
HEAT-ASSISTED EXTRACTION (HAE)						
Intercept	b_0	5.37±1.0	11.62±0.7	220.09±25.2	5.33±0.3	108.07±10.5
Linear effect	b_1	nsns	2.15±0.7	-14.12±12.6	0.16±0.0	nsns
	b_2	-0.46±0.3	0.51±0.7	38.37±18.7	0.01±0.0	10.44±7.7
	b_3	3.24±0.7	3.67±0.7	ns	1.21±0.0	-7.99±7.7
Quadratic effect	b_{11}	1.01±0.7	-0.28±0.1	-23.41±18.7	ns	-12.63±7.9
	b_{22}	ns	ns	ns	0.05±0.0	ns
	b_{33}	0.96±0.7	-1.73±0.7	-37.41±18.7	-1.07±0.0	-20.01±7.9
Interactive effect	b_{12}	0.35±0.3	ns	-39.42±18.7	ns	ns
	b_{13}	ns	-0.11±0.3	20.62±18.7	ns	ns
	b_{23}	-1.38±0.9	1.27±0.3	ns	ns	ns
Statistics (R^2)		0.8948	0.8978	0.8136	0.9104	0.8210
ULTRASOUND-ASSISTED EXTRACTION (UAE)						
Intercept	b_0	6.64±0.3	11.26±0.7	178.99±17.7	6.45±0.3	96.70±1.8
Linear effect	b_1	-0.35±0.3	ns	ns	ns	1.95±1.8
	b_2	ns	-0.62±0.5	ns	ns	3.67±1.8
	b_3	0.73±0.3	4.41±0.5	89.57±16.0	1.22±0.2	18.44±1.8
Quadratic effect	b_{11}	ns	ns	ns	-0.23±0.2	ns
	b_{22}	ns	0.55±0.5	ns	ns	ns
	b_{33}	-1.36±0.3	-0.54±0.5	30.50±16.3	-1.17±0.2	-2.53±1.8
Interactive effect	b_{12}	ns	ns	-19.32±9.9	0.21±0.2	4.55±1.8
	b_{13}	-0.27±0.3	-0.58±0.3	ns	-0.23±0.2	ns
	b_{23}	-0.41±0.3	ns	ns	-0.19±0.2	-2.55±1.8
Statistics (R^2)		0.9222	0.9349	0.9330	0.9223	0.9013

The regression coefficients related with the interactive effects of the responses, presented in **Table 7,** suggest that the use of an RSM approach to optimize the extraction responses (extraction yield and Tr and Ph (expressed as Y_1 and Y_2)) for both systems (HAE and UAE) is correctly justified. If approaches based on one-variable at a time were applied, the high level of interactions showed between the variables will make the optimum values difficult to determine. As an illustrative example, **Figure 16** shows the response of Tr in HAE representing the effect of *T & S* (at constant values of *t*), in which the related parameter shows a positive value b_{23} of 1.27±0.3 that causes an increase extraction of Tr as both variables increase (closely related with synergistic effects). However, by looking at their individual profile, at fixed values for the other, such interaction will be nearly impossible to predict without a large investment on experimental analysis.

In terms of the statistical analysis of the models fitting to the responses, the lack-of-fit test used to assess the competence of the models showed that the significant parameters in both RSM approaches (**Table 7**) were highly consistent ($p < 0.01$) and if any of them was suppressed, the reached solution would not be acceptable. This was also verified by the achieved high R^2 value, indicating the percentage of the variability explained by the model (**Table 7**). In all cases, the R^2 was higher than 0.8, with values over ~0.9 in almost all responses. The residuals distribution presented in **Figure 16** was arbitrarily around zero and no group of values or autocorrelations were observed. Additionally, the agreement between the experimental and predicted values implies an acceptable explanation of the obtained results through the used independent variables. Therefore, the models developed in Eqs. (2) to (6) for HAE and Eqs. (7) to (11) for UAE, are completely functional and adequate to be used for prediction and process optimization.

Overall effects of the process variables on the target responses

Figure 16 shows the extraction results in terms of Ph-Y_1 and Tr-Y_1 (mg/g dw) for the HAE and UAE, respectively. Each subfigure of **Figure 16** is divided into two subsections (A and B). Subsection A shows the combination of the predicted three-dimensional response surface plots with their respective second order polynomial Eq. (1) as a function of each one of the involved variables, as described by Eqs. (2) and (3) for HAE and Eqs. (7) and (8) for UAE. The binary action between variables is presented when the excluded variable is positioned at the centre of the experimental domain (see **Table 6**). Subsection B illustrates the capability to predict the obtained results and the residual distribution as a function of each one of the considered variables. The response surfaces of the different variable combinations displayed in **Figure 16** clearly shows the various trends observed when the interaction between the variables is compared. The shape of each plot indicates the significance of the interactions that occur in between the variables. The Tr-Y_1 for HAE technique showed that S was the most significant variable with an approximately linear effect. The Tr-Y_1 for the UAE technique showed a non-linear interaction for P and t suggesting saturation effects of the responses as the variables increase. The Ph-Y_1 for HAE and UAE technique showed a bell profile behaviour indicating that its extraction increases as the considered variables (t, T, P, and S) increase up to an optimum point and, then, start to decrease. Thus, the analysis of these response surface curves indicates the optimum level necessary for each variable to optimize the extraction of the compound of interest. In general terms, the information provided in **Figure 16** shows that Tr-Y_1 increases to an optimum value, meanwhile the Ph-Y_1 increases to an optimum value and then

decreases. Therefore, in almost all combinations the optimum can be found at one single point along the response, allowing computing the conditions that lead to the absolute or relative maximum.

Figure 17 shows an illustrative 3D analysis representing the effect of each one of the involved variables in HAE and UAE systems on the extraction yield (%) and Tr-Y_2 and Ph-Y_2 (mg/g R). Each one of the net surfaces represents the response predicted by the second-order polynomial Eqs. (4), (5) and (6) for HAE and Eqs. (9), (10) and (11) for UAE. The actions between the two considered variables are presented when the excluded variable is positioned at the centre of the experimental domain (**Table 6**). The Ph-Y_2 for HAE and UAE showed a bell-shaped profile indicating that an increase in t and S increases the content of Ph to a certain point, followed by a significant decrease. These patterns are also found in the Tr-Y_2 for HAE and UAE but in a lesser extent. As in SE, this behaviour is likely to be related due to the joint action of the two process. The extraction yield increases at higher rates than the Tr and Ph contents, suggesting that other compounds start to be extracted from the *G. lucidum* sample, which causes a decrease in both Tr and Ph contents since a maximum extraction level is achieved. In addition, degradation of these compounds may also occur justifying the strongest decrease visualized in the produced surfaces.

Numerical individual and global optimal conditions that maximize the extraction, statistical analysis and experimental verification of predictive models

The response optimization by RSM, for the HAE and UAE techniques, provides a strong solution by minimizing errors using a short number of experimental trials, as it was demonstrated elsewhere (Roselló-Soto et al., 2015; Wong et al., 2015). The multivariable fitting decreases the needed number of parameters to analyse the response leading to better estimations, reducing their interval of confidence and allowing to predict the response behaviour. In addition, by applying a simple procedure (considering constraints to the experimental ranges) the individual optimal conditions can be found, as well as the maximal response values (first part of **Table 8**). Relative (marked with * when the optimal value may be outside of the studied experimental range) or absolute optimal conditions were found for all the responses as follows:

- For the extraction yield, the HAE was the best solution; 21.3±1.7 % was achieved at *160.0 min, *20.0 ºC and 100.0 % ethanol.

- For the Tr-Y_1, the UAE was the best solution; 21.3±4.1 mg Equiv. UA/g dw was achieved at *7 min, *100.0 W and *100.0 % ethanol.

- For the Tr-Y_2, the UAE was the best solution; 470.5±41.7 mg Equiv. UA/g extract was achieved at *40 min, *100.0 W and *100.0 % ethanol.

- For the Ph-Y_1, the UAE technique was the best solution; 6.7±0.7 mg Equiv. GA/g dw was achieved at 29.4 min, *100.0 W and 59.7 % ethanol.

- For the Ph-Y_2, the HAE was the best solution; 125.9±12.7 mg Equiv. GA/g extract was achieved at 81.3 min, *90.0 ºC and 49.1 % ethanol.

Comparing both techniques in terms of extraction efficiency, UAE conducted to significantly higher values than HAE, probably due to compound's degradation as described previously by other authors (Jacotet-Navarro et al., 2016; Ying Li, Fabiano-Tixier, Tomao, Cravotto, & Chemat, 2013). Regarding the extraction time, UAE was the fastest extraction method for almost all responses. In the second part of **Table 8**, the global optimal conditions are found, as well as the relative response values:

- For the HAE, the global conditions that maximize the responses were 78.9 min, *90.0 ºC and 62.5 % of ethanol conducting to an extraction yield of 5.2±0.6 %, Tr content in the dry material and in the extract of 14.6±1.9 mg Equiv. UA/g dw and 285.7±31.2 mg Equiv. UA/g R, respectively; and Ph content in the dry material and in the extract of 5.8±1.2 mg Equiv. GA/g dw and 116.3±13.2 mg Equiv. GA/g R, respectively.

- For the UAE the global conditions that maximize the responses were *40 min, *100.0 W and 89.5 % of ethanol conducting to an extraction yield of 4.9±0.6 %, Tr content in the dry material and in the extract of 17.4±2.9 mg Equiv. UA/g dw and 435.6±41.2 mg

- Equiv.UA/g R, respectively; and Ph content in the dry material and in the extract of 4.6±0.2 mg Equiv. GA/g dw and 106.6±16.2 mg Equiv. GA/g extract, respectively.

Table 8. Operating conditions that maximize the extracted residue and the content of Tr and Ph compounds from *G. lucidum*.

	OPTIMAL EXTRACTION CONDITIONS			OPTIMUM RESPONSE	
	X_1: t (min)	X_2: T (ºC) or P(W)	X_3: Et (%)		
INDIVIDUAL OPTIMAL RESPONSES					
Heat-Assisted Extraction (HAE)					
Yield	* 160.0	* 20.0	* 100.0	21.3±1.7	%
Tr (Y_1)	* 160.0	* 90.0	* 100.0	22.1±2.9	mg Equiv. UA/g dw
Tr (Y_2)	* 10.0	* 90.0	35.4	362.1±33.1	mg Equiv. UA/g R
Ph (Y_1)	* 160.0	* 20.0	65.7	6.3±0.7	mg Equiv. GA/g dw
Ph (Y_2)	81.3	* 90.0	49.1	125.9±12.7	mg Equiv. GA/g R
Ultrasound-Assisted Extraction (UAE)					
Yield	* 7.0	* 100.0	70.6	7.8±0.9	%
Tr (Y_1)	* 7.0	* 100.0	* 100.0	21.3±4.1	mg Equiv. UA/g dw
Tr (Y_2)	* 40.0	* 100.0	* 100.0	470.5±41.7	mg Equiv. UA/g R
Ph (Y_1)	29.4	* 500.0	59.7	6.7±0.7	mg Equiv. GA/g dw
Ph (Y_2)	* 40.0	* 500.0	* 100.0	135.65±15.7	mg Equiv. GA/g R
GLOBAL OPTIMAL RESPONSES					
Heat-Assisted Extraction (HAE)					
Yield				5.2±0.6	%
Tr (Y_1)				14.6±1.9	mg Equiv. UA/g dw
Tr (Y_2)	78.9	* 90.0	62.5	285.7±31.2	mg Equiv. UA/g R
Ph (Y_1)				5.8±1.2	mg Equiv. GA/g dw
Ph (Y_2)				116.9±13.2	mg Equiv. GA/g R
Ultrasound-Assisted Extraction (UAE)					
Yield				4.9±0.6	%
Tr (Y_1)				17.4±2.9	mg Equiv. UA/g dw
Tr (Y_2)	* 40	* 100.0	89.5	435.6±21.1	mg Equiv. UA/g R
Ph (Y_1)				4.6±0.2	mg Equiv. GA/g dw
Ph (Y_2)				106.6±16.2	mg Equiv. GA/g R

Finally, **Figure 18** shows the summarized individual 2D responses as a function of the defined variables for HAE and UAE techniques guiding the selection of the most favourable conditions. The line represents the variable response pattern when the other responses are located at the optimal values presented in **Table 8**. The dots ($\odot$) presented alongside the line highlight the location of the optimal value. For all techniques and responses, the conditions that lead to the optimal values were re-checked to ensure the accuracy of the presented results. The interest in scale-up processes to obtain bioactives of interest, such as the ones proposed in the present work (triterpenes and phenolic compounds) can take advantages from the data reported in **Figure 18**. The data was organized in a simple format to allow an easy interpretation of the responses.
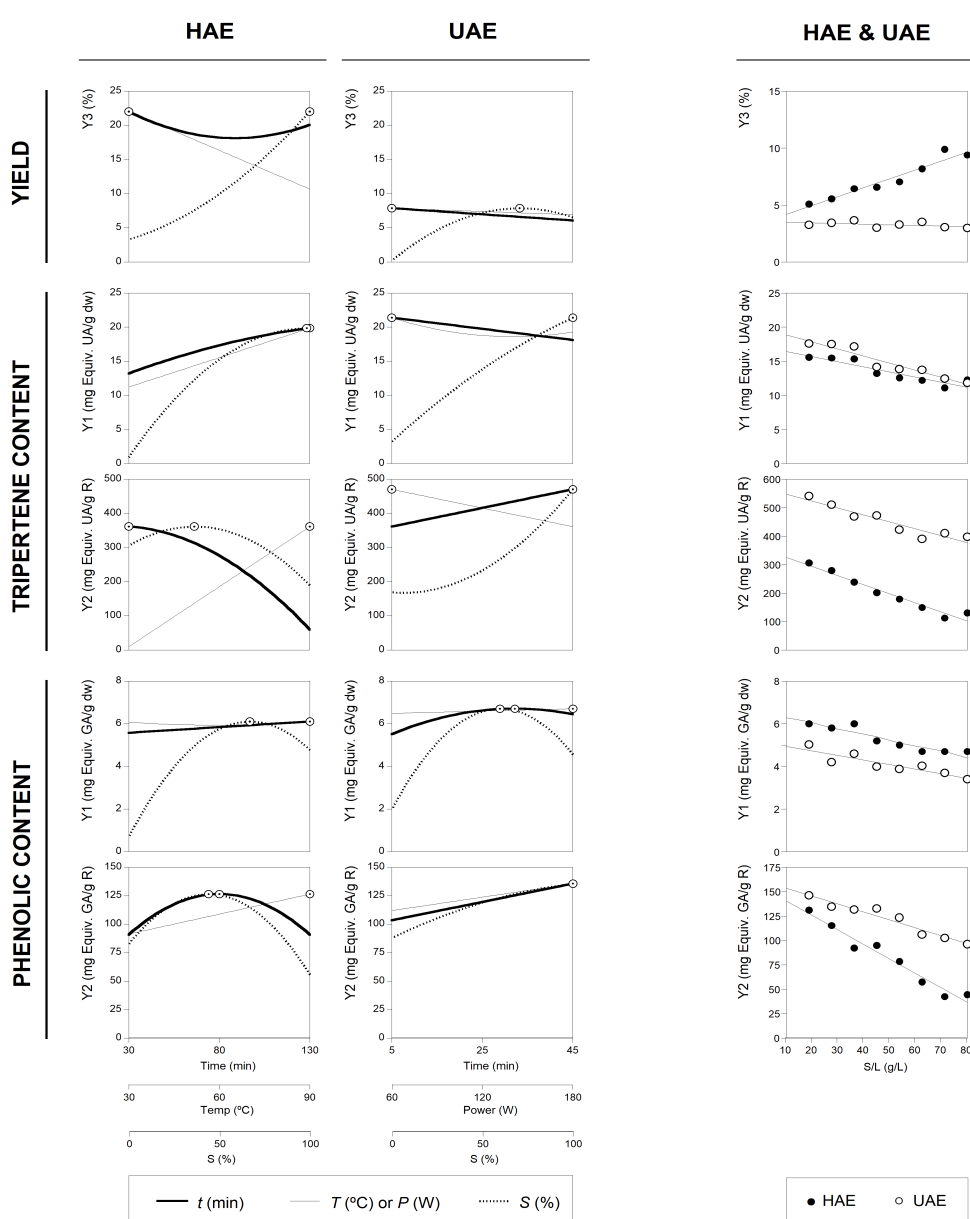
Figure 18. Shows an illustration that summarizes the effects of all variables assessed for HAE and MAE systems. _Part A_: Shows the individual 2D responses of all studied responses as a function of all the variables assessed. The variables in each of the 2D graphs were positioned at the optimal values of the others (**Table 8**). The dots (⊙) presented alongside each line highlights the location of the optimum value. Lines and dots are generated by the theoretical second order polynomial models of Eqs. (2) to (6) for ME and Eqs. (7) to (11). _Part B_: Shows the dose response of _S/L ratio_ at the optimal values of the other three variables optimized by RSM. Points (● for HAE and ○ for UAE) represent the obtained experimental results, meanwhile the line shows the predicted pattern by a simple linear relation. The limit value (80 g/L) shows the maximum achievable experimental concentration until the sample cannot be physically stirred at laboratory scale.

Dose-response analysis of the solid-to-liquid effect at the optimum conditions

The S/L studies for the HAE and UAE techniques, performed at the optimal global conditions predicted by the polynomial Eqs. (4) to (11), are presented in the third part of **Table 8**. For HAE the conditions were: 78.9 min, 90.0ºC and 62.5% of ethanol, whereas for UAE the conditions were: 40.0 min, 100.0 W and 89.5% of ethanol. Preliminary obtained results showed that the experimental limit value at lab-scale was proximal to 80 g/L. Therefore, in both techniques an experimental dose-response test was designed to verify the *S/L* behaviour between 10 g/L to 80 g/L. In all cases, the *S/L* effect can be described by a simple non-linear relationship with an intercept, and in almost all cases, the linear relationship shows a decreasing pattern as the *S/L* ratio increases. The *S/L* increase leads to a decrease in the solvent extraction ability and the observed decreasing patterns are expected due to the saturation effects. Consequently, the dose-response is explained by means of the linear parametric values of the slope (*m*) and the intercept (*b*). The effects of the *S/L* dose-response for the HAE and UAE techniques are presented in **Figure 18**. In all cases, the obtained responses through the HAE and UAE systems are consistent with the previous results obtained using a *S/L* ratio of 30 g/L. **Figure 18** shows the experimental results (dots: ● for HAE and ○ for UAE) and model predictions of the linear relationship (lines) obtained for each technique. The results derived from the linear fitting analysis are summarized as follows:

- For the extraction yield, the HAE technique conducted to a predicted intercept of *b*=4.2±0.4% of R and a slope with positive values (*m*=0.069±0.008%), which can indicate an extract increase with the *S/L*. This was the only case that presented increased patterns as a function of the rise of the *S/L*. The reasons behind may be the high values of *T* applied (90.0 ºC), which may help to dissolve other substances even at high values of *S/L*. Meanwhile, for the UAE technique *b*=3.5±0.2 % of R and *m*=-0.005±0.004% of R per g/L.

- For the Tr-Y_1 response for HAE and UAE techniques the *b* values obtained were 16.4±0.6 and 18.9±0.5 mg Equiv. UA/g dw, respectively. Regarding the decreasing *m* effect caused by the *S/L* increase were -0.066±0.012 and -0.091±0.011 mg Equiv. UA/g dw per g/L, respectively.

- For the Tr-Y_2 response for HAE and UAE techniques, the *b* values obtained were 325.6±12.7 and 547.7 ±15.3 mg Equiv. UA/g R, respectively. Regarding the decreasing *m* effect caused by the *S/L* increase were -2.80±0.25 and -2.12±0.31 mg Equiv. UA/g R per g/L, respectively.

-   For the Ph-Y_1 response for HAE and UAE techniqmodelues, the *b* values obtained were 6.3±0.2 and 4.9±0.2 mg Equiv. GA/g dw, respectively. Regarding the decreasing *m* effect caused by the *S/L* increase were -0.023±0.003 and -0.019±0.004 mg Equiv. GA/g dw per g/L, respectively.

-   For the Ph-Y_2 response for HAE and UAE techniques the *b* values obtained were 140.6±5.4 and 153.6±3.7 mg Equiv. GA/g R, respectively. Regarding the decreasing *m* effect caused by the *S/L* increase were -1.299±0.107 and -0.710±0.073 mg Equiv. GA/g R per g/L, respectively.

Consequently, the dose-response in terms of all response criteria can be explained by the parametric results derived from the linear relationships and this trend was visually interpreted in **Figure 18**, for comparison purposes, in which the modelling predictions obtained for each technique are represented jointly up to determine the experimental limit value of 80 g/L.

Characterization of the optimized extract in terms of individual triterpenoids and phenolic compounds by HPLC-DAD-ESI/MSn

The global optimum conditions for Tr and Ph extraction by HAE and UAE techniques are presented in **Table 8**. These conditions were used to obtain extracts that were further characterized by using HPLC-DAD-ESI/MSn. The HPLC profiles (λ= 280 nm) derived from *G. lucidum* regarding the content of phenolic and triterpenoid compounds at the optimal global conditions of UAE is shown in **Figure 19**.

Identification and quantification of phenolic compounds

The composition of *G. lucidum* extracts in terms of phenolic compounds is presented in T**able 9** (section A). Only phenolic acids, such as protocatechuic, *p*-hydroxybenzoic and syringic acids were identified in the SE extract, being *p*-hydroxybenzoic acid the most abundant compound. Different *G. lucidum* extracts have shown the presence of the above mentioned phenolic acid with slight dissimilarity, which could be attributed to differences in the extraction technique, origin, and variation in environmental conditions necessary for mushrooms maturation (Heleno et al., 2012). Composition in phenolic compounds of the extracts obtained using UAE and HAE systems showed the presence of syringic acid, while *p*-hydroxybenzoic acid was additionally present in the UAE ethanolic extract. Under the optimum conditions, the corresponding predicted response values for the Ph content in the SE, HAE and UAE samples (based on a spectrophotometric assay) were confirmed by HPLC-DAD-ESI/MSn. As expected,

the results showed that the predicted concentrations were slightly different from the experimental ones. The UV-Vis spectrophotometric determination of total phenolics by the Folin Ciocalteu's method is one of the most widely used methods due to its simplicity and low cost, when compared to chromatographic assays, that are highly sensitive and accurate. This methodology is known to have interferences reacting also with non-phenolic reducing compounds, which can lead to an overvaluation of the phenolic content. Therefore, there are a lot of controversies regarding the comparison of results obtained from both methods and several scientific publications have revealed conflicting results (Marques et al., 2013; Popova et al., 2004). Due to the high diversity of chemical compounds in *G. lucidum*, the spectrophotometric method is often unable to accurately quantify the phenolic compounds present in the sample, however, it can be used to conduct optimization studies because of its operational advantages.

Identification and quantification of triterpenoids

An HPLC-DAD-ESI/MSn approach was used in the present work and it has proven to be successful in screening triterpene mixtures in ethanol extracts of *G. lucidum*, using two detectors, DAD and ESI-MS, to obtain the UV absorbance and the molecular weights respectively, to ensure easy and accurate identification. ESI-MS spectra in negative modes were used in the present study and all Tr gave $[M-H]^-$ and $[2M-H]^-$ ions. Under the optimum conditions, the corresponding predicted response values for the triterpene content in the SE, HAE and UAE samples were chromatographically confirmed to validate the model. Even though not all compounds could be recognised because they share the same mass and showed similar retention times, a total of 24, 26 and 28 Tr were correctly identified in HAE, UAE and SE, respectively (section B of **Table 9**). Seven ganoderic acid derivative compounds (peaks 8, 12, 15, 18, 20, 25 and 28) were detected in all extraction techniques. The Tr identified in the present work resulted from a comparison with literature data, regarding the UV spectra, retention time and MS fragmentation pattern. The Tr profile in *G. lucidum* often depends on the extraction method employed and the geographical origin of the strain. However, most studies have reported good repeatability in the Tr profile of *G. lucidum* (Guo et al., 2012; Hadda, Djamel, & Akila, 2015; Hennicke et al., 2016; Yang et al., 2007). In all three extraction techniques evaluated, ganoderic acid A (peak 22) and ganoderic acid H (peak 23) were the most abundant Tr present. The experimental results obtained at the optimum conditions were

found not to be significantly different from what was predicted by the model, thus indicating the suitability of the model employed and the success of RSM in optimizing the extraction conditions for obtaining triterpenes from *G. lucidum*. The extraction efficiency for recovery of Tr compounds per extraction technique has been established as shown in **Table 9**. SE provided the highest results regarding the phenolic compounds; however, the SE technique requires high solvent consumption, long extraction time, and intensive manpower which often contradicts the "green chemistry" and "environmentally friendly" concept. Alternatively, the UAE technique has shown to overcome the challenges in the traditional method, because of its fast and environmentally friendly approach.
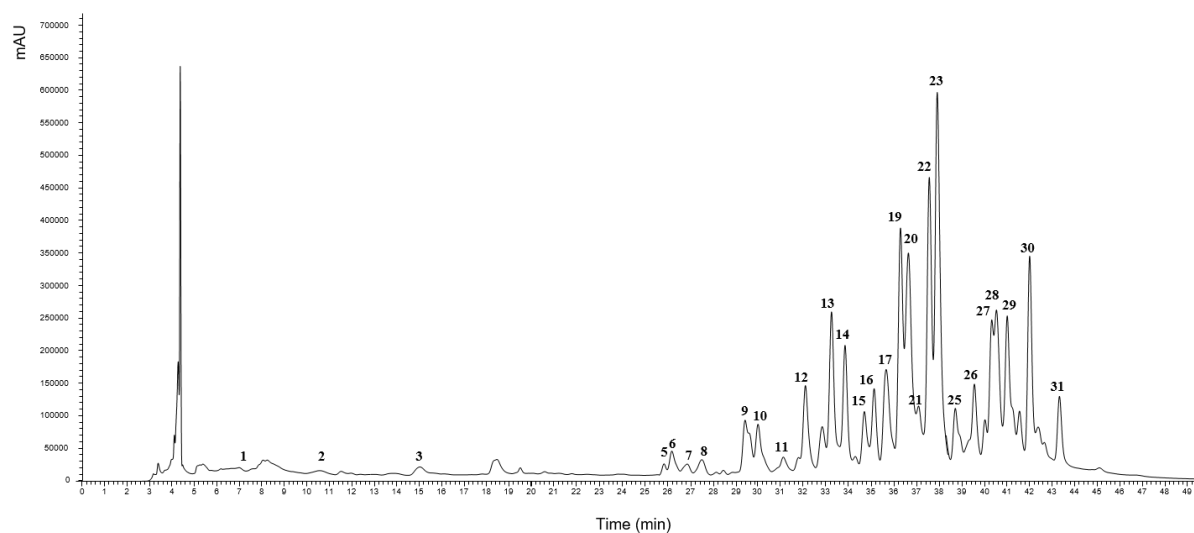
Figure 19. Example of the HPLC profiles (λ = 280 nm) derived from *G. lucidum* regarding the content of phenolic and triterpenoid compounds. A representative case at the optimal global conditions of UAE presented in **Table 8**). Compounds identification numbers are described in detail in **Table 9**.

Table 9. Identification and quantification of phenolic compounds and triterpenoids in *G. lucidum* extracts produced at the determined optimal conditions of HAE, UAE and SE.

Peak	Rt	UV λmax	[M-H]⁻ & [2M-H]	MS²	Tentative identification	Quantification (mg/g R)		
	(min)	*(nm)*	*(m/z)*	*(m/z)*		*HAE*	*UAE*	*SE*
A: Characterization of phenolic compounds								
1	7	259,293sh	153	109(100)	Protocatequic acid	-	-	1.80± 0.01
2	10.8	257	137	93(100)	*p*-Hydroxybenzoic acid	-	0.364±0.01	2.98±0.01
3	15	280	197	121(100)	Syringic acid	0.250±0.001	0.260±0.001	1.51±0.01
					Total phenolic acids	**0.250±0.001**	**0.620±0.001**	**6.30±0.01**
B: Characterization of triterpenes								
4	29.06	259	533/1067	515(5),497(12),404(100),303(12)	12-3,7,15-Trihydroxy-4-(hydroxymethyl)-11,23-dioxo-lanost-8-en-26-oic acid	3.77±0.03	7.18 ±0.05	14.21±0.02
5	30.8	256	533/1067	515(5),497(21),453(16),423(11),319(5),303(8)	12-Hydroxyganoderic acid C2	5.01±0.03	1.43±0.04	4.51±0.06
6	31.27	252	529/1059	511(10),467(100),449(11),434(5),431(15),419(8),312(8),285(5),263(11)	20-hydroxy-ganoderic acid AM1	-	5.41±0.06	11.40±0.01
7	31.73	251	529/1059	511(13),499(100),481(6),465(18),438(28),419(18),367(11),287(11)	12-deacetylganoderic acid H	2.28±0.04	3.62±0.06	6.1±0.14
8	32.28	255	547/1095	529(50),511(41),485(3),467(100),449(24),431(26),304(11),265(7)	Ganoderic acid derivative	3.78±0.03	5.27±0.04	7.3±0.1
9	33.94	258	531/1063	513(13),451(3),401(100),385(5),304(19),301(45),286(3),249(27)	Ganoderic acid η	5.50±0.03	14.13±0.08	25.41±0.04
10	34.48	254	511/1023	493(23),449(100),431(5),413(15),405(3)	Ganoderic acid F	5.34±0.03	12.46±0.05	17.97±0.02
11	35.37	265	529/1059	511(5),467(100),449(27),437(29),317(10),301(5),263(5)	12-hydroxyganoderic acid D	4.15±0.04	7.78±0.05	6.86±0.07
12	35.95	251	515/1031	497(100),453(31),437(8),303(19),287(5),235(3)	Ganoderic acid derivative	11.03±0.06	21.61±0.06	21.20±0.08
13	36.84	256	517/1035	499(100) 481(48),456(17),438(52),407(8),304(6),287(35)	Ganoderic acid C2	17.92±0.03	28.09±0.08	38.70±0.15
14	37.51	257	529/1059	511(5),481(7),467(100),451(14),438(38),424(3),319(5),303(3),301(5)	Ganoderic acid C6	10.50±0.04	21.11±0.04	29.10±0.08
15	38.16	256	529/1059	511(58),493(5),449(10),399(100),301(3)	Ganoderic acid derivative	5.22±0.06	11.07±0.06	12.77±0.01
16	38.46	256	531/1063	513(11),498(15),469(100),454(29),452(24),437(6),304(5),302(6),290(20),266(7)	Ganoderic acid G	8.04±0.02	14.31±0.29	16.84±0.07
17	38.75	248	513/1027	495(10),480(16),451(100),437(14),433(22),407(17),331(5),315(3),303(5),287(5)	Ganoderenic acid B	13.12±0.01	23.05±0.50	10.66±0.09
18	39.01	259	527/1055	509(26),465(6),397(100),355(4)	Elfvingic acid derivative	-	-	10.41±0.09
19	39.35	254	515/1031	497(10),453(100),439(5),409(5),304(21),287(12),263(3),250(14)	Ganoderic acid B	18.86±0.07	35.72±0.02	23.99±0.09
20	39.46	250	513/1027	495(100),479(27),462(12),451(30),433(31),381(25),301(15)	Ganoderic acid derivative	25.64±0.03	44.70±0.16	22.44±0.10
21	39.66	261	513/1027	495(21),480(5),451(100),433(24),381(6),301(6),247(3)	Ganoderic acid AM1	-	11.56±0.03	15.82±0.01
22	40.29	254	515/1031	497(100),480(5),454(6),436(10),302(8),301(4),285(3)	Ganoderic acid A	28.79±0.05	43.46±0.20	36.77±0.04
23	40.66	261	571/1143	553(100),511(8),481(3),468(8),437(3),423(2)	Ganoderic acid H	27.32±0.19	58.13±0.03	41.05±0.39
24	40.87	252	527/1055	509(20),479(13),465(100),435(3),421(3),317(3),301(3)	Elfvingic acid A	-	-	9.83±0.01
25	41.34	254	529/1059	511(10),496(22),493(21),467(100),449(61),434(4),319(6),317(8),301(16),300(11),299(12)	Ganoderic acid derivative	6.12±0.07	13.98±0.05	11.56± 0.04
26	41.93	246	511/1023	493(12),478(20),449(100),435(15),431(4),405(4),329(3),301(4),285(5),283(3),261(4)	Ganoderenic acid D	12.38±0.04	23.06±0.04	10.27±0.07
27	42.55	255	513/1027	495(16),451(100),437(6),433(3),407(4),301(23),286(3),284(11),247(8)	Ganoderic acid D	15.17±0.09	17.61±0.12	11.31±0.01
28	42.74	245	509/1019	491(100),476(18),461(34),447(15),429(3),417(3),300(5),299(4)	Ganoderic acid derivative	13.37±0.13	28.36±0.04	12.81±0.08
29	43.15	256	511/1023	493(100),449(65),435(3),300(5),247(4)	Ganoderic acid E	12.84±0.03	31.53±0.08	10.81±0.07
30	43.95	255	569/1139	551(100),509(35),508(21),466(8)	12-acetoxyganoderic acid F	15.91±0.03	32.59±0.12	12.08±0.07
31	44.92	272	513/1027	451(100),437(8),433(3),422(3),301(5)	Ganoderic acid J	8.41±0.16	14.05±0.42	2.92±0.05
					Total triterpenoids	**280.46±0.11**	**531.26±0.24**	**455.01±1.47**

Extraction efficiencies assessment between HAE and UAE

Extraction of bioactive compounds from natural matrices using solid-liquid extraction systems constitutes an important step to obtain ingredients to produce phytochemical-rich products. This is in accordance with current trends where a raising interest is devoted to the use of natural-derived ingredients in different industrial fields. Over the years, conventional extraction systems were predominantly applied (Azwanida, 2015; Joana Gil-Chávez et al., 2013). Traditional methods such as SE and HAE, have been used everywhere for many different purposes. They are often time-consuming and require large quantities of polluting solvents in comparison to other emerging technologies. However, in terms of efficiency (extraction yield and purity), the SE is described as the standard chemical extraction process at laboratory scale. Nonetheless, by itself, it is an optimized extraction system and in addition, literature offers a high number of practical examples that report the favourable conditions (Azmir et al., 2013). Additionally, its sister in industrial applications, the repeated-heated-extraction, has been used by food processing industries and researchers with the purpose of extracting more efficiently major and minor compounds.

However, to maximally recover compounds of interest from natural sources, while also taking into consideration environmental factors, financial feasibility, time and extraction quality, non-conventional technologies have been applied (such as UAE as well as pulsed electric field, enzyme digestion, extrusion, microwave assisted extraction, supercritical fluid extraction, etc.). New extraction techniques are continuously developed and/or modified to properly identify the most suitable technique that maximally increases the recovery of bioactive compounds.

Even though there are reports on the optimization of Tr extraction from natural matrices (Wei et al., 2015), only Ruan et al., (2014) have been able to report the effects of different extraction variables on the extraction efficiency of Tr from *G. lucidum*. The above authors reported that Tr yield was 13.23 mg/g dw when the extraction conditions were 100% ethanol, 60.2 °C, and 6 h. Wei et al., (2015) reported an increase in Tr extraction using the UAE system as the solvent proportion increased from 50 to 75% by 14.39 to 19.51 mg/g dw, respectively. Also, as the time increased from 10 to 40 min, the extraction yield increased from 12.50 to 18.93 mg/g dw, respectively. The above authors reported an optimum yield of 26.7±0.2 mg/g dw at 70% ethanol, 50 min, and 100 W, values that are consistent with Tr-Y_1 content reported in the present work of 28.4±4.1 mg/g dw at the optimal individual conditions (**Table 8**, 100% of ethanol, 40 min and 100 W). Studies conducted by Gao et al., (2011) revealed that an optimal extraction yield of 1.09% for the HAE system at 90% ethanol, 120 mins and 80 °C while 5.0± 0.6% were

obtained in the present work (**Table 8**). The dissimilarity in the above response could be due to the influence of the application of mathematical and statistic techniques to maximize the recovery. To the authors' best knowledge, no previous studies have been conducted on the optimization of Ph compound extraction from *G. lucidum* using the UAE and HAE system. However, Lin, Yu, & Weng, (2012) conducted an optimization using the supercritical fluid extraction technique, obtaining optimum extraction values at lower temperatures.

SE, HAE, and UAE extraction techniques have been examined, optimized and compared concerning the recovery of bioactive compounds from *G. lucidum*. The results showed that the main variables involved in those processes have significant effects on the extraction yield. The UAE system was found to be the most effective and faster method for Tr extraction, capable of yielding 17.4±2.9 mg Equiv. UA/g dw and producing a 4.9% R (49 mg R/g dw) with a purity of 435.6±21.1 mg Equiv. UA/g R at its optimal extraction conditions. Meanwhile, HAE was found to offer a better result for the Ph extraction showing 5.8±1.2 mg Equiv. GA/g dw and producing a 5.2% R (52 mg R/g dw) with a purity of 116.9±13.2 mg Equiv. GA/g R at its optimal extraction conditions. In global terms, applying the RSM conditions by UAE technique lead to higher amounts of compounds but also higher extraction yields than those found in HAE and SE, but the costs involving the use of this technique at industrial scale may not cover the investment needed. This work offers an overview through environmentally compatible extraction processes, in which *G. lucidum* is submitted to 'clean' technologies able to integrate a potential industrial sector in a sustainable approach. The obtained results indicate the viability of using *G. lucidum* as a productive source of an enriched extract with bioactive compounds. Under the optimum conditions, an HPLC-DAD-ESI/MSn confirmed the validity of the model with a total of 24, 26 and 28 Tr correctly identified in HAE, UAE and SE extracts, respectively. Protocatechuic, *p*-hydroxybenzoic and syringic acids were identified in the SE ethanolic extract. The HAE system showed the presence of only syringic acid while *p*-hydroxybenzoic acid was additionally present in the UAE extract. In addition, the present work can reinforce the potential of *G. lucidum* to serve as a source of bioactive compounds to be used as natural additives in functional foods, as cosmeceutical ingredients and as novel compounds with pharmaceutical potentials. Because of the widespread presence of Tr and Ph compounds in *G. lucidum*, further studies should be conducted using the optimal extraction conditions determined in the present work.

3.1.2. Optimization of ergosterol extraction from *Agaricus blazei* Murrill using response surface methodology: A comparative study between modern and conventional techniques

The RSM was applied to optimize the HAE, MAE, and UAE techniques with the purpose of finding the most favourable conditions that maximizes the recovery from ergosterol and the results were expressed according to three response (*Y*) format values: Y_1, the % of extracted material (R), which was used to evaluate the total extraction yield; Y_2, in mg of ergosterol per g of extract residue (mg E/g R), which was used to evaluate the ergosterol purity in the extract; and Y_3, in mg of ergosterol per 100 g of dry mushroom *A. blazei* (mg E/100 g M dw), which was used to analyse the extraction yield expressed in ergosterol. Studies previously conducted were taken into consideration to screen the appropriate variables to determine the experimental domain for an appropriate RSM design. Independent variables, which include *t* and *T* for HAE and MAE, and *t* and *P* for UAE, were preliminarily tested.

Experimental design

Trials were conducted based on one-at-the-time analysis of each one of the variables and each one of the selected techniques. The variables that caused significant changes, and the relevant ranges of action, were selected for each one of the studied extraction methodologies (**Table 10**). The variables were coded according to the needs of the experimental design. For each technique, the combined effect of the two relevant variables was studied using a *circumscribed central composite design* (*CCCD*) using five levels for each one with 16 response combinations (three replicates per condition). Experimental runs were randomized, to minimize the effects of unexpected variability in the observed responses.

Table 10. Experimental domain and codification of independent variables in the *CCCD* factorial design with 5 range levels and 2 factors.

CODED VALUES	NATURAL VALUES					
	HAE		*UAE*		*MAE*	
	t (min)	*T (ºC)*	*t (min)*	*P (W)*	*t (min)*	*T (ºC)*
-1.41	10.00	30.00	5.00	100.00	2.00	60.00
-1	30.50	34.10	8.66	118.31	5.37	73.18
0	80.00	60.00	17.50	250.00	13.50	105.00
+1	129.50	85.90	26.34	381.69	21.63	136.82
+1.41	150.00	90.00	30.00	400.00	25.00	150.00

Response surface models were fitted by means of least-squares calculation using the following second order polynomial equation,

$$Y = b_0 + \sum_{i=1}^{n} b_i X_i + \sum_{\substack{i=1 \\ j>i}}^{n-1} \sum_{j=2}^{n} b_{ij} X_i X_j + \sum_{i=1}^{n} b_{ii} X_i^2 \qquad [12]$$

where Y is the dependent variable (response variable) to be modelled, X_i and X_j define the defined independent variables, b_0 is the constant coefficient, b_i is the coefficient of linear effect, b_{ij} is the coefficient of the interaction effect, b_{ii} the coefficients of quadratic effect and n is the number of variables. The variables X_1 and X_2 were t and T or P (for HAE and MAE t and T were used, whereas for UAE t and P were chosen). Regarding the responses, three different response formats were used as the dependent variables: Y_1, response format value in %, to analyse the total extraction yield; Y_2, the response format value in mg/g of extract to analyse the ergosterol purity in the extract and Y_3 the response format value in mg/100 g M dw to analyse the extraction yield in ergosterol.

Procedure to optimize the variables to a maximum response

A simple method was used to optimize the predictive model by solving nonlinear problems in order to maximize the responses (Y_1, Y_2, and Y_3) individually or globally (Vieira et al., 2017). Certain limitations were imposed (*i.e.* t cannot be lower than 0) to avoid variables with unnatural and unrealistic physical conditions.

Dose-response analysis of the solid-to-liquid ratio

Once the optimal conditions (X_1 and X_2) were found by RSM, the following natural optimization step was to describe the pattern of the solid-to-liquid ratio (*S/L* or X_3, expressed in g/L) aiming at achieving a more productive process for industrial applications. To depict the response effect as a function of the *S/L* variation, the Weibull (W) equation (Prieto, Curran, Gowen, & Vázquez, 2015) for increasing (↑) and decreasing (↓) responses were used with some parametric modifications to fit the searched purposes:

$$\uparrow W(X_4) = K \exp\left[\ln\left(1 - \frac{n}{100}\right)\left(\frac{X_4}{m_n}\right)^a\right] \quad \text{or} \quad \downarrow W(X_4) = K - K \exp\left[\ln\left(1 - \frac{n}{100}\right)\left(\frac{X_4}{m_n}\right)^a\right] \qquad [13]$$

where K is the maximum extraction value (response criteria units, *i.e.*, if Y_2 units would be mg/g R), a is a shape parameter related to the maximum slope of the response, n is any desired level between 0 to 100% of the response (Y_1, Y_2, and Y_3) that would be achieved, and m_n would

be the *S/L* value (X_3) for such a response level of *n* selected (m_{10}, m_{25}, m_{75}, m_{95}, etc.). For example, if 99% was select for the *n* value, the m_n parameter will display de needed *S/L* needed to achieve 99% of the assessed response ($m_{99\%}$). When the response shows increasing patterns (↑), the Weibull equation that will be used to describe the response will present an m_n parameter with *n*=99%. When the response shows decreasing patterns (↓), an m_n parameter with *n*=50% will be used. These different levels of the response as a function of the increasing or decreasing patterns of the response are logical relations of the intrinsic solutions for industrial purposes. When the response increases, it seems to be logical to know the maximum *S/L* value needed to achieve 99% of the assessed response ($m_{99\%}$), as it is the case for Y_2 and Y_3 responses. However, when the response decreases, the value of $m_{99\%}$ will be approximately zero. Therefore, it seems to be logical to search for values that do not decrease our response more than the half of the maximum value (such as $m_{50\%}$), as it is the case for Y_1 response. If other m_n are required, Eq. [13] can be modified to produce any other desired result. However, the selected parameter values for *K* and m_n provide key information related to the pattern of the response to assess the *S/L* trend.

Numerical methods and statistical analysis

Fitting procedures, coefficient estimates, and statistical calculations were performed as previously described by Pinela et al. (2016). In brief, a) the coefficient measurement was carried out using the nonlinear least-square (quasi-Newton) method provided by the macro "Solver" in Microsoft Excel, which allows minimizing the sum of the quadratic differences between the observed and model-predicted values; b) the coefficient significance was evaluated using the '*SolverAid*' to determine the parametric confidence intervals. The non-statistically significant terms (*p*-value > 0.05) were dropped to simplify the model; and c) the model reliability was verified using the following statistical assessment criteria: i) the Fisher *F*-test (α=0.05) was used to determine whether the constructed models were adequate to describe the observed data; ii) the '*SolverStat*' macro was used for the assessment of parameter and model prediction uncertainties; iii) the R^2 and R^2_{adj} were interpreted as the proportion of variability , of the dependent variable explained by the model; and iv) bias and accuracy factors of all equations were calculated to evaluate the fittings of the experimental data, such as the mean squared error (MSE), the root mean square of the errors (RMSE), the mean absolute percentage error (MAPE) and the Durbin-Watson coefficient (DW).

RSM is a proficient tool to evaluate the effects of numerous variables and their interactions on one or more responses. The *CCCD* is a popular form of RSM and has been applied by a number

of researchers for optimization of various food processing methods (Bezerra et al., 2008). **Figure 20** shows a comprehensive summary of the different steps carried out in the optimization of ergosterol extraction from the fruiting bodies (basidiocarps) of *A. blazei*. RSM was applied to study the level of significance of each independent variable, for each one of the carried extraction methods, on their respective responses to be able to fully describe the interactive effects among the numerous factors.
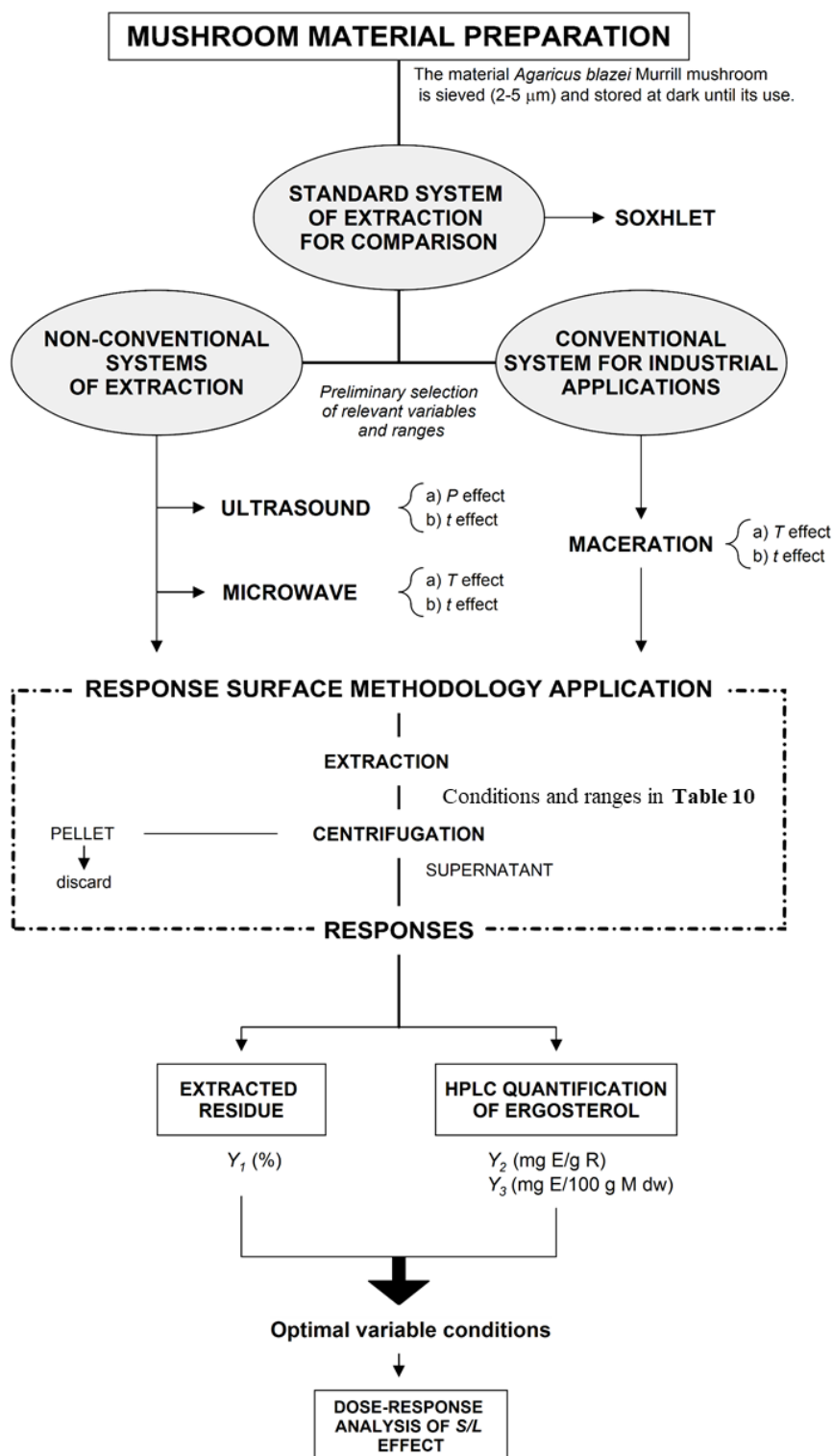
Figure 20. Diagram of the different steps carried out for optimizing the conditions that maximize the extraction responses (Y_2 in mg E/g R and Y_3 in mg E/100 g M dw) of the ergosterol compound and the total extracted residue (Y_1 in %).

Theoretical mathematical models derived from the RSM analysis

In the present study, a total of 16 experimental runs were needed to optimize the extraction and produce the parametric values for model development in HAE, UAE, and MAE with responses defined as Y_1, Y_2 and Y_3. **Table 10** shows the experimental conditions; the responses according to the statistical *CCCD* experimental design are presented in **Table 11**, for each one of the computed extraction techniques.

Table 11. Experimental RSM results for the optimization of the two main variables involved (X_1 and X_2) in the HAE, UAE, and MAE for the three response value formats assessed (Y_1, yield in %; Y_2, mg E/g R; and Y_3 mg E/100 g M dw). Variables, natural values, and ranges in **Table 10**. Three replicates were performed for each condition for each technique.

		EXPERIMENTAL RESPONSES								
CODED VALUES		HEAT-ASSISTED EXTRACTION (HAE)			ULTRASOUND-ASSISTED EXTRACTION (UAE)			MICROWAVE-ASSSISTED EXTRACTION (MAE)		
X_1	X_2	Y_1	Y_2	Y_3	Y_1	Y_2	Y_3	Y_1	Y_2	Y_3
-1	-1	3.33	1.14	3.80	1.55	1.21	1.88	13.18	0.48	6.33
-1	1	15.32	1.05	16.15	8.08	2.11	17.02	22.70	0.95	21.51
1	-1	4.25	1.66	7.07	1.87	1.23	2.31	12.05	1.52	18.39
1	1	19.20	0.67	12.87	9.24	2.13	19.74	18.59	0.70	12.99
-1.41	0	6.70	1.06	7.20	4.18	1.93	8.06	15.90	1.03	16.32
1.41	0	10.63	1.65	17.54	8.81	1.60	14.10	18.58	1.34	24.93
0	-1.41	3.51	0.50	1.75	1.70	1.14	1.94	7.49	1.15	8.60
0	1.41	14.30	1.39	19.91	11.77	1.59	18.72	24.30	1.07	26.14
-1.41	-1.41	3.34	0.79	2.66	1.89	0.71	2.74	6.91	0.98	6.81
-1.41	1.41	16.63	0.91	15.21	7.43	1.64	5.85	22.32	0.90	20.04
1.41	-1.41	4.40	1.42	6.23	1.81	1.20	2.18	8.85	1.59	14.11
1.41	1.41	20.45	1.01	20.56	9.82	2.08	20.43	23.84	0.99	23.78
0	0	8.91	1.84	16.43	6.63	1.64	10.90	19.03	1.15	21.91
0	0	9.15	1.67	15.27	6.67	1.84	12.28	18.73	1.02	19.03
0	0	9.63	1.54	14.92	6.16	2.54	15.63	18.76	1.10	20.62
0	0	9.70	1.49	14.45	6.29	2.20	13.82	19.33	1.03	19.97

By fitting the second-order polynomial model of Eq. [12] to the obtained responses, using nonlinear least-squares estimations, the parametric values are obtained and presented in **Table 12** Part A.

The coefficients showing confidence interval values (α=0.05) higher than the parameter value, considered as non-significant (*ns*) and were not accounted for in the model development. In statistical terms, the *ns* parameters of the RSM approaches do not improve the reached solution of the models, but increase the uncertainties of all significant parameters and, in addition, the *ns* parameters distort the predicted solutions in untested conditions. This has already been described in the literature (Ranic et al., 2014), and suggested as a mandatory step to avoid

irregularities in the mathematical analysis, such as response overfitting and inaccurate predictions of the results of untested operating conditions. Therefore, based on the results presented in **Table 12** A, the final resulting models for each one of the assessed extraction techniques were the following:

For the response format Y_1 (yield of the extracted R material, %):

for HAE: $\quad Y_{HAE}^{Y_1} = 9.90 + 0.86t + 5.23T + 0.42tT$ [14]

for UAE: $\quad Y_{UAE}^{Y_1} = 1.49 + 0.09t - 0.26P^2 + 0.10tP$ [15]

for MAE: $\quad Y_{MAE}^{Y_1} = 13.40 + 1.26t + 5.12T - 1.50T^2$ [16]

For the response format Y_2 (mg E/g R):

for HAE: $\quad Y_{HAE}^{Y_2} = 6.47 + 0.71t + 2.96T - 0.36t^2 - 0.24T^2 + 0.29tT$ [17]

for UAE: $\quad Y_{UAE}^{Y_2} = 1.80 + 0.03t + 0.29P - 0.21P^2 - 0.03tP$ [18]

for MAE: $\quad Y_{MAE}^{Y_2} = 13.15 + 1.97t + 5.41T - 1.15t^2 - 1.53T^2 + 1.63tT$ [19]

For the response format Y_3 (mg E/100 g M dw):

for HAE: $\quad Y_{HAE}^{Y_3} = 18.57 + 5.18T - 0.46t^2 - 1.21T^2 - 0.19tT$ [20]

for UAE: $\quad Y_{UAE}^{Y_3} = 1.09 + 0.10t - 0.12P - 0.09tP$ [21]

for MAE: $\quad Y_{MAE}^{Y_3} = 19.83 + 2.50t + 4.92T - 1.69T^2 - 0.80tT$ [22]

Table 12. Parametric results of the second-order polynomial equation of Eq. [1] for the HAE, UAE and MAE extracting techniques assessed and in terms of the extraction behaviour of the three response value formats (Y_1, yield in %; Y_2, mg E/g R; and Y_3 mg E/100 g M dw), according to the experimental design. Analysis of significance of the parameters (α=0.05) are presented in coded values. Additionally, the statistical information of the fitting procedure to the model is presented.

COEFFICIENTS		PARAMETRIC RESPONSES TO THE CENTRAL COMPOSITE DESIGNS FOR EACH TECHNIQUE								
		HEAT-ASSITED EXTRACTION (HAE)			ULTRASOUND-ASSISTED EXTRACTION (UAE)			MICROWAVE-ASSISTED EXTRACTION (MAE)		
		Y_1	Y_2	Y_3	Y_1	Y_2	Y_3	Y_1	Y_2	Y_3
Fitting coefficients obtained										
Intercept	b_0	9.90±0.63	1.49±0.17	13.40±1.58	6.47±0.48	1.80±0.07	13.15±0.56	18.57±0.88	1.09±0.05	19.83±1.42
Linear effect	b_1	0.86±0.64	0.09±0.11	1.26±1.05	0.71±0.28	0.03±0.02	1.97±0.32	ns	0.10±0.05	2.50±0.87
	b_2	5.23±0.63	ns	5.12±1.03	2.96±0.28	0.29±0.04	5.41±0.32	5.18±0.51	-0.12±0.05	4.92±0.85
Quadratic effect	b_{11}	ns	ns	ns	-0.36±0.22	ns	-1.15±0.39	-0.46±0.28	ns	ns
	b_{22}	ns	-0.26±0.13	-1.50±1.19	-0.24±0.18	-0.21±0.05	-1.53±0.39	-1.21±0.64	ns	-1.69±1.04
Interactive effect	b_{12}	0.42±0.16	-0.10±0.09	ns	0.29±0.15	-0.03±0.03	1.63±0.29	-0.19±0.13	-0.09±0.04	-0.80±0.76
Statistical information of the fitting analysis										
Obs		48	48	48	48	48	48	48	48	48
R^2		0.9179	0.8234	0.8153	0.9158	0.8123	0.8767	0.9463	0.8354	0.8849
R^2adj		0.9326	0.9533	0.8034	0.9003	0.8006	0.8795	0.8912	0.8156	0.8773
MEC		280.1	960.3	0.008	602.7	1363.9	0.016	158.0	2397.5	0.003
RMSE		16.73	30.99	0.088	24.55	36.93	0.126	12.57	48.96	0.050
MAPE		12.15	11.46	8.32	12.78	11.05	6.55	12.41	15.23	5.07
DW		2.228	2.071	2.101	1.321	2.043	2.047	2.179	1.659	2.093

ns: non-significant coefficient; Obs: Number of observations; R^2: Coefficient of determination; R^2adj: The adjusted determination coefficient for the model; MSE: The Mean Square of the Error; RMSE: The Root Mean Square of the Errors; MAPE: The Mean Absolute Percentage Error; and DW: The Durbin-Watson statistic.

The variable models of Eqs. [14] to [22] derived from Eq. [12], where X_1 (t, min) and X_2 (T, ºC or P, W); Y is the response, with the sub-indices indicating the applied technique and the super-indices the three used response criteria (Y_1 in %, Y_2 in mg E/g R and Y_3 in mg E/100 g M dw). The parametric information presented in **Table 12** or Eqs. [14] to [22], provides a complete summary of the effects caused by each one of the variables defined for each extraction system. These equations translate the response patterns, showing a relatively high complexity (higher than 5 parameters) of the possible sceneries for the Y_1 and Y_2 value formats and relatively simple solutions for the Y_3 response value format (less than 4 parameters).

Since the experimental plan is based on coded values of the variables, the obtained model coefficients are empirical and cannot be associated with physical or chemical parameters. However, their numerical values can be used for direct comparisons. In fact, the higher the absolute value of the coefficients is, the more important will be the weight of the corresponding variables. Correspondingly, when a factor has a positive effect, the response increases as the value of the involved variable increase, and when the factor has a negative effect, the response decreases.

Graphical illustrations and general analysis of the results

Figure 21, 22 and **23** show the fitting analysis, graphical descriptions of the responses as a function of each defined variable, statistical analysis and optimal conditions that maximize the assessed response format value (Y_1, Y_2, and Y_3) of each variable for the HAE, UAE and MAE techniques. In each of these figures (**Figure 21, 22** and **23**), the illustration is divided in four sections:

- Part A shows the surface plots in 3D response surface predicted with the second order polynomial Eq. [12] as a function of each one of the involved variables.

- Part B shows the 2D contour plots of the simulations achieved with the models of Eqs. [14] to [22] after fitting the experimental results to Eq. [12].

- Part C shows an illustration of the statistical robustness of the performed mathematical analysis. Two basic graphical criteria were used: the ability to simulate the changes of the response using the correlation between experimental and predicted values and the residual distribution as a function of each of the variables.

- Part D shows the summarized individual 2D responses as a function of the defined variables for the HAE, UAE and MAE extraction systems to guide the selection of the

most favourable conditions. The line represents the variable response pattern when the others are located at the optimal values. The dots ($\odot$) presented alongside the line highlight the location of the optimal value.

Observing the response surface plots for the extraction yield in the HAE system in **Figure 21**, it is possible to verify that the amount of extracted material increases up to a maximum value as t and T increase. On the other hand, in the UAE system the amount of extracted material increases to an optimum value and then starts to decrease as a function of t and P. In the MAE technique, a higher T favours a faster diffusion, thus achieving a higher content in Y_1 due to an increase in the solubility and diffusion coefficient from the solid to the liquid matrix. Despite this positive effect on the extraction yield, increasing T may also affect the stability of the compound of interest. Hence, a combination of lower t and moderate T resulted in a better extraction yield. Observing the predicted surfaces for Y_2 response format value (mg E/g R) in **Figure 22**, it is possible to draw the following conclusions: in MAE, a negative interactive effect between variables was observed (positive for t and negative for T), which indicates that higher t might be beneficial to improve exudation of active constituents from the ruptured cell walls, but prolonged exposure may cause compound deterioration, thus reducing the ergosterol purity in the extract. In the UAE system, the variable P was found to have a positive effect on Y_2. The 2D response contour plot of **Figure 22** (Part B), shows mutual interactions between the variables, whereas the circular contour plot reveals less interaction between the corresponding variables, and the elliptical contour plot shows the most significant interactions between the variables. The 2D plot for the UAE technique shows the most significant interactions, meaning that a moderate value of t and a higher P value generated the highest yield in ergosterol (mg E/g R). Observing **Figure 23** and comparing the results among all the techniques, it allows concluding that MAE gave significantly higher values at a shorter t. The results with the UAE technique indicate that Y_3 increased as a function of P and t increase, while an opposite effect was observed for HAE.
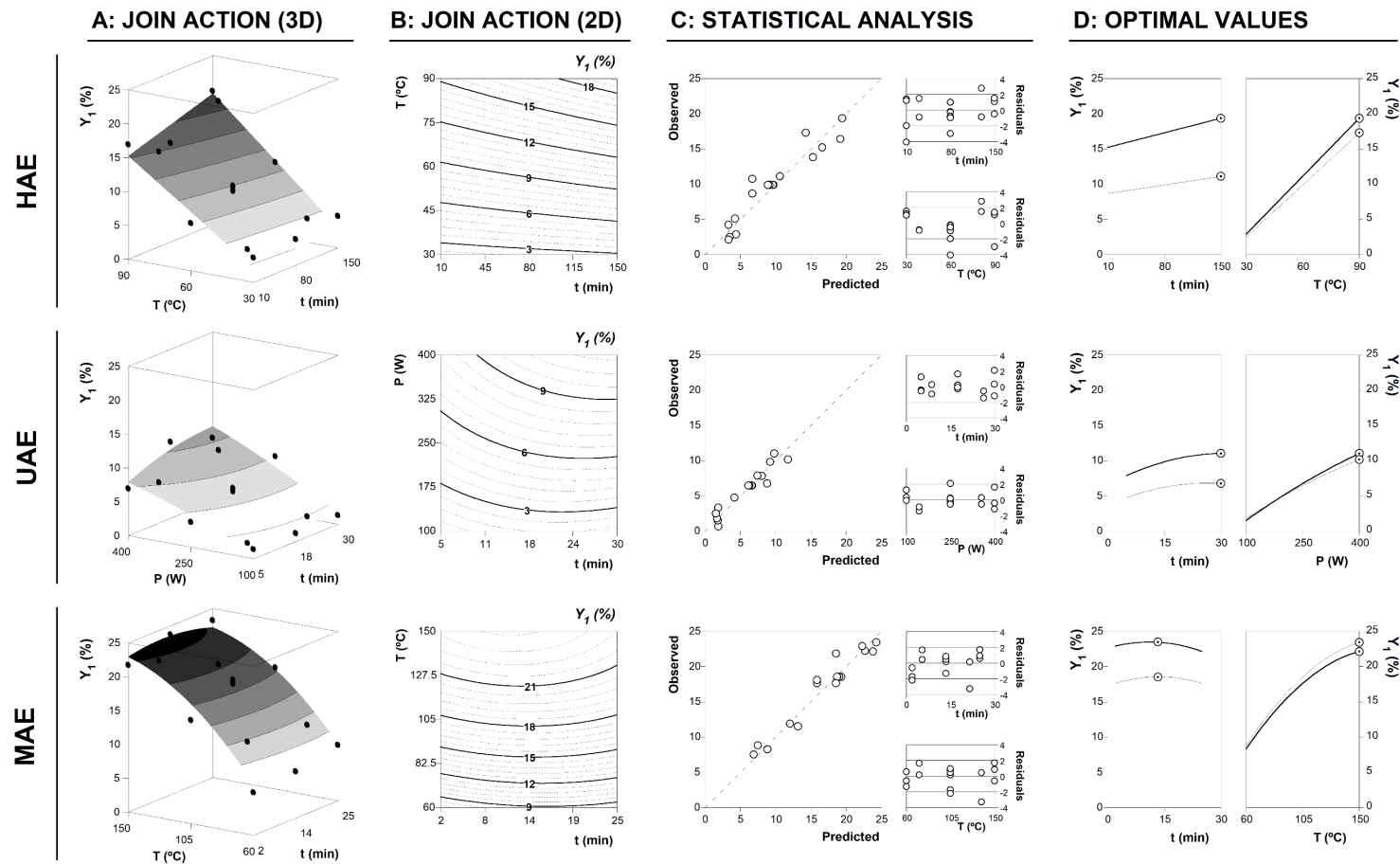
Figure 21. Graphical results in terms of response value format Y_1 (%) using HAE, UAE, and MAE extraction techniques. ***Part A***: Points (●) represent the obtained experimental results (**Table 11**) and the net surface represents the theoretical 3D response surface predicted with the second order polynomial Eq. [12] as a function of each of the variables involved. Estimated parametric values are shown in **Table 12**. ***Part B***: Two-dimensional representation of the fitting results of Eq. [12]. The binary actions between variables are presented when the excluded variable is positioned at the optimum of the experimental domain (**Table 13**). ***Part C***: To illustrate the statistical description, two basic graphical criteria are used: the ability to simulate the changes of the response and the residual distribution as a function of each of the variables. ***Part D***: The dots (⊙) presented alongside each line highlight the location of the optimum value. Lines are generated by Eq. [12]

Figure 22. Graphical results in terms of response value format Y_2 (mg E/g R) using HAE, UAE, and MAE extraction techniques. ***Part A*:** Points (●) represent the obtained experimental results (**Table 11**) and the net surface represents the theoretical 3D response surface predicted with the second order polynomial Eq. [12] as a function of each of the variables involved. Estimated parametric values are shown in **Table 12**. ***Part B*:** Two-dimensional representation of the fitting results of Eq. [12]. The binary actions between variables are presented when the excluded variable is positioned at the optimum of the experimental domain (**Table 13**). ***Part C*:** To illustrate the statistical description, two basic graphical criteria are used: the ability to simulate the changes of the response and the residual distribution as a function of each of the variables. ***Part D*:** The dots (⊙) presented alongside each line highlight the location of the optimum value. Lines are generated by Eq. [12].

Figure 23. Graphical results in terms of response value format Y_3 (mg E/100 g M dw) using HAE, UAE, and MAE extraction techniques.

Statistical and experimental verification of predictive models

To assess the competence of the obtained models of Eqs. [14] to [22], several statistical tests were used, and the results are presented in **Table 12**. In general, for all the developed models, the statistical tests merge into the same conclusions: the models are practical and can be applied effectively in subsequent prediction stages. In fact, the most common statistical criteria presented in **Table 12**, coefficients R^2 and R^2_{adj}, in all cases, displayed values higher than 0.8, which indicates a good agreement between the experimental and predicted values. The distribution of the experimental and predicted values can be visualized in part C of **Figure 21** to **23**. Indeed, it suggests that more than 80% of variability was successfully explained by the model, thus indicating the suitability of the model and a high level of correlation between the observed and predicted values. For all extraction methodologies, all experimental points were found to be close to the line of perfect fit, suggesting an accurate correlation between the predicted and experimental values, what further confirms the suitability of the employed model. Additionally, the residuals distribution presented in Part C of **Figure 21** to **23** was in all cases arbitrarily distributed around zero, and no group of values or autocorrelations were observed. This implies that the variation of the experimental results can be explained by the independent processing variables by using the specific parametric values presented in **Table 12**, which validates the models of Eqs. [14] to [22], and allows the determination of the optimal conditions that will maximize the responses.

Numerical optimal conditions that maximize the extraction and experimental verification of predictive models

By applying a simple method to solve nonlinear problems, the optimum individual condition maximizing the recovery of ergosterol were determined for the three possible response format values. In addition, the global optimum conditions can also be determined. Both individual and global optimal conditions are presented in **Table 13**. The best results of the found optimal individual values, for each of the responses, are as follows:

- For the extraction yield, response value Y_1, the MAE was the best solution: 23.50±4.3% was achieved at 11.1±1.2 min and 150±10.2 ºC.

- For the ergosterol purity in the extract, response value Y_2, the UAE was the best solution: 1.92±0.2 mg/100 g E, was achieved at 30.0±1.5 min and 311.7±31.2 W

- For the response yield in ergosterol, response value Y_3, the MAE was the best solution; 25.50±3.5 mg/100 g M dw was achieved at 25.0±3.4 min and 140.7±12.1 ºC.

The global optimal conditions found are as follow:

- For the response value Y_1, the MAE was the best solution: 21.16±2.3% was achieved at 25.0±2.6 min and 134.6±10.9 ºC.

- For the response value Y_2, the UAE was the best solution: 1.77±0.6 mg/100 g E, was achieved at 30.0±4.3 min and 400.0±18.7 W

- For the response value Y_3, the MAE was the best solution: 25.44±5.1 mg/100 g M dw was achieved at 25.0±2.6 min and 134.6±10.9 ºC.

Table 13. Variable conditions in natural values that lead to optimal response values for RSM according to the experimental design (**Table 10**) for each of the extracting techniques assessed (HAE, UAE and MAE), for the three individual response value formats (Y_1, yield in %; Y_2, mg E/g R; and Y_3 mg E/100 g M dw) and for the global optimal conditions.

CRITERIA		OPTIMAL VARIABLE CONDITIONS		OPTIMUM RESPONSE	
		X_1: t (min)	X_2: T (ºC) or P(W)		
A) Individual optimal variable conditions:					
Maceration (ME)	Y_1	150.0±5.3	90.0±6.4	19.37±1.2	%
	Y_2	150.0±6.2	54.3±7.1	1.64±0.2	mg E/g R
	Y_3	150.0±4.9	90.0±8.6	19.43±3.1	mg E/100 g M dw
Ultrasound (UAE)	Y_1	30.0±7.9	400.0±15.2	11.03±0.9	%
	Y_2	30.0±1.5	311.7±31.2	1.92±0.2	mg E/g R
	Y_3	30.0±6.2	400.0±51.1	21.49±1.9	mg E/100 g M dw
Microwave (MAE)	Y_1	11.1±1.2	150.0±10.2	23.50±4.3	%
	Y_2	25.0±4.2	60.0±11.5	1.59±0.4	mg E/g R
	Y_3	25.0±3.4	140.7±12.1	25.50±3.5	mg E/100 g M dw
B) Global optimal variable conditions:					
Maceration (ME)	Y_1			17.05±1.9	%
	Y_2	150.0±6.1	81.6±2.6	1.21±0.1	mg E/g R
	Y_3			18.84±2.3	mg E/100 g M dw
Ultrasound (UAE)	Y_1			11.03±3.1	%
	Y_2	30.0±4.3	400.0±18.7	1.77±0.6	mg E/g R
	Y_3			21.49±0.9	mg E/100 g M dw
Microwave (MAE)	Y_1			21.16±2.3	%
	Y_2	25.0±2.6	134.6±10.9	1.01±0.1	mg E/g R
	Y_3			25.44±5.1	mg E/100 g M dw

Considering both the individual and global values, the higher extract yield was obtained using the MAE technique. HAE also conducted to high extraction yields but requiring higher extraction times. In terms of Y_2, UAE reached maximum results by consuming less energy and time, while providing higher ergosterol purity in the extract, which is aligned with the requirements of green technology. The results herein obtained are in accordance with

conclusions previously reported (Chemat et al., 2017; Montesano et al., 2008; Zhu et al., 2016). UAE is an eco-friendly alternative to conventional techniques. The main benefits are the time and energy reduction, and type of applied solvents, consequently minimizing industrial emissions (Chemat et al., 2017), which is an objective of the sustainable ''green'' chemistry. The extraction processes are completed in minutes with high reproducibility, simplifying manipulation and work conditions, giving products with higher purity and eliminating further treatment as it occurs in conventional extraction methods such as Soxhlet extraction or maceration (Chemat et al., 2017).

Optimization of solid-liquid extraction using HAE, MAE and UAE technique

As already described elsewhere, the ideal *S/L* should be one that allows the solvent to penetrate the structure of the solid matrix (Pinela et al., 2017), allowing also the solvent to dissolve all the target compounds (Albuquerque et al., 2016). Therefore, a study aiming to evaluate the *S/L* effect was conducted at the global optimal conditions predicted by the polynomial models obtained for HAE, UAE, and MAE techniques (**Table 13**, part B). Preliminary experiments indicated a limit value of *S/L* near to 120 g/L. Therefore, the dose-response analysis process was designed to analyse the *S/L* from 5 to 120 g/L.

The dose-response results to the study of the *S/L* effects for the three response value formats (Y_1, Y_2, and Y_3), and each one of the used three techniques was evaluated by fitting the Weibull model of Eq. [13] (in its increasing or decreasing form) to the obtained responses using nonlinear least-squares estimations. The obtained parametric values are presented in **Table 14**.

The effects caused by the increase of the *S/L* on the response value formats are graphically shown in **Figure 24** for the three studied techniques. **Figure 24** part A shows the experimental dose-response results (in which: Y_1 ○, Y_2 □ and Y_3●) at the global optimal values of the two variables defined for each of the three assessed techniques (HAE, UAE and MAE), and their respective predictions made by the mathematical model of Eq. [13] (lines). In general, a non-linear effect can be observed for all responses as the *S/L* dose-response increases, causing a saturated-decreasing effect (↓) for the Y_1 (%) value format and saturated-increasing effects (↑) for the Y_2 (mg E/g R) and Y_3 (mg E/100 g M dw) value formats. **Figure 24**, part B shows, jointly, the dose-response simulation trends for HAE, UAE and MAE for comparison purposes.

Table 14. Parametric results of the second-order polynomial equation of Eq. [13] or the HAE, UAE, and MAE techniques assessed in terms of the variation of the *S/L*.

	PARAMETRIC VALUES			STATISTICS
	K	*m*$_{50\%}$ or *m*$_{99\%}$	*A*	*R*^{2}
Y$_1$ (%)				
HAE	33.43±2.19	41.14±4.51	0.79±0.08	0.9848
UAE	22.00±3.65	53.85±6.28	0.65±0.17	0.8604
MAE	26.98±3.51	82.76±8.58	1.60±0.19	0.9030
Y$_2$ (mg E/g R)				
HAE	2.57±0.63	155.46±12.61	1.22±0.09	0.9916
UAE	2.92±0.33	102.44±17.96	1.17±0.11	0.9750
MAE	1.01±0.19	12.70±2.11	7.40±0.87	0.9363
Y$_3$ (mg E/100 g M dw)				
HAE	22.60±3.45	25.34±2.17	2.32±0.26	0.9430
UAE	25.07±4.12	36.35±2.25	1.38±0.18	0.8955
MAE	28.01±3.76	26.57±3.85	1.71±0.37	0.9895

The analysis of the results can be interpreted by means of the two main parameters K and m_n (at 50% or 99% of the response). The parameter K shows the maximum extraction value that can be obtained as a function of the *S/L* dose-response. Thus, the lower the m_n values are, the higher are the extraction levels reached in a shorter dose-response, which would limit the possibility of reducing the amount of needed solvent for industrial purposes. Given these considerations, both values are important to understanding the trends of the *S/L* dose-response effect. In a more detailed analysis, the following aspects can be observed:

A: FITTING ANALYSIS OF ALL RESPONSES

Heat-assisted extraction (HAE)
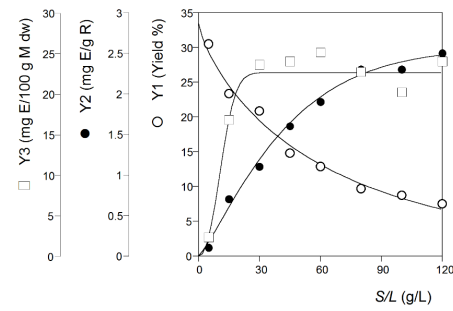
Ultrasound-assisted extraction (UAE)
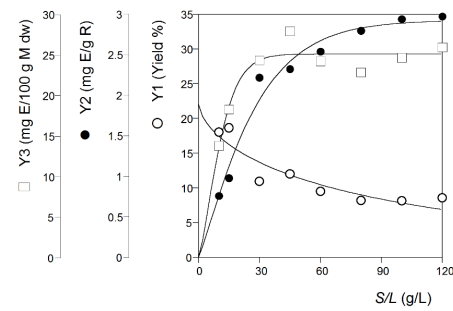
Microwave-assisted extraction (MAE)
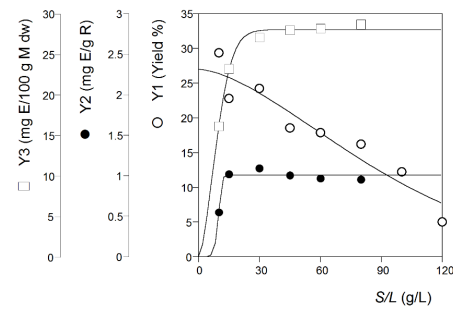
B: SIMULATION ANALYSIS OF THE RESPONSES

HAE ——— UAE ——— MAE ·········
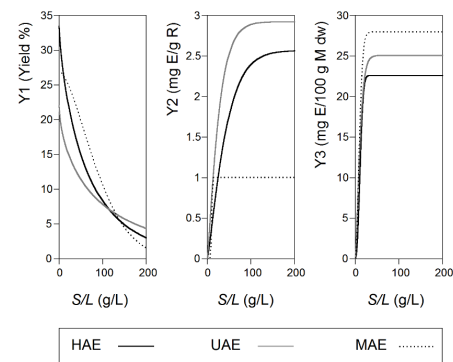
Figure 24. Graphical illustration of the effects caused by the S/L on the response value formats for the three studied techniques. ***Part A*** shows the fitting analysis of the experimental dose-response results (in which: Y_1 ○, Y_2 □ and Y_3 ●) at the global optimal values of the two other variables for each of the three techniques assessed (HAE, UAE and MAE) and their respective predictions made by the mathematical model of Eq. [13] (lines). Meanwhile, ***part B*** shows the dose-response simulation trends for HAE, UAE, and MAE jointly for comparison purposes.

- For Y_1 values, a response that translates the extraction yield: a saturated-decreasing dose-response pattern was found, which means that Y_2 initially decreases to zero as S/L increases. For HAE, UAE, and MAE the $m_{50\%}$ values obtained were 41.14±4.51, 53.85±6.28, and 82.76±8.58 g/L, respectively, with a maximum extraction yield (parametric value of K) of 33.43±2.19, 22.00±3.65 and 26.98±3.51%, for all the assessed techniques. The R^2 values obtained for the fitting results of the experimental values to Eq [13] in its saturated-decreasing form (↓) were 0.9848, 0.8604 and 0.9030 for HAE, UAE, and MAE, respectively.

- For Y_2 values, a response that gives the ergosterol purity in the extracted: a saturated-increasing (↑) dose-response pattern was observed, which means that Y_1 initially increases as the S/L increases, but when certain S/L levels are reached the ergosterol purity in the extract remains constant. For HAE, the response increases until S/L reaches values close to 155.46±12.61 g/L (parametric value $m_{99\%}$ from Eq. [13], **Table 14**), allowing a content of 2.57±0.63 mg E/g R (parametric value K from Eq. [13], **Table 14**, positive). For UAE, the $m_{99\%}$ value was 102.44±17.96 g/L, with a K value of 2.92±0.33 mg E/g R, and for MAE, 12.70±2.11 g/L was obtained as $m_{99\%}$, with K giving 1.01±0.19 mg E/g R. In HAE and MAE, the achieved increased levels of ergosterol purity by varying the S/L are not as pronounced as those observed with UAE, a fact that may be related to instrumental limitations. The R^2 values obtained for the fitting results of the experimental values of Eq [13] in its saturated-decreasing form (↓) were 0.9916, 0.9750 and 0.9363 for HAE, UAE, and MAE, respectively.

- For Y_3 values, a response that reflects the yield in ergosterol: a saturated-increasing (↑) dose-response pattern was noticed, which means that Y_2 initially increases as the S/L values increase. For HAE, UAE, and MAE the $m_{99\%}$ the obtained values were 25.34±2.17, 36.35±2.25, and 26.57±3.85 g/L, respectively, presenting K values of 22.60±3.45, 25.07±4.12 and 28.01±3.76 E/100 g M dw, respectively. These results may reflect the total ergosterol content available in the mushroom fruiting body, once the maximum concentration is achieved. In the non-conventional techniques (UAE and MAE) the decreasing effect is less noticeable, comparatively with the used conventional extraction method (HAE). In fact, for UAE and MAE, the S/L effect remains almost constant until ~120 g/L.

In conclusion, UAE was the best extraction technique, closely followed by MAE. The less effective extraction system was HAE. These results prove that alternative solid-liquid

extraction methods are more suitable than the conventional ones for the extraction of ergosterol from ABM fruiting bodies. The findings of this work are in accordance with the ones of Tomšik et al. (2016), which stated that UAE enhances the extraction process by increasing the mass transfer between the solvent and the plant material. The collapse of cavitation bubbles leads to a better cell disruption facilitating the release of extractable compounds, allowing greater penetration of solvent into the sample matrix, thus increasing the contact surface area between the solid and liquid phase (Chemat et al., 2017; Tomšik et al., 2016).

Comparison of the efficiency of ergosterol extraction by conventional and non-conventional techniques

Chemical synthesis of ergosterol and other valuable sterols can be carried out by chemical esterification and lipase-catalysed esterification that requires several energy and material consuming steps (He et al., 2014). Production of these valuable ingredients using these routes presents disadvantages, making alternative processes, such as extraction from ergosterol-rich matrices, attractive methods for ergosterol obtainment. Several authors have reported the extraction of ergosterol from mushrooms using the Soxhlet system (Barreira et al., 2014; Heleno, Diz, et al., 2016; Taofiq, Heleno, et al., 2016). *A. bisporus* and other edible or medicinal mushrooms belonging to the *Agaricus* genus have been reported to be novel sources of ergosterol (**Table 15**). *A. bisporus* presented the higher content of ergosterol (J. Deng et al., 2017), when compared to other species, however, *A. blazei* can be valorised as a viable source of ergosterol, considering the surplus amount of its fruiting bodies that are discarded in the production/processing chain. From previous studies also reported in **Table 15**, extraction of ergosterol has been carried out using conventional techniques, as well as non-conventional methods, with the latter requiring milder conditions. Most of the methods reported in **Table 15** were conducted using one variable at a time, what in most cases does not guarantee maximization of the ergosterol recovery. Hence, carrying out RSM using a series of experimental domains, and possible combination of independent variables, presents advantages (Heleno, Diz, et al., 2016; Heleno, Prieto, et al., 2016).

Table 15. Ergosterol content reported in some *Agaricus* genus.

| TECHNIQUE | MUSHROOM MATERIAL | | SOLVENT | | CONDITIONS | CONTENT | REFERENCE |
	Source	Used parts	Type	Proportion (%)		(mg E/100 g)	
HAE	*Agaricus bisporus*	Mycelium	Methanol	100	25°C, 1hr, non-saponified	17.49 ± 1.45	(Cardoso et al., 2017)
HAE	*Agaricus bisporus*	Fruiting bodies	Ethanol	95	1M NaOH, 80°C, 1hr saponified	33.54 ± 6.34	(Shao et al., 2010)
HAE	*Agaricus bisporus P*	Fruiting bodies	Ethanol	95	1M NaOH, 80°C, 1hr saponified	48.24± 3.12	(Shao et al., 2010)
HAE	*Agaricus bisporus*	Fruiting bodies	Ethanol	95	80°C, 1hr, saponified	43.22±5.11	(N. K. Lee & Aan, 2016)
HAE	*Agaricus arvensis*	Fruiting bodies	Methanol	100	2M NaOH, saponified	26.83 ± 8.71	(Gąsecka et al., 2017)
HAE	*Agaricus bisporus P*	Fruiting bodies	Methanol	100	2M NaOH, saponified	26.46± 1.52	(Gąsecka et al., 2017)
HAE	*Agaricus bisporus*	Fruiting bodies	Methanol	100	2M NaOH, saponified	1.15 ± 36.16	(Gąsecka et al., 2017)
HAE	*Agaricus bitorquis*	Fruiting bodies	Methanol	100	2M NaOH, saponified	35.35 ± 0.55	(Gąsecka et al., 2017)
HAE	*Agaricus brasiliensis*	Fruiting bodies	Methanol	100	2M NaOH, saponified	6.01 ± 0.32	(Gąsecka et al., 2017)
HAE	*Agaricus campestris*	Fruiting bodies	Methanol	100	2M NaOH, saponified	42.34± 0.48	(Gąsecka et al., 2017)
HAE	*Agaricus silvaticus*	Fruiting bodies	Methanol	100	2M NaOH, saponified	45.82 ± 2.11	(Gąsecka et al., 2017)
PLE	*Agaricus bisporus*	Fruiting bodies	Ethanol	--	10.68 MPa, 50°C	93.06 ± 4.21	(Gil-Ramírez et al., 2013)
CAE	*Agaricus bisporus*	Fruiting bodies	Hexane	--	4000 rpm,10 min	612.65 ± 9.45	(Guan et al., 2016)
CAE	*Agaricus bisporus P*	Fruiting bodies	Hexane	--	4000 rpm,10 min	759.34 ± 13.56	(Guan et al., 2016)
CAE	*Agaricus brazilienses*	Mycelium	Ethanol	95	4000 rpm, 20 min	74.67 ± 4.87	(H. Gao & Gu, 2007)
MAE	*Agaricus bisporus*	Fruiting bodies	Ethanol	--	19.4 min, 132.8°C	555.3 ± 23.6	(Heleno, Prieto, et al., 2016)
SFAE	*Agaricus bisporus*	Fruiting bodies	Ethanol	10	9-30 MPa, 40 °C,	532.45 ± 4.85	(Gil-Ramírez et al., 2013)
UAE	*Agaricus bisporus*	Fruiting bodies	Ethanol	100	15 min, 375W	19.49 ± 0.74	(C. R. L. Francisco et al., 2018)
UAE	*Agaricus bisporus*	Fruiting bodies	Hexane		15 min, 375W	152.22 ± 6.53	(Heleno, Diz, et al., 2016)
UAE	*Agaricus bisporus*	Fruiting bodies	Ethanol	100	15 min, 375W	671.53 ± 10.51	(Heleno, Diz, et al., 2016)
UAE	*Agaricus bisporus*	Fruiting bodies	Limonene	--	15 min, 375W	372.02 ± 0.17	(Heleno, Diz, et al., 2016)
UAE	*Agaricus bisporus*	Fruiting bodies	Ethanol	100	15 mins, 375W	36.72 ± 0.01	(Heleno et al., 2017)
SE	*Agaricus bisporus P*	Fruiting bodies	Hexane	100	2hr	77.34 ± 1.45	(Barreira et al., 2014)
SE	*Agaricus bisporus*	Fruiting bodies	Hexane	100	2hr	352.32 ± 1.64	(Barreira et al., 2014)
SE	*Agaricus bisporus*	Fruiting bodies	Hexane	100	4hr, 12 cycles	186.11 ± 0.33	(Heleno, Diz, et al., 2016)
SE	*Agaricus bisporus*	Fruiting bodies	Ethanol	100	4hr, 12 cycles	676.12 ± 31.23	(Heleno, Diz, et al., 2016)
SE	*Agaricus bisporus*	Fruiting bodies	Limonene	100	4hr, 12 cycles	261.86 ± 11.75	(Heleno, Diz, et al., 2016)

HAE-Heat assisted extraction; PLE-Pressurized liquid extraction; CAE-Centrifuge assisted extraction; MAE--Microwave assisted extraction; SFAE-Supercritical fluid assisted extraction; UAE-Ultrasound assisted extraction, SE- Soxhlet extraction.

Conventional techniques such as SE and HAE have been used for decades requiring large solvent consumption and being high time-consuming processes, leading often to the degradation of compounds with health-related risks (Heleno, Diz, et al., 2016). However, non-conventional extraction techniques such as the UAE and the MAE are being applied to maximize the extraction of several valuable compounds from natural matrices using shorter times and with high reproducibility (Rezende, Nogueira, & Narain, 2017). The MAE optimum conditions provided the highest extraction yield, while the UAE under the optimum achieved conditions conducted to the highest ergosterol purity in the extract. The simplicity of using conventional extraction methodologies (HAE or maceration) *vs* the advantages of using non-conventional technologies (microwave, ultrasound) to recover bioactive compounds from natural matrices, from an environmental and economic point of view, has received special attention in the last decades. In the present study, the optimum conditions of (*t, T,* and *P*; depending on the chosen technique), to recover ergosterol from *A. blazei* using HAE, MAE and UAE were established using RSM. The used response criteria account with the extraction yield, ergosterol purity in the extract, and yield in ergosterol. The results showed that the optimum conditions to maximize responses lie in the selected experimental domains that were selected. The values predicted by the models are in close agreement with the experimental observations, proving the validity of the model and the utility of the predictions for a future scale-up of the studied process, production of ABM-based ergosterol-rich extracts. The UAE technology, at the optimum conditions, was identified as the most appropriate to obtain high content ergosterol-rich extracts, followed by MAE and HAE. The obtained ergosterol-rich extracts can be applied as bioactive ingredients for food, pharmaceutical, cosmeceutical and nutraceutical purposes.

3.2. The bioactive and chemical composition of mushroom extracts towards the development of mushroom-based cosmeceutical formulation.

The cosmeceutical potential of *A. bisporus*, *L. edodes*, and *P. ostreatus* ethanolic extracts was establish through the assessment of their anti-inflammatory, antimicrobial, antioxidant, and anti-tyrosinase activities, and further incorporation in a cosmetic base cosmetic cream. The bioactive properties of the final formulations were confirmed and related to the chemical ingredients present in the extracts, namely phenolic acids and ergosterol.

3.2.1. The chemical composition of mushroom ethanolic extracts

The chemical composition of the mushroom extracts is presented in **Table 16**. *P. ostreatus* showed the highest content in phenolic acids and cinnamic acid (a related compound), followed by *L. edodes* and, finally, *A. bisporus.* The highest content in *P. ostreatus* is due to the contribution of cinnamic and *p*-hydroxybenzoic acids, found in much higher amounts in this species, followed by *p*-coumaric acid. Protocatechuic acid was only identified in *L. edodes*, while *A. bisporus* only revealed the presence of cinnamic acid. The results are consistent with the ones published by Taofiq et al. (2015) that reported the presence of all those three phenolic acids in *P. ostreatus* ethanolic extract obtained by maceration and only cinnamic acid in *A. bisporus*. Carneiro et al. (2013) described the presence of vanillic and *p*-coumaric acids in methanol/water (80:20, *v/v*) extract of *L. edodes* from Brazil. The differences between the used extraction procedures and mushroom origin can justify the dissimilarity observed in the achieved phenolic acids profile. In the present study, the magnitude of the ergosterol content was: *P. ostreatus* > *A. bisporus* > *L. edodes*, even though Barreira et al. (2014) reported a different order, namely *A. bisporus* > *L. edodes* > *P. ostreatus*, but these authors used Soxhlet extraction with a different solvent (*n*-hexane).

3.2.2. Bioactive properties of the mushroom ethanolic extracts

The anti-inflammatory effects of the ethanolic extracts were assessed upon stimulation of RAW 264.7 macrophages with lipopolysaccharide for the production of the inflammatory mediator (NO). The most efficient species were *A. bisporus* and *L. edodes,* presenting the lowest EC_{50} values, followed by *P. ostreatus* (**Table 17**). The high activity exhibited by *L. edodes* extract

may be related to its high content of protocatechuic acid, but without discarding the presence of other metabolites from different chemical classes such as terpenes, polysaccharide and lipid metabolites that have also been reported as important contributors to the anti-inflammatory activity of mushroom extracts (Elsayed et al., 2014). *A. bisporus* displayed the highest anti-tyrosinase activity among the studied mushroom species (**Table 17**). *P. ostreatus* and *L. edodes* exhibited very similar activities. To the author's best knowledge, there are no reports on the anti-tyrosinase activity of *A. bisporus*. The activity displayed by the studied mushroom extracts were related with the identified phenolic acids and ergosterol and the studied mushroom extracts can be considered good candidates to be further explored as inhibitors of tyrosinase. *A. bisporus* and *P. ostreatus* showed the highest radical scavenging activity and reducing power (**Table 17**). The obtained results are consistent with the ones reported by Reis, Martins, Barros, & Ferreira, (2012), where *A. bisporus* methanolic extracts obtained by maceration gave the highest DPPH radical scavenging activity. Heleno, Ferreira, et al., (2015) reported that the reducing power of *L. edodes* methanolic extracts obtained by maceration revealed an EC_{50} of 3.19±0.03 mg/mL, like the one reported in the present study. All the mushroom extracts showed antibacterial potential against MSSA and MRSA (**Table 18**). Regarding the Gram-positive bacteria strains, in general, *L. edodes* showed the highest activity against the tested bacteria by presenting the lowest MIC values, while *A. bisporus* revealed the weakest activity presenting the highest MIC values against MSSA and MRSA and no activity against *E. faecalis*. *P. ostreatus* and *L. edodes* showed antibacterial activity against *E. faecalis*. None of the extracts was able to inhibit the growth of Gram-negative bacteria strains, even at the highest tested concentration (20 mg/mL). These results are in agreement with the ones reported by Barros, Cruz, Baptista, Estevinho, & Ferreira (2008) that described the absence of antibacterial activity in *A. bisporus* methanolic extracts against *P. aeruginosa*. Alves et al. (2013) also reported no activity for *A. bisporus* against resistant *P. aeruginosa* and *E. coli*. However, Stojković et al. (2014a) reported antibacterial activity of this mushroom (methanolic and ethanolic extracts) against *E. coli* and *P. aeruginosa*, but this may be due to the fact that these authors used ATCC bacteria whereas in the present work all the bacteria strains were clinical isolates with an antibiotics resistance profile (**Annex**). The normal microflora of the skin includes *S. epidermis*, *S. aureus* and *P. aeruginosa*, among others (Rodrigues et al., 2013). Taking into account that these microorganisms are opportunistic and have high resistance profiles, they are a threat when skin lesions occur, causing severe localized infections even with systemic invasion (Russo et al., 2016). Thus, finding extracts/compounds with high antibacterial activity against these species can be considered beneficial in the design of

cosmeceutical formulations. The mechanism of phenolic compound's antibacterial activity has been attributed to its ability to interfere with the bacteria membrane causing their disruption and subsequent DNA damage (Martins, Barros, Henriques, Silva, & Ferreira, 2015).

3.2.3. Chemical profile and bioactivity of the final cosmeceutical formulations

In the base cosmetic creams incorporated with the extracts, the presence of phenolic acids, including cinnamic acid, and ergosterol were monitored by HPLC-PDA and HPLC-UV. By analysing **Table 16** it can be concluded that all the target compounds were stable when incorporated in the base cosmetic cream matrix. In fact, they were detected at almost the same amount as firstly found in the extracts. It was possible to quantify in the final cosmeceutical formulations up to 85% of the content quantified in the extracts before incorporation.

The anti-inflammatory, anti-tyrosinase, antioxidant and antibacterial activities of the final cosmeceutical formulations were also evaluated, and the results are given in **Table 17**. The final formulations incorporated with *A. bisporus* and *L. edodes* showed the highest anti-inflammatory activity like it was observed with the individual ethanolic extracts; while *P. ostreatus* presented the lowest anti-inflammatory potential. The cosmeceutical formulation incorporated with *A. bisporus* extract revealed the highest anti-tyrosinase, while *P. ostreatus* and *L. edodes* revealed the lowest one, also in agreement with the individual activity of the extracts before incorporation. *A. bisporus* and *P. ostreatus* cream formulations showed the highest antioxidant activity, while *L. edodes* presented the lowest DPPH scavenging activity and reducing power. All the cosmeceutical formulations showed inhibition against MSSA and MRSA (**Table 18**). *A. bisporus* cream formulation revealed the lowest activity for MSSA and MRSA and did not present activity against *E. faecalis*. *L. edodes* cream formulation showed the highest activity against *E. faecalis*, MSSA and MRSA. The cosmeceutical formulations displayed antibacterial activity against the same bacteria species that were inhibited by the extracts. All the bioactivities were affected when extracts were incorporated into the base cosmetic cream formulations, increasing the EC_{50} values to higher concentrations, but still displaying all the bioactivities evaluated and maintaining the levels of the analysed bioactive compounds. This increase in the EC_{50} values can be due to some interferences of the base cosmetic cream that may affect the extract availability to exert the same bioactivity. Considering the antioxidant and the antibacterial activities exhibited by the final cream formulations, mushroom extracts can also act as preservatives in the final formulations.

Table 16. Phenolic acids and ergosterol content in the mushrooms ethanolic extract and in the cosmeceutical formulations.

	Mushroom extracts			Cosmeceutical formulations		
Phenolic acids (µg/g)	*A. bisporus*	*P. ostreatus*	*L. edodes*	*A. bisporus* cream	*P. ostreatus* cream	*L. edodes* cream
Cinnamic acid	90.06± 0.74[b]	362.7 ± 1.28[a]	7.31± 0.14[c]	87.73 ± 1.63[b]	317.43±1.32[a]	6.10 ± 0.56[c]
p-Hydroxybenzoic acid	nd	157.78 ± 4.13	83.05± 2.15	nd	138.88 ± 2.30	73.67 ± 1.56
p-Coumaric acid	nd	63.74 ± 0.15	nd	nd	53.16 ± 2.94	nd
Protocatechuic acid	nd	nd	52.45±0.38	nd	nd	39.85±1.53
Total (µg/g)	90.06± 0.74[c]	584.24 ± 3.01[a]	142.81 ± 2.39[b]	87.73 ± 1.63[c]	509.47 ± 3.93[a]	119.61± 2.54[b]
Ergosterol (mg/g)	44.79 ± 0.37[b]	78.20 ± 0.54[a]	8.94± 0.04[c]	41.43±1.38[b]	71.62±0.29[a]	8.60±0.25[c]

nd- not detected. In each row and within each group of samples (mushroom extracts and final cosmeceutical formulations), different letters mean significant statistical differences ($p<0.05$).

Table 17. Anti-inflammatory, anti-tyrosinase, and antioxidant activities of the mushroom ethanolic extracts and of the cosmeceutical formulations.

	Mushroom extracts			Cosmeceutical formulations		
Bioactivities	*A. bisporus*	*P. ostreatus*	*L. edodes*	*A. bisporus* cream	*P. ostreatus* cream	*L. edodes* cream
Anti-inflammatory (EC$_{50}$ value, mg/mL)	0.18 ± 0.01[b]	0.29 ±0.03[a]	0.16 ±0.01[b]	2.52±0.23[b]	3.81±0.23[a]	2.59±0.23[b]
Anti-tyrosinase (EC$_{50}$ value, mg/mL)	0.16 ± 0.01[b]	0.86 ± 0.07[a]	0.82 ± 0.08[a]	3.22±0.37[b]	11.01±0.35[a]	11.89±0.85[a]
Antioxidant (EC$_{50}$ value, mg/mL)						
DPPH radical-scavenging activity	7.04 ± 0.32[b]	7.69 ± 0.20[b]	23.36 ± 1.11[a]	234.3±10.9[b]	239.5±10.4[b]	321.8±16.4[a]
Reducing power	2.34 ± 0.05[b]	2.36 ± 0.08[b]	3.03 ± 0.04[a]	35.91±0.31[b]	32.18±2.73[c]	48.90±0.64[a]

Dexamethasone was used as a positive control for anti-inflammatory activity (EC$_{50}$=0.016 mg/mL). Ascorbic acid was used as positive control for anti-tyrosinase activity (EC$_{50}$=0.031 mg/mL). Trolox was used as a positive control for antioxidant activity (EC$_{50}$=0.041 mg/mL for reducing power and 0.042 mg/mL for DPPH scavenging activity). In each row and within each group of samples (mushrooms extract and final cosmeceutical formulations), different letters mean significant statistical differences ($p<0.05$).

Table 18. Antimicrobial activity (MIC, mg/mL) of mushroom extracts and prepared formulations.

Bacteria strains	Mushroom extracts			Cosmeceutical formulations		
	A. bisporus	*P. ostrearus*	*L. edodes*	*A. bisporus* cream	*P. ostreatus* cream	*L. edodes* cream
Gram-positive						
Enterococcus faecalis	>20	10	5	>200	200	100
Methicillin sensitive *Staphylococcus aureus*	10	2.5	2.5	200	50	50
Methicillin resistant *Staphylococcus aureus*	10	2.5	2.5	200	50	50
Gram-negative						
Escherichia coli	>20	>20	>20	>200	>200	>200
Pseudomonas aeruginosa	>20	>20	>20	>200	>200	>200

MIC- Minimum Inhibitory concentration

Based on the above findings, it can be concluded that ethanolic extracts of *A. bisporus*, *P. ostreatus*, and *L. edodes* own antioxidant activity which suggests that they have the ability to cope with oxidative stress promoting ROS generation and acting as skin anti-ageing ingredients. The extracts revealed antibacterial activity against MSSA and MRSA, which are microorganisms found to colonize the skin during injury and inflammation. After incorporating the extracts into the base cosmetic cream, the mushroom cosmetic formulations still display antioxidant and anti-inflammatory activity by inhibition of NO production and by suppression of tyrosinase activity. Furthermore, the final cosmeceutical formulations containing the mushroom extracts were found to inhibit important bacterial strains responsible for skin damage. These diverse functions displayed by the mushroom extracts before and after incorporation in the base cosmetic cream formulations suggest that the studied mushrooms contain bioactive compounds that can be the basis of cosmeceutical formulations capable to tackle skin ageing, inflammation, and hyperpigmentation. Hence, studies in dermal and epidermal cells should be conducted to clarify the role of the compounds responsible for the assessed bioactive properties. Further studies are currently being conducted regarding the evaluation of the stability of the cosmeceutical formulations.

3.3. The potential of *Ganoderma lucidum* extracts as bioactive ingredients in topical formulations, beyond its nutritional benefits

Herein, the fruiting bodies of *G. lucidum* were studied: i) in terms of nutritional and chemical composition to highlight its potential to be consumed as functional foods; ii) as a source of bioactive compounds, namely, triterpenic and phenolic acids which show antioxidant, anti-inflammatory, anti-tyrosinase, antitumor and antimicrobial activities, for cosmeceutical purposes. This last concept was studied by incorporating *G. lucidum* ethanolic extracts in a base cosmetic cream, which was further characterized in terms of physico-chemical and bioactive parameters.

3.3.1. The nutritional and chemical composition of *G. lucidum* fruiting bodies

The results for the nutritional composition of *G. lucidum* are presented in **Table 19**. Carbohydrates were the most abundant compounds, followed by proteins, fat, ash and salt. The results are fairly consistent with the ones reported by Stojković et al. (2014b) even though the

origin of the samples was different (Serbia). Regarding the free sugars, fructose was the only one identified in *G. lucidum*. Concerning the fatty acids (**Table 20)**, polyunsaturated fatty acids (PUFA) were the most abundant ones due to the high contribution of linoleic acid followed by saturated fatty acids (SFA) and monounsaturated fatty acids (MUFA). These results suggest *G. lucidum* as an important dietary source of PUFAs, which have been reported as effective agents in the support of the general body well-being by preventing several chronic diseases (J. Wang, Luo, Li, & Zhao, 2012). Concerning the tocopherols, the alpha and delta isoforms were found in *G. lucidum*, being δ-tocopherol the most abundant one (**Table 19**). This molecule has received special attention due to its reported health-promoting benefits and potent antioxidant properties, being highly used in clinical dermatology, as photoprotective skin agents against UV radiation (Thiele & Ekanayake-Mudiyanselage, 2007).

Table 19. The nutritional and chemical composition of *G. lucidum* fruiting bodies

Component	Mean ± SD
Nutritional value (g/100 g)	
Lipids	2.50±0.02
Proteins	6.72±0.04
Ash	2.4±0.2
Available carbohydrates	38.0±0.7
Total carbohydrate	88.4±0.2
Energy (kcal/100 g)	201±3
Free sugars (g/100 g)	
Fructose	2.15±0.04
Tocopherols (µg/100 g)	
alpha-Tocopherol	18.1±0.2
delta-Tocopherol	123±7
Total content of biomolecules	
Terpenoids (mg linalool/g)	27.2±0.7
Triterpenoids (mg ursolic acid/g)	5.6±0.5

Values are expressed in dry weight basis.

A very common trend in the pharmaceutical and cosmetic industries involve the use of nutritional supplements to manage health conditions; including a popular term used among dermatologist and cosmetic formulators referred to as ″beauty pills″. They involve the use of compounds such as vitamins, lycopene, retinol, essential fatty acids and other compounds with antioxidant properties to improve skin appearance (Draelos, 2010).

G. lucidum is therefore considered a complete "package" of healthy food, being an excellent source of nutritional components, as well as, of other non-nutritional compounds and as such when orally ingested, it can improve body function and wellbeing.

Table 20. Fatty acids (relative percentage) of *G. lucidum.*

Fatty acids	Amount (%)
C6:0	0.57±0.04
C8:0	0.37±0.02
C10:0	0.24±0.01
C12:0	0.283±0.007
C14:0	1.16±0.02
C15:0	2.84±0.06
C16:0	21.32±0.34
C16:1	0.46±0.04
C17:0	1.88±0.11
C18:0	5.79±0.17
C18:1n9	12.68±0.10
C18:2n6	42.42±0.13
C18:3n3	1.35±0.05
C20:0	0.71±0.04
C20:1	0.141±0.006
C20:2	0.27±0.02
C20:5n3	0.86±0.03
C22:0	2.88±0.13
C22:1n9	1.05±0.09
C22:6n3	1.48±0.10
C24:0	1.28±0.07
SFA (%)	**39.30±0.35**
MUFA (%)	**14.33±0.13**
PUFA (%)	**46.37±0.26**

SFA- Saturated Fatty Acids; MUFA- Monounsaturated Fatty Acids; PUFA- Polyunsaturated Fatty Acids. Caproic acid (C6:0); Caprylic acid (C8:0); Capric acid (C10:0); ; Lauric acid (C12:0); Myristic acid (C14:0); Pentadecanoic acid (C15:0); Palmitic acid (C16:0); Palmitoleic acid (C16:1); Heptadecanoic acid (C17:0); Stearic acid (C18:0); Oleic acid (C18:1n-9c); Linoleic acid (C18:2n-6c); a-Linolenic acid (C18:3n-3); ; Arachidic acid (C20:0); cis-11-Eicosenoic acid (C20:1); cis-11,14-Eicosadienoic acid (C20:2); Eicosapentaenoic acid (C20:5n-3); Behenic acid (C22:0); Erucic acid (C22:1n-9); Lignoceric acid (C24:0)

The Total terpenoids and triterpenoids were determined, and the results are shown in **Table 19**. The triterpene content reported in the present work was consistent with the one recently described by Liu et al. (2017), where the triterpene amount of *G. lucidum* was about 5.90 mg ursolic acid equiv/g dw. Commercially, there are already available nutraceutical products

containing *G. lucidum* extract, either alone or in combination with other mushroom species. Some of them include Organic Rare Red Reishi[TM] (100% *G. lucidum*); Organic ReiShi-Gen (50% *G. lucidum* and 50% *L. edodes*); Organic Trimyco-Gen[TM] (33% *Cordyceps sinensis* 33% *G. lucidum* 33% *L. Edodes*). These products are either formulated in pills or capsules, rich in triterpenes and β-glucans, and have been recently reported by Rathore et al. (2017) to protect the body against oxidative stress and support the immune system.

3.3.2. *G. lucidum* ethanolic extracts as relevant bioactive extracts

The ethanolic extracts of *G. lucidum* were analysed by HPLC-DAD-ESI/MS and the obtained profiles included phenolic acids and triterpenic acids. Data regarding retention time, maximum wavelengths, pseudo-molecular ion and main fragment ions observed in MS[2], compounds identification, and individual quantification are presented in **Table 21**. A total of three phenolic acids (peaks 1-3), identified by comparing their UV spectra, retention time and MS fragmentation pattern with the ones of commercial standards, were found in the *G. lucidum* extract, with *p*-hydroxybenzoic acid being the most abundant. Concerning published data, protocatechuic and *p*-hydroxybenzoic acids are the most widely reported phenolic acids in *G. lucidum*. Nevertheless, Yildiz et al. (2015) have also detected the presence of syringic acid in the methanolic extracts from this matrix, which is consistent with results achieved in this work. Heleno et al. (2012) and Stojković et al. (2014b) also reported the presence of *p*-coumaric and cinnamic acids in the fruiting body of *G. lucidum*, but differences in the extraction procedure and used environment for mushroom maturation can justify the dissimilarity found in the achieved phenolic composition and other secondary metabolites profiles.

A total of 26 triterpenoids (peaks 4-7, 9-27 and 29-31) were identified (**Table 21**), being six of them identified as ganoderic acid derivatives. In fact, an ESI-MS spectrum in negative mode was used in the present study and all triterpenoids gave [M - H]⁻ and [2M - H]⁻ ions in their negative ion mass spectra. The triterpenoids identified in the present work resulted from a comparison with literature data, regarding the UV spectra, retention time and MS fragmentation pattern, namely with the one reported for triterpenoids in the works of Guo et al. (2012); Liu et al. (2014); Pecić et al. (2015); Qi et al. (2012) &Yang et al. (2007), which also studied *G. lucidum* samples.

Ganoderic acid H, followed by ganoderic acid C2 and ganoderic acid A were the most abundant triterpenoids acids present. Yang et al. (2007) and Hadda et al. (2015) reported the presence of ganoderenic acid K in chloroform extracts of *G. lucidum* from China and Algeria, suggesting

that the triterpenoids profile might depends on the extraction method employed (namely used solvent and extraction conditions) and the geographical origin of the strain. However, most studies have reported good repeatability in the triterpenoids profile of *G. lucidum* (Hadda et al., 2015; Hennicke et al., 2016; Yang et al., 2007).

Table 21. Identification and quantification of phenolic compounds and triterpenoids in *G. lucidum* extracts produced using the SE.

Peak	Rt (min)	UV λmax (nm)	[M-H]⁻ & [2M-H] (m/z)	MS² (m/z)	Tentative identification	Quantification (mg/g R)
Phenolic acid						
1	5.23	259,293sh	153	109(100)	Protocatequic acid	1.80± 0.01
2	8.39	257	137	93(100)	*p*-Hydroxybenzoic acid	2.98±0.01
3	11.51	280	197	121(100)	Syringic acid	1.51±0.01
					Total phenolic acids	**6.30±0.01**
Triterpenes						
4	29.06	259	533/1067	515(5),497(12),404(100),303(12)	12-3,7,15-Trihydroxy-4-(hydroxymethyl)-11,23-dioxo-lanost-8-en-26-oic acid	14.21±0.02
5	30.8	256	533/1067	515(5),497(21),453(16),423(11),319(5),303(8)	12-Hydroxyganoderic acid C2	4.51±0.06
6	31.27	252	529/1059	511(10),467(100),449(11),434(5),431(15),419(8),312(8),285(5),263(11)	20-hydroxy-ganoderic acid AM1	11.40±0.01
7	31.73	251	529/1059	511(13),499(100),481(6),465(18),438(28),419(18),367(11),287(11)	12-deacetylganoderic acid H	6.1±0.14
8	32.28	255	547/1095	529(50),511(41),485(3),467(100),449(24),431(26),304(11),265(7)	Ganoderic acid derivative	7.3±0.1
9	33.94	258	531/1063	513(13),451(3),401(100),385(5),304(19),301(45),286(3),249(27)	Ganoderic acid η	25.41±0.04
10	34.48	254	511/1023	493(23),449(100),431(5),413(15),405(3)	Ganoderic acid F	17.97±0.02
11	35.37	265	529/1059	511(5),467(100),449(20),437(29),317(10),301(5),263(5)	12-hydroxyganoderic acid D	6.86±0.07
12	35.95	251	515/1031	497(100),453(31),437(8),303(19),287(5),235(3)	Ganoderic acid derivative	21.20±0.08
13	36.84	256	517/1035	499(100) 481(48),456(17),438(52),407(8),304(6),287(35)	Ganoderic acid C2	38.70±0.15
14	37.51	257	529/1059	511(5),481(7),467(100),451(14),438(38),424(3),319(5),303(3),301(5)	Ganoderic acid C6	29.10±0.08
15	38.16	256	529/1059	511(58),493(5),449(10),399(100),301(3)	Ganoderic acid derivative	12.77±0.01
16	38.46	256	531/1063	513(11),498(15),469(100),454(29),452(24),437(6),304(5),302(6),290(20),266(7)	Ganoderic acid G	16.84±0.07
17	38.75	248	513/1027	495(10),480(16),451(100),437(14),433(22),407(17),331(5),315(3),303(5),287(5)	Ganoderenic acid B	10.66±0.09
18	39.01	259	527/1055	509(26),465(6),397(100),355(4)	Elfvingic acid derivative	10.41±0.09
19	39.35	254	515/1031	497(10),453(100),439(5),409(5),304(21),287(12),263(3),250(14)	Ganoderic acid B	23.99±0.09
20	39.46	250	513/1027	495(100),479(27),462(12),451(30),433(31),381(25),301(15)	Ganoderic acid derivative	22.44±0.10
21	39.66	261	513/1027	495(21),480(5),451(100),433(24),381(6),301(6),247(3)	Ganoderic acid AM1	15.82±0.01
22	40.29	254	515/1031	497(100),480(5),454(6),436(10),302(8),301(4),285(3)	Ganoderic acid A	36.77±0.04
23	40.66	261	571/1143	553(100),511(8),481(3),468(8),437(3),423(2)	Ganoderic acid H	41.05±0.39
24	40.87	252	527/1055	509(20),479(13),465(100),435(3),421(3),317(3),301(3)	Elfvingic acid A	9.83±0.01
25	41.34	254	529/1059	511(10),496(22),493(21),467(100),449(61),434(4),319(6),317(8),301(16),300(11),299(12)	Ganoderic acid derivative	11.56± 0.04
26	41.93	246	511/1023	493(12),478(20),449(100),435(15),431(4),405(4),329(3),301(4),285(5),283(3),261(4)	Ganoderenic acid D	10.27±0.07
27	42.55	255	513/1027	495(16),451(100),437(6),433(3),407(4),301(23),286(3),284(11),247(8)	Ganoderic acid D	11.31±0.01
28	42.74	245	509/1019	491(100),476(18),461(34),447(15),429(3),417(3),300(5),299(4)	Ganoderic acid derivative	12.81±0.08
29	43.15	256	511/1023	493(100),449(65),435(3),300(5),247(4)	Ganoderic acid E	10.81±0.07
30	43.95	255	569/1139	551(100),509(35),508(21),466(8)	12-acetoxyganoderic acid F	12.08±0.07
31	44.92	272	513/1027	451(100),437(8),433(3),422(3),301(5)	Ganoderic acid J	2.92±0.05
					Total triterpenoids	**455.01±1.47**

The results regarding the bioactivity of *G. lucidum* extracts are presented in **Table 22**. The antioxidant results obtained are very similar to the ones reported by Heleno et al. (2012) for DPPH radical scavenging and reducing power, even though the authors performed a different extraction procedure (maceration in methanol:water mixture (80:20, *v/v*)). These authors also conducted studies concerning phenolic and polysaccharide extracts of *G. lucidum*, being the antioxidant activity slightly lower in the latter, suggesting that phenolic compounds play a more prominent role in the free radical scavenging activity.

G. lucidum ethanolic extract also revealed tyrosinase inhibition activity. To the authors best knowledge only Chien et al. (2008) have reported the tyrosinase inhibition activity for ethanolic extract of *G. lucidum* from Taiwan with a reported EC_{50} reaching 0.32 mg/mL, lower than the one obtained herein, possibly justified by the used slightly different procedures. Kim et al. (2016) were able to identify a bioactive compound, ganodermanondiol, which suppressed the expression of the tyrosinase-related protein (TRP-1, TRP-2) and microphthalmia-associated transcription factor (MITF) thereby inhibiting the synthesis of melanin. Tyrosinase inhibitors have shown to be effective ingredients towards skin lightening, and among the bioactive compounds found in mushrooms, phenolics have been reported as the ones that contribute most significantly to their anti-tyrosinase activity (Taofiq, González-Paramás, et al., 2016). Therefore, the ethanolic extract studied in the present work can be further exploited as a tyrosinase inhibitor to reduce the severity of hyperpigmentation and decrease melanin biosynthesis, partly due to the registered amount on phenolic acids and triterpenoids. Regarding the anti-inflammatory activity, aqueous, methanolic and ethanolic extracts of *G. lucidum* presented activity mainly by inhibiting NO, PGE2, TNF-α IL1-β production (Taofiq, Martins, et al., 2016). In the present study, the ethanolic extract of *G. lucidum* revealed anti-inflammatory activity by inhibiting NO production. Even though the phenolic compounds of mushrooms have been identified as the most important contributors to their anti-inflammatory activity (Taofiq et al., 2015), triterpenic acids such as ganoderic acid C1 and lanostane in *G. lucidum*, have also contributed significantly to its anti-inflammatory activity (Taofiq, Martins, et al., 2016).

The numerous secondary metabolites contained in this mushroom have attracted huge interest and one of the most complete reported studies is the one on its cytotoxic effect (Amen et al., 2016; Li et al., 2013). In the present work, no toxicity was observed in non-tumor porcine liver cells (PLP2) at the maximum tested concentration (400 µg/mL). However, the extract was able to inhibit all human tumor cell lines evaluated; with breast carcinoma cells showing to be the most susceptible cells, followed by non-small cell lung, hepatocellular and cervical carcinoma

cells. Our results against cervical carcinoma cells were mostly in line with the ones reported by Ćilerdžić et al. (2014) with a growth inhibitory effect of 61.17 ± 0.75 µg/mL, even though mushroom origin (Serbia) and applied extraction procedure (maceration) were different. The results also correlated well with the statements reported by Reis et al. (2015) for methanolic extract, namely a similar trend on the registered activity was observed (MCF-7 > NCI-H460). Overall, a lot of studies have been able to identify the triterpenes as the most prominent class of compounds contributing to the shown cytotoxic effect (Amen et al., 2016; S. Y. Chen, Chang, Chen, Chang, & Lin, 2016; P. Li et al., 2013). The mechanism of antitumor effect of this mushroom has been associated with inducing autophagy (Reis et al., 2015), leading to apoptosis, inhibition of tumor invasion and metastasis (Patel & Goyal, 2012).

Finally, among the analysed bacterial strains, *G. lucidum* extract showed the highest antibacterial activity against MSSA and MRSA with corresponding lowest minimum inhibitory concentrations (**Table 22**). Regarding the Gram-positive bacteria strains, *Listeria monocytogenes* was the least inhibited followed by *Enteroccocus faecalis.* For Gram-negative bacteria, the extract was not able to inhibit the growth of *Morganella morganii* and *Pseudomonas aeruginosa* even at the highest tested concentration, while the two *E. coli* and the two *Klebsiella* strains were inhibited. In brief, the extract was able to inhibit both Gram-negative and Gram-positive bacteria. The antimicrobial activity of *G. lucidum* has been widely studied, and according to the review conducted by Alves et al. (2013), extracts of *G. lucidum* revealed antimicrobial activity against *B. subtilis*, *S. aureus*, *E. coli*, *K. pneumoniae*, *P. aeruginosa*, *S. typhi*, and *S. Typhimurium*. The phenolic acids present in this mushroom have been identified as the most important contributors to this activity (Heleno et al., 2013). These authors went further to evaluate the antimicrobial activity of these phenolic acid derivatives (glucuronated and methylated) to confirm if they reveal activity in their *in vivo* form after undergoing metabolism. In the review conducted by Ferreira et al., (2015), the polysaccharide fractions was also described to contribute significantly to the antimicrobial activity of this mushroom. Thus, further studies need to be conducted with this extract by testing other bacterial and fungal strains to confirm if it presents broad spectrum antimicrobial activity.

Table 22. Bioactive properties of *G. lucidum* ethanolic extract.

	G. lucidum ethanolic extract
Antioxidant activity (EC$_{50}$ values, mg/mL)	
DPPH scavenging activity	0.73 ± 0.01
Reducing power	0.15 ± 0.01
Cytotoxic activity (GI$_{50}$ values, µg/mL)	
MCF-7 (breast carcinoma)	61 ± 4
NCI-H460 (non-small cell lung carcinoma)	64 ± 3
HeLa (cervical carcinoma)	73 ± 3
HepG2 (hepatocellular carcinoma)	68.44 ± 0.08
PLP2 (non-tumour primary liver porcine cells)	> 400
Anti-inflammatory activity (EC$_{50}$, µg/mL)	
NO Inhibition	112 ± 1
Anti-tyrosinase activity (EC$_{50}$ values, mg/mL)	
L-DOPA assay	2.81 ± 0.01
Antimicrobial activity (MIC, mg/mL)	
Gram-positive	
Enterococcus faecalis	10
Listeria monocytogenes	20
MSSA	5
MRSA	5
Gram-negative	
Eschericia coli	10
Eschericia coli ESBL	10
Klebsiella pneumoniae	20
Klebsiella pneumoniae ESBL	20
Morganella morganii	>20
Pseudomonas aeruginosa	>20
Proteus mirabilis	20
Candida albicans	>20

The antioxidant activity was expressed as EC$_{50}$ values, where lower values correspond to higher antioxidant potential. Trolox (positive control) EC$_{50}$ values: 41 µg/mL (reducing power), 42 µg/mL (DPPH scavenging activity). Anti-inflammatory activity is expressed as EC$_{50}$ values corresponding to 50% of inhibition of the NO production in comparison with the negative control (100% of NO production). Dexamethasone (positive control) EC$_{50}$ values: 16 µg/mL. Anti-tyrosinase activity is expressed as EC$_{50}$ values corresponding to 50% of inhibition of tyrosinase. Ascorbic acid (positive control) EC$_{50}$ values: 31 µg/mL. Cytotoxicity results are expressed as GI$_{50}$ values corresponding to the sample concentration responsible for 50% of growth inhibition in human tumor cell lines or in liver primary culture PLP2. Ellipticine (positive control) GI$_{50}$ values: 1.21 µg/mL (MCF-7), 1.03 µg/mL (NCI-H460), 0.91 µg/mL (HeLa), 1.10 µg/mL (HepG2) and 2.29 (PLP2). Minimum Inhibitory concentration-MIC, MRSA- Methicillin-resistant *Staphylococcus aureus*; MSSA methicillin-susceptible *S. aureus*; ESBL- spectrum extended producer of β – lactamase.

3.3.3. *G. lucidum* ethanolic extracts in cosmeceutical formulations

The use of bioactive products such as vitamins, peptides, phenolic compounds, polyhydroxy acids, obtained from plant, mushroom and other natural matrices, as cosmeceutical ingredients, has received increased attention because of their multifunctional benefits on skin (e.g. antioxidant, anti-tyrosinase, anti-hyaluronidase, anti-collagenase, anti-elastase, photoprotective, antimicrobial and anti-inflammatory activities) (Hyde et al., 2010; Y. Wu et al., 2016).

In the present study, the results of antioxidant, antimicrobial and anti-tyrosinase activities for the produced cosmeceutical formulation are presented in **Table 23**. The cosmeceutical formulations maintain the bioactivities exhibited by the extract. This achievement is quite interesting regarding the concern of cosmetic industry in reducing the presence of synthetic ingredients, and its gradual replacement by natural counterparts, due to the increased awareness on the negative effects reported for some artificial antimicrobial agents. In fact, natural bioactive compounds with a broad spectrum of antimicrobial properties are being slowly introduced in this industrial field, also justified by their multifunctional properties (Kerdudo et al., 2016). The formulations incorporated with *G. lucidum* extract were able to significantly inhibit the growth of MSSA and MRSA by presenting a low minimum inhibitory concentration. Also, this work demonstrates that extracts of *G. lucidum* have interesting biological properties that can be exploited in the design of cosmeceutical formulations either as tyrosinase inhibitors, anti-inflammatory agents or as preservatives to prolong the shelf life of the formulated product. The compounds earlier identified in the ethanolic extract were monitored by HPLC-DAD-ESI/MS and found to be present in the produced cosmeceutical formulation.

The relevance of *G. lucidum* properties is evident from the number of commercial cosmeceutical products in the market formulated from their extracts, either alone or in combination with other natural ingredients. Examples include Body Repair Lotion (*G. lucidum* extract and medicinal plant), Dr. Andrew Weil for Origins[TM] Mega-Mushroom Skin Relief Face Mask (*G. lucidum*, *C. sinensis* and medicinal plants) and Menard Embellir Refresh Massage cream (*G. lucidum* and *G. sinense*). These products have all been used to suppress the severity of hyperpigmentation, to brighten skin appearance, prevent ageing effects, and to protect skin against UV radiation (Taofiq, González-Paramás, et al., 2016).

Table 23. Physico-chemical and bioactive properties of *G. lucidum* cosmeceutical formulation

	G. lucidum cosmeceutical formulation
Physico-chemical properties	
Colour	
L^*	70.3 ± 0.7
a^*	12.1 ± 0.5
b^*	32.9 ± 0.9
pH	4.61 ± 0.03
Bioactive properties	
Antioxidant activity (EC$_{50}$ values, mg/mL)	
DPPH scavenging activity	34 ± 1
Reducing power	13.60 ± 0.09
Anti-tyrosinase activity (EC$_{50}$ values, mg/mL)	
L-DOPA assay	23.80 ± 0.03
Antimicrobial activity (MIC, mg/mL)	
Enterococcus faecalis	200
Listeria monocytogenes	400
MSSA	100
MRSA	100
Eschericia coli	200
Eschericia coli ESBL	200
Klebsiella pneumoniae	400
Klebsiella pneumoniae ESBL	400
Morganella morganii	>400
Pseudomonas aeruginosa	>400
Proteus mirabilis	400
Candida albicans	>400

Even though the individual contribution of their constituents needs to be established, there are reports claiming that terpenes such as monoterpenes and sesquiterpenes have potential to enhance compound penetration across the skin by decreasing skin barrier resistance of the *stratum corneum* (Lane, 2013). Thus, the content of terpenoids determined for *G. lucidum* can play an important role by enhancing the topical availability of other constituents in cosmeceutical formulations.

In today's cosmetic market a wide variety of choices is offered to consumers, being colour attributes an important characteristic for their acceptance. Hence, companies have paid lots of attention to managing colour display during product design and formulation. In the present work, the colour attributes of the produced cosmeceutical formulation showed a light-yellow colouration. The rate of dermal absorption of topical formulations such as lotions and creams are often influenced by the pH of the product. The pH of skin external surface is around 5.5, and at this condition, the skin micro-flora, barrier homeostasis, and *stratum corneum* are maintained (Ali & Yosipovitch, 2013; Martínez-Pla, Martín-Biosca, Sagrado, Villanueva-Camañas, & Medina-Hernández, 2004). Most reports have suggested that a pH between 4 and 6.5 can be considered as adequate for cosmetic formulations since most pathogenic bacteria (e.g. *S. aureus*), thrive best at neutral pH levels (Ali & Yosipovitch, 2013). In the present work, the cosmeceutical formulation presented a pH 4.6, which is considered within the favourable pH range.

3.4. *Agaricus blazei* Murrill: an ingredient for nutraceutical and cosmeceutical applications

The fruiting bodies (basidiocarps) of *Agaricus blazei* Murrill (ABM) were donated by a local producer in Maringá, Paraná, Brazil (23°24′S 51°55′W). ABM fruiting bodies that are considered off-market and grouped as an agro-industrial residue, were used in the present work. The nutraceutical and cosmeceutical potential of this residue was studied herein by evaluating its nutritional and chemical composition. Ethanolic extracts, obtained by Soxhlet extraction, were evaluated regarding the effects on cell viability and death in Caco-2 and HT29-MTX cells lines (MTT and LDH assays; preliminary safety tests for nutraceutical applications). To evaluate the dermatological potential, the extract was incorporated into a semi-solid base formulation that, together with the ethanolic extract itself, were studied for the effects on cell viability of a keratinocyte cell line (preliminary safety tests for cosmeceutical applications).

3.4.1. The nutritional and chemical composition of ABM

Studies on the chemical and bioactive composition of mushrooms have been reported over years, aiming at identifying species with relevant biological properties and high nutritional value (Heleno, Ferreira, et al., 2015; Stojković et al., 2014b; Taofiq, Heleno, et al., 2017). The proximate composition of the studied ABM bio-residues, expressed on a dry weight (dw) basis, are presented in **Table 24**. Its components include carbohydrates (48±2 g/100 g dw), crude protein (31.6±0.5 g/100 g dw), ash (6.2±0.5 g/100 g dw), and total fat (0.66±0.08 g/100 g dw). Carbohydrates were the major constituents, followed by proteins and ash; the fat content was low. The energy contribution was 325.3 ± 0.5 kcal/100 g dw, mainly attributed to the high carbohydrate content. Comparatively, with a commercial *A. blazei* supplement obtained from Brazil, there were no significant differences in the nutritional profile (ash, 7.47 ± 0.04 g/100 g dw; proteins, 31 ± 2 g/100 g dw; fat, 1.82 ± 0.03 g/100 g dw) (Carneiro et al., 2013). Regarding free sugars, mannitol and trehalose were the only ones detected, and found in similar amounts to the ones reported by Stojković et al. (2014a).

Table 24. Nutritional and chemical composition of ABM bio-residues.

Component	Mean ± SD
Nutritional value (g/100 g)	
Lipids	0.66±0.08
Proteins	31.6±0.5
Ash	6.2±0.5
Available carbohydrate	48±2
Total Carbohydrates	61.5±2
Energy (kcal/100 g)	325.3±0.5
Free sugars (g/100 g)	
Mannitol	34.4±0.2
Trehalose	5.1±0.2
Total Sugars	39.5±0.4
Tocopherols (µg/100 g)	
α-Tocopherol	17±0.6
Organic acids (g/100 g)	
Oxalic acid	0.98±0.01

In what concerns organic acids, oxalic acid was the unique detected compound, even though Stojković et al. (2014a) reported the presence of fumaric acid in *A. blazei* samples obtained from the Netherlands. Regarding the fatty acids profile, twenty-two molecules were identified (**Table 25**), with polyunsaturated fatty acids (PUFA) predominating (a high contribution of linoleic acid was identified), followed by saturated fatty acids (SFA) and monounsaturated fatty acids (MUFA). The distribution of fatty acids in the studied dried powder mushroom was similar to the ones reported by Carneiro et al. (2013).

Most of the literature reports refer to intact fruiting bodies of ABM, while the present results show that discarded bio-residues are still promising sources of interesting biomolecules. To the author's best knowledge, only Corrêa et al. (2018) have reported the re-utilisation of ABM bio-residues to produce an ergosterol rich fraction with antioxidant and antimicrobial properties. Those authors went further by fortifying a commercial yoghurt with the obtained ergosterol rich extract, and the final formulation was found to present an enhanced antioxidant activity. ABM bio-residues studied in the present work is therefore considered a useful source of nutritional components as well as non-nutritional compounds, which can be utilised as food supplements.

Table 25. Fatty acids (relative percentage, %) in ABM bio-residues.

Fatty acids	Amount (%)
C6:0	0.225±0.006
C8:0	0.459±0.009
C10:0	0.319±0.003
C12:0	2.36±0.01
C14:0	1.36±0.02
C15:0	1.22±0.01
C15:1	0.056±0.001
C16:0	20.6±0.1
C16:1	0.170±0.005
C17:0	1.34±0.01
C18:0	5.58±0.02
C18:1n9	2.66±0.02
C18:2n6	51.04±0.05
C18:3n6	1.47±0.02
C20:0	1.88±0.02
C20:1	0.046±0.002
C20:2	0.201±0.007
C21:0	0.572±0.001
C22:0	4.36±0.07
C22:1	2.1±0.1
C23:0	0.516±0.004
C24:0	1.52±0.04
SFA	**42.2±0.1**
MUFA	**5.0±0.1**
PUFA	**52.71±0.02**

The results are presented as mean ± SD. Caproic acid (C6:0); caprylic acid (C8:0); capric acid (C10:0); lauric acid (C12:0); myristic acid (C14:0); pentadecanoic acid (C15:0); *cis*-10-pentadecenoic acid (C15:1); palmitic acid (C16:0); palmitoleic acid (C16:1); heptadecanoic acid (C17:0) stearic acid (C18:0); oleic acid (C18:1n9); linoleic acid (C18:2n6); Gamma linolenic acid (C18:3n6); arachidic acid (C20:0); *cis*-11-eicosenoic acid (C20:1); *cis*-11,14 - eicosadienoic acid (C20:2); heneicosanoic acid (C21:0); behenic acid (C22:0); erucic acid (C22:1); tricosanoic acid (C23:0); lignoceric acid (C24:0); SFA – saturated fatty acids; MUFA – monounsaturated fatty acids; PUFA – polyunsaturated fatty acids.

3.4.2. Preliminary safety tests with the ABM ethanolic extract for nutraceutical ingredients

To fully confirm the nutraceutical potential of the obtained ABM ethanolic extracts, the major challenge still lies on the access of their safety throughout the GIT since the intestinal epithelium is the major area for the absorption of bioactive molecules allowing them to reach systemic circulation. Hence, *in vitro* models were used to mimic intestinal epithelium and access the safety of the bioactive extracts (Pan, Han, Zhang, Yu, & Liu, 2015). In the present work, the cell viability effect of the ethanolic extract prepared from ABM bio-residues was evaluated on Caco-2 and HT29-MTX cells following a concentration-dependent manner (1-10000 µg/mL). Caco-2 cells are similar to enterocytes in the gut epithelium, while HT29-MTX cells are like the mucus-producing goblet cells. Both cell lines have been widely used as intestinal models to evaluate the safety of novel nutraceutical ingredients (de Francisco et al.,

2018). Concerning Caco-2 cells, at 100 µg/mL, cell viability was not influenced up to 80% (**Figure 25**). Regarding HT29-MTX cells, up to 80% cell viability was maintained at 1 mg/mL, while the highest tested concentration (10 mg/mL) was found to significantly reduce the cell viability (**Figure 26**).
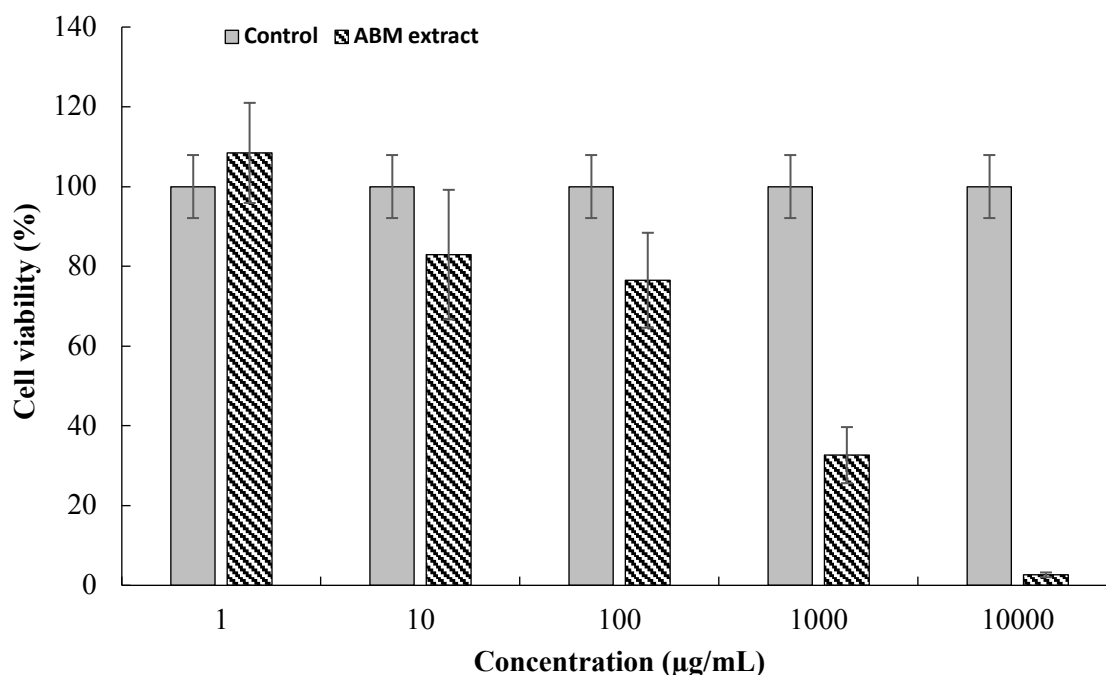
Figure 25. Cell viability effects of the ABM ethanolic extract at different concentrations on Caco-2 cells as measured by the MTT assay (n = 4).

The LDH assay has been utilised as a good marker to ascertain cytotoxicity of bioactive ingredients. The mechanism behind it involves the measurement of lactate dehydrogenase (LDH), an enzyme found in the surroundings of compromised cell membranes. In the present work, both Caco-2 and HT29-MTX cells were found to have no significant effect on LDH leakage up to 100 µg/mL (**Figure 27**). However, the LDH level was significantly detected in Caco-2 at 1 mg/mL and 10 mg/mL, while LDH was only detected at 10 mg/mL for HT29-MTX cells. From the obtained results, the cell viability studies in the MTT assay were complementary with what was observed in the LDH assay.
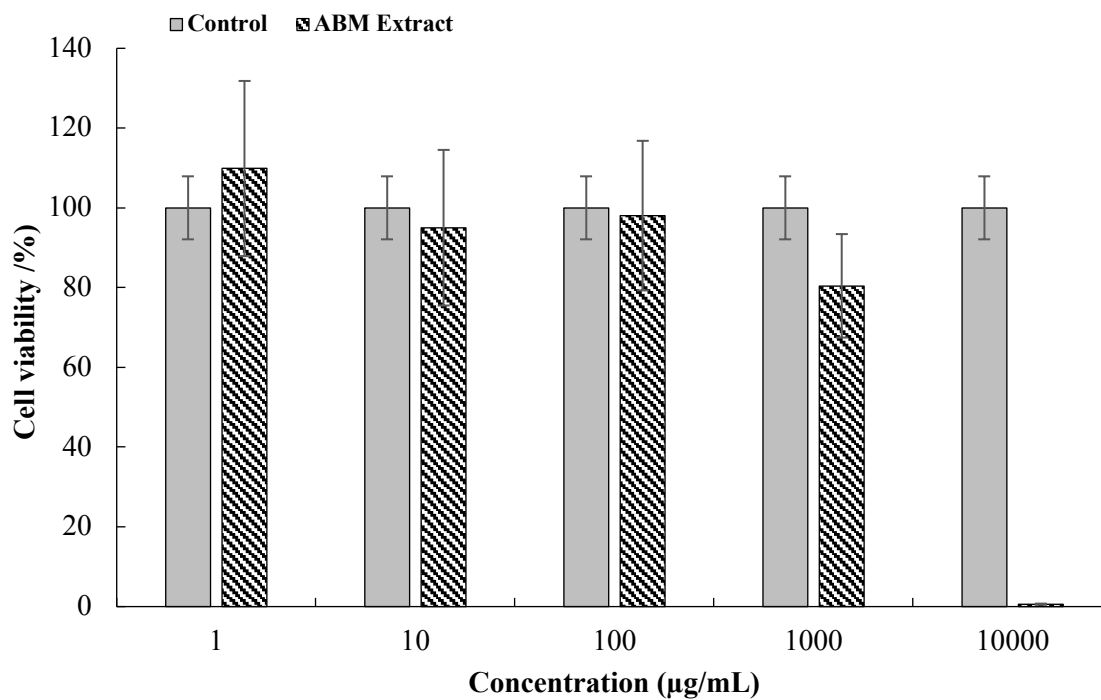
Figure 26. Cell viability effects of the ABM ethanolic extract at different concentrations on HT29-MTX as measured by the MTT assay (n = 4).
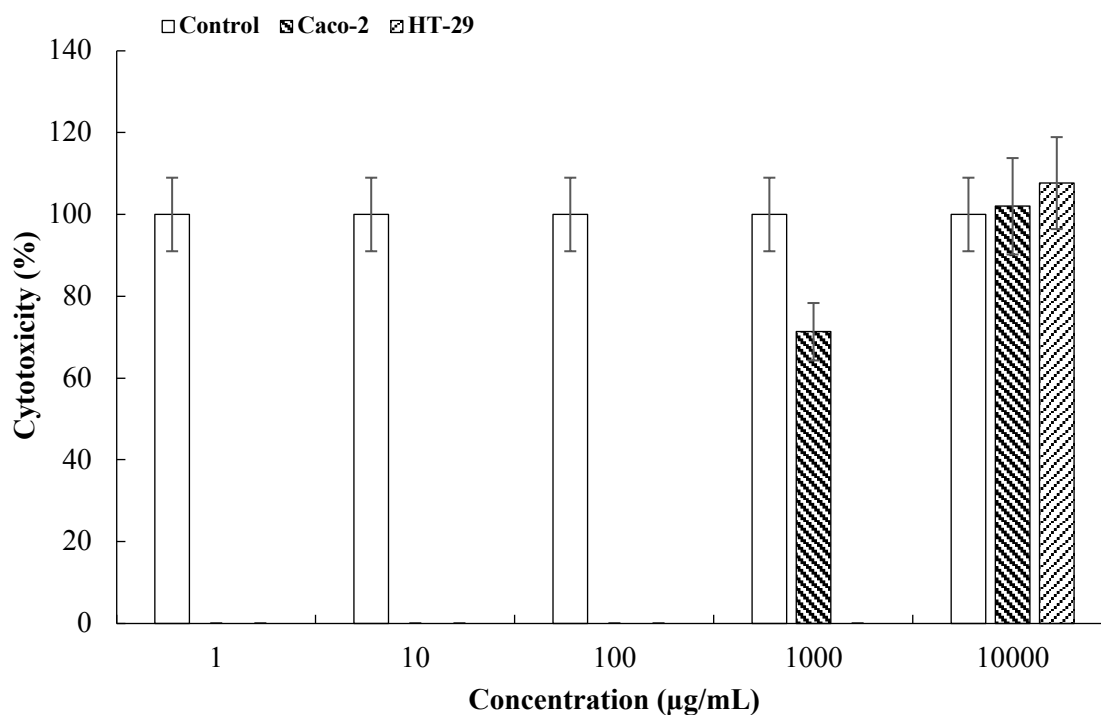
Figure 27. Cytotoxicity effects of the ABM ethanolic extract on HT29-MTX and Caco-2 cells at different concentrations as measured by LDH assay (n = 4).

3.4.3. Preliminary safety tests with the ABM ethanolic extract and final cream formulation for cosmeceutical applications

The global cosmetic industry has been a successful industrial sector over the years. Due to the increased awareness, coupled with the higher demand for safer and natural-based cosmetic products, innovative natural ingredients able to exert multifunctional benefits to the skin are an utmost of this industrial sector (Kerdudo et al., 2016; F. Rodrigues et al., 2015; Taofiq, González-Paramás, et al., 2016). In this context, mushroom-based cosmeceutical ingredients are gaining increased importance, even though they are still exploited at modest levels. Moreover, some of the bioactive properties displayed by mushroom extracts and/or their individual metabolites have lead dermatologists and researchers linked to the cosmetic field to become optimistic considering the future of mushrooms and their compounds in this sector.

In the present work, the incorporation of the ethanolic extract into a base cosmetic cream resulted in a formulation with a lower level of lightness (L^*) when compared with the former base cosmetic cream (control). The following colour attributes, using the $L^*a^*b^*$ scale, were obtained (74.30 ± 0.8, 9.16 ± 0.31, 19.31 ± 0.48). The final pH of the mushroom-based formulation was 4.31 ± 0.03, while for the control was 4.84 ± 0.02. Some studies have reported that formulations with pH between 3.5 and 6.0 can be considered favourable as most pathogenic bacteria thrive best at neutral pH levels and, at these conditions, the skin micro-flora and barrier homeostasis are maintained (Ali & Yosipovitch, 2013; Martínez-Pla et al., 2004). Additionally, some of the biomolecules identified and quantified in the studied ABM bio-residues, namely tocopherols, fatty acids, organic acids and sugars, can play major roles on skin antioxidant defence, protection against photoageing, regulation of collagen synthesis, suppression of inflammatory response, normalization of epidermal lipid profiles and improvement of skin hydration and elasticity (De Vaugelade et al., 2017; Hyde et al., 2010; Kayashima, 2002; Rhimi et al., 2018; Shapiro & Saliou, 2001; Taieb, Gay, Sebban, & Secnazi, 2012). Noteworthy is the detected high content of mannitol in the analysed ABM bioresidues (**Table 25**). Mannitol is largely used in cosmetics as a humectant to preserve the product from dehydration, and as a moisturising agent to prevent the dryness of the skin. In the last years, mannitol has been considered as the ideal excipient to be used with hyaluronic acid (HA) fillers, thanks to its hydrating and antioxidant properties (André & Villain, 2017). Thus, the action of these molecules incorporated in the final formulation prepared herein can contribute to a better skin function.
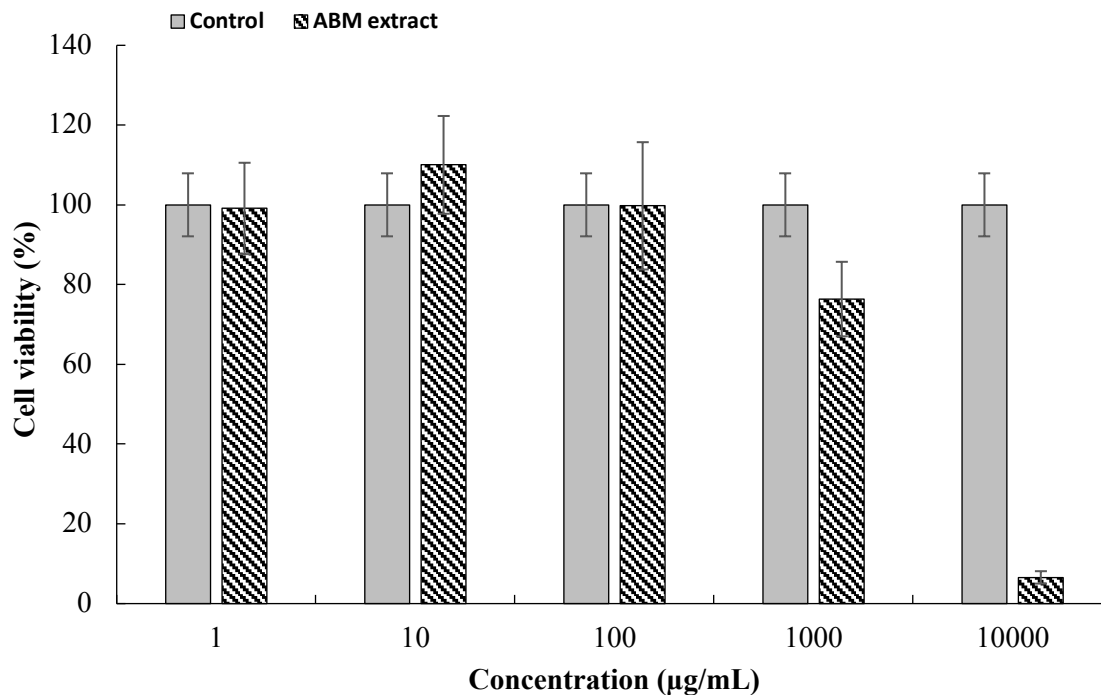
Figure 28. Cell viability effects of the ABM ethanolic extract at different concentrations on keratinocytes (HaCaT) cell line as measured by the MTT assay (n = 4).

Even though progress have been made in what concerns the use of natural extracts as cosmeceutical ingredients, their safety and efficacy lack appropriate reporting and dissemination. This constraint makes consumer's acceptance difficult, since they may not perceive that bioactive claims are true. In addition, the safety evaluation of ingredients for cosmeceutical applications is a critical step as some of these natural extracts contain different compounds and biomolecules that may be irritant to skin cells. In the present work, the effects of the obtained ethanolic extract on keratinocyte (HaCaT) cells viability was evaluated using MTT and LDH assays, as this cell line was previously documented as a reliable *in vitro* model to access the safety of cosmeceutical ingredients (Rodrigues et al., 2013).
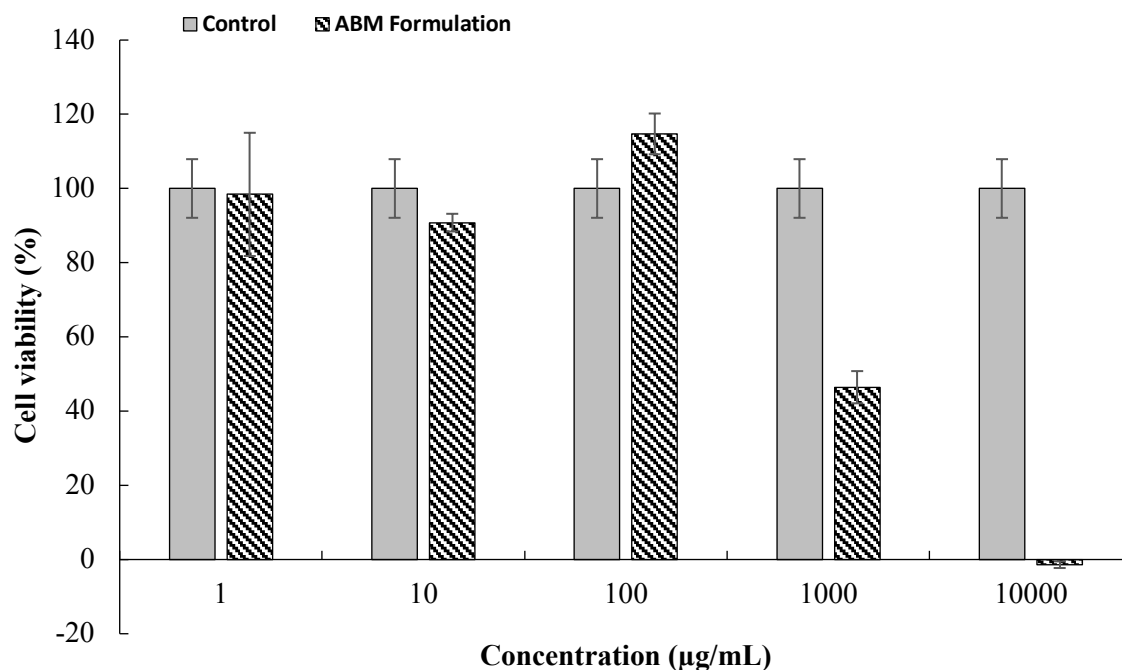
Figure 29. Cell viability effects of the final cream formulation with the ABM ethanolic extract at different concentrations on keratinocytes (HaCaT) cell line as measured by the MTT assay (n = 4).

From the results shown in **Figure 28** for the MTT assay, ABM ethanolic extract did not show cytotoxicity on HaCaT cell line up to 100 µg/mL. However, at 1 mg/mL, there was a reduction in the cell viability up to 30%, while a significant decrease was observed at the highest tested concentration (10 mg/mL). These results showed that higher concentrations of the extract can be deleterious for skin cells. It can also be seen that the obtained cell viability results for the corresponding formulation, showed maintenance of 50% cell viability at 1 mg/mL (**Figure 29**). Cytotoxicity of *A. blazei* extracts and their individual metabolites in different cell lines have been reported, (Cardozo et al., 2013; C. F. Kim, Jiang, Leung, Fung, & Lau, 2009; K. A. Yamamoto et al., 2013) and in the case of Shahirah et al. (2014) the *in vitro* cytotoxicity effect of ABM using the MTT assay in a fibroblast cell line (V79-4), was determined. According to the authors, the extracts displayed cytotoxicity effects above 1 mg/mL, which is consistent with the results achieved in the present work.

The present study is the first report evaluating the potential of re-utilisation of *A. blazei* by-products, based on its nutritional and chemical composition, for nutraceutical and cosmeceutical applications. Also, the dermatological potential of an ethanolic extract was accessed through cell viability effects in a skin cell line. The presence of essential nutrients

such as carbohydrates, proteins, and fatty acids was demonstrated. The ethanolic extract maintained the cell viability on Caco-2 and HT29-MTX cells at 100 µg/mL. The richness in sugars, α-tocopherol, and organic acids make *A. blazei* by-residues a potential ingredient for developing nutraceutical ingredients and/or functional foods, which may contribute to better nutrition and health improvement. It is also important to note that the oral administration of extracts rich in compounds with antioxidant capacity can be used to prevent the effects of cutaneous sun damage, but the efficacy of these extracts as nutricosmetics still needs to pass proper long-term clinical trials. To further confirm the cosmeceutical potential of ABM, skin permeation studies using Franz diffusion cells to determine topical bioavailability of the active ingredients are needed, as well as dermal and ocular irritability tests to ascertain safety. The results presented herein support the sustainable re-use of mushroom wastes, here demonstrated with ABM, which are generated in significant quantities during their production chain. This is highly meaningful since global mushrooms' cultivation has been predicted to increase significantly in the coming years.

3.5. Mushrooms as cosmeceutical ingredients: stability and use of microencapsulation techniques to ensure a controlled release

Following studies conducted in section 3.2, where ethanolic extracts of *A. bisporus*, *L. edodes* and *P. ostreatus* demonstrated cosmeceutical potential, *A. bisporus* and *P. ostreatus*, due to their highest bioactivity, was selected to be used in the present section. Thus, ethanolic extracts obtained from these mushroom species were prepared and further microencapsulated by the atomization/coagulation method with sodium alginate as the polymeric matrix. The produced microspheres were fully characterised and thereafter incorporated in a base cosmetic cream. The bioactive and physico-chemical properties imparted by these microencapsulated extracts, comparatively with the use of the respective free forms, were evaluated over a 6 months'time period. These studies were performed to ascertain the stability of the prepared formulations, compare microencapsulated versus free forms, and monitor the *in vitro release* profile of selected bioactive compounds (phenolic acids and ergosterol) in the developed cosmeceutical formulations.

3.5.1. Microencapsulation of the extracts

Table 26 summarizes the results obtained for the encapsulation efficiency, yield, and load. The concentration of the phenolic acids and related compounds in the coagulation and washing solutions was determined using the HPLC to calculate the EE (%), conducting to values of 72.8 and 99.6% for A and P, respectively, corroborating the successful encapsulation of the extracts. The EY (%), which represent the effectiveness of the process, conducted to values of 60.2 and 55.0 % for A and P, which might be considered satisfactory considering that the technique was applied at a laboratory scale. The EL%, which depicts the content of bioactive in the microparticles was 14.6% and 19.9% for A and P, respectively. It allows to determine the quantity of microspheres needed to be incorporated in the base cosmetic cream.

Table 26. Comparison of encapsulation efficiency, load, and yield of the microparticles prepared using alginate

Samples	EE (%)	EL (%)	EY (%)
A	72.8	14.6	60.2
P	99.6	19.9	55.0
E	na	na	60.2

na-not applied; A, P and E represent samples prepared with *A. bisporus*, *P. ostreatus* and empty microparticles respectively.

The surface morphology of the prepared microparticles, immediately after production, was visualized by optical microscopy and the respective images (acquired at magnifications of 40x, 100x and 400x) are shown in **Figure 30**. It is possible to observe a consistent spherical morphology with few particles displaying crumpled shapes of various sizes (consistent with a polydisperse sample), and no agglomeration. The lyophilized microspheres were rehydrated in distilled water and analysed again (magnification of 100x). The final shape of the rehydrated microspheres was quite irregular, but despite their deformation, the final size was close to that obtained immediately after encapsulation.

40x 100x 400x 100x (lyophylized)
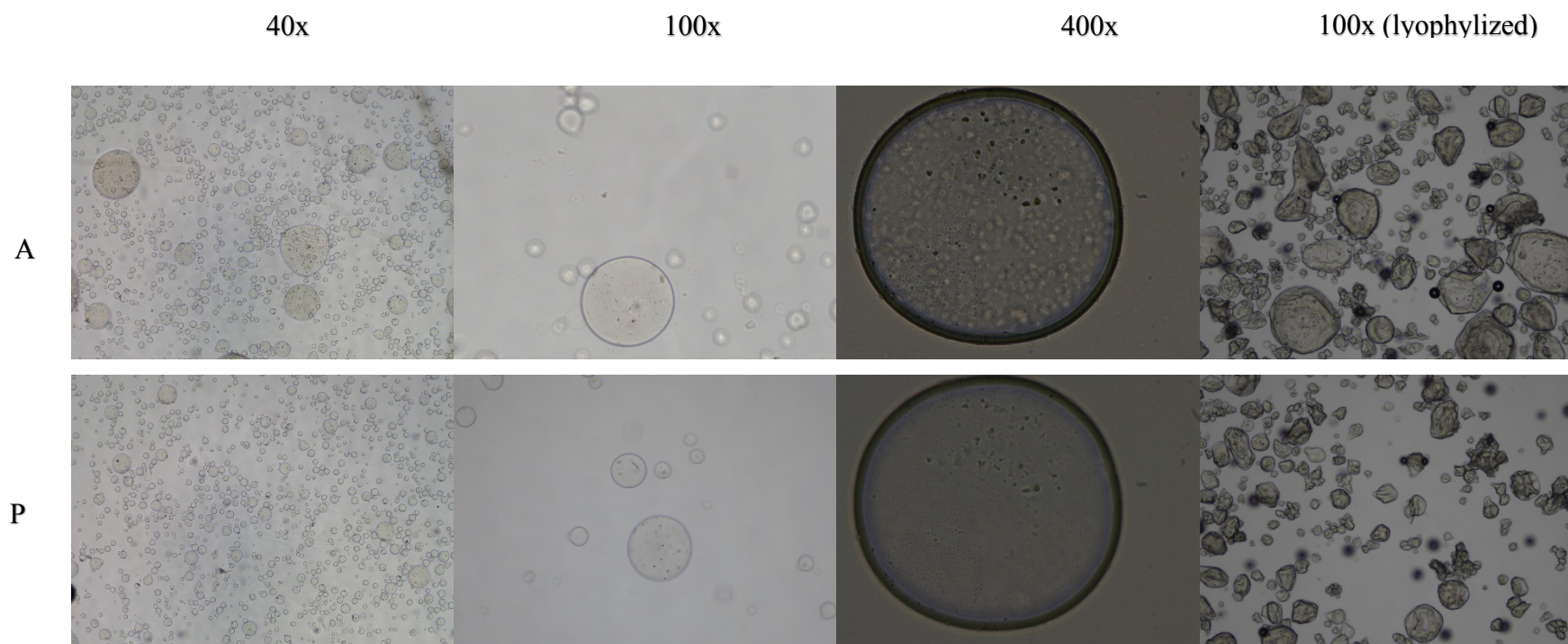
Figure 30. Optical Microscopy analysis with magnifications of 40, 100 and 400x of the microspheres after 4 h of coagulation under stirring. with A, and P representing samples prepared with *A. bisporus* and *P. ostreatus* respectively
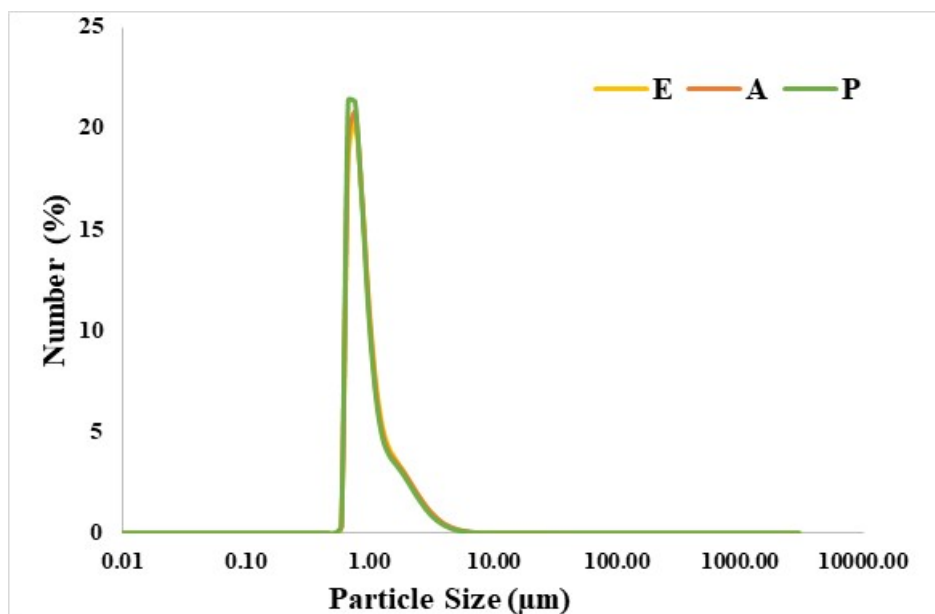
Figure 31. Microparticles size distributions expressed as mean number distribution, with A, P and E representing samples prepared with *A. bisporus*, *P. ostreatus* and empty microparticles respectively.

The results for the particle size distributions, in number and volume, represented in terms of percentiles (D_{10}, D_{50}, and D_{90}) are presented in **Table 27**. The respective average particle size (in number and volume) are also presented in **Table 27**. The achieved average sizes in volume for A, P and E were 122, 110 and 102 μm respectively.

Table 27. Comparison of particle size distribution in terms of number and volume, encapsulation efficiency, load and yield of the microparticles prepared using alginate.

Samples	Particle size distribution							Mean particle size (μm)	
	Volume distribution				Number distribution				
	D_{10}	D_{50}	D_{90}	Span	D_{10}	D_{50}	D_{90}	Volume	Number
A	27.1	100	254	2.27	0.72	0.94	2.05	122	1.14
P	27.7	94.7	240	2.24	0.72	0.92	1.96	110	1.11
E	19.5	79.2	235	2.72	0.82	1.15	2.83	102	1.50
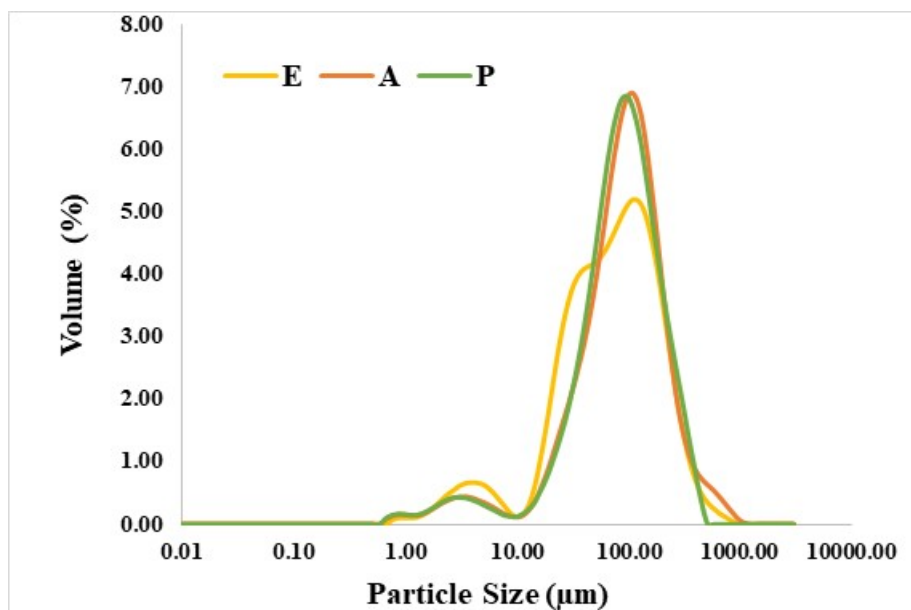
Figure 32. Microparticles size distributions expressed as mean volume distribution, with A, P and E representing samples prepared with *A. bisporus*, *P. ostreatus* and empty microparticles respectively.

From the analysis of the particle size distributions shown in **Figure 31 and 32**, distributions in number (**Figure 31**) were unimodal (or proximately unimodal), whereas distributions in volume showed a bimodal pattern (**Figure 32**). Considering the span (dispersity) parameter which reveals how homogenous the particle's size is (**Table 27)**, there is no significant dissimilarity among all three produced types of microparticles.

3.5.2. Bioactivity of mushroom-based cosmeceutical formulations – use of free forms

In the present work, the cosmeceutical potential of each prepared formulation was investigated based on their ability to display antioxidant, anti-tyrosinase and antimicrobial activities. The *in vitro* antioxidant activity of the cosmeceutical formulations prepared with the ethanolic extracts are presented in **Table 29**. The formulations revealed both DPPH scavenging activity and reducing power. The antioxidant activity decreased over time, which can be partly attributed to the oxidation of the extracts. A similar study was reported by Gezina et al. (2015) in which the authors prepared semi-solid formulations containing two species of Honeybush (*Cyclopia maculata* Vent and *Cyclopia genistoides* Vent). The active bioflavonoids present in their hydromethanolic extracts were found to lack sufficient stability in semi-solid formulations to

sustain the antioxidant activity. The phenolic acids, and related compounds composing the ethanolic extracts of *P. ostreatus* and *A. bisporus* have been previously described (section 3.2; Taofiq, Heleno, et al., 2016). These compounds have been reported to contribute significantly to the antioxidant activity (Heleno, Martins, et al., 2015). The quantification of these compounds in the corresponding semisolid formulations are presented in **Table 28**. For the cosmeceutical formulations prepared with *A. bisporus* extract (BCAb), and *P. ostreatus* extract (BCPo), phenolic acids, related compounds and ergosterol revealed no significant changes in their content over the storage time (6 months). Considering that there was no significant loss of bioactive compounds under the used storage temperature (4 ˚C), further studies are needed to be conducted at different environmental conditions (temperature and relative humidity) to confirm this observation.

Table 28. Phenolic acids and ergosterol content in the developed cosmeceutical formulations.

Samples	Ergosterol, Phenolic acids and Related Compounds in each cosmeceutical formulation			
	Cinnamic acid (µg)	*p*-Hydroxybenzoic acid (µg)	*p*-Coumaric acid (µg)	Ergosterol (mg)
BCAbT0	2.20±0.07[a]	nd	nd	1.11±0.01[a]
BCAbT3	2.19±0.07[a]	nd	nd	1.10±0.01[a]
BCAbT6	2.18±0.03[a]	nd	nd	1.08±0.01[a]
BCPoT0	8.84±0.02[a]	3.87±0.02[a]	1.52±0.02[a]	1.93±0.01[a]
BCPoT3	8.82±0.14[a]	3.84±0.06[a]	1.51±0.07[a]	1.92±0.03[a]
BCPoT6	8.80±0.03[a]	3.80±0.07[a]	1.50±0.02[a]	1.89±0.03[a]

In each column, different letters mean significant differences in bioactive compounds content between formulations (p<0.05).

Table 29. Bioactive properties of the developed cosmeceutical formulations

| Creams | Anti-tyrosinase activity EC$_{50}$ values (mg/mL) | | | Antioxidant activity EC$_{50}$ values (mg/mL) | | | | | |
| | | | | DPPH | | | Reducing power | | |
	Time 0	Time 3	Time 6	Time 0	Time 3	Time 6	Time 0	Time 3	Time 6
BCAb	25.1±0.5*	89±8*	>100	347± 1[b]	380±2[a]	385±13[a]	69±1[b]	69±5[b]	74±1[a]
BCPo	23±2[c]	40±3[b]	56±1[a]	339±2[c]	355±2[b]	378 ±6[a]	51±1[c]	57.8±0.6[b]	62±2[a]
BCMAb	>100	31±1*	69±3*	>400	>400	>400	>400	>400	>400
BCMPo	>100	46±4	46±1	>400	>400	>400	>400	>400	>400
BCEM	>100	>100	>100	>400	>400	>400	>400	>400	>400
BC	>100	>100	>100	>400	>400	>400	>400	>400	>400

In each row, different letters mean significant differences between formulations (p<0.05). When only two samples were present a Student´s t-test was used to determine the significant difference between two different samples, with α = 0.05. *Means a significant difference between the samples (p>0.001).

Table 30. Antimicrobial activity of the developed cosmeceutical formulations.

	MIC (mg/mL)																	
	Enterococcus faecalis			MSSA			MRSA			*E. coli*			*Proteus mirabilis*			*Candida albicans*		
	T_0	T_3	T_6	T_0	T_3	T_6	T_0	T_3	T_6	T_0	T_3	T_6	T_0	T_3	T_6	T_0	T_3	T_6
BCAb	>400	>400	> 400	400	400	> 400	400	400	> 400	>400	>400	>400	200	200	> 400	400	400	> 400
BCPo	400	400	>400	200	200	400	200	200	400	> 400	> 400	> 400	400	400	> 400	400	400	> 400
BCMAb	>400	>400	> 400	>400	>400	400	> 400	> 400	400	> 400	> 400	> 400	> 400	> 400	> 400	> 400	> 400	> 400
BCMPo	>400	>400	400	>400	>400	400	> 400	> 400	400	> 400	> 400	> 400	> 400	> 400	400	> 400	> 400	400
BCEM	>400	>400	>400	>400	>400	>400	>400	>400	>400	>400	>400	>400	>400	>400	>400	>400	>400	>400
BC	>400	>400	>400	>400	>400	>400	>400	>400	>400	>400	>400	>400	>400	>400	>400	>400	>400	>400

Table 31. Physico-chemical properties of the semi-solid cosmeceutical formulations.

Sample	Colour T0			Colour T3			Colour T6			pH T0	pH T3	pH T6
	l*	*a**	*b**	*l**	*a**	*b**	*l**	*a**	*b**			
BCAb	85.8±0.7[a]	0.8±0.3[a]	18.9±0.6[a]	81.42± 2[b]	0.597±0.03[b]	18.5±0.1[ab]	79.4±0.5[b]	0.26 ±0.02[c]	18.400±0.03[b]	3.88 ± 0.01[b]	3.88 ± 0.04[b]	4.12±0.01[a]
BCPo	88.3±0.5[a]	0.21±0.02[c]	19.0±0.4[b]	87.3±0.4[b]	0.37±0.02[a]	22.6±0.1[a]	78.4±0.5[c]	0.28 ±0.03[b]	19.2±0.1[b]	3.42 ± 0.02[b]	3.46 ± 0.02[b]	3.69±0.01[a]
BCMAb	75.7±0.7[a]	-0.65±0.05[a]	5.3±0.2[c]	72.4±0.3[b]	-1.29 ±0.02[c]	6.0±0.2[b]	69.7±0.3[c]	-1.08±0.01[b]	7.0±0.2[a]	3.82 ± 0.03[b]	3.75 ± 0.03[b]	4±0.01[a]
BCMPo	72.0±0.3[a]	-0.71±0.05[a]	5.9±0.3[c]	71.02±0.05[b]	-1.24 ±0.01[c]	6.23±0.02[b]	68.02±0.07[c]	-0.91 ±0.01[b]	7.23±0.02[a]	3.67 ± 0.02[b]	3.7 ± 0.01[b]	3.96±0.01[a]
BCEM	85.6± 0.8[a]	-0.63±0.05[a]	7.9±0.3[a]	81.8± 0.2[b]	-1.55±0.04[c]	6.18±0.05[b]	77.5± 0.4[c]	-1.26±0.02[b]	6.35±0.06[b]	3.64±0.03[b]	3.75±0.05[b]	3.92±0.01[a]
BC	92.2± 0.4[a]	-0.99±0.07[b]	3.65±0.07[b]	89.4± 0.3[b]	-1.15±0.04[c]	4.8±0.2[a]	85.6± 0.4[c]	-0.86±0.04[a]	3.04±0.09[c]	4.78±0.01[b]	4.83±0.03[ab]	4.84±0.02[a]

In each row and between each colour parameter during the different times, different letters mean significant differences between formulations ($p<0.05$). T0-immediately after formulation preparation, T3-3 months and T6-6 months.

Another interesting potential of bioactive ingredients in cosmeceuticals is their tyrosinase inhibition potential, making them suppressors of melanin that largely contribute to hyperpigmentation and photoageing (Taofiq, González-Paramás, et al., 2016). The search for tyrosinase inhibitors has also intensified in the last decade due to the negative consequences associated with the use of synthetic ingredients that present several negative effects on the skin (Taofiq, González-paramás, et al., 2017). In the present study, the results for the tyrosinase inhibition activity of the developed formulations are presented in **Table 29**. For the formulations prepared with mushroom extracts (BCAb and BCPo), an anti-tyrosinase activity was observed and the results show that both formulations contain compounds that can inhibit tyrosinase, thus indicating their potential to be used in hyperpigmentation correction formulations. Like what was observed with the antioxidant activity; a gradual loss of tyrosinase inhibition activity from time 0 to 6 months in the formulations prepared with mushroom ethanolic extracts, was observed. This can be attributed to possible interactions with the different ingredients present in the base formulation along time.

The life span of cosmetic and personal care products has been extended using synthetic preservatives due to their broad spectrum of antimicrobial activity, low price and to the fact that these compounds do not origin degradation products that affect physico-chemical properties (colour, pH, viscosity) (Kerdudo et al., 2016). Over the years some of these synthetic preservatives have become more controversial because of some negative effects associated with their use. Bearing in mind these challenges, cosmetic companies are now in search of non-harmful alternatives for consumers, and bioactive compounds with multifunctional properties are slowly been used for this purpose (Taofiq, González-paramás, et al., 2017). In the present study, the antimicrobial activity of each cosmeceutical formulation against Gram-negative, Gram-positive and yeast strains is presented in **Table 30**.

In all cases, the prepared formulations were found to be effective against Gram-negative, Gram-positive bacteria and *Candida albicans*. However, at the effective minimum inhibitory concentration, the antimicrobial activity failed to be maintained, highlighting a loss of bioactivity of the extracts. However, the results suggest that the compounds present in the studied extracts have the potential to be used as preservatives, capable of preventing microbial contamination in cosmeceutical formulations, but need strategies to increase effectiveness maintenance along storage time.

3.5.3. Bioactivity of mushroom-based cosmeceutical formulations – use of microencapsulated forms

Real-time *in vitro* release of bioactive compounds from polymeric microspheres is typically done to evaluate control release at appropriate environmental and physiological conditions. This process may, sometimes, take weeks, months, or even years (Andhariya et al., 2017). The real-time *in vitro* release of the mushroom extracts loaded in the prepared microparticles was performed under controlled temperature during a 6-month period. The microparticles prepared in the present work showed high encapsulation efficiencies and the manifestation of bioactivity, due to compounds release from the microparticles, was evaluated on the base cosmetic cream added with microencapsulated extracts. From the obtained results, it can be seen that the formulations prepared with BCMAb and BCMPo particles, respectively, did not display significant antioxidant and antimicrobial effects up to month 3, which can be due to a very slow release of the encapsulated bioactives, whose concentration is not enough to exert a bioactive effect. The slow release makes the process suitable to be used in the design of cosmeceutical formulations, whose shelf life span varies from months to even years.

Therefore, the gradual release ensures continuous effectiveness against microbial growth. However, and from the point of view of skin beneficial effects, their slow release can be disadvantageous as the formulated product may not release the bioactive compounds at the required levels for the intended effect. Nevertheless, it is expected that the application process of the cream favour mechanical disruption of the capsules, and thus the prompt release of the protected bioactive compounds on the skin surface. About the anti-tyrosinase activity, the released compounds were sufficient to cause activity manifestation of the formulations at the 3rd month of storage, as shown in **Table 29**. From the anti-tyrosinase bioactivity evolution profile presented in **Figure 33**, it can be observed that both formulations, BCMAb and BCMPo, showed comparable patterns until the 3rd month of storage time (no bioactivity). After this time-period, they start to reveal significant activity (31 ± 1 and 46 ± 4 mg/mL, for BCMAb and BCMPo respectively) but with a decreasing profile until the 6 months. In particular, BCMPo was able to maintain a more sustained release (no significant decrease was observed), comparatively with BCMAb that showed an important decrease up to the 6th month. As expected BCEM did not show any contribution to the tested bioactivities. Most studies on bioactive compounds release, consider various conditions such as temperature, solvent, pH, presence of enzymes or even stirring rate (J. Shen & Burgess, 2012).
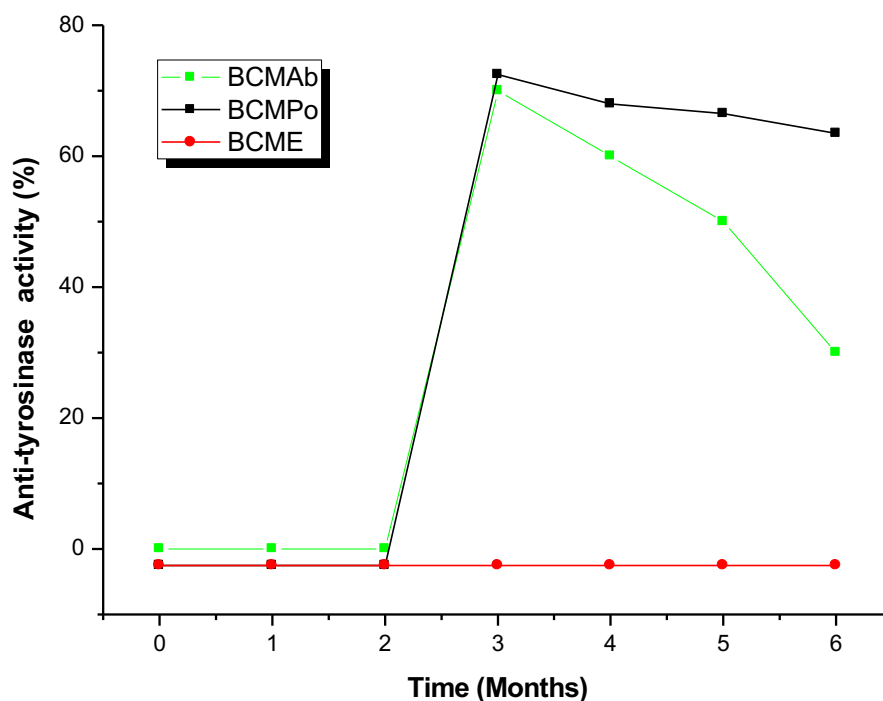
Figure 33. Extrapolated real-time *in vitro* release profile of formulations designed with microparticles (BCMAb-base cosmetic cream with microparticles of *A. bisporus* extract, BCMPo- base cosmetic cream with microparticles of *P. ostreatus* extract and BCEM- base cosmetic cream with empty microparticles (control)).

However, some of these conditions do not mimic the real environment, or the mechanism behind the release, making the real-time release evaluation, such as the assays done in the present work, an important contribute despite the long time required. In what concerns release profiles evaluation, Acosta et al. (2015) reported that the release of polyphenols from olive extract microencapsulated with chitosan was pH dependent, and the release rate at pH 7.4 doubled the one obtained at pH 5.5. Hence, more studies need to be conducted to find the best conditions that might promote the degradation of the polymeric material allowing for faster delivery of the bioactive compounds, when applied.

3.5.4. Physico-chemical parameters

During product development, especially when bioactive ingredients are added either to improve products shelf life or to functionalise the formulations, several procedures need to be conducted to ascertain the safety and efficacy of the product. Some of the preliminary tests include pH, viscosity, colour and odour evaluation. **Table 31** summarizes the pH values of

each formulation and the behaviour in terms of colour changes. Over the course of incubation, no significant colour changes were observed suggesting that the compounds present in the extracts were stable and their possible degradation did not lead to products imparting colour changes. From data on **Table 31**, it is possible to conclude that the formulations incorporated with the mushroom ethanolic extracts (BCAb and BCPo) presented a lower level of lightness (l^*) as the storage time increase and this may be due to oxidation of the incorporated extracts. The colour coordinates for the formulations prepared with microparticles revealed a deeper red (greater a^* value) mainly due to the contribution of alginate. Overall, the initial colour were maintained and without significant variations over the course of storage, and these are crucial parameters during preliminary stability testing analysis.

In the present work, all the cosmeceutical formulations presented a pH between 3.4 and 5.0 suggesting that these formulations have a large pH range, that was maintained even after months under storage. Samples were stored at 4°C and the lack of significant pH variations is a clear indication of formulation stability. However, because most of the products exhibit excellent stability at this temperature, temperature variation studies are necessary at 50°C, 25°C and -10°C in order to fulfill the cycle stability tests and to evaluate the behaviour of the developed formulations under temperature stress (Moraes, 2018).

The above findings reveal that ethanolic extracts of *A. bisporus* and *P. ostreatus*, display strong antioxidant, antimicrobial and anti-tyrosinase activities, mainly due to the contribution of their bioactive components, being suitable as multifunctional cosmeceutical ingredients. The atomization/coagulation technique was successfully applied to encapsulate the bioactives. After incorporating the extracts into the base cosmetic cream, they displayed bioactivity; even with a decreasing pattern along the 6 months, for the free extracts. For the microencapsulated extracts, no demonstration of significant antioxidant and antimicrobial activity was observed, with anti-tyrosinase bioactivity being displayed after 3 months. Key findings in the present study revealed that it is important to study the release profile of the bioactive compounds from the microspheres, under different environmental conditions, in order to promote a faster release of the active ingredient, which might be interesting for certain applications. Results presented in the present work reveal the promising potential of mushroom extracts in what concerns bioactivity and stability.

3.6. Individual bioactive compounds as cosmeceutical ingredients: stabilization by microencapsulation to ensure a controlled release

The present section intends to evaluate the anti-inflammatory, antimicrobial and anti-tyrosinase activities of *p*-hydroxybenzoic, *p*-coumaric, protocatechuic and cinnamic acids, and ergosterol. Based on the exhibited bioactivity, and interest to be used in cosmeceuticals formulations, these compounds were microencapsulated using the atomization/coagulation method with calcium alginate as the matrix material. The produced microspheres were fully characterised and tested against the use of the non-encapsulated forms (free compounds) in a base cosmetic (semi-solid formulation). Each produced formulation was submitted to bioactivity evaluation over a period of 6 months to ascertain stability and monitor the *in vitro* release of compounds responsible for the effect. Additionally, target compounds (phenolic acids, cinnamic acid, and ergosterol), incorporated in its free form were monitored using the HPLC.

3.6.1. Bioactive properties of the individual compounds

In the present work, the potential of the studied compounds to suppress NO production was evaluated (**Table 32**). Regarding the results, *p*-coumaric acid showed the highest potential presenting the lowest EC_{50} values (152.17 ± 6.22 µg/mL), followed by cinnamic (180.12 ± 14.18 µg/mL), protocatechuic (182.16 ± 9.76 µg/mL) and *p*-hydroxybenzoic acids (195.21 ± 8.70 µg/mL). These results are in agreement with the ones reported previously by our research group for cinnamic and *p*-hydroxybenzoic acids (Taofiq et al., 2015). On the other hand, ergosterol showed lower activity (338 ± 23 µg/mL), possibly due to its low solubility in the culture medium. To our best knowledge, only Kuo et al. (2011) have reported an anti-inflammatory potential for commercial ergosterol at 10 µg/mL by inhibiting NO production in RAW. 7 macrophage cells.

Table 32. Anti-inflammatory and anti-tyrosinase activities of the individual compounds.

Individual compounds	Anti-inflammatory activity (EC$_{50}$ values, µg/mL)	Anti-tyrosinase activity (EC$_{50}$ values, mg/mL)
Cinnamic acid	180 ± 14^c	0.31 ± 0.05*
Protocatechuic acid	182 ± 10^c	>2.0
p-Hydroxybenzoic acid	195 ± 9^b	1.86 ± 0.01*
p-Coumaric acid	152 ± 6^d	>2.0
Ergosterol	338 ± 23^a	>2.0

Anti-inflammatory activity is expressed as EC$_{50}$ values corresponding to 50% of inhibition of the NO production in comparison with the negative control (100% of NO production). Dexamethasone (positive control) EC$_{50}$ values: 16 µg/mL. Anti-tyrosinase activity is expressed as EC$_{50}$ values corresponding to 50% of inhibition of tyrosinase. Ascorbic acid (positive control) EC$_{50}$ values: 31 µg/mL. In the column different letters mean significant differences *(p < 0.05)*. *Statistically different values, Student´s *t*-test *p*-value <0.001.

Concerning the anti-tyrosinase activity (**Table 32**), cinnamic acid displayed the strongest activity exhibiting the lowest EC$_{50}$ value (0.31 ± 0.05 mg/mL). The other tested compounds, showing EC$_{50}$ values above the highest tested concentration of 2.0 mg/mL, presented limited activity. To the author's best knowledge, no studies have been previously reported for the tyrosinase inhibitory activity of protocatechuic, *p*-hydroxybenzoic and cinnamic acids; however, some other phenolic acids such as caffeic acid (43.09 ± 2.3 µM), ferulic acid (51.85 ± 1.7µM) and gallic acid (18.30 µM) have been reported as significantly suppress tyrosinase activity (Kumar et al., 2013; Thangboonjit et al., 2014). Although in the present study it was not possible to report anti-tyrosinase activity for *p*-coumaric acid, studies conducted by An et al. (2010) related that *p*-coumaric acid at 10 µg/mL showed activity at levels comparable to kojic acid, whereas Jun et al., (2012) confirmed that the anti-tyrosinase activity mechanism of *p*-coumaric acid was due to its ability to reduce MITF and tyrosinase mRNA expression by 73 and 82 %, respectively. The results show that these compounds display a promising potential to be used, either alone or in combination with other bioactive ingredients, to provide protection against hyperpigmentation.

The results for the antimicrobial activity expressed as MIC values are shown in **Table 33** for the studied compounds. All the individual compounds showed considerable antimicrobial capacity against gram-positive, gram negative bacteria and *Candida*, with cinnamic acid and ergosterol exhibiting a similar antimicrobial pattern. Interestingly, *p*-coumaric and protocatechuic acids presented the highest activity against methicillin-sensitive *Staphylococcus aureus* (SA), similarly to what was reported by Parkar et al. (2008). All the compounds showed

inhibitory activity against *E. coli* in accordance with the results reported by Cueva et al. (2010). Due to the well-known constraints associated with the use of synthetic antimicrobial agents, this study highlights the potential of the studied polyphenols and sterols as viable alternatives.

Table 33. Antimicrobial activity of the individual compounds.

		MIC (mg/mL)				
	Bacterial strains	cinnamic acid	*p*-hydroxybenzoic acid	*p*-coumaric acid	protocatechuic acid	Ergosterol
Gram +	*MRSA*	1	1	0.5	2.5	1
	MSSA	1	1	0.5	2.5	1
	E. faecalis	1	1	1	1	1
Gram -	*E. coli*	1	1	2.5	0.25	1
	P. mirabilis	1	2.5	2.5	2.5	1
	Yeast strain					
	C. albicans	2.5	2.5	2.5	2.5	2.5

MIC-Minimum Inhibitory concentration

Phenolic acids such as ferulic and caffeic acid have been reported to be interesting anti-wrinkling and photoprotective ingredients for skin care products, as reported by Pluemsamran et al. (2012), while Seok and Boo (2015) have reported anti-ageing potential for *p*-coumaric acid in dermal fibroblasts cell lines. However, most of the cosmeceutical properties were only evaluated for the individual compounds, and the compounds seldom incorporated in base cosmetic creams to evaluate if the bioactive properties are maintained.

3.6.2. Morphology and characteristics of the developed microspheres

The surface morphology images of the prepared microspheres, immediately visualised by optical microscopy after preparation, and at magnifications of 40x, 100x and 400x, are shown in **Figure 34**. It is possible to observe a consistent spherical morphology with particles of various sizes showing no agglomeration.
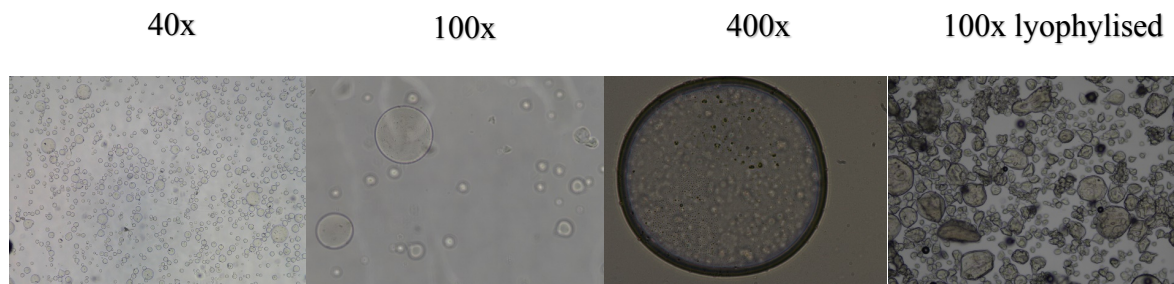
Figure 34. Optical Microscopy analysis with magnifications of 40, 100 and 400x of the microspheres after 4 h of coagulation under stirring.
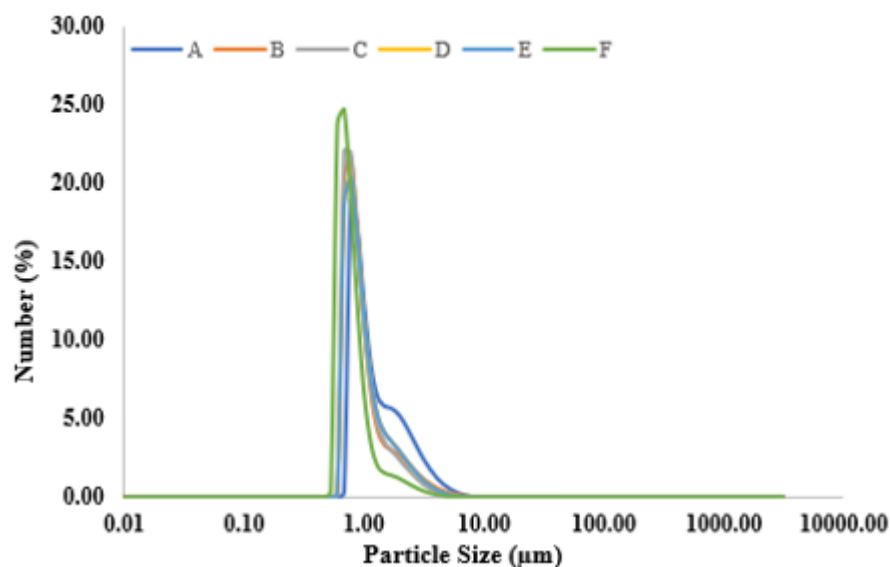
Figure 35. Microparticles size distribution in number.

The results for the particle size distribution, in terms of number and volume, represented as percentiles (D_{10}, D_{50}, and D_{90}), are presented in **Table 34**. From the analysis of particle size distribution, the distributions in number (**Figure 35**) were unimodal whereas the distributions in volume were bimodal (**Figure 36**). Another important parameter to consider is the Span (dispersity) which indicates the width of the particle size distribution and gives an indication of particle size homogeneity. The lyophilized microspheres were rehydrated in distilled water and analysed using the optical microscope at a magnification of 100x. The final shape of the rehydrated microspheres was quite irregular but close to what was observed with microspheres right after the encapsulation process.
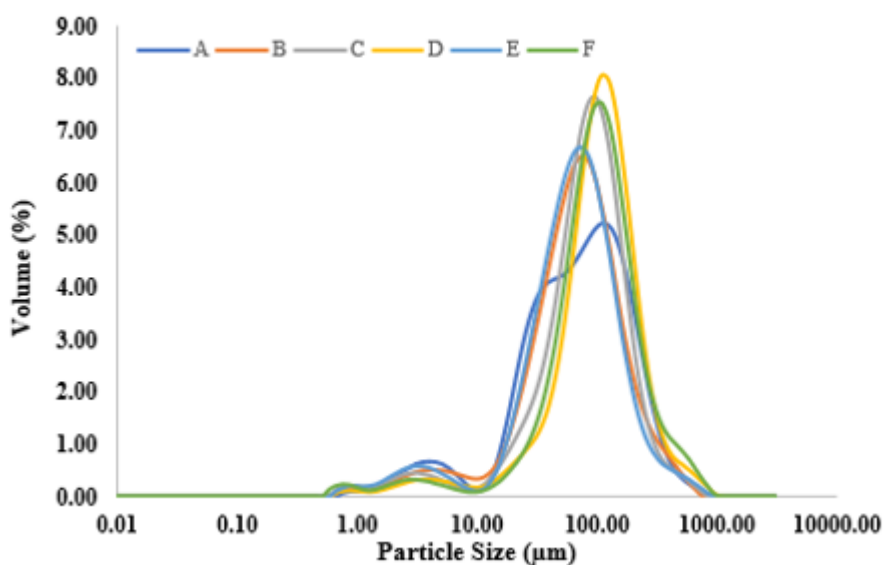
Figure 36. Microparticles size distribution in volume.

Table 34. Particle size distribution in number and volume (D_{10}, D_{50} and D_{90} and mean particle size) of the prepared microspheres.

Samples	Particle size distribution (µm)							Mean particle size (µm)	
	Volume distribution				Number distribution			Number	Volume
	D_{10}	D_{50}	D_{90}	Span	D_{10}	D_{50}	D_{90}		
A	19.5	79.2	235	2.72	0.82	1.15	2.83	1.50	102
B	20.5	74.6	206	2.28	0.72	0.93	2.10	1.63	95.1
C	25.4	90.7	208	2.01	0.71	0.91	1.84	1.07	104
D	36.1	115	261	1.95	0.72	0.91	1.95	1.10	132
E	21.3	71.0	186	2.31	0.72	0.95	2.05	1.15	90.1
F	36.3	108	273	2.19	0.63	0.77	1.26	0.86	132

A - empty microparticles B - *p*-hydroxybenzoic acid, C - *p*-coumaric acid, D - cinnamic acid, E - protocatechuic acid, F - Ergosterol.

From the obtained data, there is no significant dissimilarity among the particles incorporating the various bioactive ingredients. **Table 35** summarizes the results obtained for the encapsulation yield, loading, and efficiency of the produced alginate microspheres. To determine EE %, the concentration of the analysed compounds was determined both in the coagulation and washing solutions using the HPLC and the amount effectively encapsulated obtained by difference.

The results showed that the compounds were successfully encapsulated with EE % greater than 50% for all the studied cases. The EY %, which represents the weight of dry microspheres,

recovered after encapsulation process, relatively to the weight of raw-materials initially used, was found to be over 45% in all the samples. These values are quite satisfactory considering that the applied technique was conducted at a laboratory scale. Some authors reported the encapsulation of phenolic acids such as caffeic, chlorogenic and rosmarinic acids, using similar scales, with a EY (%) only over 37%, for all the studied cases (Aguiar, Costa, Rocha, Estevinho, & Santos, 2017). The EL (%,) representing the compound content per gram of microspheres, allows the determination of the microsphere's amount needed to be incorporated in the base cosmetic creams. By analysing the results listed in **Table 35**, the EL (%) was above 5% in all the cases.

Table 35. Encapsulation efficiency, load and yield of the prepared microspheres.

Samples	EE (%)	EY (%)	EL (%)
A	na	60.2	na
B	88.3	57.8	9.80
C	73.7	55.7	8.19
D	98.4	58.9	10.9
E	50.3	62.2	5.59
F	63.2	45.5	7.02

na- not applied

3.6.3. Bioactive properties of cosmeceutical formulations

In the present work, the cosmeceutical potential of each prepared formulation was investigated based on their ability to display anti-inflammatory, anti-tyrosinase and antimicrobial activities. The results for the *in vitro* anti-tyrosinase activity of the prepared cosmeceutical formulations containing the individual compounds are presented in **Table 36.** From the results, all the developed formulations (CFHA, CFCoA, CFCA, CFPA) were able to inhibit tyrosinase activity over 6 months under storage. On the other hand, the formulation prepared with ergosterol (CFE) was also able to inhibit the tyrosinase activity, however, a significant loss was observed as the storage time increased, which can be attributed to the interaction between ergosterol and other ingredients present in the base cosmetic cream (**Table 36**). Several studies have reported that phenolic acids and related compounds are the most significant contributors to anti-tyrosinase activity, but most of these studies only investigated pure compounds without

performing their incorporation in topical semi-solid formulations (T. S. Chang, 2009; Taofiq, González-paramás, et al., 2017). An exception was the work of Seo et al. (2011), who conducted clinical trials by exposing the forearms of 21 persons after topical application of a *p*-coumaric acid-based cream twice daily. The results showed that there was a significant improvement in the hyperpigmentation formation.

For the anti-inflammatory activity, all the developed formulations containing the individual phenolic acids, cinnamic acid and ergosterol were able to inhibit NO production (**Table 36**). As observed for the other bioactive properties there was a gradual loss of bioactivity as the storage time increased, with the ergosterol-based formulation (CFE) showing the lower anti-inflammatory activity. The formulation prepared with *p*-coumaric acid (CFCoA) was the most promising one, as determined based on the observations made with the individual compounds. The antimicrobial activity of the developed cosmeceutical formulations, against Gram-negative, Gram-positive and yeast microbial strains, are presented in **Table 37.** In all the cases, the prepared formulations were found to be effective against Gram-negative, Gram-positive bacteria, and *C. albicans*. The antimicrobial activity of the formulations incorporated with the free individual agents decreased along the storage time, probably due to the interaction with the ingredients present in the base cosmetic cream. Our findings suggest that these bioactive compounds have the potential to be used as preservatives capable of preventing microbial contamination in cosmeceutical formulations.

The identification and quantification of the individual compounds present in the prepared formulations, determined by HPLC, are presented in **Table 36**. It can be concluded that all the target compounds were stable and where identified in their corresponding formulation. The validation of an extraction protocol for phenolic acids extraction from semi-solid formulation still poses some challenges. However, it was possible to effectively identify and quantify the amount of phenolic acids and related compounds present in each prepared cosmeceutical formulation over the storage time. The results showed that there was no significant loss of phenolic compounds, or ergosterol, over the course of the incubation period for all the considered semi-solid formulations.

3.6.4. Physico-chemical parameters

Although it is possible to find in the market, a wide range of cosmetic colours, the majority of consumers still prefer products with a basic white colour. Hence, the cosmetic industry has paid attention to colour management during the design of new products. Responding to this requisite, the physico-chemical evaluation of the prepared semisolid formulations in terms of colour, and pH, was carried out during the storage period at time 0, 3 and 6 months (**Table 38**). Over the course of the six-month incubation period, no significant colour changes were observed, suggesting that the individual compounds are stable, and their degradation does not lead to end products causing significant colour changes. It was possible to observe that the formulations presented lower levels of lightness (l^*) as the storage time increase, which may be derived from the oxidation of the incorporated compounds. Lower l^* values and higher yellowness (b^*) was observed for the formulations prepared with the individual compounds, whereas the colour coordinates for the formulations prepared with the microspheres revealed a deeper red (greater a^* value), mainly due to the contribution of alginate. Overall, the initial odour (qualitative evaluation) and colour were maintained, i.e. they were not significantly different over the course of the storage time, which are crucial parameters for the preliminary analysis of stability. In this work, all the developed cosmeceutical formulations presented a pH in the range $3.4 - 6.0$, suggesting that they have a favourable pH along the storage time. The samples, stored at 4 °C in darkness, presented no significant pH variation, which is a clear indication of their stability. Also, most of the products exhibited excellent stability under this temperature.

Table 36. Bioactive properties of the individual compounds developed cosmeceutical formulations and compounds monitoring over the storage time.

Creams	Anti-tyrosinase activity (EC_{50} values, mg/mL)			Anti-inflammatory activity (EC_{50} values, mg/mL)			Bioactive compounds profile (mg/g)		
	Time 0	Time 3	Time 6	Time 0	Time 3	Time 6	Time 0	Time 3	Time 6
CFHA	54±4[b]	55.3±0.1 [b]	59.9±0.5[a]	30.66±1[c]	41.92±2.17 [b]	54.13±0.93[a]	6.80± 0.07[a]	6.83± 0.04[a]	6.39± 0.02[b]
CFCoA	37.6±0.9[b]	41±7 [b]	51±6[a]	22.64±0.76[c]	33.04±1.51 [b]	45.29±1.63[a]	6.67± 0.03[a]	6.52± 0.08 [b]	6.48± 0.07[b]
CFCA	32.3±0.2[b]	36±5[ab]	40±3[a]	33.47±0.46[c]	40.03±1.09 [b]	47.05±1.01[a]	6.50± 0.01[a]	6.4± 0.2[a]	6.39± 0.02[a]
CFPA	40±3[b]	43±2[b]	61±7[a]	36.28±1.62*	47.59±0.55*	>60	6.64± 0.08[a]	6.5± 0.1[b]	6.42± 0.01[b]
CFE	24±2[c]	51±5 [b]	98.2±0.7[a]	53.35±1.62	>60	>60	6.9±0.01[a]	6.81±0.01[b]	6.78±0.02[b]
CFEM	>100	>100	>100	>60	>60	>60	nd	nd	nd
CFMHA	>100	>100	48±12	>60	50.56±0.57*	42.66±0.94*	nd	nd	nd
CFMCoA	>100	73±1*	45±4*	>60	42.34±1.02*	34.57±0.43*	nd	nd	nd
CFMCA	>100	80.8±0.7*	43.0±0.8*	>60	48.440.5±*	40.33±1.13*	nd	nd	nd
CFMPA	>100	>100	49±8	>60	46.99±1.43*	40.07±0.17*	nd	nd	nd
CFME	>100	47±4*	32.6±0.6*	>60	>60	>60	nd	nd	nd
BA	>100	>100	>100	>60	>60	>60	nd	nd	nd

nd-not determined, for easy identification of the samples, each formulation was labelled as follows: i) Cosmeceutical formulations incorporated with free Individual compounds: CFHA- *p*-hydroxybenzoic acid, CFCoA- *p*-coumaric acid, CFCA- cinnamic acid, CFPA- protocatechuic acid, CFE- ergosterol; ii) Cosmeceutical formulations incorporated with microencapsulated compounds: CFEM- empty microspheres (control), CFMHA- microspheres with *p*-hydroxybenzoic acid, CFMCoA- microspheres with *p*-coumaric acid, CFMCA- microspheres with cinnamic acid, CFMPA- microspheres with protocatechuic acid, CFME- microspheres with ergosterol. For all the assays a negative control was analysed with base cosmetic cream (BA). In each row different letters mean significant differences ($p < 0.05$). *Statistically different values, Student´s t-test p-value <0.001.

Table 37. Antimicrobial activity of the final cosmeceutical formulations.

	Mic (mg/mL)																	
	Bacterial strains															**Yeast**		
Samples	*E. faecalis*			MSSA			MRSA			*E. coli*			*P. mirabilis*			*C. albicans*		
	T_0	T_3	T_6	T_0	T_3	T_6	T_0	T_3	T_6	T_0	T_3	T_6	T_0	T_3	T_6	T_0	T_3	T_6
BA	>400	>400	>400	>400	>400	>400	>400	>400	>400	>400	>400	>400	>400	>400	>400	>400	>400	>400
CFHA	200	200	400	200	200	400	200	200	400	200	200	400	400	400	400	400	400	400
CFCoA	200	200	400	100	100	200	100	100	200	400	400	400	200	200	400	400	400	400
CFCA	200	200	400	200	200	400	200	200	400	200	200	400	200	200	400	400	400	400
CFPA	200	200	400	100	100	200	100	100	200	400	400	400	400	400	400	400	400	400
CFE	200	200	400	200	200	400	200	200	400	200	200	400	200	200	400	400	400	400
CFEM	>400	> 400	>400	>400	400	>400	>400	>400	>400	>400	>400	>400	>400	>400	>400	>400	> 400	>400
CFMHA	>400	400	200	>400	400	200	>400	400	200	>400	400	200	>400	>400	400	>400	> 400	400
CFMCoA	>400	400	200	>400	200	>400	>400	200	100	>400	>400	400	>400	>400	200	>400	> 400	>400
CFMCA	>400	400	200	>400	400	200	>400	400	200	>400	>400	400	>400	>400	400	>400	> 400	>400
CFMPA	>400	400	200	>400	200	100	>400	200	100	>400	>400	400	>400	>400	400	>400	> 400	>400
CFME	>400	400	200	>400	400	200	>400	400	200	>400	>400	400	>400	>400	400	>400	> 400	400

Table 38. Physico-chemical properties of the developed cosmeceutical formulations.

Sample	Colour T0			Colour T3			Colour T6			pH T0	pH T3	pH T6
	L^*	a^*	b^*	L^*	a^*	b^*	L^*	a^*	b^*			
CFHA	93.0±0.3[a]	-0.85±0.07[a]	4.31±0.08[a]	86.35±0.2[b]	-0.88±0.02[a]	3.71±0.04[b]	81± 1[c]	-0.9±0.2[a]	3.4±0.3[b]	5.43±0.02[ab]	5.49±0.05[a]	5.4±0.02[b]
CFCoA	93.0±0.4[a]	-0.79±0.05[a]	4.6±0.1[a]	85.06±0.5[b]	-0.80±0.02[a]	3.48±0.08[b]	80.4± 0.3[c]	-0.82±0.02[a]	2.9±0.3[c]	4.37±0.02[a]	4.41±0.04[a]	4.4±0.04[a]
CFCA	93.1±0.2[a]	-0.98±0.07[c]	4.21±0.07[a]	84.29±0.5[b]	-0.64±0.01[a]	2.82±0.02[c]	81.0± 0.1[c]	-0.74±0.01[b]	3.0±0.1[b]	4.35±0.01c	4.4±0.02[b]	4.47±0.02[a]
CFPA	92.7±0.4[a]	-1.01±0.02[c]	3.68±0.06[a]	84.70±0.2[b]	-0.94±0.01[b]	3.23±0.04[b]	80.7± 0.2[c]	-0.84±0.01[a]	3.1±0.1[c]	3.75±0.01[c]	3.8±0.01[b]	3.89±0.01[a]
CFE	92.8±0.4[a]	-1.05±0.09[b]	4.6±0.2[a]	83.53±0.03[b]	-0.72±0.04[a]	3.10±0.01[c]	81.3± 0.2[c]	-0.78±0.03[a]	3.58±0.01[b]	4.57±0.04[b]	4.61±0.02[a]	4.65±0.02[a]
CFEM	85.6±0.8[a]	-0.63±0.05[a]	7.9±0.3[a]	81.8±0.2[b]	-1.55±0.04[c]	6.18±0.05[b]	77.5± 0.4[c]	-1.26±0.02[b]	6.35±0.06[b]	3.64±0.03[c]	3.75±0.05[b]	3.92±0.01[a]
CFMHA	77.9±0.5[a]	-0.09±0.03[a]	6.3±0.1[a]	77.3± 0.5[a]	-0.64±0.01[b]	6.11±0.03[ab]	76.8± 0.3[a]	-0.84±0.02[c]	5.9±0.3[b]	4.54±0.01[b]	4.55±0.05[b]	4.68±0.02[a]
CFMCoA	81.7±0.6[a]	-0.81±0.06[a]	5.1±0.2[a]	79.4±0.3[b]	-0.81±0.06[a]	4.96±0.02[ab]	78.7± 0.3[b]	-0.83±0.04[a]	4.7±0.2[b]	4.07±0.02[b]	4.1±0.02[b]	4.22±0.01[a]
CFMCA	65.1±0.9[a]	-0.89±0.03[c]	-0.5±0.1[a]	64.25±0.04[a]	-0.58±0.02[a]	-0.38±0.03[a]	64.3± 0.3[a]	-0.63±0.05[a]	-0.46±0.04[b]	4.39±0.01[b]	4.33±0.01[c]	4.47±0.01[a]
CFMPA	79.7±0.5[a]	-0.59±0.06[a]	4.6±0.2[a]	79.7±0.1[a]	-0.74±0.03[b]	4.61±0.02[a]	78.7± 0.1[a]	-0.81±0.03[b]	4.64±0.02[a]	3.92±0.01[c]	3.98±0.02[b]	4.1±0.01[a]
CFME	80.8±0.4[a]	-0.84±0.07[a]	5.5±0.4[a]	78.2± 0.3[b]	-1.25±0.08[c]	5.4±0.2[ab]	77.3± 0.3[c]	-1.02±0.02[b]	4.8±0.2[b]	3.81±0.01[b]	3.83±0.03[b]	4.00±0.01[a]
BA	92.2±0.4[a]	-0.99±0.07[b]	3.65±0.07[b]	89.4±0.3[b]	-1.15±0.04[c]	4.8±0.2[a]	85.6± 0.4[c]	-0.86±0.04[a]	3.04±0.09[c]	4.78±0.01[b]	4.83±0.03[ab]	4.84±0.02[a]

In each row and between each colour parameter (L, a and b) during the different times, different letters mean significant differences between samples ($p < 0.05$)

3.6.5. Real-time *in vitro* release

The real-time *in vitro* release of the microencapsulated bioactive agents was performed under controlled temperature medium. Their release was evaluated based on their potential to increase the bioactive properties of the corresponding formulations. From the obtained data, microspheres showed a very slow release of the encapsulated bioactives up to the 6th month under storage. Throughout the process of microencapsulation, the anti-tyrosinase, anti-inflammatory, and antimicrobial activities were not compromised since the bioactivity was kept in almost all cases, highlighting the potential of alginate particles as effective delivery vehicles. Regarding the anti-tyrosinase activity, a fast release, sufficient to cause activity, was achieved for the formulations at the 3rd month of storage as shown by the data of **Table 36**. It was also observed that both formulations CFMCoA and CFMCA showed similar profile relative to the anti-tyrosinase and anti-inflammatory activity. The release in both cases was able to sustain the bioactivities up to the 6th month. As expected BCEM did not show any contribution to the tested bioactivities. CFMPA and CFMHA were able to maintain an anti-tyrosinase activity lower than the one obtained for CFMCoA and CFMCA, regardless they showed the best anti-inflammatory activity. BCE was able to sustain the anti-tyrosinase activity, however, no anti-inflammatory activity was perceived. The slow release supports the suitability of the microencapsulation process to be used in the design of cosmeceutical formulations, whose shelf life span from months to even years, making the gradual release adequate to ensure the continued effectiveness against microbial growth. It is also interesting to note that the compounds not released during the evaluated storage time can be further released in the skin during the application of the cosmeceutical formulation. In fact, due to the applied pressure, capsules breakage will occur with the subsequent release of the encapsulated compounds, which will result in skin benefits derived from the fraction of preserved bioactives. From the obtained results, the alginate microcapsules showed potential to ensure the controlled release of the bioactive agents, which will add in the cosmetic preservation during storage and will provide benefits for the skin upon application (preserved fraction).

Some relevant reports have been presented on the use of microencapsulation techniques to protect bioactive compounds for cosmeceutical purposes. Biswick et al. (2012) microencapsulated caffeic acid, with the produced microparticles able to withstand both UVA and UVB radiation, indicating their suitability to be used in the design of sunscreen cosmetic formulations. Ouimet et al. (2015) microencapsulated ferulic acid, whose slow release was reported as acting for days, but able to achieve antioxidant activity. Different factors such as

polymer nature and molecular weight and microparticle's size have been reported by Sharma et al. (2016), as influencing the release rate making these issues worthy of further investigation. The studies performed under the context of the present work is a valuable strategy to access the long-lasting effect of the encapsulated bioactive compounds. The overall results show that microencapsulation can provide efficient tools to support the development of cosmetic formulations promoting the preservation of the cosmeceutical ingredients, and the sustained release of the compounds (i.e. bioactivity maintenance).

The findings achieved in this work reveal that the studied compounds (*p*-hydroxybenzoic, *p*-coumaric, protocatechuic and cinnamic acids, and ergosterol) displayed anti-tyrosinase, antimicrobial and anti-inflammatory activities making them suitable to be explored as multifunctional cosmeceutical ingredients. The atomization/coagulation technique was successfully applied to encapsulate the bioactive agents, conducting to EE% values above 50% for all the tested compounds. After incorporating the individual compounds in the cosmetic formulations, bioactive properties were only partially maintained while their microencapsulated formulations have shown a sustained release able to better preserve bioactivity. Moreover, over the course of storage time, no significant changes were observed in the tested stability parameters, namely colour, and pH. By the obtained results, the analysed bioactive agents revealed promising bioactivity and stability.

3.7. Safety and topical bioavailability of mushroom extracts as cosmeceutical ingredients

Following studies conducted in section 3.2 and 3.3 where interesting cosmeceutical potential was displayed for ethanolic extracts of *P. ostreatus* and *G. lucidum*, both extracts were selected for further studies. Both extracts, obtained by Soxhlet extraction, and their corresponding final cosmetic formulations, prepared from a selected base cosmetic cream, were tested regarding cell viability and cytotoxic effects using MTT and LDH assays in keratinocytes (HaCaT) and fibroblasts (HFF-1). Additionally, the extracts and the final formulations were submitted to skin permeation assays using the Franz diffusion cell with pig ear skin as the permeation membrane.

Natural extracts, or their individual metabolites, offer many advantages as cosmeceutical ingredients and are being increasingly used nowadays. They assume an importance not just because of the bioactive potential but also due to the commercial and market appeal, making them positively recognized and accepted by consumers. Ethanolic extracts obtained from *G.*

lucidum and *P. ostreatus* (E1 and E2, respectively) were incorporated into base cosmetic creams and the generated formulations designated as F1 and F2 for *G. lucidum* and *P. ostreatus*, respectively. The incorporated extracts may have a positive effect on the skin when applied topically due to their content in different bioactive molecules (e.g triterpenoids, phenolic acids and related compounds), as well as the bioactive properties previously reported (Taofiq, Heleno, et al., 2017, 2016; Taofiq et al., 2018). The colour attributes of the produced formulations in the *L*a*b** system were 70.3±0.7, 12.1±0.5, 32.9±0.9 and 88.3±0.5, 0.21±0.02, 19.01±0.4 for F1 and F2, respectively. Both formulations present pH between 3.4 - 4.7 and can be considered adequate for topical application.

3.7.1. Safety of ethanolic extracts as cosmeceutical ingredients

Most products introduced into the market by cosmeceutical manufacturers undergo self-policing since no dedicated regulation for safety is available. Some of these ingredients can cause several allergies; hence, setting up approaches and methods to identify allergens and evaluate the potential toxicity of some of these products is of huge importance (Draelos, 2009). The presence of a diversity of chemical compounds in bioactive extracts may trigger some unwanted skin irritations, contact dermatitis, photosensitivity, hair and nail damage, hyperpigmentation, hypopigmentation and systemic effects (X. H. Gao et al., 2008). Since these ingredients are going to be in contact with the skin, it is vital to evaluate their safety and potential toxicity against skin cells. Over the years, *in vitro* models were developed to mimic skin cells and assess the safety and potential toxicity of bioactive extracts intended for dermatological use (Rodrigues et al., 2013). In the present work, the cell viability effect of the ethanolic extracts prepared from *G. lucidum* and *P. ostreatus* was evaluated on HaCaT (keratinocytes) and HFF-1 (fibroblast) cells, following a concentration-dependent manner (1-10000 µg/mL). Keratinocytes are a biologically relevant target for skin irritants because they are the first living cells that contact topically with the applied compounds. Also, HaCaT cells present several morphological and functional features typical of normal epidermal keratinocytes, making them a good model for skin toxicity tests (Abruzzo et al., 2017). The chemical profile of the ethanolic extracts from *G. lucidum* and *P. ostreatus* (**Tables 16 and 21**) correspond to a mixture of different bioactive compounds, which could potentiate the development of reactions (allergic or irritant) when applied for dermatologic purposes,

imposing the need to perform cytotoxicity evaluation and access the minimum concentration reducing the viability of the tested cell lines.
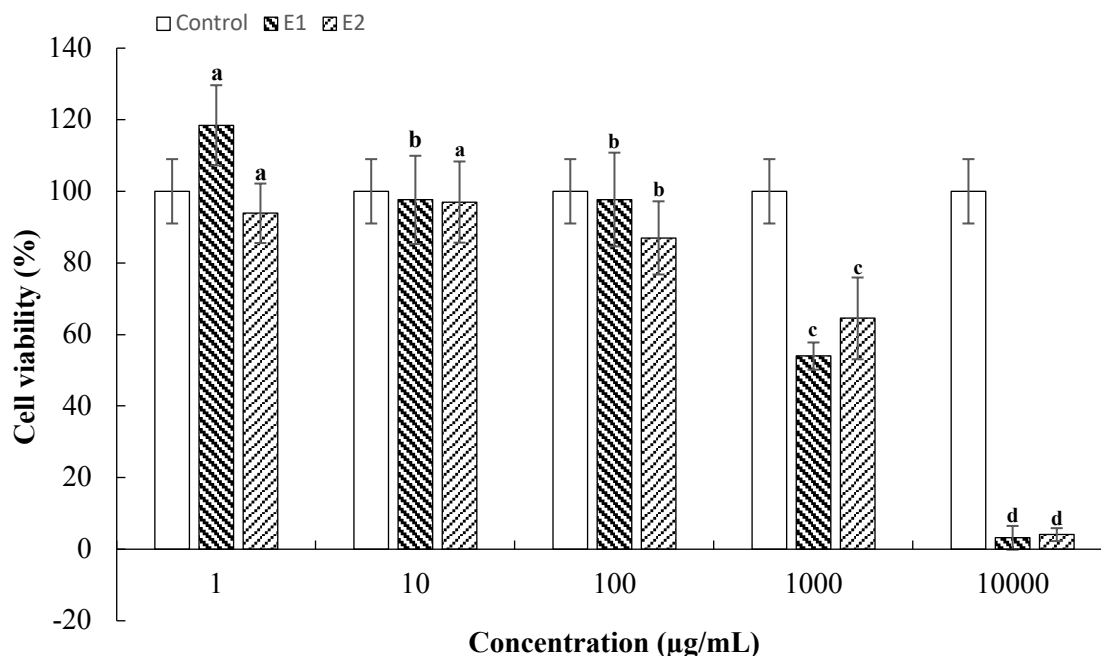
Figure 37. Effect of ethanolic extracts of *G. lucidum* (E1) and *P. ostreatus* (E2) exposure on the viability of HaCaT cells at different concentrations, as measured by the MTT assay. Values are expressed as means ± SD (n = 3). In each extract, different letters mean significant differences between the concentrations ($p<0.05$).

Regarding HaCaT cells after exposure to both extracts (**Figure 37**), up to 90% cell viability was maintained at 100 µg/mL, while the highest tested concentration (10 mg/mL) was found to significantly inhibit cell viability. Concerning HFF-1 cells, the cell viability was maintained up to 60% at 100 µg/mL for E1, and up to 90% when the same concentration was used with E2. Above 100 µg/mL, both extracts were found to significantly affect the viability of HFF-1 cells as shown in **Figure 38**. This result can be used to compare the potential toxicity of the studied mushroom ethanolic extracts, based on which further experiments can be conducted.
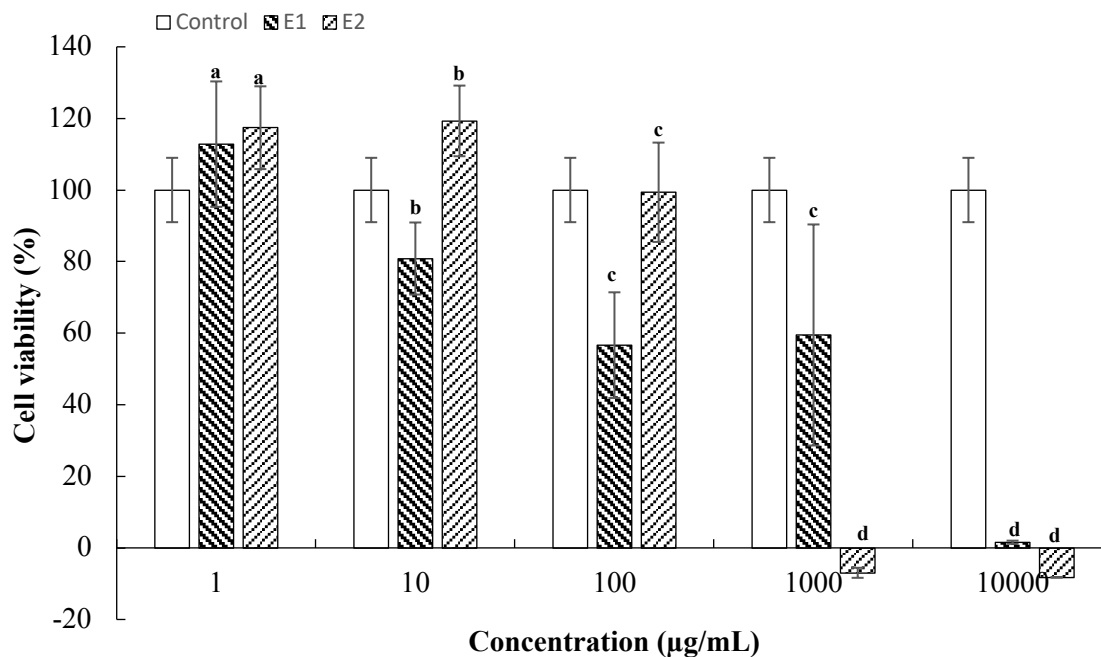
Figure 38. Effect of ethanolic extracts of *G. lucidum* (E1) and *P. ostreatus* (E2) exposure on the viability of HFF-1 cells at different concentrations, as measured by the MTT assay. Values are expressed as means ± SD (n = 3). In each extract, different letters mean significant differences between the concentrations ($p<0.05$).

The LDH assay has been utilised as a good marker to ascertain cytotoxicity of bioactive ingredients. The mechanism behind it involves the measurement of lactate dehydrogenase (LDH), an enzyme found in the surroundings of compromised cell membranes. As shown in **Figure 39**, E2 did not show any potential to cause LDH leakage after exposure to HaCaT cells. This low toxicity was achieved at 100 µg/mL, more than 50% toxicity was found above 1 mg/mL. In what concerns E1, a lower level of toxicity was found in the range of 4-100 µg/mL, while increased cellular LDH efflux was found above 100 µg/mL. Similarly, **Figure 40** showed that both extracts present low toxicity to HFF-1cells between 1-10 µg/mL, but increased LDH level was observed between 100-10000 µg/mL for both extracts, comparable to Triton X-100 (negative control). The results indicate that the fibroblasts cells were more sensitive when compared to the keratinocytes after exposure to different concentrations of the extracts. These results are in agreement with those obtained for hydroalcoholic extract obtained from the leaves of six species of *Medicago* (Rodrigues et al., 2013). The authors observed that the keratinocytes were more resistant than fibroblasts when exposed to different concentrations of the extract. Based on the achieved results described, the extract concentration that was able to maintain cell viability up to 50% can be selected for further experiments or applications.
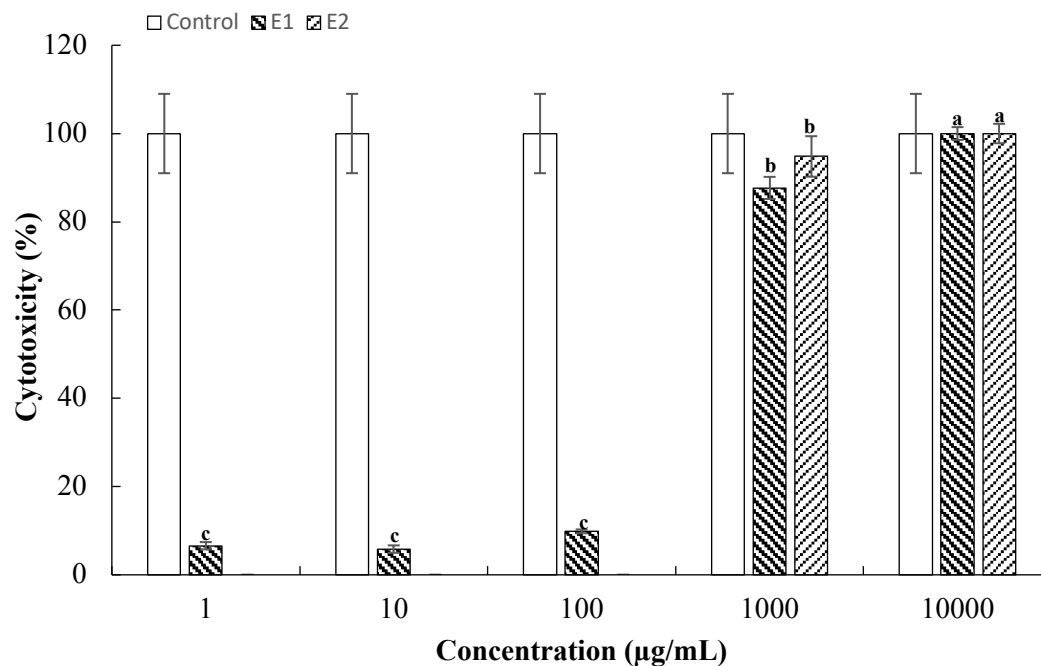
Figure 39. Cytotoxicity (%) of LDH in HaCaT cells after exposure to extracts E1 and E2. Values are expressed as means ± SD (n = 3). In each extract, different letters mean significant differences between the concentrations ($p<0.05$).
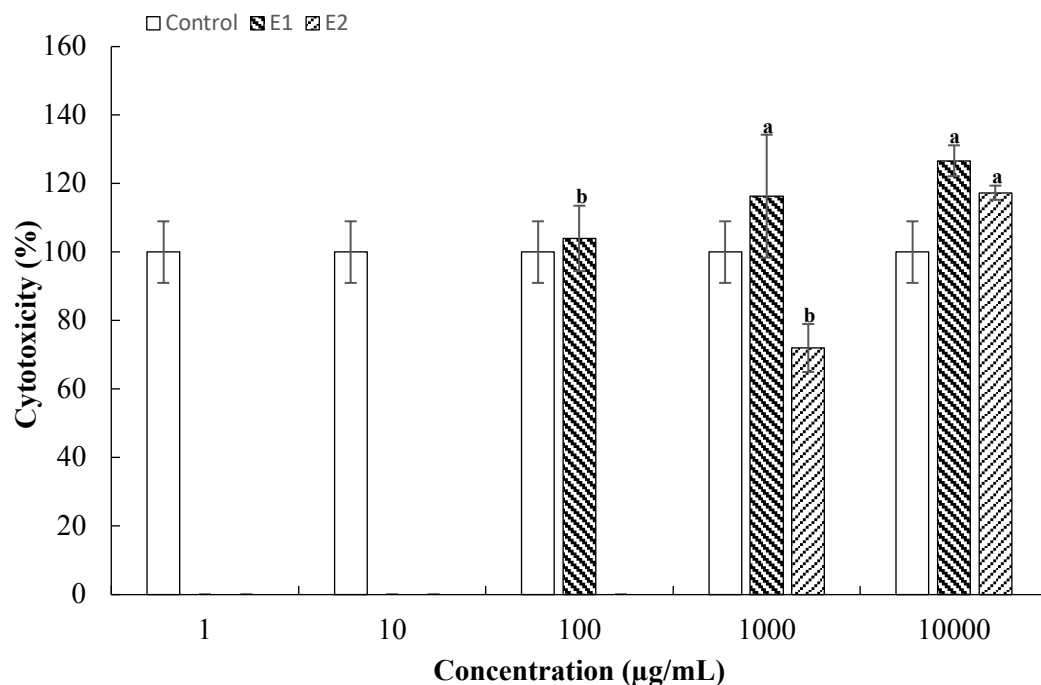
Figure 40. Cytotoxicity (%) of LDH in HFF-1 cells after exposure to extracts E1 and E2. Values are expressed as means ± SD (n = 3). In each extract, different letters mean significant differences between the concentrations ($p<0.05$).

The final cosmeceutical creams formulated with the extracts were also submitted to studies evaluating their cell viability and cytotoxicity effect on fibroblasts and keratinocyte cell lines. Data of **Figure 41** indicates that the cell viability of HaCaT cell lines, after exposure to F1, undergo, up to 60%, maintenance of cell viability at 1 mg/mL.
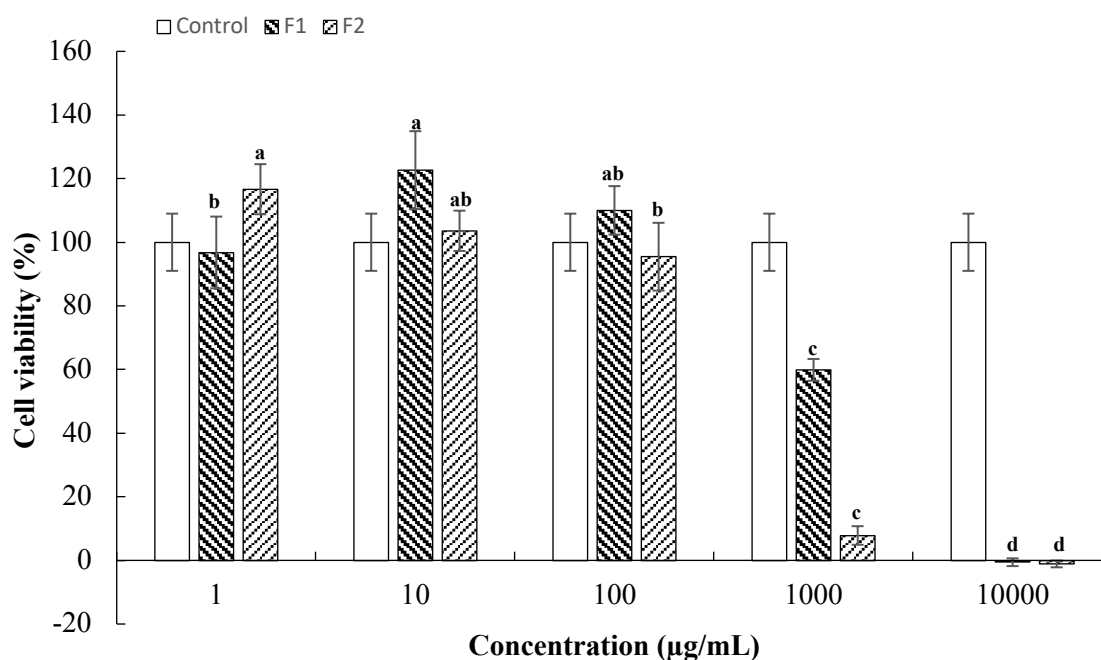
Figure 41. Effect of formulations (F1 and F2) exposure on the viability of HaCaT cells at different concentrations, as measured by the MTT assay. Values are expressed as means ± SD (n = 3). In each extract, different letters mean significant differences between the concentrations ($p<0.05$).

The effect of F2 on cell viability of HFF-1 (**Figure 42**) showed a cell survival rate of ~60% for all concentrations below 100 μg/mL, while 1 mg/mL and 10 mg/mL were found to be deleterious to the cells as compared to Triton X-100 (negative control). In fact, it is difficult to deduce the cytotoxic contribution of each component present in the base cosmetic cream, as well as the contribution of the individual compounds identified in the extracts.
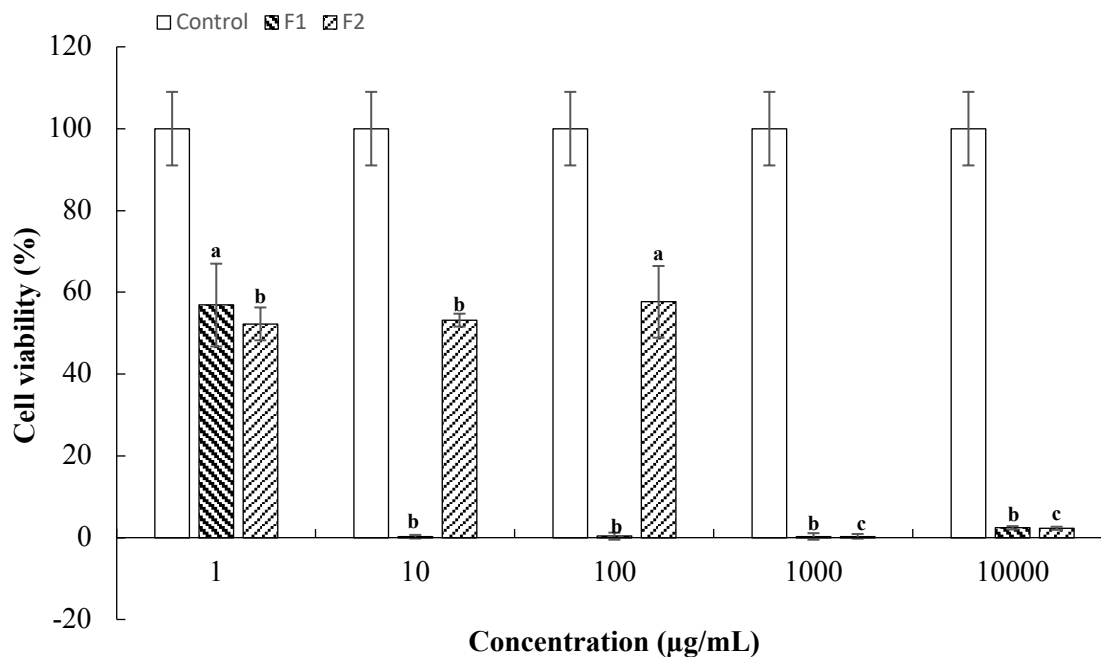
Figure 42. Effect of formulations (F1 and F2) exposure on the viability of HFF-1 cells at different concentrations, as measured by the MTT assay. Values are expressed as means ± SD (n = 3). In each extract, different letters mean significant differences between the concentrations ($p<0.05$).

3.7.2. *Ex vivo* Skin permeation studies

To identify which of the naturally occurring compounds of the prepared ethanolic extracts from *G. lucidum* and *P. ostreatus* were able to penetrate through the skin, and to evaluate their permeability, *ex vivo* experiments were conducted using a pigskin model. From the results described in **Table 39**, in what concerns skin penetration profile of E1, significant amounts of compounds were found to penetrate the skin, but these compounds were not detected in the receptor compartment. The results showed that a significant percentage of the compounds earlier detected in the extract were retained in the skin layers. It will be of utmost significance if these compounds retained in the skin layers can elicit a local cosmeceutical effect.

Bioactive ingredients present in cosmeceutical formulations must be released from the carrier (base cosmetic cream) and be able to penetrate the *stratum corneum* of the skin in order to deliver a cosmeceutical effect (Rodrigues et al., 2016). Because of the ban on the use of *in vivo* assays for testing cosmetics ingredients, in the cosmetic directive 76/768/EEC there is a demand for novel *in vitro* methods to determine the bioavailability of topically applied

chemicals (Gerstel et al., 2016). Skin permeation studies have been conducted in the past using human skin as a membrane, but these experiments are expensive and sometimes limited due to ethical issues. Penetration studies with human and pig skin have been conducted and the results have shown that both skin cells demonstrate positive correlation and bioavailability distribution in the different skin layers with comparable and reproducible results (Barbero & Frasch, 2009). Histologically, many similarities are observed such as the tissue turnover time, the SC thickness, the hair-follicle density and the characteristics of their keratinous proteins. However, dissimilarities exist in the level of vascularization, fat component of the SC organized in a hexagonal lattice in pigs and orthorhombic lattice in human (Praça et al., 2018). The goal is the permeation of active ingredients in *stratum corneum*, which is popularly referred to as the rate-limiting barrier before successfully permeating through the epidermis (Haq, Goodyear, Ameen, Joshi, & Michniak-Kohn, 2018).

Table 39. Identification and quantification of phenolic compounds and triterpenoids during *ex vivo* permeation study.

Rt (min)	UV λmax (nm)	[M-H]⁻ & [2M-H] (m/z)	MS² and MS³ (m/z)	Tentative identification	Quantification Initial	Final	Expected penetration
Phenolic compounds					**μg/g**		
5.31	259,293sh	153	109(100)	Protocatequic acid	377±7	tr	377±7
8.5	257	137	93(100)	*p*-Hydroxybenzoic acid	285±7	tr	285±7
11.45	280	197	121(100)	Syringic acid	612±8	tr	612±8
				Total phenolic acids	**1275±22**		**1275±22**
Triterpenes					**mg/g**		
35.5	265	529/1059	511(5),467(100),449(20),437(29),317(10),301(5),263(5)	12-Hydroxyganoderic acid D	3.37±0.06	1.12±0.07	2.25±0.01
36.8	251	515/1031	497(100),453(31),437(8),303(19),287(5),235(3)	Ganoderic acid derivative	7.0±0.1	2.166±0.003	4.8±0.1
36.9	256	517/1035	499(100) 481(48),456(17),438(52),407(8),304(6),287(35)	Ganoderic acid C2	12.57±0.07	5.8±0.4	6.8±0.3
37.5	257	529/1059	511(5),481(7),467(100),451(14),438(38),424(3),319(5),303(3),301(5)	Ganoderic acid C6	6.6±0.1	tr	6.6±0.1
38.2	256	529/1059	511(58),493(5),449(10),399(100),301(3)	Ganoderic acid derivative	1.65±0.04	tr	1.65±0.04
38.5	256	531/1063	513(11),498(15),469(100),454(29),452(24),437(6),304(5),302(6),290(20),266(7)	Ganoderic acid G	12.0±0.4	tr	12.0±0.4
38.8	248	513/1027	495(10),480(16),451(100),437(14),433(22),407(17),331(5),315(3),303(5),287(5)	Ganoderenic acid B	5.83±0.07	3.5±0.1	2.3±0.2
39.4	254	515/1031	497(10),453(100),439(5),409(5),304(21),287(12),263(3),250(14)	Ganoderic acid B	24.4±0.4	21.0±0.1	3.4±0.5
40.4	254	515/1031	497(100),480(5),454(6),436(10),302(8),301(4),285(3)	Ganoderic acid A	14.8±0.6	9.0±0.2	5.8±0.4
40.7	261	571/1143	553(100),511(8),481(3),468(8),437(3),423(2)	Ganoderic acid H	9.24±0.02	tr	9.24±0.02
40.9	252	527/1055	509(20),479(13),465(100),435(3),421(3),317(3),301(3)	Elfvingic acid A	11.9±0.5	6.92±0.09	5.0±0.4
41.9	246	511/1023	493(12),478(20),449(100),435(15),431(4),405(4),329(3),301(4),285(5),283(3),261(4)	Ganoderenic acid D	8.47±0.05	6.7±0.2	1.8±0.02
42.6	255	513/1027	495(16),451(100),437(6),433(3),407(4),301(23),286(3),284(11),247(8)	Ganoderic acid D	14.3±0.3	9.7±0.2	4.6±0.1
42.8	245	509/1019	491(100),476(18),461(34),447(15),429(3),417(3),300(5),299(4)	Ganoderic acid derivative	10.7±0.3	3.34±0.01	7.4±0.3
43.2	256	511/1023	493(100),449(65),435(3),300(5),247(4)	Ganoderic acid E	8.9±0.5	7.5±0.1	1.4±0.1
44.0	255	569/1139	551(100),509(35),508(21),466(8)	12-Acetoxyganoderic acid F	7.26±0.02	2.38±0.03	4.88±0.02
45.1	272	513/1027	451(100),437(8),433(3),422(3),301(5)	Ganoderic acid J	4.7±0.2	tr	4.7±0.2
				Total triterpenoids	**163±4**	**79±1**	**85±3**

Each value represents the mean ± SD

Different factors such as higher molecular weight, lipophilicity, and aqueous solubility have been reported to be the most important determining factors that explain the tendency of compounds to permeate or to be retained on the skin surface (Žilius et al., 2013). Protocatechuic and syringic acids were the unique compounds that permeated from the E1 extract suspension through the skin in an amount that could be quantified between 1 - 8 h, as shown in **Table 40**.

Table 40. Skin permeation profile of the extract E1 (*Ganoderma lucidum*).

Time	Compounds	Amount detected in the receptor compartment (μg/g)
15 min	-	-
30 min	-	-
45 min	-	-
1 h	Protocatechuic acid	51.5±0.4
2 h	Protocatechuic acid	35.3±0.2
4 h	Protocatechuic acid	11.5±0.1
	Syringic acid	37.2±0.4
6 h	Protocatechuic acid	12.1±0.1
	Syringic acid	tr
8hr	Protocatechuic acid	tr
	Syringic acid	tr

Each value represents the mean ± SD

Both compounds were also detected in the receptor compartment of formulation F1 test. Phenolic acids and related compounds identified in the E2 extract are cinnamic, *p*-hydroxybenzoic and *p*-coumaric acids, and none of these compounds were detected in the receptor fluid, up to 8 h of assayed time. This finding was an indication of the low skin permeation of compounds found in extracts prepared from *P. ostreatus*. Similarly, the penetration and permeation of compounds in formulation F2 were very low and no compounds were detected in the receptor compartment. The results showed that the penetration ability of the phenolic acids identified in the receptor compartment of the assays with sample E1 and F1 might be due to the enhanced contribution of the high size triterpenes of E1 and corresponding formulation. Studies have identified triterpenes, terpenes, and sesquiterpenes as promising non-toxic, highly advanced, non-irritating transdermal penetration enhancers, which were classified as generally regarded as safe (GRAS) by the Food and Drug Administration (Aqil, Ahad, Sultana, & Ali, 2007). The results of E1 and F1 samples showed that the amounts of compounds penetrating in the F1 case were higher than the ones of E1 extract suspension (**Figure 43**). These results are in agreement with the ones reported by Tachaprutinun et al. (2014) in which

the authors confirmed that the properties of the base cosmetic cream (vehicle) have a significant impact on the penetration of the active ingredients.
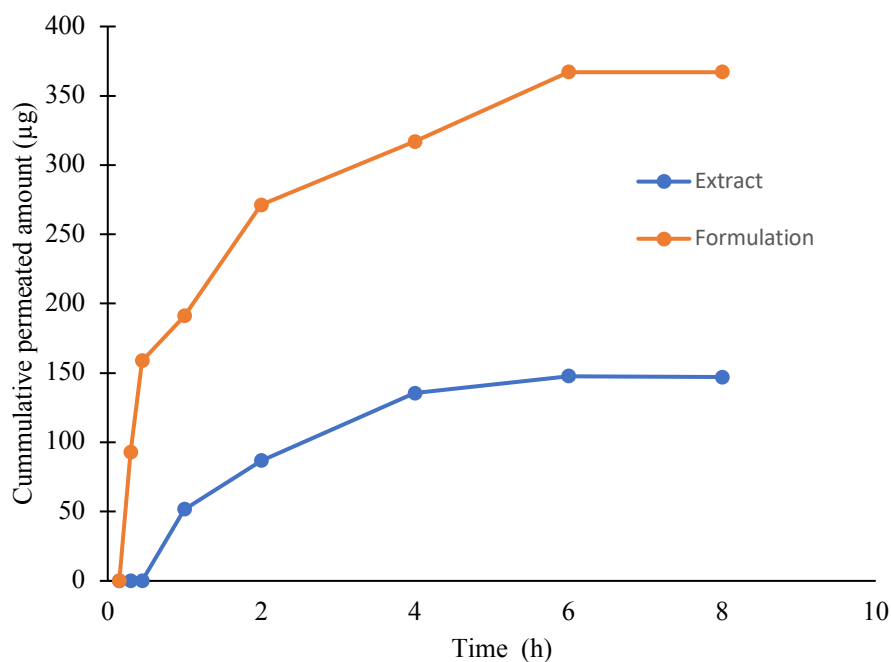
Figure 43. Permeation profile of compounds in E1 and F1.

Various types of bioactivities have been reported for triterpenes and phenolic acids, such as antimicrobial, anti-inflammatory and antioxidant properties (M. J. Alves et al., 2013; Heleno, Martins, et al., 2015; Taofiq et al., 2015). *In vitro* studies have shown that syringic acid present anti-inflammatory activity due to the ability to suppress iNOS and COX-2 activity (M. H. Lee et al., 2013; Stanikunaite et al., 2009). On the other hand, protocatechuic acid presents hyperpigmentation potential due to its ability to inhibit the tyrosinase enzyme (Sahin, 2018). Hence, when applied to the skin, F1 will be able to deliver these health promoting potentials namely antioxidants and anti-inflammatory effects. Abla and Banga (2013) have reported the permeation of catechin and resveratrol using porcine ear skin, which was favoured due to the use of propylene glycol that acts as a penetration enhancer. A more significant amount of catechin was retained in the *stratum corneum* whereas only 10% was able to be quantified in the underlying skin. Other authors suggested that the release of phenolic compounds from semisolid vehicles is influenced, not only by the physiochemical properties of the bioactive ingredient but also by the properties of the used vehicle, as well as by the concentration of the bioactive in the formulation.

The above phenomena were reported by Žilius et al. (2013) after 8h of *ex vivo* skin permeation experiments, where over 90% of the phenolic compounds were released from a hydrophilic gel, and only up to 5% and 22% of phenolic compounds were released from ointment and water-in-oil (w/o) cream, respectively. These results demonstrated that the E1 ethanolic extract can be utilised as an ingredient for cosmeceutical application due to the beneficial biological properties of its individual compounds (protocatechuic and syringic acids). After topical application, they penetrate the skin, offering advantages as antioxidative support to the skin, suppressing oxidative stress and protecting the skin against photoageing.

Conclusions and Future Perspectives

Mushrooms are a source of biologically active metabolites that present an interesting potential to be utilised as cosmeceutical and nutricosmetic ingredients. The present study was aimed to strengthen the knowledge of mushrooms and their individual metabolites as potential ingredients for cosmetic application. Optimization studies were successfully conducted to obtain extracts from *G. lucidum* and *A. blazei*, rich in bioactive compounds, by comparing conventional and more sustainable non-conventional approaches. Regarding *G. lucidum*, in global terms at the optimum conditions predicted by the RSM model, the UAE led to the obtainment of extracts richer in triterpenes than those obtained by HAE and SE, mainly due to the higher amounts of ganoderic acid C2, A and H. Regarding *A. blazei*, the MAE, at the optimum conditions, was identified as the most appropriate to obtain higher extraction yield and ergosterol content, followed by UAE and HAE. The values predicted by the models were in close agreement with the experimental observations, proving the validity of the model and the utility of the predictions for future scale-up towards the production of an ergosterol-rich extract from *A. blazei*.

The ethanolic extracts of *A. bisporus*, *P. ostreatus*, *L. edodes* and *G. lucidum* displayed strong antioxidant activity which suggests that they can prevent/minimize the oxidative stress related to ROS generation, thus acting as skin anti-ageing ingredients. The magnitudes of the other bioactive properties were as follows: anti-tyrosinase: *A. bisporus > L. edodes > P. ostreatus*, *L. edodes > A. blazei > G. lucidum;* anti-inflammatory: *G. lucidum > L. edodes > A. bisporus > P. ostreatus > A. blazei;* antimicrobial: *G. lucidum > L. edodes > A. bisporus > P. ostreatus*. *G. lucidum* was found to present the highest amount of phenolic acids and related compounds, due to the contribution of protocatechuic, *p*-hydroxybenzoic and syringic acids, closely followed by *P. ostreatus* which presented *p*-hydroxybenzoic, protocatechuic and cinnamic acids. After incorporating the extracts into the base cosmetic cream, the mushroom cosmetic formulations still preserved some of its bioactivities, which highlights that mushrooms contain sustainable bioactive compounds that can be utilised as cosmeceutical ingredients.

After incorporating the extracts into the base cosmetic creams, they displayed bioactivity; even with a decreasing pattern along the 6 months, for the free extracts. Microparticles were then developed to ensure topical delivery of *A. bisporus* and *P. ostreatus* ethanolic extracts. The release profile after incorporating microparticles in semi-solid base formulation showed no demonstration of significant antioxidant and antimicrobial activities, but with the anti-

tyrosinase activity being displayed even after 3 months. The produced microparticles effectively offered protection, and when compared to the free forms they were able to allow for a sustained release of the bioactive compounds.

In the study related to the cosmeceutical potential of the individual compounds, the magnitude of the bioactivities displayed were as follows: anti-tyrosinase activity: cinnamic acid > *p*-hydroxybenzoic acid; antimicrobial activity: *p*-coumaric acid > cinnamic acid > ergosterol > *p*-hydroxybenzoic acid > protocatechuic acid; anti-inflammatory activity: *p*-coumaric acid > cinnamic acid > protocatechuic acid > *p*-hydroxybenzoic acid > ergosterol. The multifunctional properties displayed by these compounds make them suitable candidates to be explored as cosmeceutical ingredients. The atomization/coagulation technique was successfully applied to encapsulate the bioactive agents, conducting to encapsulation efficiency percentages above 50% for all the tested compounds. After incorporating the individual compounds in the cosmetic formulations, bioactive properties were only partially maintained while their microencapsulated formulations have shown a sustained release able to better preserve bioactivity. Moreover, over the course of storage time, no significant changes were observed in the tested stability parameters, namely colour and pH. By the obtained results, the analysed bioactive agents revealed promising bioactivity and stability.

Besides the interesting biological properties displayed by *G. lucidum* and *A. blazei* ethanolic extracts, these mushroom species also showed high nutritional contribution. α-Tocopherol, oxalic acid, and twenty-one fatty acids (mainly polyunsaturated fatty acids) were quantified in *A. blazei*. In *G. lucidum*, a similar fatty acid profile was observed with the presence of α-tocopherol and δ-tocopherol. Comparatively, *A. blazei* was found to present lower fat content, but a higher energy contribution. The cell viability effect of the extract prepared from *A. blazei* on Caco-2 and HT29-MTX cells were found to be maintained in a concentration-dependent manner. It is interesting to note that the oral administration of extracts rich in compounds with antioxidant capacity can be utilised to prevent damages caused by cutaneous sun damage resulting in better and healthy skin, but the efficacy of these extracts as nutricosmetics is still subjected to proper long-term clinical trials.

Following previous results, *G. lucidum* and *P. ostreatus* demonstrated the best cosmeceutical potential, due to their highest bioactivity; both extracts and their corresponding formulations were selected for further studies. Regarding HaCaT cells, after exposure to the extracts, up to 90% cell viability was maintained after the MTT assay, while HFF-1 cells were found to be

more sensitive to *G. lucidum* extract. In the LDH assay, *P. ostreatus* extract did not show any potential to cause LDH leakage after exposure to HFF-cell. This low toxicity was achieved at 100 µg/mL, while up to > 50% toxicity was found above 1 mg/mL. The results showed the absence of toxicity for keratinocytes and fibroblasts in a concentration-dependent manner, which is indicative of the safety of these extracts for cosmeceutical ingredients' purposes. Protocatechuic and syringic acids were the only compounds permeating from *G. lucidum* extract, while very low detection was observed for compounds from the *P. ostreatus* extract. These results pointed out for the suitability of using mushroom extracts as skin care ingredients.

The studies conducted here successfully optimized extraction techniques to maximize the recovery of different compounds from mushrooms; highlighted the biological properties of mushroom extracts; and were validated in final applications in cosmetic matrices. Furthermore, the nutritional and chemical composition of the mushroom fruiting bodies were also determined, and the microencapsulation with polymeric materials were applied to modulate the release of bioactive compounds and provide protection against degradation factors. The absence of toxicity of the extracts and their final formulations was confirmed, and skin permeation studies were conducted to evaluate the topical availability of the bioactive compounds. Overall, it can be concluded that the studied mushrooms represent an important source of bioactives with multifunctional biological properties, which can be used as ingredients to formulate cosmetic creams or lotions.

Future perspectives

1. From a sustainable point of view, focus should be placed on residues generated during mushrooms' production processes to suppress the negative impact of these wastes on the environment, while contributing effectively as sources of biologically active cosmeceutical ingredients;

2. Mushroom extract and individual compounds revealed intereting biological properties and as such determine the biochemical mechanism behind each bioactive property by testing the levels of expression of the respective protein markers by western blot analysis can be further carried out;

3. Comprehensive safety and toxicity assessment of the extracts and the individual compounds can also be conducted using validated cell-based *in vitro* models as proposed by the European Centre for the Validation of Alternative Methods (ECVAM) to predict carcinogenicity, repeat dose toxicity and reproductive toxicity;

4. Because of the limitations on testing cosmetic ingredients on animals, technological advancements have led to the development of 3D models, either as epidermal models (containing keratinocytes) or full thickness models (containing keratinocytes and fibroblasts) such as EpiSkin[TM], EpiDerm[TM], StrataTest[TM], SkinEthic[TM], Epiderm FT[TM,] and epiCS[TM]. Therefore, evaluation of the permeability and topical availability of the bioactive metabolites in the studied extracts and individual compounds in these models will further strengthen the knowledge on their use as cosmeceutical ingredients;

5. Studies related to the *in vivo* effects of the extracts and their corresponding cosmeceutical formulations should be conducted. Volunteers can be asked about their perception of the formulation based on properties such as skin hydration, wrinkles depth, skin roughness and transepidermal water loss.

References

Abla, M. J., & Banga, A. K. (2013). Quantification of skin penetration of antioxidants of varying lipophilicity. *International Journal of Cosmetic Science*, 35(1), 19–26.

Abreu, R. M. V, Ferreira, I. C. F. R., Calhelha, R. C., Lima, R. T., Vasconcelos, M. H., Adega, F., Chaves, R., Queiroz, M. J. R. P. (2011). Anti-hepatocellular carcinoma activity using human HepG2 cells and hepatotoxicity of 6-substituted methyl 3-aminothieno[3,2-*b*] pyridine-2-carboxylate derivatives: *In vitro* evaluation, cell cycle analysis and QSAR studies. *European Journal of Medicinal Chemistry*, 46(12), 5800–5806.

Abruzzo, A., Armenise, N., Bigucci, F., Cerchiara, T., Gösser, M. B., Samorì, C., Galletti, P., Tagliavini, E., Brown, D. M., Helinor, J. Johnston, J. J., Fernandes, T. F., Luppi, B. (2017). Surfactants from itaconic acid toxicity to HaCaT keratinocytes *in vitro*, micellar solubilization, and skin permeation enhancement of hydrocortisone. *International Journal of Pharmaceutics*, 524(1–2), 9–15.

Acosta, N., Sanchez, E., Calderon, L., Cordoba-Diaz, M., Cordoba-Diaz, D., Dom, S., & Heras, A. (2015). Physical stability studies of semi-solid formulations from natural compounds loaded with Chitosan Microspheres. *Marine Drugs*, 13(9), 5901–5919.

Agrawal, S., Adholeya, A., Barrow, C. J., & Deshmukh, S. K. (2018). Marine fungi: An untapped bioresource for future cosmeceuticals. *Phytochemistry Letters*, 23, 15–20.

Aguiar, J., Costa, R., Rocha, F., Estevinho, B. N., & Santos, L. (2017). Design of microparticles containing natural antioxidants: Preparation, characterization and controlled release studies. *Powder Technology*, 313, 287–292.

Aguiar, J., Estevinho, B. N., & Santos, L. (2016). Microencapsulation of natural antioxidants for food application − The specific case of coffee antioxidants − A review. *Trends in Food Science and Technology*, 58, 21–39.

Akdis, C., Akdis, M., Trautmann, A., & Blaser, K. (2000). Immune regulation in atopic dermatitis. *Current Opinion in Immunology*, 12, 641–646.

Akihisa, T., Nakamura, Y., Tagata, M., Tokuda, H., Yasukawa, K., Uchiyama, E., Suzuki, E., Kimura, Y. (2007). Anti-inflammatory and anti-tumor-promoting effects of triterpene acids and sterols from the fungus *Ganoderma lucidum*. *Chemistry and Biodiversity*, 4(2), 224–231.

Alam, N., Yoon, K. N., Lee, J. S., Cho, H. J., & Lee, T. S. (2012). Consequence of the antioxidant activities and tyrosinase inhibitory effects of various extracts from the fruiting bodies of *Pleurotus ferulae*. *Saudi Journal of Biological Sciences*, 19(1), 111–118.

Alam, N., Yoon, K. N., Lee, K. R., Shin, P. G., Cheong, J. C., Yoo, Y. B., Shim, M. J., Lee, M. J., Lee, U. Y., Lee, T. S. (2010). Antioxidant Activities and Tyrosinase Inhibitory Effects of Different Extracts from *Pleurotus ostreatus* Fruiting Bodies. *Mycobiology*, 38(4), 295.

Albuquerque, B. R., Prieto, M. A., Barreiro, M. F., Rodrigues, A., Curran, T. P., Barros, L., & Ferreira, I. C. F. R. (2016). Catechin-based extract optimization obtained from *Arbutus unedo* L. fruits using maceration/microwave/ultrasound extraction techniques. *Industrial Crops and Products*, 95, 404–415.

Ali, S. A., Choudhary, R. K., Naaz, I., & S Ali, A. (2015). Melanogenesis: Key Role of Bioactive Compounds in the Treatment of Hyperpigmentory Disorders. *Journal of Pigmentary Disorders*, 2(11), 1–9.

Ali, S. M., & Yosipovitch, G. (2013). Skin pH: From basic science to basic skin care. *Acta Dermato-Venereologica*, 93(3), 261–267.

Alsterholm, M., Karami, N., & Faergemann, J. (2010). Antimicrobial activity of topical skin pharmaceuticals - An *in vitro* study. *Acta Dermato-Venereologica*, 90(3), 239–245.

Alves, M. J., Ferreira, I. C. F. R., Dias, J., Teixeira, V., Martins, A., & Pintado, M. (2013). a Review on Antimicrobial Activity of Mushroom Extracts and Isolated Compounds. *Planta Medica*, 78, 1707–1718.

Alves, M. J., Ferreira, I. C. F. R., Froufe, H. J. C., Abreu, R. M. V, Martins, A., & Pintado, M. (2013). Antimicrobial activity of phenolic compounds identified in wild mushrooms, SAR analysis and docking studies. *Journal of Applied Microbiology*, 115(2), 346–357.

Ambothi, K., Prasad, N. R., & Balupillai, A. (2015). Ferulic acid inhibits UVB-radiation induced photocarcinogenesis through modulating inflammatory and apoptotic signalling in Swiss albino mice. *Food and Chemical Toxicology*, 82, 72–78.

Amen, Y. M., Zhu, Q., Afifi, M. S., Halim, A. F., Ashour, A., & Shimizu, K. (2016). New cytotoxic lanostanoid triterpenes from *Ganoderma lingzhi*. *Phytochemistry Letters*, 17, 64–70.

Amer, M., & Maged, M. (2009). Cosmeceuticals versus pharmaceuticals. *Clinics in Dermatology*, 27(5), 428–430.

Amin, Z. A., Ali, H. M., Alshawsh, M. A., Darvish, P. H., & Abdulla, M. A. (2015). Application of *Antrodia camphorata* promotes Rat's wound healing *in vivo* and facilitates Fibroblast cell proliferation *in vitro*. *Evidence-Based Complementary and Alternative Medicine*, 317693, 1-14

Amirullah, N. A., Zainal Abidin, N., & Abdullah, N. (2018). The potential applications of mushrooms against some facets of atherosclerosis: A review. *Food Research International*, 105, 517–536.

An, S. M., Koh, J. S., & Boo, Y. C. (2010). *p*-coumaric acid not only inhibits human tyrosinase activity *in vitro* but also melanogenesis in cells exposed to UVB. *Phytotherapy Research*, 24(8), 1175–1180.

Andhariya, J. V., Choi, S., Wang, Y., Zou, Y., Burgess, D. J., & Shen, J. (2017). Accelerated *in vitro* release testing method for naltrexone loaded PLGA microspheres. *International Journal of Pharmaceutics*, 520, 79–85.

André, P., & Villain, F. (2017). Free radical scavenging properties of mannitol and its role as a constituent of hyaluronic acid fillers: a literature review. *International Journal of Cosmetic Science*, 39(4), 355–360.

Aqil, M., Ahad, A., Sultana, Y., & Ali, A. (2007). Status of terpenes as skin penetration enhancers. *Drug Discovery Today*, 12, 1061–1067.

Ashraf, Z., Rafiq, M., Seo, S. Y., Babar, M. M., & Zaidi, N. U. S. S. (2015). Synthesis, kinetic mechanism and docking studies of vanillin derivatives as inhibitors of mushroom tyrosinase. *Bioorganic and Medicinal Chemistry*, 23(17), 5870–5880.

Azmi, N., Hashim, P., Hashim, D. M., Halimoon, N., & Majid, N. M. N. (2014). Anti-elastase, anti-tyrosinase and matrix metalloproteinase-1 inhibitory activity of earthworm extracts as potential new anti-aging agent. *Asian Pacific Journal of Tropical Biomedicine*, 4, S348–S352.

Azmir, J., Zaidul, I. S. M., Rahman, M. M., Sharif, K. M., Mohamed, A., Sahena, F., Jahurul, M. H. A., Ghafoor, K., Norulaini, N. A. N., & Omar, A. K. M. (2013). Techniques for extraction of bioactive compounds from plant materials: A review. *Journal of Food Engineering*, 117(4), 426–436.

Azwanida, N. N. (2015). A Review on the Extraction Methods Use in Medicinal Plants, Principle, Strength and Limitation. *Medicinal & Aromatic Plants*, 4(3), 3–8.

Baby, S., Johnson, A. J., & Govindan, B. (2015). Secondary metabolites from *Ganoderma*. *Phytochemistry*, 114, 66–101.

Bae, J. T., Sim, G. S., Lee, D. H., Lee, B. C., Pyo, H. B., Choe, T. B., & Yun, J. W. (2005). Production of exopolysaccharide from mycelial culture of *Grifola frondosa* and its inhibitory effect on matrix metalloproteinase-1 expression in UV-irradiated human dermal fibroblasts. *FEMS Microbiology Letters*, 251(2), 347–354.

Bae, J. Y., Choi, J. S., Kang, S. W., Lee, Y. J., Park, J., & Kang, Y. H. (2010). Dietary compound ellagic acid alleviates skin wrinkle and inflammation induced by UV-B irradiation. *Experimental Dermatology*, 19(8), 182–190.

Bai, J., Lu, Y., Li, P. Y., Liu, C. M., Wu, H. C., Wen, R., & Du, S. Y. (2014). Development and *in vitro* evaluation of a transdermal hydrogel patch for ferulic acid. *Pakistan Journal of Pharmaceutical Sciences*, 27(2), 369–375.

Bajko, E., Kalinowska, M., Borowski, P., Siergiejczyk, L., & Lewandowski, W. (2016). 5-*O*-Caffeoylquinic acid: A spectroscopic study and biological screening for antimicrobial activity. *LWT - Food Science and Technology*, 65, 471–479.

Barba, F. J., Zhu, Z., Koubaa, M., Sant'Ana, A. S., & Orlien, V. (2016). Green alternative methods for the extraction of antioxidant bioactive compounds from winery wastes and by-products: A review. *Trends in Food Science and Technology*, 49, 96–109.

Barbero, A. M., & Frasch, H. F. (2009). Pig and guinea pig skin as surrogates for human *in vitro* penetration studies: A quantitative review. *Toxicology in Vitro*, 23(1), 1–13.

Barbulova, A., Colucci, G., & Apone, F. (2015). New Trends in Cosmetics: By-Products of Plant Origin and Their Potential Use as Cosmetic Active Ingredients. *Cosmetics*, 2(2), 82–92.

Barreira, J. C. M., Oliveira, M. B. P. P., & Ferreira, I. C. F. R. (2014). Development of a Novel Methodology for the Analysis of Ergosterol in Mushrooms. Food Analytical Methods, 7(1), 217–223.

Barros, L., Pereira, C., & Ferreira, I. C. F. R. (2013). Optimized Analysis of Organic Acids in Edible Mushrooms from Portugal by Ultra Fast Liquid Chromatography and Photodiode Array Detection. *Food Analytical Methods*, 6(1), 309–316.

Barros, L., Cruz, T., Baptista, P., Estevinho, L. M., & Ferreira, I. C. F. R. (2008). Wild and commercial mushrooms as source of nutrients and nutraceuticals. *Food and Chemical Toxicology*, 46(8), 2742–2747.

Baumann, L. (2012). Inside Cosmeceutical Marketing Claims. *Practical Dermatology*, 35–39.

Bellik, Y., Boukraâ, L., Alzahrani, H. A., Bakhotmah, B. A., Abdellah, F., Hammoudi, S. M., & Iguer-Ouada, M. (2013). Molecular mechanism underlying anti-inflammatory and anti-allergic activities of phytochemicals: an update. *Molecules*, 18, 322–353.

Bernstein, E. F., Underhill, C. B., Lakkakorpi, J., Ditre, C. M., Uitto, J., Yu, R. J., & Van Scott, O. E. (1997). Citric acid increases viable epidermal thickness and glycosaminoglycan content of sun-damaged skin. *Dermatologic Surgery*, 23(8), 689–694.

Bessada, S. M. F., Barreira, J. C. M., Barros, L., Ferreira, I. C. F. R., & Oliveira, M. B. P. P. (2016). Phenolic profile and antioxidant activity of *Coleostephus myconis* (L.) Rchb.f.: An underexploited and highly disseminated species. *Industrial Crops and Products*, 89, 45–51.

Bezerra, M. A., Santelli, R. E., Oliveira, E. P., Villar, L. S., Escaleira, E. A., & Escaleira, L. A. (2008). Response surface methodology (RSM) as a tool for optimization in analytical chemistry. *Talanta*, 76(5), 965–977.

Bishop, K. S., Kao, C. H. J., Xu, Y., Glucina, M. P., Paterson, R. R. M., & Ferguson, L. R. (2015). From 2000 years of *Ganoderma lucidum* to recent developments in nutraceuticals. *Phytochemistry*, 114, 56–65.

Biswick, T., Park, D. H., & Choy, J. H. (2012). Enhancing the UV A1 screening ability of caffeic acid by encapsulation in layered basic zinc hydroxide matrix. *Journal of Physics and Chemistry of Solids*, 73(12), 1510–1513.

Bolzinger, M. A., Briançon, S., Pelletier, J., & Chevalier, Y. (2012). Penetration of drugs through skin, a complex rate-controlling membrane. *Current Opinion in Colloid and Interface Science*, 17(3), 156–165.

Borges, A., Saavedra, M. J., & Simões, M. (2012). The activity of ferulic and gallic acids in biofilm prevention and control of pathogenic bacteria. *Biofouling*, 28(7), 755–767.

Box, G. E. P., Hunter, J. S., & Hunter, W. G. (2005). Statistics for Experimenters: Design, Innovation, and Discovery, 2nd Edition. Wiley.

Box, G., & Hunter, J. (1957). Multi-factor experimental designs for exploring response surfaces. *The Annals of Mathematical Statistics*, 28(1), 195–241.

Brandt, F. S., Cazzaniga, A., & Hann, M. (2011). Cosmeceuticals: Current Trends and Market Analysis. *Seminars in Cutaneous Medicine and Surgery*, 30(3), 141–143.

Briones-Labarca, V., Giovagnoli-Vicuña, C., & Cañas-Sarazúa, R. (2018). Optimization of extraction yield, flavonoids and lycopene from tomato pulp by high hydrostatic pressure-assisted extraction. *Food Chemistry*, 278, 751–759.

Búfalo, M. C., Ferreira, I., Costa, G., Francisco, V., Liberal, J., Cruz, M. T., Lopes, M. C., Batista, M. T., Sforcin, J. M. (2013). Propolis and its constituent caffeic acid suppress LPS-stimulated pro-inflammatory response by blocking NF-κB and MAPK activation in macrophages. *Journal of Ethnopharmacology*, 149(1), 84–92.

Cai, T. G., & Cai, Y. (2011). Triterpenes from the fungus *Poria cocos* and their inhibitory activity on nitric oxide production in mouse macrophages via blockade of activating protein-1 pathway. *Chemistry and Biodiversity*, 8(11), 2135–2143.

Caleja, C., Ribeiro, A., Barros, L., Barreira, J. C. M., Antonio, A. L., Oliveira, M. B. P. P., Barreiro, M. F., Ferreira, I. C. F. R. (2016). Cottage cheeses functionalized with fennel and chamomile extracts: Comparative performance between free and microencapsulated forms. *Food Chemistry*, 199, 720–726.

Cardoso, R. V. C., Fernandes, Â., Oliveira, M. B. P. P., Calhelha, R. C., Barros, L., Martins, A., & Ferreira, I. C. F. R. (2017). Development of nutraceutical formulations based on the mycelium of *Pleurotus ostreatus* and *Agaricus bisporus*. *Food and Function*, 8(6), 2155–2164.

Cardozo, F. T. G. S., Camelini, C. M., Cordeiro, M. N. S., Mascarello, A., Malagoli, B. G., Larsen, I. V., Rossia, M. J. Nunes, R. J. , Bragad, F. C. Brandte, C. R., & Siẽes, C. M. O. (2013). Characterization and cytotoxic activity of sulfated derivatives of polysaccharides from *Agaricus brasiliensis*. *International Journal of Biological Macromolecules*, 57, 265–272.

Carneiro, A. A. J., Ferreira, I. C. F. R., Dueñas, M., Barros, L., Da Silva, R., Gomes, E., & Santos-Buelga, C. (2013). Chemical composition and antioxidant activity of dried powder formulations of *Agaricus blazei* and *Lentinus edodes*. *Food Chemistry*, 138(4), 2168–2173.

Carocho, M., & Ferreira, I. C. F. R. (2013a). A review on antioxidants, prooxidants and related controversy: Natural and synthetic compounds, screening and analysis methodologies and future perspectives. *Food and Chemical Toxicology*, 51(1), 15–25.

Carocho, M., & Ferreira, I. C. F. R. (2013b). The role of phenolic compounds in the fight against cancer - a review. *Anti-Cancer Agents in Medicinal Chemistry*, 13, 1236–1258.

Carvalho, I. T., Estevinho, B. N., & Santos, L. (2016). Application of microencapsulated essential oils in cosmetic and personal healthcare products - A review. *International Journal of Cosmetic Science*, 38(2), 109–119.

Casanova, F., Estevinho, B. N., & Santos, L. (2016). Preliminary studies of rosmarinic acid microencapsulation with chitosan and modified chitosan for topical delivery. *Powder Technology*, 297, 44–49.

Casanova, F., & Santos, L. (2016). Encapsulation of cosmetic active ingredients for topical application - a review. *Journal of Microencapsulation*, 33(1), 1–17.

Casiraghi, A., Ranzini, F., Musazzi, U. M., Franzè, S., Meloni, M., & Minghetti, P. (2017). *In vitro* method to evaluate the barrier properties of medical devices for cutaneous use. *Regulatory Toxicology and Pharmacology*, 90, 42–50.

Castro, A. J. G., Castro, L. S. E. P. W., Santos, M. S. N., Faustino, M. G. C., Pinheiro, T. S., Dore, C. M. P. G., Baseia, I. G., & Leite, E. L. (2014). Anti-inflammatory, anti-angiogenenic

and antioxidant activities of polysaccharide-rich extract from fungi *Caripia montagnei*. *Biomedicine and Preventive Nutrition*, 4(2), 121–129.

Chaiprasongsuk, A., Onkoksoong, T., Pluemsamran, T., Limsaengurai, S., & Panich, U. (2016). Photoprotection by dietary phenolics against melanogenesis induced by UVA through Nrf2-dependent antioxidant responses. *Redox Biology*, 8, 79–90.

Chang, C. L., Lin, C. S., & Lai, G. H. (2012). Phytochemical characteristics, free radical scavenging activities, and neuroprotection of five medicinal plant extracts. *Evidence-Based Complementary and Alternative Medicine*, 984295, 1–8.

Chang, C. W., Lur, H. S., Lu, M. K., & Cheng, J. J. (2013). Sulfated polysaccharides of *Armillariella mellea* and their anti-inflammatory activities via NF-κB suppression. *Food Research International*, 54(1), 239–245.

Chang, T. S. (2009). An updated review of tyrosinase inhibitors. *International Journal of Molecular Sciences*, 10(6), 2440–2475.

Chanioti, S., & Tzia, C. (2018). Extraction of phenolic compounds from olive pomace by using natural deep eutectic solvents and innovative extraction techniques. *Innovative Food Science and Emerging Technologies*, 48, 228–239.

Chaowattanapanit, S., Silpa-archa, N., Kohli, I., Lim, H. W., & Hamzavi, I. (2017). Post inflammatory hyperpigmentation: A comprehensive overview: Treatment options and prevention. *Journal of the American Academy of Dermatology*, 77(4), 607–621.

Chemat, F., Rombaut, N., Sicaire, A. G., Meullemiestre, A., Fabiano-Tixier, A. S., & Abert-Vian, M. (2017). Ultrasound assisted extraction of food and natural products. Mechanisms, techniques, combinations, protocols and applications. A review. *Ultrasonics Sonochemistry*, 34, 540–560.

Chemat, F., Zill-E-Huma, & Khan, M. K. (2011). Applications of ultrasound in food technology: Processing, preservation and extraction. *Ultrasonics Sonochemistry*, 18(4), 813–835.

Chen, J.-N., Gonzalez de Mejia, E., & Swi-Bea Wu, J. (2011). Inhibitory Effect of a Glycoprotein Isolated from Golden Oyster Mushroom (*Pleurotus citrinopileatus*) on the Lipopolysaccharide-Induced Inflammatory Reaction in RAW 264.7 Macrophage. *Journal of Agricultural and Food Chemistry*, 59, 7092–7097.

Chen, L., Hu, J. Y., & Wang, S. Q. (2012). The role of antioxidants in photoprotection: A critical review. *Journal of the American Academy of Dermatology*, 67(5), 1013–1024.

Chen, M., Bai, H., Zhai, J., Meng, X., Guo, X., Wang, C., Wang, P., Lei, H., Niu, Z., Ma, Q. (2019). Comprehensive screening of 63 colouring agents in cosmetics using matrix solid-phase dispersion and ultra-high-performance liquid chromatography coupled with quadrupole-Orbitrap high-resolution mass spectrometry. *Journal of Chromatography A*, (2018), 1–12.

Chen, S. Y., Chang, C. L., Chen, T. H., Chang, Y. W., & Lin, S. Bin. (2016). Colossolactone H, a new *Ganoderma* triterpenoid exhibits cytotoxicity and potentiates drug efficacy of gefitinib in lung cancer. *Fitoterapia*, 114, 81–91.

Chen, W.-P., & Wu, L.-D. (2014). Chlorogenic acid suppresses interleukin-1β-induced inflammatory mediators in human chondrocytes. *International Journal of Clinical and Experimental Pathology*, 7(12), 8797–8801.

Chen, Y. S., Lee, S. M., Lin, C. C., & Liu, C. Y. (2014). Hispolon decreases melanin production and induces apoptosis in melanoma cells through the downregulation of tyrosinase and microphthalmia-associated transcription factor (MITF) expressions and the activation of caspase-3, -8 and -9. *International Journal of Molecular Sciences*, 15(1), 1201–1215.

Cheng, P., Phan, C., Sabaratnam, V., Abdullah, N., Abdulla, M. A., & Kuppusamy, U. R. (2013). Polysaccharides-Rich Extract of *Ganoderma lucidum* Accelerates Wound Healing in Streptozotocin-Induced Diabetic Rats. Evidence-Based Complementary and Alternative Medicine, 671252, 1-9.

Chien, C. C., Tsai, M. L., Chen, C. C., Chang, S. J., & Tseng, C. H. (2008). Effects on tyrosinase activity by the extracts of *Ganoderma lucidum* and related mushrooms. *Mycopathologia*, 166(2), 117–120.

Chien, S. C., Chen, M. L., Kuo, H. T., Tsai, Y. C., Lin, B. F., & Kuo, Y. H. (2008). Anti-inflammatory activities of new succinic and maleic derivatives from the fruiting body of *Antrodia camphorata*. *Journal of Agricultural and Food Chemistry*, 56(16), 7017–7022.

Choe, J. H., Yi, Y. J., Lee, M. S., Seo, D. W., Yun, B. S., & Lee, S. M. (2015). Methyl 9-Oxo-(10E,12E)-octadecadienoate isolated from *Fomes fomentarius* attenuates lipopolysaccharide-induced inflammatory response by blocking phosphorylation of STAT3 in murine macrophages. *Mycobiology*, 43(3), 319–326.

Choi, E. J., Lee, S., Kim, H. H., Singh, T. S. K., Choi, J. K., Choi, H. G., Suh, W. M., Lee, S. H., Kim, S. H. (2011). Suppression of dust mite extract and 2,4-dinitrochlorobenzene-induced atopic dermatitis by the water extract of *Lindera obtusiloba*. *Journal of Ethnopharmacology*, 137(1), 802–807.

Choi, S., Nguyen, V. T., Tae, N., Lee, S., Ryoo, S., Min, B. S., & Lee, J. H. (2014). Anti-inflammatory and heme oxygenase-1 inducing activities of lanostane triterpenes isolated from mushroom *Ganoderma lucidum* in RAW264.7 cells. *Toxicology and Applied Pharmacology*, 280(3), 434–442.

Choi, Y. H., Kim, G. Y., & Lee, H. H. (2014). Anti-inflammatory effects of cordycepin in lipopolysaccharide-stimulated RAW 264.7 macrophages through Toll-like receptor 4-mediated suppression of mitogen-activated protein kinases and NF-κB signaling pathways. *Drug Design, Development and Therapy*, 8, 1941–1953.

Chu, C., Ye, S., Wu, H., & Chiu, C. (2015). The *Ganoderma* Extracts from Tein-Shan *Ganoderma* Capsule Suppressed LPS-Induced Nitric Oxide Production in RAW 264.7 Cells. *MC-Transaction on Biotechnology*, 7(1), 1–11.

Chu, X., Ci, X., He, J., Jiang, L., Wei, M., Cao, Q., Guan, M., Xie, X., Deng, X., He, J. (2012). Effects of a natural prolyl oligopeptidase inhibitor, rosmarinic acid, on lipopolysaccharide-induced acute lung injury in mice. *Molecules*, 17(3), 3586–3598.

Ćilerdžić, J., Vukojević, J., Stajić, M., Stanojković, T., & Glamočlija, J. (2014). Biological activity of *Ganoderma lucidum* basidiocarps cultivated on alternative and commercial substrate. *Journal of Ethnopharmacology*, 155(1), 312–319.

Cirino, G., Distrutti, E., & Wallace, J. (2006). Nitric Oxide and Inflammation. *Inflammation & Allergy-Drug Targets*, 5(2), 115–119.

Comuzzi, C., Polese, P., Melchior, A., Portanova, R., & Tolazzi, M. (2003). SOLVERSTAT: a new utility for multipurpose analysis. An application to the investigation of dioxygenated Co (II) complex formation in dimethylsulfoxide solution. *Talanta*, 59(1), 67–80.

Cong-cong, X. U., Bing, W., Yi-qiong, P. U., Jian-sheng, T. A. O., & Tong, Z. (2017). Advances in extraction and analysis of phenolic compounds from plant materials. *Chinese Journal of Natural Medicines*, 15(10), 721–731.

Corrêa, R., Barros, L., Fernandes, A., Sokovic, M., Bracht, A., Peralta, R. M., & Ferreira, I. C. F. R. (2018). A natural food ingredient based on ergosterol: optimization of the extraction from *Agaricus blazei*, evaluation of bioactive properties and incorporation in yogurts. *Food & Function*, 9, 1465–1474.

Costa, R., & Santos, L. (2017). Delivery systems for cosmetics - From manufacturing to the skin of natural antioxidants. *Powder Technology*, 322, 402–416.

Cueva, C., Moreno-Arribas, M. V., Martín-Álvarez, P. J., Bills, G., Vicente, M. F., Basilio, A., Rivas, C. L., Requena, T., Rodrıguez, J. M., Bartolomé, B. (2010). Antimicrobial activity of phenolic acids against commensal, probiotic and pathogenic bacteria. *Research in Microbiology*, 161(5), 372–382.

da Cunha, F. M., Duma, D., Assreuy, J., Buzzi, F. C., Niero, R., Campos, M. M., & Calixto, J. B. (2004). Caffeic acid derivatives: *in vitro* and *in vivo* anti-inflammatory properties. *Free Radical Research*, 38(11), 1241–1253.

Dai, J., & Mumper, R. J. (2010). Plant phenolics: Extraction, analysis and their antioxidant and anticancer properties. *Molecules*, 15(10), 7313–7352.

de Francisco, L., Pinto, D., Rosseto, H., Toledo, L., Santos, R., Tobaldini-Valério, F., Svidzinski, T., Bruschi, M., Sarmento, B., Oliveira, M. B. P. P., & Rodrigues, F. (2018). Evaluation of radical scavenging activity, intestinal cell viability and antifungal activity of Brazilian propolis by-product. *Food Research International*, 105, 537–547.

de Mattos-Shipley, K. M. J., Ford, K. L., Alberti, F., Banks, A. M., Bailey, A. M., & Foster, G. D. (2016). The Good, the Bad and the Tasty: The Many Roles of Mushrooms. *Studies in Mycology*, 85, 125–157.

De Vaugelade, S., Nicol, E., Vujovic, S., Bourcier, S., Pirnay, S., & Bouchonnet, S. (2017). UV-vis degradation of α-tocopherol in a model system and in a cosmetic emulsion-Structural elucidation of photoproducts and toxicological consequences. *Journal of Chromatography A*, 1517, 126–133.

De Vita, D., Friggeri, L., D'Auria, F. D., Pandolfi, F., Piccoli, F., Panella, S., Palamara, A. T., Simonetti, G., Scipione, L., Di Santo, R., Costi, R., Tortorella, S. (2014). Activity of caffeic

acid derivatives against *Candida albicans* biofilm. *Bioorganic and Medicinal Chemistry Letters*, 24(6), 1502–1505.

Deng, J. S., Huang, S. S., Lin, T. H., Lee, M. M., Kuo, C. C., Sung, P. J., Hou, W. C., Huang, G. J., & Kuo, Y. H. (2013). Analgesic and anti-inflammatory bioactivities of eburicoic acid and dehydroeburicoic acid isolated from *Antrodia camphorata* on the inflammatory mediator expression in mice. *Journal of Agricultural and Food Chemistry*, 61(21), 5064–5071.

Deng, J., Xu, Z., Xiang, C., Liu, J., Zhou, L., Li, T., Yang, Z., & Ding, C. (2017). Comparative evaluation of maceration and ultrasonic-assisted extraction of phenolic compounds from fresh olives. *Ultrasonics Sonochemistry*, 37, 328–334.

Dias, M. I., Sousa, M. J., Alves, R. C., & Ferreira, I. C. F. R. (2016). Exploring plant tissue culture to improve the production of phenolic compounds: A review. *Industrial Crops and Products*, 82, 9–22.

Dias, M. I., Ferreira, I. C. F. R., & Barreiro, M. F. (2015). Microencapsulation of bioactives for food applications. *Food & Function*, 6(4), 1035–1052.

Diyabalanage, T., Mulabagal, V., Mills, G., DeWitt, D. L., & Nair, M. G. (2008). Health-beneficial qualities of the edible mushroom, *Agrocybe aegerita*. *Food Chemistry*, 108(1), 97–102.

Draelos, Z. D. (2010). Nutrition and enhancing youthful-appearing skin. *Clinics in Dermatology*, 28(4), 400–408.

Draelos, Z. D. (2009). Cosmeceuticals: undefined, unclassified, and unregulated. *Clinics in Dermatology*, 27(5), 431–434.

Duarte, N., Ferreira1, M.-J. U., Martins, M., Viveiros, M., & Amaral, L. (2007). Antibacterial Activity of Ergosterol Peroxide against *Mycobacterium tuberculosis*: Dependence upon System and Medium Employed. *Phytotherapy Research*, 21, 601–604.

Dudhgaonkar, S., Thyagarajan, A., & Sliva, D. (2009). Suppression of the inflammatory response by triterpenes isolated from the mushroom *Ganoderma lucidum*. *International Immunopharmacology*, 9(11), 1272–1280.

Działo, M., Mierziak, J., Korzun, U., Preisner, M., Szopa, J., & Kulma, A. (2016). The potential of plant phenolics in prevention and therapy of skin disorders. *International Journal of Molecular Sciences*, 17(2), 1–41.

Edward, T. L., Kirui, M. S. K., Omolo, J. O., Ngumbu, R. G., Odhiambo, P. M., & Paul K. K. (2015). Change in Concentration of Vitamin D2 in Oyster Mushrooms Exposed to 254nm and 365nm UV-light During Growth. *International Journal of Biochemistry and Biophysics*, 3(1), 1–5.

Elsayed, E. A., El Enshasy, H., Wadaan, M. A. M., & Aziz, R. (2014). Mushrooms: A potential natural source of anti-inflammatory compounds for medical applications. *Mediators of Inflammation*, 805841, 1–15.

Elsner, P. (2006). Antimicrobials and the Skin Physiological and Pathological Flora. Current Problems in Dermatology, 33, 35–41.

Epstein, H. (2009). Cosmeceuticals and polyphenols. *Clinics in Dermatology*, 27(5), 475–478.

Ergün, B. Ç., Çoban, T., Onurdag, F. K., & Banoglu, E. (2011). Synthesis, antioxidant and antimicrobial evaluation of simple aromatic esters of ferulic acid. *Archives of Pharmacal Research*, 34(8), 1251–1261.

Fangkrathok, N., Junlatat, J., & Sripanidkulchai, B. (2013). *In vivo* and *in vitro* anti-inflammatory activity of *Lentinus polychrous* extract. *Journal of Ethnopharmacology*, 147(3), 631–637.

Faria, N. C. G., Kim, J. H., Gonçalves, L. A. P., Martins, M. D. L., Chan, K. L., & Campbell, B. C. (2011). Enhanced activity of antifungal drugs using natural phenolics against yeast strains of *Candida* and *Cryptococcus*. *Letters in Applied Microbiology*, 52(5), 506–513.

Fernandes, Â., Barreira, J. C. M., Antonio, A. L., Oliveira, M. B. P. P., Martins, A., & Ferreira, I. C. F. R. (2016). Extended use of gamma irradiation in wild mushrooms conservation: Validation of 2 kGy dose to preserve their chemical characteristics. *LWT - Food Science and Technology*, 67, 99–105.

Fernandes, A. S., Mazzei, J. L., Evangelista, H., Marques, M. R. C., Ferraz, E. R. A., & Felzenszwalb, I. (2018). Protection against UV-induced oxidative stress and DNA damage by Amazon moss extracts. *Journal of Photochemistry and Photobiology B: Biology*, 183, 331–341.

Ferraro, V., Anton, M., & Santé-Lhoutellier, V. (2016). The "sisters" α-helices of collagen, elastin and keratin recovered from animal by-products: Functionality, bioactivity and trends of application. *Trends in Food Science and Technology*, 51, 65–75.

Ferreira, I. C. F. R., Heleno, S. A., Reis, F. S., Stojkovic, D., Queiroz, M. J. R. P., Vasconcelos, M. H., & Sokovic, M. (2015). Chemical features of *Ganoderma* polysaccharides with antioxidant, antitumor and antimicrobial activities. *Phytochemistry*, 114, 38–55.

Ferreira, I. C. F. R., Barros, L., & Abreu, R. (2009). Antioxidants in Wild Mushrooms. *Current Medicinal Chemistry*, 16(12), 1543–1560.

Fisk, W. A., Agbai, O., Lev-Tov, H. A., & Sivamani, R. K. (2014). The use of botanically derived agents for hyperpigmentation: A systematic review. *Journal of the American Academy of Dermatology*, 70(2), 352–365.

FitzGerald, G. A. (2004). Coxibs and Cardiovascular Disease. *New England Journal of Medicine*, 351(17), 1709–1711.

Fiume, M. M., Heldreth, B. A., Bergfeld, W. F., Belsito, D. V., Hill, R. A., Klaassen, C. D., Liebler, D. C., Marks Jr, J. G., Shank, R. C., Slaga, T. J., Snyder, P. W., Andersen, F. A. (2014). Safety Assessment of Citric Acid, Inorganic Citrate Salts, and Alkyl Citrate Esters as Used in Cosmetics. *International Journal of Toxicology*, 33, 16S–46S.

Fotakis, G., & Timbrell, J. A. (2006). *In vitro* cytotoxicity assays: Comparison of LDH, neutral red, MTT and protein assay in hepatoma cell lines following exposure to cadmium chloride. *Toxicology Letters*, 160(2), 171–177.

Francisco, C. R. L., Heleno, S. A., Fernandes, I. P. M., Barreira, J. C. M., Calhelha, R. C., Barros, L., Gonçalves, O. H., Ferreira, I. C. F. R., & Barreiro, M. F. (2018). Functionalization of yogurts with *Agaricus bisporus* extracts encapsulated in spray-dried maltodextrin crosslinked with citric acid. *Food Chemistry*, 245, 845–853.

Francisco, V., Costa, G., Figueirinha, A., Marques, C., Pereira, P., Miguel Neves, B., Lopes, M. C., García-Rodríguez, M., Cruz, M. T., & Batista, M. T (2013). Anti-inflammatory activity of *Cymbopogon citratus* leaves infusion via proteasome and nuclear factor-kB pathway inhibition: Contribution of chlorogenic acid. *Journal of Ethnopharmacology*, 148(1), 126–134.

Freedman, B. M. (2009). Topical antioxidant application enhances the effects of facial microdermabrasion. *Journal of Dermatological Treatment*, 20(2), 82–87.

Freeman, B. L., Eggett, D. L., & Parker, T. L. (2010). Synergistic and antagonistic interactions of phenolic compounds found in navel oranges. *Journal of Food Science*, 75(6), 570–576.

Gangan, V. D., Jazly, L., Chakraborty, C. T., Bhatia, D. S., Dubey, R. S., Sankhe, S. S., Pujari, J. S., Satpute, M. S., & Shastri, I. (2014). Synthesis and Antibacterial Activity of Novel Caffeic Acid Hybrid Derivatives. *International Journal of Chemical and Pharmaceutical Analysis*, 2(1), 28–34.

Gao, H., & Gu, W. Y. (2007). Optimization of polysaccharide and ergosterol production from *Agaricus brasiliensis* by fermentation process. *Biochemical Engineering Journal*, 33(3), 202–210.

Gao, X. H., Zhang, L., Wei, H., & Chen, H. D. (2008). Efficacy and safety of innovative cosmeceuticals. *Clinics in Dermatology*, 26(4), 367–374.

Gao, Y., Zhang, R., Zhang, J., Gao, S., Gao, W., Zhang, H., Wang, H., & Han, B. (2011). Study of the extraction process and *in vivo* inhibitory effect of *Ganoderma* triterpenes in oral mucosa cancer. *Molecules*, 16(7), 5315–5332.

Garcia-Salas, P., Morales-Soto, A., Segura-Carretero, A., & Fernández-Gutiérrez, A. (2010). Phenolic-compound-extraction systems for fruit and vegetable samples. *Molecules*, 15(12), 8813–8826.

Gąsecka, M., Magdziak, Z., Siwulski, M., & Mleczek, M. (2017). Profile of phenolic and organic acids, antioxidant properties and ergosterol content in cultivated and wild growing species of *Agaricus*. *European Food Research and Technology*, 244(2), 1–10.

Gebhardt, P., Dornberger, K., Gollmick, F. A., Gräfe, U., Härtl, A., Görls, H., Schlegel, B., & Hertweck, C. (2007). Quercinol, an anti-inflammatory chromene from the wood-rotting fungus *Daedalea quercina* (Oak Mazegill). *Bioorganic and Medicinal Chemistry Letters*, 17(9), 2558–2560.

Geethangili, M., & Tzeng, Y.-M. (2011). Review of Pharmacological Effects of *Antrodia camphorata* and Its Bioactive Compounds. *Evidence-Based Complementary and Alternative Medicine*, 212641, 1–17.

Geng, Y., Zhu, S., Cheng, P., Lu, Z. M., Xu, H. Y., Shi, J. S., & Xu, Z. H. (2017). Bioassay-guided fractionation of ethyl acetate extract from *Armillaria mellea* attenuates inflammatory response in lipopolysaccharide (LPS) stimulated BV-2 microglia. *Phytomedicine*, 26, 55–61.

Gerber, G. S. F. W., Fox, L. T., Gerber, M., du Preez, J. L., van Zyl, S., Boneschans, B., & Jeanetta du, P. (2015). Stability, clinical efficacy, and antioxidant properties of Honeybush extracts in semi-solid formulations. *Pharmacognosy Magazine*, 11(44), 337–351.

Gerstel, D., Jacques-Jamin, C., Schepky, A., Cubberley, R., Eilstein, J., Grégoire, S., Hewitt, N., Klaric, M., Rothe, H., & Duplan, H. (2016). Comparison of protocols for measuring cosmetic ingredient distribution in human and pig skin. *Toxicology in Vitro*, 34, 153–160.

Ghafoor, K., AL-Juhaimi, F. Y., & Choi, Y. H. (2012). Supercritical Fluid Extraction of Phenolic Compounds and Antioxidants from Grape (*Vitis labrusca* B.) Seeds. *Plant Foods for Human Nutrition*, 67(4), 407–414.

Gil-Ramírez, A., Aldars-García, L., Palanisamy, M., Jiverdeanu, R. M., Ruiz-Rodríguez, A., Marín, F. R., Reglero, G., & Soler-Rivas, C. (2013). Sterol enriched fractions obtained from Agaricus bisporus fruiting bodies and by-products by compressed fluid technologies (PLE and SFE). *Innovative Food Science and Emerging Technologies*, 18, 101–107.

Govindan, S., Johnson, E. E. R., Christopher, J., Shanmugam, J., Thirumalairaj, V., & Gopalan, J. (2016). Antioxidant and anti-aging activities of polysaccharides from *Calocybe indica* var. APK2. *Experimental and Toxicologic Pathology*, 68(6), 329–334.

Green, B. A., Yu, R. J., & Van Scott, E. J. (2009). Clinical and cosmeceutical uses of hydroxyacids. *Clinics in Dermatology*, 27(5), 495–501.

Grosser, T., Fries, S., & FitzGerald, G. A. (2006). Biological basis for the cardiovascular consequences of COX-2 inhibition: therapeutic challenges and opportunities. *Journal of Clinical Investigation*, 116(1), 4–15.

Guan, W., Zhang, J., Yan, R., Shao, S., Zhou, T., Lei, J., & Wang, Z. (2016). Effects of UV-C treatment and cold storage on ergosterol and Vitamin D2 contents in different parts of white and brown mushroom (*Agaricus bisporus*). *Food Chemistry*, 210, 129–134.

Guerra-Tapia, A., & Gonzalez-Guerra, E. (2014). Hair cosmetics: Dyes. *Actas Dermo-Sifiliograficas*, 105(9), 833–839.

Guerra Dore, C. M. P., Azevedo, T. C. G., de Souza, M. C. R., Rego, L. A., de Dantas, J. C. M., Silva, F. R. F., Rocha, H. A. O., Baseia, I. G., & Leite, E. L. (2007). Anti-inflammatory, antioxidant and cytotoxic actions of β-glucan-rich extract from *Geastrum saccatum* mushroom. *International Immunopharmacology*, 7(9), 1160–1169.

Gunawardena, D., Bennett, L., Shanmugam, K., King, K., Williams, R., Zabaras, D., Head, R., Ooi, L., Gyengesi, E., Münch, G. (2014). Anti-inflammatory effects of five commercially available mushroom species determined in lipopolysaccharide and interferon-γ activated murine macrophages. *Food Chemistry*, 148, 92–96.

Guo, X.-Y., Han, J., Ye, M., Ma, X.-C., Shen, X., Xue, B.-B., & Che, Q.-M. (2012). Identification of major compounds in rat bile after oral administration of total triterpenoids of *Ganoderma lucidum* by high-performance liquid chromatography with electrospray ionization tandem mass spectrometry. *Journal of Pharmaceutical and Biomedical Analysis*, 63, 29–39.

Guzman, J. D., Mortazavi, P. N., Munshi, T., Evangelopoulos, D., McHugh, T. D., Gibbons, S., Malkinson, J., Bhakta, S. (2014). 2-Hydroxy-substituted cinnamic acids and acetanilides are selective growth inhibitors of *Mycobacterium tuberculosis*. MedChemComm, 5(1), 47–50.

Habtemariam, S. (2013). Targeting the production of monocytes/macrophages-derived cytokines by anti-inflammatory herbal drugs. *Phytopharmacology*, 4(1), 131–148.

Hadda, M., Djamel, C., & Akila, O. (2015). Production and Qualitative Analysis of Triterpenoids and Steroids of *Ganoderma* Species Harvested from Cork Oak Forest of North-Eastern Algeria. *Research Journal of Microbiology*, 10(8), 366–376.

Haining, Z., & Yongkun, M. (2017). Optimisation of High Hydrostatic Pressure Assisted Extraction of Anthocyanins from Rabbiteye Blueberry Pomace. *Czech Journal of Food Sciences*, 35(2), 180–187.

Hämäläinen, M., Nieminen, R., Vuorela, P., Heinonen, M., & Moilanen, E. (2007). Anti-inflammatory effects of flavonoids: Genistein, kaempferol, quercetin, and daidzein inhibit STAT-1 and NF-κB activations, whereas flavone, isorhamnetin, naringenin, and pelargonidin inhibit only NF-κB activation along with their inhibitory effect on i. *Mediators of Inflammation*, 45673, 1–10.

Han, C., & Cui, B. (2012). Pharmacological and pharmacokinetic studies with agaricoglycerides, extracted from *Grifola frondosa*, in animal models of pain and inflammation. *Inflammation*, 35(4), 1269–1275.

Han, E. S., Oh, J. Y., & Park, H. J. (2011). *Cordyceps militaris* extract suppresses dextran sodium sulfate-induced acute colitis in mice and production of inflammatory mediators from macrophages and mast cells. *Journal of Ethnopharmacology*, 134(3), 703–710.

Han, J., Chen, Y., Bao, L., Yang, X., Liu, D., Li, S., Zhao, F., & Liu, H. (2013). Anti-inflammatory and cytotoxic cyathane diterpenoids from the medicinal fungus *Cyathus africanus*. *Fitoterapia*, 84(1), 22–31.

Han, R. M., Li, D. D., Chen, C. H., Liang, R., Tian, Y. X., Zhang, J. P., & Skibsted, L. H. (2011). Phenol acidity and ease of oxidation in isoflavonoid/β-carotene antioxidant synergism. *Journal of Agricultural and Food Chemistry*, 59(18), 10367–10372.

Hapsari, R., Elya, B., & Amin, J. (2012). Formulation and evaluation of antioxidant and tyrosinase inhibitory effect from gel containing the 70% ethanolic *Pleurotus ostreatus* extract. *International Journal of Medicinal and Aromatic Plants*, 2(1), 135–140.

Haq, A., Goodyear, B., Ameen, D., Joshi, V., & Michniak-Kohn, B. (2018). Strat-M® synthetic membrane: Permeability comparison to human cadaver skin. International Journal of Pharmaceutics, 547, 432–437.

Haruta-Ono, Y., Setoguchi, S., Ueno, H. M., Higurashi, S., Ueda, N., Kato, K., Saito, T., Matsunaga, K., & Takata, J. (2012). Orally administered sphingomyelin in bovine milk is incorporated into skin sphingolipids and is involved in the water-holding capacity of hairless mice. *Journal of Dermatological Science*, 68(1), 56–62.

Harwansh, R. K., Mukherjee, P. K., Bahadur, S., & Biswas, R. (2015). Enhanced permeability of ferulic acid loaded nanoemulsion based gel through skin against UVA mediated oxidative stress. *Life Sciences*, 141, 202–211.

Hasnat, M. A., Pervin, M., Cha, K. M., Kim, S. K., & Lim, B. O. (2015). Anti-inflammatory activity on mice of extract of Ganoderma lucidum grown on rice via modulation of MAPK and NF-KB pathways. *Phytochemistry*, 114, 125–136.

He, W. Sen, Yin, J., Xu, H. S., Qian, Q. Y., Jia, C. S., Ma, H. Le, & Feng, B. (2014). Efficient synthesis and characterization of ergosterol laurate in a solvent-free system. *Journal of Agricultural and Food Chemistry*, 62(48), 11748–11755.

Hearst, R., Nelson, D., McCollum, G., Millar, B. C., Maeda, Y., Goldsmith, C. E., Rooney, P.J., Anne Loughrey, A., Rao, J. R., & Moore, J. E. (2009). An examination of antibacterial and antifungal properties of constituents of Shiitake (*Lentinula edodes*) and Oyster (*Pleurotus ostreatus*) mushrooms. *Complementary Therapies in Clinical Practice*, 15(1), 5–7.

Heffernan, A. L., Baduel, C., Toms, L. M. L., Calafat, A. M., Ye, X., Hobson, P., Broomhall, S., Mueller, J. F. (2015). Use of pooled samples to assess human exposure to parabens, benzophenone-3 and triclosan in Queensland, Australia. *Environment International*, 85, 77–83.

Heleno, S. A., Rudke, A. R., Calhelha, R. C., Carocho, M., Barros, L., Gonçalves, O. H., Barreiro, M. F., & Ferreira, I. C. F. R. (2017). Development of dairy beverages functionalized with pure ergosterol and mycosterol extracts: an alternative to phytosterol-based beverages. *Food & Function*, 8(1), 103–110.

Heleno, S. A., Prieto, M. A., Barros, L., Rodrigues, A. A., Barreiro, M. F., & Ferreira, I. C. F. R. (2016). Optimization of microwave-assisted extraction of ergosterol from *Agaricus bisporus* L. by-products using response surface methodology. *Food and Bioproducts Processing*, 100, 25–35.

Heleno, S. A., Diz, P., Prieto, M. A., Barros, L., Rodrigues, A., Barreiro, M. F., & Ferreira, I. C. F. R. (2016). Optimization of ultrasound-assisted extraction to obtain mycosterols from *Agaricus bisporus* L. by response surface methodology and comparison with conventional Soxhlet extraction. *Food Chemistry*, 197, 1054–1063.

Heleno, S. A., Ferreira, R. C., Antonio, A. L., Queiroz, M.-J. R. P., Barros, L., & Ferreira, I. C. F. R. (2015). Nutritional value, bioactive compounds and antioxidant properties of three edible mushrooms from Poland. *Food Bioscience*, 11, 48–55.

Heleno, S. A., Martins, A., Queiroz, M. J. R. P., & Ferreira, I. C. F. R. (2015). Bioactivity of phenolic acids: Metabolites versus parent compounds: A review. *Food Chemistry*, 173, 501–513.

Heleno, S. A., Ferreira, I. C. F. R., Calhelha, R. C., Esteves, A. P., Martins, A., & Queiroz, M. J. R. P. (2014). Cytotoxicity of *Coprinopsis atramentaria* extract, organic acids and their synthesized methylated and glucuronate derivatives. *Food Research International*, 55, 170–175.

Heleno, S. A., Ferreira, I. C. F. R., Esteves, A. P., Ćirić, A., Glamočlija, J., Martins, A., Sokovic, M., Queiroz, M. J. R. P. (2013). Antimicrobial and demelanizing activity of

Ganoderma lucidum extract, *p*-hydroxybenzoic and cinnamic acids and their synthetic acetylated glucuronide methyl esters. *Food and Chemical Toxicology*, 58, 95–100.

Heleno, S. A., Barros, L., Martins, A., Queiroz, M. J. R. P., Santos-Buelga, C., & Ferreira, I. C. F. R. (2012). Fruiting body, spores and *in vitro* produced mycelium of *Ganoderma lucidum* from Northeast Portugal: A comparative study of the antioxidant potential of phenolic and polysaccharidic extracts. *Food Research International*, 46(1), 135–140.

Hennicke, F., Cheikh-Ali, Z., Liebisch, T., Maclá-Vicente, J. G., Bode, H. B., & Piepenbring, M. (2016). Distinguishing commercially grown *Ganoderma lucidum* from Ganoderma lingzhi from Europe and East Asia on the basis of morphology, molecular phylogeny, and triterpenic acid profiles. *Phytochemistry*, 127, 29–37.

Hirobe, T. (2014). Keratinocytes regulate the function of melanocytes. *Dermatologica Sinica*, 32(4), 200–204.

Ho, C. Y., Lau, C. B. S., Kim, C. F., Leung, K. N., Fung, K. P., Tse, T. F., Chan, H. H. L., & Chow, M. S. S. (2004). Differential effect of *Coriolus versicolour* (Yunzhi) extract on cytokine production by murine lymphocytes *in vitro*. *International Immunopharmacology*, 4(12), 1549–1557.

Hong, Y.-H., Jung, E. Y., Noh, D. O., & Suh, H. J. (2014). Physiological effects of formulation containing tannase-converted green tea extract on skin care: physical stability, collagenase, elastase, and tyrosinase activities. *Integrative Medicine Research*, 3(1), 25–33.

Hseu, Y. C., Huang, H. C., & Hsiang, C. Y. (2010). Antrodia camphorata suppresses lipopolysaccharide-induced nuclear factor-κB activation in transgenic mice evaluated by bioluminescence imaging. *Food and Chemical Toxicology*, 48(8–9), 2319–2325.

Hseu, Y. C., Wu, F. Y., Wu, J. J., Chen, J. Y., Chang, W. H., Lu, F. J., Lai, Y.C., & Yang, H. L. (2005). Anti-inflammatory potential of *Antrodia camphorata* through inhibition of iNOS, COX-2 and cytokines via the NF-κB pathway. *International Immunopharmacology*, 5, 1914–1925.

Hsieh, Y. U. H., Chu, F. H., Wang, Y. A. S., Chien, S. C., Chang, S. T., Shaw, J. F., Chen C. Y., Hsiao, W. W., Kuo, Y. H., Wang, S. Y. (2010). Antrocamphin A, an anti-inflammatory principal from the fruiting body of Taiwanofungus camphoratus, and its mechanisms. *Journal of Agricultural and Food Chemistry*, 58(5), 3153–3158.

Hu, S., Zhou, G., & Wang, Y. (2017). Tyrosinase Inhibitory Activity of Total Triterpenes and Poricoic Acid A Isolated from *Poria cocos*. *Chinese Herbal Medicines*, 9(4), 321–327.

Hu, Y. H., Liu, X., Jia, Y. L., Guo, Y. J., Wang, Q., & Chen, Q. X. (2014). Inhibitory kinetics of chlorocinnamic acids on mushroom tyrosinase. *Journal of Bioscience and Bioengineering*, 117(2), 142–146.

Huang, G. J., Huang, S. S., & Deng, J. S. (2012). Anti-inflammatory activities of inotilone from *Phellinus linteus* through the inhibition of MMP-9, NF-κB, and MAPK activation *in vitro* and *in vivo*. *PLoS ONE*, 7(5), 1–12.

Huang, G. J., Huang, S. S., Lin, S. S., Shao, Y. Y., Chen, C. C., Hou, W. C., & Kuo, Y. H. (2010). Analgesic effects and the mechanisms of anti-inflammation of ergostatrien-3β-ol from

Antrodia camphorata submerged whole broth in mice. *Journal of Agricultural and Food Chemistry*, 58(12), 7445–7452.

Huang, H., Hsu, T., Chao, H., Chen, C., Chiu, S., & Chang, T. (2014). Inhibition of melanogenesis in murine melanoma cells by *Agaricus brasiliensis* methanol extract and anti-reactive oxygen species (ROS) activity. *African Journal of Microbiology Research*, 8(6), 519–524.

Hugo, P. C., Gil-Chávez, J., Sotelo-Mundo, R. R., Namiesnik, J., Gorinstein, S., & González-Aguilar, G. A. (2012). Antioxidant interactions between major phenolic compounds found in "Ataulfo" mango pulp: Chlorogenic, gallic, protocatechuic and vanillic acids. *Molecules*, 17(11), 12657–12664.

Hui, X., Pin-ru, W., Shen, Z., & Xiang-dong, C. (2010). Chemical analysis of *Hericium erinaceum* polysaccharides and effect of the polysaccharides on derma antioxidant enzymes, MMP-1 and TIMP-1 activities. *International Journal of Biological Macromolecules*, 47(1), 33–36.

Hwang, S. J., Kim, Y.-W., Park, Y., Lee, H.-J., & Kim, K.-W. (2014). Anti-inflammatory effects of chlorogenic acid in lipopolysaccharide-stimulated RAW 264.7 cells. *Inflammation Research*, 63(1), 81–90.

Hyde, K. D., Bahkali, A. H., & Moslem, M. A. (2010). Fungi - An unusual source for cosmetics. *Fungal Diversity*, 43, 1–9.

Ignatova, M. G., Manolova, N. E., Rashkov, I. B., Markova, N. D., Toshkova, R. A., Georgieva, A. K., & Nikolova, E. B. (2016). Poly(3-hydroxybutyrate)/caffeic acid electrospun fibrous materials coated with polyelectrolyte complex and their antibacterial activity and *in vitro* antitumor effect against HeLa cells. *Materials Science and Engineering C*, 65, 379–392.

Imamura, K., Asai, M., Sugamoto, K., Matsumoto, T., Yamasaki, Y., Kamei, I., Hattori, T., Kishimoto, M., Niisaka, S., Kubo, M., Nishiyama, K., & Yamasaki, M. (2015). Suppressing effect of cordycepin on the lipopolysaccharide-induced nitric oxide production in RAW 264.7 cells. *Bioscience, Biotechnology and Biochemistry*, 79(6), 1021–1025.

Jacotet-Navarro, M., Rombaut, N., Deslis, S., Fabiano-Tixier, A.-S., Pierre, F.-X., Bily, A., & Chemat, F. (2016). Towards a "dry" bio-refinery without solvents or added water using microwaves and ultrasound for total valorization of fruit and vegetable by-products. *Green Chemistry*, 18(10), 3106–3115.

Jang, E. J., Shin, Y., Park, H. J., Kim, D., Jung, C., Hong, J. Y., Kim, S., & Lee, S. K. (2017). Anti-melanogenic activity of phytosphingosine via the modulation of the microphthalmia-associated transcription factor signalling pathway. *Journal of Dermatological Science*, 87(1), 19–28.

Jasinghe, V. J., & Perera, C. O. (2006). Ultraviolet irradiation: The generator of Vitamin D2 in edible mushrooms. *Food Chemistry*, 95(4), 638–643.

Jeong, J. W., Jin, C. Y., Kim, G. Y., Lee, J. D., Park, C., Kim, G. D, Kim W. J., Jung, W. K., Seo, S. K., Choi, I. W Choi, Y. H. (2010). Anti-inflammatory effects of cordycepin via suppression of inflammatory mediators in BV2 microglial cells. *International Immunopharmacology*, 10(12), 1580–1586.

Jiménez L., C., Caleja, C., Prieto, M. A., Barreiro, M. F., Barros, L., & Ferreira, I. C. F. R. (2018). Optimization and comparison of heat and ultrasound assisted extraction techniques to obtain anthocyanin compounds from *Arbutus unedo* L. fruits. *Food Chemistry*, 264, 81–91.

Jing, H., Li, J., Zhang, J., Wang, W., Li, S., Ren, Z., Gao, Z., Song, X., Wang, X., & Jia, L. (2018). The antioxidative and anti-aging effects of acidic- and alkalic-extractable mycelium polysaccharides by *Agrocybe aegerita* (Brig.) Sing. *International Journal of Biological Macromolecules*, 106, 1270–1278.

Joana Gil-Chávez, G., Villa, J. A., Fernando Ayala-Zavala, J., Basilio Heredia, J., Sepulveda, D., Yahia, E. M., & González-Aguilar, G. A. (2013). Technologies for Extraction and Production of Bioactive Compounds to be Used as Nutraceuticals and Food Ingredients: An Overview. *Comprehensive Reviews in Food Science and Food Safety*, 12(1), 5–23.

Joo, M., & Sadikot, R. T. (2012). PGD synthase and PGD 2 in immune response. *Mediators of Inflammation*, 503128, 1–6.

Joo, T., Sowndhararajan, K., Hong, S., Lee, J., Park, S. Y., Kim, S., & Jhoo, J. W. (2014). Inhibition of nitric oxide production in LPS-stimulated RAW 264.7 cells by stem bark of *Ulmus pumila* L. *Saudi Journal of Biological Sciences*, 21(5), 427–435.

Jun, H. jin, Lee, J. H., Cho, B. R., Seo, W. D., Kim, D. W., Cho, K. J., & Lee, S. J. (2012). *p*-Coumaric acid inhibition of CREB phosphorylation reduces cellular melanogenesis. *European Food Research and Technology*, 235(6), 1207–1211.

Juráňová, J., Franková, J., & Ulrichová, J. (2017). The role of keratinocytes in inflammation. *Journal of Applied Biomedicine*, 15(3), 169–179.

Kaewnarin, K., Suwannarach, N., Kumla, J., & Lumyong, S. (2016). Phenolic profile of various wild edible mushroom extracts from Thailand and their antioxidant properties, anti-tyrosinase and hyperglycaemic inhibitory activities. *Journal of Functional Foods*, 27, 352–364.

Kamble, P., Sadarani, B., Majumdar, A., & Bhullar, S. (2017). Nanofiber based drug delivery systems for skin: A promising therapeutic approach. *Journal of Drug Delivery Science and Technology*, 41, 124–133.

Kammeyer, A., & Luiten, R. M. (2015). Oxidation events and skin aging. *Ageing Research Reviews*, 21, 16–29.

Kamo, T., Asanoma, M., Shibata, H., & Hirota, M. (2003). Anti-inflammatory lanostane-type triterpene acids from *Piptoporus betulinus*. *Journal of Natural Products*, 66(8), 1104–1106.

Kayashima, T. (2002). Oxalic acid is available as a natural antioxidant in some systems. *Biochimica et Biophysica Acta*, 1573(1), 1–3.

Keller, S., Le, H. Y., Rödiger, C., Hipler, U. C., Kertscher, R., Malarski, A., Hunstock, L.S., Kiehntopf, M., Kaatz, M., Norgauer, J., & Jahreis, G. (2014). Supplementation of a dairy drink enriched with milk phospholipids in patients with atopic dermatitis - A double-blind, placebo-controlled, randomized, cross-over study. *Clinical Nutrition*, 33(6), 1010–1016.

Kerdudo, A., Burger, P., Merck, F., Dingas, A., Rolland, Y., Michel, T., & Fernandez, X. (2016). Development of a natural ingredient – Natural preservative: A case study. *Comptes Rendus Chimie*, 19(9), 1077–1089.

Khatkar, A., Nanda, A., Kumar, P., & Narasimhan, B. (2017). Synthesis, antimicrobial evaluation and QSAR studies of *p*-coumaric acid derivatives. *Arabian Journal of Chemistry*, 10, S3804–S3815.

Kim, B. C., Choi, J. W., Hong, H. Y., Lee, S. A., Hong, S., Park, E. H., Kim, S.J., Lim, C. J. (2006). Heme oxygenase-1 mediates the anti-inflammatory effect of mushroom Phellinus linteus in LPS-stimulated RAW264.7 macrophages. *Journal of Ethnopharmacology*, 106(3), 364–371.

Kim, C. F., Jiang, J. J., Leung, K. N., Fung, K. P., & Lau, C. B. S. (2009). Inhibitory effects of *Agaricus blazei* extracts on human myeloid leukaemia cells. *Journal of Ethnopharmacology*, 122(2), 320–326.

Kim, D. E., Kim, B., Shin, H. S., Kwon, H. J., & Park, E. S. (2014). The protective effect of hispidin against hydrogen peroxide-induced apoptosis in H9c2 cardiomyoblast cells through Akt/GSK-3β and ERK1/2 signalling pathway. *Experimental Cell Research*, 327(2), 264–275.

Kim, J.-W., Kim, H.-I., Kim, J.-H., Kwon, O.-C., Son, E.-S., Lee, C.-S., & Park, Y.-J. (2016). Effects of Ganodermanondiol, a New Melanogenesis Inhibitor from the Medicinal Mushroom *Ganoderma lucidum*. *International Journal of Molecular Sciences*, 17, 1798, 1-12

Kim, K. M., Kwon, Y. G., Chung, H. T., Yun, Y. G., Pae, H. O., Han, J. A., Ha, K.S., Kim, T. W., Kim, Y. M. (2003). Methanol extract of *Cordyceps pruinosa* inhibits *in vitro* and *in vivo* inflammatory mediators by suppressing NF-κB activation. *Toxicology and Applied Pharmacology*, 190(1), 1–8.

Kim, S. H., Song, Y. S., Kim, S. K., Kim, B. C., Lim, C. J., & Park, E. H. (2004). Anti-inflammatory and related pharmacological activities of the *n*-BuOH subfraction of mushroom *Phellinus linteus*. *Journal of Ethnopharmacology*, 93(1), 141–146.

Kim, S. W., Hwang, H. J., Lee, B. C., & Yun, J. W. (2007). Submerged production and characterization of *Grifola frondosa* Polysaccharides- A new application to cosmeceuticals. *Food Technology and Biotechnology*, 45(3), 295–305.

Kim, S. Y., Go, K. C., Song, Y. S., Jeong, Y. S., Kim, E. J., & Kim, B. J. (2014). Extract of the mycelium of *T. matsutak*e inhibits elastase activity and TPA-induced MMP-1 expression in human fibroblasts. *International Journal of Molecular Medicine*, 34(6), 1613–1621.

Kim, Y. J. (2007). Antimelanogenic and Antioxidant Properties of Gallic Acid. *Biological & Pharmaceutical Bulletin*, 30(6), 1052–1055.

Kimura, T., Hashimoto, M., Yamada, M., & Nishikawa, Y. (2013). *Sparassis crispa* (Hanabiratake) Ameliorates Skin Conditions in Rats and Humans. *Bioscience, Biotechnology, and Biochemistry*, 77(9), 1961–1963.

Klančnik, A., Možina, S. S., & Zhang, Q. (2012). Anti-Campylobacter Activities and Resistance Mechanisms of Natural Phenolic Compounds in Campylobacter. *PLoS ONE*, 7(12), 1–10.

Kohno, K., Miyake, M., Sano, O., Tanaka-Kataoka, M., Yamamoto, S., Koya-Miyata, S., Arai, N., Fujii, M., Watanabe, H., Ushio, S., Iwaki, K., & Fukuda, S. (2008). Anti-inflammatory and immunomodulatory properties of 2-amino-3*H*-phenoxazin-3-one. *Biological & Pharmaceutical Bulletin*, 31(10), 1938–1945.

Kornhauser, A., Coelho, S. G., & Hearing, V. J. (2012). Effects of cosmetic formulations containing hydroxyacids on sun-exposed skin: Current applications and future developments. *Dermatology Research and Practice*, 2012(710893), 1–6.

Kot, B., Wicha, J., Piechota, M., Wolska, K., & Grużewska, A. (2015). Antibiofilm activity of trans-cinnamaldehyde, *p*-coumaric, and ferulic acids on uropathogenic Escherichia coli. *Turkish Journal of Medical Sciences*, 45(4), 919–924.

Krupodourova, T. A., Klymenko, P. P., Barshteyn, V. Y., Leonov, Y. I., Shytikov, D. W., & Orlova, T. N. (2015). Effects of *Ganoderma lucidum* (Curtis) P. Karst and *Crinipellis schevczenkovi* Buchalo aqueous extracts on skin wound healing. *Journal of Phytopharmacology*, 4(4), 197–201.

Kubota, K., Shibata, A., & Yamaguchi, T. (2016). The molecular assembly of the ionic liquid/aliphatic carboxylic acid/aliphatic amine as effective and safety transdermal permeation enhancers. *European Journal of Pharmaceutical Sciences*, 86, 75–83.

Kuete, V., Ango, P. Y., Fotso, G. W., Kapche, G. D. W. F., Dzoyem, J. P., Wouking, A. G., Ngadjui, B. T., & Abegaz, B. M. (2011). Antimicrobial activities of the methanol extract, fractions and compounds from *Artocarpus communis* (Moraceae). *BMC Complementary and Alternative Medicine*, 11, 42, 1-5.

Kular, J. K., Basu, S., & Sharma, R. I. (2014). The extracellular matrix: Structure, composition, age-related differences, tools for analysis and applications for tissue engineering. *Journal of Tissue Engineering*, 5, 1–17.

Kumar, K. J. S., Vani, M. G., Wang, S. Y., Liao, J. W., Hsu, L. S., Yang, H. L., & Hseu, Y. C. (2013). *In vitro* and *in vivo* studies disclosed the depigmenting effects of gallic acid: A novel skin lightening agent for hyperpigmentary skin diseases. *BioFactors*, 39(3), 259–270.

Kuo, C. F., Hsieh, C. H., & Lin, W. Y. (2011). Proteomic response of LAP-activated RAW 264.7 macrophages to the anti-inflammatory property of fungal ergosterol. *Food Chemistry*, 126(1), 207–212.

Kwak, J. Y., Park, S., Seok, J. K., Liu, K. H., & Boo, Y. C. (2015). Ascorbyl coumarates as multifunctional cosmeceutical agents that inhibit melanogenesis and enhance collagen synthesis. *Archives of Dermatological Research*, 307(7), 635–643.

Kwon, A. H., Qiu, Z., Hashimoto, M., Yamamoto, K., & Kimura, T. (2009). Effects of medicinal mushroom (*Sparassis crispa*) on wound healing in streptozotocin-induced diabetic rats. *American Journal of Surgery*, 197(4), 503–509.

Lall, N., & Kishore, N. (2014). Are plants used for skin care in South Africa fully explored? *Journal of Ethnopharmacology*, 153, 61–84.

Landi, N., Pacifico, S., Ragucci, S., Iglesias, R., Piccolella, S., Amici, A., Di Giuseppe A. M. A., & Di Maro, A. (2017). Purification, characterization and cytotoxicity assessment of

Ageritin: The first ribotoxin from the basidiomycete mushroom *Agrocybe aegerita*. *Biochimica et Biophysica Acta*, 1861(5), 1113–1121.

Lane, M. E. (2013). Skin penetration enhancers. *International Journal of Pharmaceutics*, 447, 12–21.

Latimer, G.W., Jr. (Ed.) AOAC Official Methods of Analysis of AOAC INTERNATIONAL, 20th ed. *AOAC International*: Rockville, MD, USA, 2016.

Lavi, I., Levinson, D., Peri, I., Nimri, L., Hadar, Y., & Schwartz, B. (2010). Orally administered glucans from the edible mushroom *Pleurotus pulmonarius* reduce acute inflammation in dextran sulfate sodium-induced experimental colitis. *British Journal of Nutrition*, 103(3), 393–402.

Lee, B. C., Bae, J. T., Pyo, H. B., Choe, T. B., Kim, S. W., Hwang, H. J., & Yun, J. W. (2003). Biological activities of the polysaccharides produced from submerged culture of the edible Basidiomycete *Grifola frondosa*. *Enzyme and Microbial Technology*, 32(5), 574–581.

Lee, B. R., Kim, S. Y., Kim, D. W., An, J. J., Song, H. Y., Yoo, K. Y., Kang, T. C., Won, M. H., Lee, K. J. Kim, K. H., Joo, J. H., Ham, H. J., Hur, J. H., Cho, S. W., Han, K. H., Lee, K. S., Park, J. Choi, S.Y., & Eum, W. S. (2009). *Agrocybe chaxingu* polysaccharide prevent inflammation through the inhibition of COX-2 and NO production. *BMB Reports*, 42(12), 794–799.

Lee, C.-L., Huang, C.-H., Wang, H.-C., Chuang, D.-W., Wu, M.-J., Wang, S.-Y., Hwang, T. L., Wu, C. C., Chen, Y. L., Chang, F. R Wu, Y.-C. (2011). First total synthesis of antrocamphin A and its analogs as anti-inflammatory and anti-platelet aggregation agents. *Organic & Biomolecular Chemistry*, 9, 70–73.

Lee, D. G., Kang, H. W., Park, C. G., Ahn, Y. S., & Shin, Y. (2016). Isolation and identification of phytochemicals and biological activities of *Hericium ernaceus* and their contents in *Hericium* strains using HPLC/UV analysis. *Journal of Ethnopharmacology*, 184, 219–225.

Lee, D. S., Woo, J. Y., Ahn, C. B., & Je, J. Y. (2014). Chitosan-hydroxycinnamic acid conjugates: Preparation, antioxidant and antimicrobial activity. *Food Chemistry*, 148, 97–104.

Lee, J. W., Choi, Y. J., Park, J. H., Sim, J. Y., Kwon, Y. S., Lee, H. J., Kim, S.S., Chun, W. (2013). 3,4,5-Trihydroxycinnamic acid inhibits lipopolysaccharide-induced inflammatory response through the activation of Nrf2 pathway in BV2 microglial cells. *Biomolecules and Therapeutics*, 21(1), 60–65.

Lee, M. H., Kang, H., Lee, K., Yang, G., Ham, I., Bu, Y., Kim, H., & Choi, H. Y. (2013). The aerial part of *Taraxacum coreanum* extract has an anti-inflammatory effect on peritoneal macrophages *in vitro* and increases survival in a mouse model of septic shock. *Journal of Ethnopharmacology*, 146(1), 1–8.

Lee, N. K., & Aan, B.-Y. (2016). Optimization of ergosterol to vitamin D2 synthesis in *Agaricus bisporus* powder using ultraviolet-B radiation. *Food Science and Biotechnology*, 25(6), 1627–1631.

Lee, S. M., Lee, Y. R., Cho, K. S., Cho, Y. N., Lee, H. A., Hwang, D. Y., Jung, Y. J., Son, H. J. (2015). Stalked sea squirt (*Styela clava*) tunic waste as a valuable bioresource: Cosmetic and antioxidant activities. *Process Biochemistry*, 50(11), 1977–1984.

Lee, S. S., Tan, N. H., Fung, S. Y., Sim, S. M., Tan, C. S., & Ng, S. T. (2014). Anti-inflammatory effect of the sclerotium of *Lignosus rhinocerotis* (Cooke) Ryvarden, the Tiger Milk mushroom. *BMC Complementary and Alternative Medicine*, 14(359), 1–8.

Lee, Y. G., Lee, W. M., Kim, J. Y., Lee, J. Y., Lee, I. K., Yun, B. S., Rhee, M. H., Cho, J. Y. (2008). Src kinase-targeted anti-inflammatory activity of davallialactone from *Inonotus xeranticus* in lipopolysaccharide-activated RAW264.7 cells. *British Journal of Pharmacology*, 154(4), 852–863.

Lee, Y. H., Lee, N. H., Bhattarai, G., Kim, G. E., Lee, I. K., Yun, B. S., Hwang P. H., & Yi, H. K. (2013). Anti-inflammatory effect of pachymic acid promotes odontoblastic differentiation via HO-1 in dental pulp cells. *Oral Diseases*, 19(2), 193–199.

Leiva, F. J., Saenz-Díez, J. C., Martínez, E., Jiménez, E., & Blanco, J. (2015). Environmental impact of *Agaricus bisporus* cultivation process. *European Journal of Agronomy*, 71, 141–148.

Lembo, S., Balato, A., Caprio, R. Di, Cirillo, T., Giannini, V., Gasparri, F., & Monfrecola, G. (2014). The Modulatory Effect of Ellagic Acid and Rosmarinic Acid on Ultraviolet-B-Induced Cytokine / Chemokine Gene Expression in Skin Keratinocyte (HaCaT) Cells. *BioMed Research International*, 346793, 1–8.

Lemos, M., Borges, A., Teodósio, J., Araújo, P., Mergulhão, F., Melo, L., & Simões, M. (2014). The effects of ferulic and salicylic acids on *Bacillus cereus* and *Pseudomonas fluorescens* single- and dual-species biofilms. *International Biodeterioration and Biodegradation*, 86, 42–51.

Lenochová, P., Vohnoutová, P., Roberts, S. C., Oberzaucher, E., Grammer, K., & Havlíček, J. (2012). Psychology of fragrance use: Perception of individual odour and perfume blends reveals a mechanism for idiosyncratic effects on fragrance choice. *PLoS ONE*, 7(3), 1–10.

Li, H. R., Habasi, M., Xie, L. Z., & Aisa, H. A. (2014). Effect of chlorogenic acid on melanogenesis of B16 melanoma cells. *Molecules*, 19(9), 12940–12948.

Li, M., Zhao, Y., Hao, H., Han, W., & Fu, X. (2017). Theoretical and practical aspects of using fetal fibroblasts for skin regeneration. *Ageing Research Reviews*, 36, 32–41.

Li, P., Deng, Y.-P., Wei, X.-X., & Xu, J.-H. (2013). Triterpenoids from Ganoderma lucidum and their cytotoxic activities. *Natural Product Research*, 27(1), 17–22.

Li, S., Liu, H., Wang, W., Wang, X., Zhang, C., Zhang, J., Jing, H., Ren, Z., Gao, Z., & Jia, L. (2018). Antioxidant and anti-aging effects of acidic-extractable polysaccharides by *Agaricus bisporus*. *International Journal of Biological Macromolecules*, 106, 1297–1306.

Li, S., Liu, M., Zhang, C., Tian, C., Wang, X., Song, X., Jing, H., Gao, Z., Ren, Z., Liu, W., Zhang, J., & Jia, L. (2018). Purification, *in vitro* antioxidant and *in vivo* anti-aging activities of soluble polysaccharides by enzyme-assisted extraction from *Agaricus bisporus*. *International Journal of Biological Macromolecules*, 109, 457–466.

Li, S., & Shah, N. P. (2016). Anti-inflammatory and anti-proliferative activities of natural and sulphonated polysaccharides from *Pleurotus eryngii*. *Journal of Functional Foods*, 23, 80–86.

Li, W., Zhou, W., Lee, D. S., Shim, S. H., Kim, Y. C., & Kim, Y. H. (2014). Hericirine, a novel anti-inflammatory alkaloid from *Hericium erinaceum*. *Tetrahedron Letters*, 55(30), 4086–4090.

Li, Y., Bao, L., Song, B., Han, J., Li, H., Zhao, F., & Liu, H. (2013). A new benzoquinone and a new benzofuran from the edible mushroom *Neolentinus lepideus* and their inhibitory activity in NO production inhibition assay. *Food Chemistry*, 141(3), 1614–1618.

Li, Y., Fabiano-Tixier, A. S., Tomao, V., Cravotto, G., & Chemat, F. (2013). Green ultrasound-assisted extraction of carotenoids based on the bio-refinery concept using sunflower oil as an alternative solvent. *Ultrasonics Sonochemistry*, 20(1), 12–18.

Liao, Y.-R., Kuo, P.-C., Liang, J.-W., Shen, Y.-C., & Wu, T.-S. (2012). An Efficient Total Synthesis of a Potent Anti-Inflammatory Agent, Benzocamphorin F, and Its Anti-Inflammatory Activity. *International Journal of Molecular Sciences*, 13(12), 10432–10440.

Lima, C. U. J. O., Gris, E. F., & Karnikowski, M. G. O. (2016). Antimicrobial properties of the mushroom *Agaricus blazei* – integrative review. *Revista Brasileira de Farmacognosia*, 26(6), 1–7.

Lin, C. J., Lien, H. M., Chang, H. Y., Huang, C. L., Liu, J. J., Chang, Y. C., Chen, C.C., & Lai, C. H. (2014). Biological evaluation of *Phellinus linteus*-fermented broths as anti-inflammatory agents. *Journal of Bioscience and Bioengineering*, 118(1), 88–93.

Lin, M. K., Lee, M. S., Chang, W. Te, Chen, H. Y., Chen, J. F., Li, Y. R., Li, C. C., & Wu, T. S. (2015). Immunosuppressive effect of zhankuic acid C from Taiwanofungus camphoratus on dendritic cell activation and the contact hypersensitivity response. *Bioorganic and Medicinal Chemistry Letters*, 25(20), 4637–4641.

Lin, M. S., Yu, Z. R., & Weng, Y. M. (2012). Study of Continuous Extraction Process Utilizing Supercritical Fluid for *Ganoderma lucidum*. *Advanced Materials Research*, 524–527, 2310–2315.

Lin, Y. S., Chen, S. H., Huang, W. J., Chen, C. H., Chien, M. Y., Lin, S. Y., & Hou, W. C. (2012). Effects of nicotinic acid derivatives on tyrosinase inhibitory and antioxidant activities. *Food Chemistry*, 132(4), 2074–2080.

Lintner, K., Mas-Chamberlin, C., Mondon, P., Peschard, O., & Lamy, L. (2009). Cosmeceuticals and active ingredients. *Clinics in Dermatology*, 27(5), 461–468.

Liu, C., Yang, N., Song, Y., Wang, L., Zi, J., Zhang, S., Dunkin, D., Busse, P., Weir, D., Tversky, J., Miller, R. L., Goldfarb, J., Zhan, J., Li, X. M. (2015). Ganoderic acid C1 isolated from the anti-asthma formula, ASHMITM suppresses TNF-α production by mouse macrophages and peripheral blood mononuclear cells from asthma patients. *International Immunopharmacology*, 27(2), 224–231.

Liu, L.-Y., Chen, H., Liu, C., Wang, H.-Q., Kang, J., Li, Y., & Chen, R.-Y. (2014). Triterpenoids of *Ganoderma theaecolum* and their hepatoprotective activities. *Fitoterapia*, 98, 254–259.

Liu, M., Song, S., Li, H., Jiang, X., Yin, P., Wan, C., Liu, X., Liu, F., Xu, J. (2014). The protective effect of caffeic acid against inflammation injury of primary bovine mammary epithelial cells induced by lipopolysaccharide. *Journal of Dairy Science*, 97(5), 2856–2865.

Liu, S.-R., Ke, B.-R., Zhang, W.-R., Liu, X.-R., & Wu, X.-P. (2017). Breeding of new *Ganoderma lucidum* strains simultaneously rich in polysaccharides and triterpenes by mating basidiospore-derived monokaryons of two commercial cultivars. *Scientia Horticulturae*, 216, 58–65.

Lohani, A., Verma, A., Joshi, H., Yadav, N. & Karki, N. (2014). Nanotechnology-Based Cosmeceuticals. *ISRN Dermatology*, 843687, 1-14.

López-Giral, N., González-Arenzana, L., González-Ferrero, C., López, R., Santamaría, P., López-Alfaro, I., & Garde-Cerdán, T. (2015). Pulsed electric field treatment to improve the phenolic compound extraction from Graciano, Tempranillo and Grenache grape varieties during two vintages. *Innovative Food Science and Emerging Technologies*, 28, 31–39.

López, N., Puértolas, E., Condón, S., Álvarez, I., & Raso, J. (2008). Effects of pulsed electric fields on the extraction of phenolic compounds during the fermentation of must of Tempranillo grapes. *Innovative Food Science and Emerging Technologies*, 9(4), 477–482.

Lorencini, M., Brohem, C. A., Dieamant, G. C., Zanchin, N. I. T., & Maibach, H. I. (2014). Active ingredients against human epidermal aging. *Ageing Research Reviews*, 15(1), 100–115.

Lou, L., Zhou, J., Liu, Y., Wei, Y. I., Zhao, J., & Deng, J. (2016). Chlorogenic acid induces apoptosis to inhibit inflammatory proliferation of IL-6-induced fibroblast-like synoviocytes through modulating the activation of JAK / STAT and NF- κ B signalling pathways. *Experimental and Therapeutic Medicine*, 11, 2054–2060.

Lou, Z., Wang, H., Rao, S., Sun, J., Ma, C., & Li, J. (2012). *p*-Coumaric acid kills bacteria through dual damage mechanisms. *Food Control*, 25(2), 550–554.

Lou, Z., Wang, H., Zhu, S., Ma, C., & Wang, Z. (2011). Antibacterial activity and mechanism of action of chlorogenic acid. *Journal of Food Science*, 76(6).

Lu, M. Y., Chen, C. C., Lee, L. Y., Lin, T. W., & Kuo, C. F. (2015). N6-(2-Hydroxyethyl) adenosine in the Medicinal Mushroom *Cordyceps cicadae* Attenuates Lipopolysaccharide-Stimulated Pro-inflammatory Responses by Suppressing TLR4-Mediated NF-κB Signaling Pathways. *Journal of Natural Products*, 78(10), 2452–2460.

Lu, Y. Y., Ao, Z. H., Lu, Z. M., Xu, H. Y., Zhang, X. M., Dou, W. F., & Xu, Z. H. (2008). Analgesic and anti-inflammatory effects of the dry matter of culture broth of *Termitomyces albuminosus* and its extracts. *Journal of Ethnopharmacology*, 120(3), 432–436.

Luque de Castro, M. D. (2011). Cosmetobolomics as an incipient "-omics" with high analytical involvement. *TrAC - Trends in Analytical Chemistry*, 30(9), 1365–1371.

Ma, L., Chen, H., Dong, P., & Lu, X. (2013). Anti-inflammatory and anticancer activities of extracts and compounds from the mushroom *Inonotus obliquus*. *Food Chemistry*, 139(1–4), 503–508.

Maack, A., & Pegard, A. (2016). *Populus nigra* (Salicaceae) absolute rich in phenolic acids, phenylpropanoïds and flavonoids as a new potent tyrosinase inhibitor. *Fitoterapia*, 111, 95–101.

Malongane, F., McGaw, L. J., & Mudau, F. N. (2017). The synergistic potential of various teas, herbs and therapeutic drugs in health improvement: a review. *Journal of the Science of Food and Agriculture*, 97(14), 4679–4689.

Marques, G. S., Leão, W. F., Lyra, M. A. M., Peixoto, M. S., Monteiro, R. P. M., Rolim, L. A., Xavier, H. S., Neto, P. J. R., & Soares, L. A. L. (2013). Comparative evaluation of UV/VIS and HPLC analytical methodologies applied for quantification of flavonoids from leaves of *Bauhinia forficata*. *Brazilian Journal of Pharmacognosy*, 23(1), 51–57.

Martínez-Pla, J. J., Martín-Biosca, Y., Sagrado, S., Villanueva-Camañas, R. M., & Medina-Hernández, M. J. (2004). Evaluation of the pH effect of formulations on the skin permeability of drugs by biopartitioning micellar chromatography. *Journal of Chromatography A*, 1047(2), 255–262.

Martins, N., Barros, L., Henriques, M., Silva, S., & Ferreira, I. C. F. R. (2015). *In vivo* anti-Candida activity of phenolic extracts and compounds: future perspectives focusing on effective clinical interventions. *BioMed Research International*, 247382, 1–14.

Masaki, H. (2010). Role of antioxidants in the skin: Anti-aging effects. *Journal of Dermatological Science*, 58(2), 85–90.

Maske, P. P., Lokapure, S. G., Nimbalkar, D., Malavi, S., & D'souza, J. I. (2013). *In vitro* determination of sun protection factor and chemical stability of *Rosa kordesii* extract gel. *Journal of Pharmacy Research*, 7(6), 520–524.

Medina-Torres, N., Ayora-Talavera, T., Espinosa-Andrews, H., Sánchez-Contreras, A., & Pacheco, N. (2017). Ultrasound Assisted Extraction for the Recovery of Phenolic Compounds from Vegetable Sources. *Agronomy*, 7(3), 47.

Meek, I. L., van de Laar, M. A. F. J., & Vonkeman, H. E. (2010). Non-steroidal anti-inflammatory drugs: An overview of cardiovascular risks. *Pharmaceuticals*, 3(7), 2146–2162.

Meng, T.-X. (2012). The Melanin Biosynthesis Stimulating Compounds Isolated from the Fruiting Bodies of *Pleurotus Citrinopileatus*. *Journal of Cosmetics, Dermatological Sciences and Applications*, 2(3), 151–157.

Meng, T. X., Furuta, S., Fukamizu, S., Yamamoto, R., Ishikawa, H., Arung, E. T., Shimizu, K., Ohga, S., & Kondo, R. (2011). Evaluation of biological activities of extracts from the fruiting body of *Pleurotus citrinopileatus* for skin cosmetics. *Journal of Wood Science*, 57(5), 452–458.

Meng, X., Liang, H., & Luo, L. (2016). Antitumor polysaccharides from mushrooms: A review on the structural characteristics, antitumor mechanisms and immunomodulating activities. *Carbohydrate Research*, 424, 30–41.

Milhorini, S. da S., Smiderle, F. R., Biscaia, S. M. P., Rosado, F. R., Trindade, E. S., & Iacomini, M. (2018). Fucogalactan from the giant mushroom *Macrocybe titans* inhibits melanoma cells migration. *Carbohydrate Polymers*, 190, 50–56.

Miyake, M., Yamamoto, S., Sano, O., Fujii, M., Kohno, K., Ushio, S., Iwaki, K., & Fukuda, S. (2010). Inhibitory Effects of 2-Amino-3 *H* -phenoxazin-3-one on the Melanogenesis of Murine B16 Melanoma Cell Line. *Bioscience, Biotechnology, and Biochemistry*, 74(4), 753–758.

Mizuno, M., Nishitani, Y., Hashimoto, T., & Kanazawa, K. (2009). Different suppressive effects of fucoidan and lentinan on IL-8 mRNA expression in *in vitro* gut inflammation. *Bioscience, Biotechnology, and Biochemistry*, 73(10), 2324–2325.

Moghimipour, E. (2012). Hydroxy acids, the most widely used anti-aging agents. *Jundishapur Journal of Natural Pharmaceutical Products*, 7(1), 9–10.

Money, N. P. (2016). Are mushrooms medicinal? *Fungal Biology*, 120(4), 449–453.

Montesano, D., Fallarino, F., Cossignani, L., Bosi, A., Simonetti, M. S., Puccetti, P., & Damiani, P. (2008). Innovative extraction procedure for obtaining high pure lycopene from tomato. *European Food Research and Technology*, 226(3), 327–335.

Monti, D., Tampucci, S., Chetoni, P., Burgalassi, S., Saino, V., Centini, M., Staltari, L., & Anselmi, C. (2011). Permeation and distribution of ferulic acid and its α-cyclodextrin complex from different formulations in hairless rat skin. *AAPS PharmSciTech*, 12(2), 514–520.

Moraes, A. R. U. and C. A. P. (2018). Development and Stability Evaluation of Liquid Crystal-Based Formulations Containing Glycolic Plant Extracts and Nano-Actives. *Cosmetics*, 5, 1–7.

Moro, C., Palacios, I., Lozano, M., D'Arrigo, M., Guillamón, E., Villares, A., Martínez, M. A., García-Lafuente, A. (2012). Anti-inflammatory activity of methanolic extracts from edible mushrooms in LPS activated RAW 264.7 macrophages. *Food Chemistry*, 130(2), 350–355.

Mota, A. H., Rijo, P., Molpeceres, J., & Reis, C. P. (2017). Broad overview of engineering of functional nanosystems for skin delivery. *International Journal of Pharmaceutics*, 532(2), 710–728.

Mujica Ascencio, S., Choe, C. S., Meinke, M. C., Müller, R. H., Maksimov, G. V., Wigger-Alberti, W., Lademann, J., & Darvin, M. E. (2016). Confocal Raman microscopy and multivariate statistical analysis for determination of different penetration abilities of caffeine and propylene glycol applied simultaneously in a mixture on porcine skin *ex vivo*. *European Journal of Pharmaceutics and Biopharmaceutics*, 104, 51–58.

Nagasaka, R., Chotimarkorn, C., Shafiqul, I. M., Hori, M., Ozaki, H., & Ushio, H. (2007). Anti-inflammatory effects of hydroxycinnamic acid derivatives. *Biochemical and Biophysical Research Communications*, 358(2), 615–619.

Nascimento, M. S., Magalhães, J. E. M., Pinheiro, T. S., da Silva, T. A., Coutinho, L. G., Baseia, I. G., Lima, L. F. A., & Leite, E. L. (2011). Polysaccharides from the fungus Scleroderma nitidum with anti-inflammatory potential modulate cytokine levels and the expression of nuclear factor KB. *Brazilian Journal of Pharmacognosy*, 22(1), 60–68.

Nazaré, A. C., De Faria, C. M. Q. G., Chiari, B. G., Petrônio, M. S., Regasini, L. O., Silva, D. H. S., Corrêa, M. A., Isaac, V. L. B. da Fonseca, L. M., & Ximenes, V. F. (2014). Ethyl ferulate, a component with anti-inflammatory properties for emulsion-based creams. *Molecules*, 19(6), 8124–8139.

Nesy, E. A., & Mathew, L. (2014). Studies on Antimicrobial and Antioxidant Efficacy of *Thevetia neriifolia* Juss Leaf Extracts against Human Skin Pathogens. *International Journal of Pharmacy and Pharmaceutical Sciences and Drug Research*, 6(2), 164–168.

Newburger, A. E. (2009). Cosmeceuticals: myths and misconceptions. *Clinics in Dermatology*, 27(5), 446–452.

Nikmaram, N., Leong, S. Y., Koubaa, M., Zhu, Z., Barba, F. J., Greiner, R., Oey, I., & Roohinejad, S. (2017). Effect of extrusion on the anti-nutritional factors of food products: An overview. *Food Control*, 79, 62–73.

Nili Ruimi, Haithem Rwashdeh, Solomon Wasser, Badireenath Konkimalla, Thomas Efferth, Monica Borgatti, Roberto Gambari, J. M. (2010). *Daedalea gibbosa* substances inhibit LPS-induced expression of iNOS by suppression of NF-κB and MAPK activities in RAW 264.7 macrophage cells. *International Journal of Molecular Medicine*, 25(4), 421–432.

Noreen, Y., Ringbom, T., Perera, P., Danielson, H., & Bohlin, L. (1998). Development of a Radiochemical Cyclooxygenase-1 and -2 *in Vitro* Assay for Identification of Natural Products as Inhibitors of Prostaglandin Biosynthesis. *Journal of Natural Products*, 61, 2–7.

Norman, G. A. Van. (2016). Drugs, Devices, and the FDA: Part 1: An Overview of Approval Processes for Drugs. *JACC: Basic to Translational Science*, 1(3), 170–179.

Nowak, J. Z. (2012). Non-steroidal anti-inflammatory drugs (NSAIDs) in ophthalmology: pharmacological and clinical characteristics. *Military Pharmacy and Medicine*, 4, 33–50.

Nuhu, A., Ki, N. Y., & Tae, S. L. (2011). Evaluation of the antioxidant and anti-tyrosinase activities of three extracts from *Pleurotus nebrodensis* fruiting bodies. *African Journal of Biotechnology*, 10(15), 2978–2986.

Oliveira, M., Reis, F. S., Sousa, D., Tavares, C., Lima, R. T., Ferreira, I. C. F. R., dos Santos, T., Vasconcelos, M. H. (2014). A methanolic extract of *Ganoderma lucidum* fruiting body inhibits the growth of a gastric cancer cell line and affects cellular autophagy and cell cycle. *Food & Function*, 5, 1389–1394.

Oludemi, T., Barros, L., Prieto, M. A., Heleno, S. A., Barreiro, M. F., & Ferreira, I. C. F. R. (2018). Extraction of triterpenoids and phenolic compounds from Ganoderma lucidum: optimization study using the response surface methodology. *Food & Function*, 9(1), 209-226.

Otte, N., Borelli, C., & Korting, H. C. (2005). Nicotinamide - Biologic actions of an emerging cosmetic ingredient. *International Journal of Cosmetic Science*, 27(5), 255–261.

Ouimet, M. A., Faig, J. J., Yu, W., & Uhrich, K. E. (2015). Ferulic Acid-Based Polymers with Glycol Functionality as a Versatile Platform for Topical Applications. *Biomacromolecules*, 16(9), 2911–2919.

Pan, F., Han, L., Zhang, Y., Yu, Y., & Liu, J. (2015). Optimization of Caco-2 and HT29 co-culture *in vitro* cell models for permeability studies. *International Journal of Food Sciences and Nutrition*, 66(6), 680–685.

Panwar, R., Pemmaraju, S. C., Sharma, A. K., & Pruthi, V. (2016). Efficacy of ferulic acid encapsulated chitosan nanoparticles against *Candida albicans* biofilm. *Microbial Pathogenesis*, 95, 21–31.

Panya, A., Kittipongpittaya, K., Laguerre, M., Bayrasy, C., Lecomte, J., Villeneuve, P., McClements, D. J., & Decker, E. A. (2012). Interactions between α-tocopherol and rosmarinic acid and its alkyl esters in emulsions: Synergistic, additive, or antagonistic effect? *Journal of Agricultural and Food Chemistry*, 60(41), 10320–10330.

Park, K. M., Kwon, K. M., & Lee, S. H. (2015). Evaluation of the Antioxidant Activities and Tyrosinase Inhibitory Property from Mycelium Culture Extracts. *Evidence-Based Complementary and Alternative Medicine*, 616298, 1–7.

Park, S. Y., Jin, M. L., Kim, Y. H., Kim, Y., & Lee, S. J. (2011). Aromatic-turmerone inhibits α-MSH and IBMX-induced melanogenesis by inactivating CREB and MITF signaling pathways. *Archives of Dermatological Research*, 303(10), 737–744.

Parkar, S. G., Stevenson, D. E., & Skinner, M. A. (2008). The potential influence of fruit polyphenols on colonic microflora and human gut health. *International Journal of Food Microbiology*, 124(3), 295–298.

Patel, S., & Goyal, A. (2012). Recent developments in mushrooms as anti-cancer therapeutics: a review. *3 Biotech*, 2, 1–15.

Pauwels, M., Dejaegher, B., Heyden, Y. Vander, and Rogiers, V. (2009). Critical analysis of the SCCNFP / SCCP safety assessment of cosmetic ingredients (2000 – 2006). *Food and Chemical Toxicology*, 47, 898–905.

Pecić, S., Nikićević, N., Veljović, M., Jardanin, M., Tešević, V., Belović, M., & Nikšić, M. (2015). The influence of extraction parameters on physico-chemical properties of special grain brandies with *Ganoderma lucidum*. *Chemical Industry and Chemical Engineering Quarterly*, 22(2), 1–22.

Pei, K., Ou, J., Huang, J., & Ou, S. (2016). *p*-Coumaric acid and its conjugates: dietary sources, pharmacokinetic properties and biological activities. *Journal of the Science of Food and Agriculture*, 96(9), 2952–2962.

Pereira, D. M., Valentão, P., Pereira, J. A., & Andrade, P. B. (2009). Phenolics: From chemistry to biology. *Molecules*, 14(6), 2202–2211.

Phan, M. A. T., Paterson, J., Bucknall, M., & Arcot, J. (2018). Interactions between phytochemicals from fruits and vegetables: Effects on bioactivities and bioavailability. *Critical Reviews in Food Science and Nutrition*, 58(8), 1310–1329.

Pinela, J., Prieto, M. A., Antonio, A. L., Carvalho, A. M., Oliveira, M. B. P. P., Barros, L., & Ferreira, I. C. F. R. (2017). Ellagitannin-rich bioactive extracts of *Tuberaria lignosa*: insights into the radiation-induced effects in the recovery of high added-value compounds. *Food & Function*, 8, 2485–2499.

Pinela, J., Prieto, M. A., Barreiro, M. F., Carvalho, A. M., Oliveira, M. B. P. P., Curran, T. P., & Ferreira, I. C. F. R. (2017). Valorisation of tomato wastes for development of nutrient-rich

antioxidant ingredients: A sustainable approach towards the needs of the today's society. *Innovative Food Science & Emerging Technologies*, 41, 160–171.

Pinela, J., Prieto, M. A. A., Carvalho, A. M., Barreiro, M. F., Oliveira, M. B. P., Barros, L., & Ferreira, I. C. F. R. (2016). Microwave-assisted extraction of phenolic acids and flavonoids and production of antioxidant ingredients from tomato: A nutraceutical-oriented optimization study. *Separation and Purification Technology*, 164, 114–124.

Pinela, J., Prieto, M. A., Barreiro, M. F., Carvalho, A. M., Oliveira, M. B. P. P., Vázquez, J. A., & Ferreira, I. C. F. R. (2016). Optimization of microwave-assisted extraction of hydrophilic and lipophilic antioxidants from a surplus tomato crop by response surface methodology. *Food and Bioproducts Processing*, 98, 283–298.

Pinelo, M., Manzocco, L., Nuñez, M. J., & Nicoli, M. C. (2004). Interaction among Phenols in Food Fortification: Negative Synergism on Antioxidant Capacity. *Journal of Agricultural and Food Chemistry*, 52(5), 1177–1180.

Pitz, H. D. S., Pereira, A., Blasius, M. B., Voytena, A. P. L., Affonso, R. C. L., Fanan, S., Trevisan, A. C. D., Ribeiro-do-Valle, R. M., & Maraschin, M. (2016). *In Vitro* Evaluation of the Antioxidant Activity and Wound Healing Properties of Jaboticaba (*Plinia peruviana*) Fruit Peel Hydroalcoholic Extract. *Oxidative Medicine and Cellular Longevity*, 2016.

Pluemsamran, T., Onkoksoong, T., & Panich, U. (2012). Caffeic acid and ferulic acid inhibit UVA-induced matrix metalloproteinase-1 through regulation of antioxidant defense system in keratinocyte HaCaT cells. *Photochemistry and Photobiology*, 88(4), 961–968.

Popova, M., Bankova, V., Butovska, D., Petkov, V., Nikolova-Damyanova, B., Sabatini, A. G., Marcazzan, G. L., & Bogdanov, S. (2004). Validated methods for the quantification of biologically active constituents of poplar-type propolis. *Phytochemical Analysis*, 15(4), 235–340.

Praça, F. S. G., Medina, W. S. G., Eloy, J. O., Petrilli, R., Campos, P. M., Ascenso, A., & Bentley, M. V. L. B. (2018). Evaluation of critical parameters for *in vitro* skin permeation and penetration studies using animal skin models. *European Journal of Pharmaceutical Sciences*, 111, 121–132.

Pragasam, S. J., & Rasool, M. (2013). Dietary component p-coumaric acid suppresses monosodium urate crystal-induced inflammation in rats. *Inflammation Research*, 62(5), 489–498.

Prieto, M. A., Curran, T. P., Gowen, A., & Vázquez, J. A. A. (2015). An efficient methodology for quantification of synergy and antagonism in single electron transfer antioxidant assays. *Food Research International*, 67, 284–298.

Prieto, M. A., Vázquez, J. A., & Murado, M. A. (2015). Crocin bleaching antioxidant assay revisited: Application to microplate to analyse antioxidant and pro-oxidant activities. *Food Chemistry*, 1(167), 299–310.

Qi, Y., Zhao, L., & Sun, H. H. (2012). Development of a rapid and confirmatory method to identify ganoderic acids in *Ganoderma* mushrooms. *Frontiers in Pharmacology*, 3(85), 1–7.

Quang, D. N., Harinantenaina, L., Nishizawa, T., Hashimoto, T., Kohchi, C., Soma, G. I., & Asakawa, Y. (2006). Inhibitory activity of nitric oxide production in RAW 264.7 cells of daldinals A-C from the fungus *Daldinia childiae* and other metabolites isolated from inedible mushrooms. *Journal of Natural Medicines*, 60(4), 303–307.

Quang, D. N., Hashimoto, T., Arakawa, Y., Kohchi, C., Nishizawa, T., Soma, G. I., & Asakawa, Y. (2006). Grifolin derivatives from *Albatrellus caeruleoporus*, new inhibitors of nitric oxide production in RAW 264.7 cells. *Bioorganic and Medicinal Chemistry*, 14(1), 164–168.

Queiroz, L. S., Nascimento, M. S., Cruz, A. K. M., Castro, A. J. G., Moura, M. de F. V., Baseia, I. G., Araújo, R. M., Benevides, N. M. B., Lima, L. F. A., & Leite, E. L. (2010). Glucans from the *Caripia montagnei* mushroom present anti-inflammatory activity. *International Immunopharmacology*, 10(1), 34–42.

Ramli, N. S. (2015). Immigrant Entrepreneurs on the World's Successful Global Brands in the Cosmetic Industry. *Procedia - Social and Behavioural Sciences*, 195, 113–122.

Ramos-e-Silva, M., Celem, L. R., Ramos-e-Silva, S., & Fucci-da-Costa, A. P. (2013). Anti-aging cosmetics: Facts and controversies. *Clinics in Dermatology*, 31(6), 750–758.

Rampersad, S. N. (2012). Multiple applications of alamar blue as an indicator of metabolic function and cellular health in cell viability bioassays. *Sensors*, 12(9), 12347–12360.

Ranic, M., Nikolic, M., Pavlovic, M., Buntic, A., Siler-Marinkovic, S., & Dimitrijevic-Brankovic, S. (2014). Optimization of microwave-assisted extraction of natural antioxidants from spent espresso coffee grounds by response surface methodology. *Journal of Cleaner Production*, 80, 69–79.

Rao, Y. K., Fang, S. H., Wu, W. S., & Tzeng, Y. M. (2010). Constituents isolated from *Cordyceps militaris* suppress enhanced inflammatory mediator's production and human cancer cell proliferation. *Journal of Ethnopharmacology*, 131(2), 363–367.

Rao, Y. K., Fang, S. H., & Tzeng, Y. M. (2007). Evaluation of the anti-inflammatory and anti-proliferation tumoral cells activities of *Antrodia camphorata*, *Cordyceps sinensis*, and *Cinnamomum osmophloeum* bark extracts. *Journal of Ethnopharmacology*, 114(1), 78–85.

Rathore, H., Prasad, S., & Sharma, S. (2017). Mushroom nutraceuticals for improved nutrition and better human health: A review. *PharmaNutrition*, 5(2), 35–46.

Reis, F. S., Martins, A., Vasconcelos, M. H., Morales, P., & Ferreira, I. C. F. R. (2017). Functional foods based on extracts or compounds derived from mushrooms. *Trends in Food Science and Technology*, 66, 48–62.

Reis, F. S., Lima, R. T., Morales, P., Ferreira, I. C. F. R., & Vasconcelos, M. H. (2015). Methanolic extract of *Ganoderma lucidum* induces autophagy of AGS human gastric tumor cells. *Molecules*, 20(10), 17872–17882.

Reis, F. S., Martins, A., Barros, L., & Ferreira, I. C. F. R. (2012). Antioxidant properties and phenolic profile of the most widely appreciated cultivated mushrooms: A comparative study between *in vivo* and *in vitro* samples. *Food and Chemical Toxicology*, 50(5), 1201–1207.

Rezende, Y. R. R. S., Nogueira, J. P., & Narain, N. (2017). Comparison and optimization of conventional and ultrasound assisted extraction for bioactive compounds and antioxidant activity from agro-industrial acerola (*Malpighia emarginata* DC) residue. *LWT - Food Science and Technology*, 85, 158–169.

Rhimi, W., Ben Salem, I., Iatta, R., Chaabane, H., Saidi, M., Boulila, A., & Cafarchia, C. (2018). *Dittrichia viscosa* L. leaves lipid extract: An unexploited source of essential fatty acids and tocopherols with antifungal and anti-inflammatory properties. *Industrial Crops and Products*, 113, 196–201.

Ribeiro, A., Estanqueiro, M., Oliveira, M., & Sousa Lobo, J. (2015). Main Benefits and Applicability of Plant Extracts in Skin Care Products. *Cosmetics*, 2(2), 48–65.

Rodrigues, F., Alves, A. C., Nunes, C., Sarmento, B., Amaral, M. H., Reis, S., & Oliveira, M. B. P. P. (2016). Permeation of topically applied caffeine from a food by-product in cosmetic formulations: Is nanoscale *in vitro* approach an option? *International Journal of Pharmaceutics*, 513, 496–503.

Rodrigues, F., Pereira, C., Pimentel, F. B., Alves, R. C., Ferreira, M., Sarmento, B., Amaral, M. H., & Oliveira, M. B. P. P. (2015). Are coffee silverskin extracts safe for topical use? An *in vitro* and *in vivo* approach. *Industrial Crops and Products*, 63, 167–174.

Rodrigues, F., Pimentel, F. B., & Oliveira, M. B. P. P. (2015). Olive by-products: Challenge application in cosmetic industry. *Industrial Crops and Products*, 70, 116–124.

Rodrigues, F., Palmeira-de-Oliveira, A., das Neves, J., Sarmento, B., Amaral, M. H., & Oliveira, M. B. (2013). *Medicago* spp. extracts as promising ingredients for skin care products. *Industrial Crops and Products*, 49, 634–644.

Roselló-Soto, E., Galanakis, C. M., Brnčić, M., Orlien, V., Trujillo, F. J., Mawson, R., Knoerzer, K., Tiwari, B. K., & Barba, F. J. (2015). Clean recovery of antioxidant compounds from plant foods, by-products and algae assisted by ultrasounds processing. Modelling approaches to optimize processing conditions. *Trends in Food Science & Technology*, 42(2), 134–149.

Royer, M., Prado, M., García-Pérez, M. E., Diouf, P. N., & Stevanovic, T. (2013). Study of nutraceutical, nutricosmetics and cosmeceutical potentials of polyphenolic bark extracts from Canadian forest species. *PharmaNutrition*, 1(4), 158–167.

Ruan, W., Lim, A. H. H., Huang, L. G., & Popovich, D. G. (2014). Extraction optimisation and isolation of triterpenoids from *Ganoderma lucidum* and their effect on human carcinoma cell growth. *Natural Product Research*, 28(24), 2264–2272.

Ruan, Y., Li, H., Pu, L., Shen, T., & Jin, Z. (2018). *Tremella fuciformis* Polysaccharides Attenuate Oxidative Stress and Inflammation in Macrophages through miR-155. *Analytical Cellular Pathology*, 5762371, 1-10.

Ruifeng, G., Yunhe, F., Zhengkai, W., Ershun, Z., Yimeng, L., Minjun, Y., Xiaojing S., Zhengtao, Y., & Naisheng, Z. (2014). Chlorogenic acid attenuates lipopolysaccharide-induced mice mastitis by suppressing TLR4-mediated NF-KB signaling pathway. *European Journal of Pharmacology*, 729(1), 54–58.

Ruiz, P. a, & Haller, D. (2006). Nutritional Immunology Functional Diversity of Flavonoids in the Inhibition of the Proinflammatory Epithelial Cells. *Nutritional Immunology*, 664–671.

Ruksiriwanich, W., Sirithunyalug, J., Boonpisuttinant, K., Jantrawut, P. (2014). Potent *in Vitro* Collagen Biosynthesis Stimulating and Antioxidant Activities. *International Journal of Pharmacy and Pharmaceutical Sciences*, 6(1), 406–412.

Russo, A., Concia, E., Cristini, F., De Rosa, F. G., Esposito, S., Menichetti, F., Petrosillo, N., Tumbarello, M., Venditti, M., Viale, P., Viscoli, C., & Bassetti, M. (2016). Current and future trends in antibiotic therapy of acute bacterial skin and skin-structure infections. *Clinical Microbiology and Infection*, 22, S27–S36.

Ruthes, A. C., Carbonero, E. R., Córdova, M. M., Baggio, C. H., Sassaki, G. L., Gorin, P. A. J., Santos, A. R. S., & Iacomini, M. (2013). Fucomannogalactan and glucan from mushroom *Amanita muscaria*: Structure and inflammatory pain inhibition. *Carbohydrate Polymers*, 98(1), 761–769.

Ruthes, A. C., Rattmann, Y. D., Malquevicz-Paiva, S. M., Carbonero, E. R., Córdova, M. M., Baggio, C. H., Santos, A. R. S., Gorin, P. A. J., & Iacomini, M. (2013). *Agaricus bisporus* fucogalactan: Structural characterization and pharmacological approaches. *Carbohydrate Polymers*, 92(1), 184–191.

Saba, E., Son, Y., Jeon, B. R., Kim, S. E., Lee, I. K., Yun, B. S., & Rhee, M. H. (2015). Acetyl eburicoic acid from *Laetiporus sulphureus* var. miniatus suppresses inflammation in murine macrophage RAW 264.7 cells. *Mycobiology*, 43(2), 131–136.

Sahin, S. C. (2018). The potential of *Arthrospira platensis* extract as a tyrosinase inhibitor for pharmaceutical or cosmetic applications. *South African Journal of Botany*, 119, 236–243.

Saija, A., Tomaino, A., Trombetta, D., De Pasquale, A., Uccella, N., Barbuzzi, T., Paolino, D., & Bonina, F. (2000). *In vitro* and *in vivo* evaluation of caffeic and ferulic acids as topical photoprotective agents. *International Journal of Pharmaceutics*, 199(1), 39–47.

Saija, A., Tomaino, A., Lo Cascio, R., Trombetta, D., Proteggente, A., De Pasquale, A., Uccella, N., & Bonina, F. (1999). Ferulic and caffeic acids as potential protective agents against photooxidative skin damage. *Journal of the Science of Food and Agriculture*, 79(3), 476–480.

Salah, L. A., & Faergemann, J. (2015). A retrospective analysis of skin bacterial colonisation, susceptibility and resistance in atopic dermatitis and impetigo patients. *Acta Dermato-Venereologica*, 95(5), 532–535.

Sams, R. L., Couch, L. H., Miller, B. J., Okerberg, C. V., Warbritton, A., Wamer, W. G., Beer, J. Z., & Howard, P. C. (2001). Basal cell proliferation in female SKH-1 mice treated with α- and β-hydroxy acids. *Toxicology and Applied Pharmacology*, 175(1), 76–82.

Sanjeewa, K. K. A., Kim, E. A., Son, K. T., & Jeon, Y. J. (2016). Bioactive properties and potentials cosmeceutical applications of phlorotannins isolated from brown seaweeds: A review. *Journal of Photochemistry and Photobiology B: Biology*, 162, 100–105.

Santos, A., Barros, L., Calhelha, R. C., Dueñas, M., Carvalho, A. M., Santos-Buelga, C., & Ferreira, I. C. F. R. (2013). Leaves and decoction of *Juglans regia* L.: Different performances

regarding bioactive compounds and *in vitro* antioxidant and antitumor effects. *Industrial Crops and Products*, 51, 430–436.

Santos, S. A. O., Villaverde, J. J., Silva, C. M., Neto, C. P., & Silvestre, A. J. D. (2012). Supercritical fluid extraction of phenolic compounds from *Eucalyptus globulus* Labill bark. *Journal of Supercritical Fluids*, 71, 71–79.

Sasaki, S. H., Linhares, R. E. C., Nozawa, C. M., Montalván, R., & Paccola-Meirelles, L. D. (2001). Strains of *Lentinula edodes* suppress growth of phytopathogenic fungi and inhibit Alagoas serotype of vesicular stomatitis virus. *Brazilian Journal of Microbiology*, 32(1), 52–55.

Sathishkumar, T., Baskar, R., Aravind, M., Tilak, S., Deepthi, S., & Bharathikumar, V. M. (2013). Simultaneous Extraction Optimization and Analysis of Flavonoids from the Flowers of *Tabernaemontana heyneana* by High Performance Liquid Chromatography Coupled to Diode Array Detector and Electron Spray Ionization/Mass Spectrometry. *ISRN Biotechnology*, 2013(450948), 1–10.

Satooka, H., Cerda, P., Kim, H. J., Wood, W. F., & Kubo, I. (2017). Effects of matsutake mushroom scent compounds on tyrosinase and murine B16-F10 melanoma cells. *Biochemical and Biophysical Research Communications*, 487(4), 840–846.

Seo, Y. K., Kim, S. J., Boo, Y. C., Baek, J. H., Lee, S. H., & Koh, J. S. (2011). Effects of *p*-coumaric acid on erythema and pigmentation of human skin exposed to ultraviolet radiation. *Clinical and Experimental Dermatology*, 36(3), 260–266.

Seok, J. K., & Boo, Y. C. (2015). *p*-Coumaric acid attenuates UVB-induced release of stratifin from keratinocytes and indirectly regulates matrix metalloproteinase 1 release from fibroblasts. *Korean Journal of Physiology and Pharmacology*, 19(3), 241–247.

Shahirah, N. N., Zuraina, M. Y. F., Fadilah, R. N., Zaila, C. F. S., Florinsiah, L., Norfazlina, M. N., & Mun, L. L. (2014). Cytotoxicity Effect of *Agaricus blazei*, *Grifola frondosa* and *Hericium erinaceus* Used in Traditional Medicine. *Bentham Open*, 5, 27–30.

Shao, S., Hernandez, M., Kramer, J. K. G., Rinker, D. L., & Tsao, R. (2010). Ergosterol profiles, fatty acid composition, and antioxidant activities of button mushrooms as affected by tissue part and developmental stage. *Journal of Agricultural and Food Chemistry*, 58(22), 11616–11625.

Shapiro, S. S., & Saliou, C. (2001). Role of vitamins in skin care. *Nutrition*, 17(10), 839–844.

Sharma, J. N., Al-Omran, A., & Parvathy, S. S. (2007). Role of nitric oxide in inflammatory diseases. *Inflammopharmacology*, 15(6), 252–259.

Sharma, N., Madan, P., & Lin, S. (2016). Effect of process and formulation variables on the preparation of parenteral paclitaxel-loaded biodegradable polymeric nanoparticles: A co-surfactant study. *Asian Journal of Pharmaceutical Sciences*, 11(3), 404–416.

Sharma, P. (2011). Cosmeceuticals: Regulatory scenario in US, Europe & India. *International Journal of Pharmacy and Technology*, 3(4), 1512–1535.

Shen, J., & Burgess, D. C. (2012). Accelerated *in vitro* release testing methods for extended release parenteral dosage form. *Journal of Pharmacy and Pharmacology*, 64(7), 986–996.

Shen, T., Duan, C., Chen, B., Li, M., Ruan, Y., Xu, D., Shi, D., Yu, D., Li, J., & Wang, C. (2017). *Tremella fuciformis* polysaccharide suppresses hydrogen peroxide-triggered injury of human skin fibroblasts via upregulation of SIRT1. *Molecular Medicine Reports*, 16(2), 1340–1346.

Shimizu, T., Kawai, J., Ouchi, K., Kikuchi, H., Osima, Y., & Hidemi, R. (2016). Agarol, an ergosterol derivative from *Agaricus blazei*, induces caspase-independent apoptosis in human cancer cells. *International Journal of Oncology*, 48(4), 1670–1678.

Šiler, B., Živković, S., Banjanac, T., Cvetković, J., Nestorović Živković, J., Ćirić, A., Soković, M., & Mišić, D. (2014). Centauries as underestimated food additives: Antioxidant and antimicrobial potential. *Food Chemistry*, 147, 367–376.

Silveira, M. L. L., Smiderle, F. R., Agostini, F., Pereira, E. M., Bonatti-Chaves, M., Wisbeck, E., Ruthes, A. C., Sassaki, G. L. Cipriani, T. R., Furlan, S. A. & Iacomini, M. (2015). Exopolysaccharide produced by *Pleurotus sajor-caju*: Its chemical structure and anti-inflammatory activity. *International Journal of Biological Macromolecules*, 75, 90–96.

Silveira, M. L. L., Smiderle, F. R., Moraes, C. P., Borato, D. G., Baggio, C. H., Ruthes, A. C., Sassaki, G. L. Cipriani, T. R., Furlan, S. A. & Iacomini, M. (2014). Structural characterization and anti-inflammatory activity of a linear β-d-glucan isolated from *Pleurotus sajor-caju*. *Carbohydrate Polymers*, 113, 588–596.

Singdevsachan, S. K., Auroshree, P., Mishra, J., Baliyarsingh, B., Tayung, K., & Thatoi, H. (2016). Mushroom polysaccharides as potential prebiotics with their antitumor and immunomodulating properties: A review. *Bioactive Carbohydrates and Dietary Fibre*, 7(1), 1–14.

Skalicka-Woźniak, K., Szypowski, J., Łoś, R., Siwulski, M., Sobieralski, K., Głowniak, K., & Malm, A. (2012). Evaluation of polysaccharides content in fruit bodies and their antimicrobial activity of four *Ganoderma lucidum* strains cultivated on different wood type substrates. *Acta Societatis Botanicorum Poloniae*, 81(1), 17–21.

Slawinska, A., Fornal, E., Radzki, W., Skrzypczak, K., Zalewska-Korona, M., Michalak-Majewska, M., Parfieniuk, E., & Stachniuk, A. (2016). Study on Vitamin D2 stability in dried mushrooms during drying and storage. *Food Chemistry*, 199, 203–209.

Song, K., An, S. M., Kim, M., Koh, J. S., & Boo, Y. C. (2011). Comparison of the antimelanogenic effects of *p*-coumaric acid and its methyl ester and their skin permeabilities. *Journal of Dermatological Science*, 63(1), 17–22.

Spagnol, C. M., Ferreira, G. A., Chiari-Andréo, B. G., Borges Isaac, V. L., Corrêa, M. A., & Nunes Salgado, H. R. (2016). Ascorbic Acid in Cosmetic Formulations: Stability, in vitro release, and permeation using rapid, inexpensive, and simple methods. *Journal of Dispersion Science and Technology*, 38(6), 901-908.

Staniforth, V., Huang, W. C., Aravindaram, K., & Yang, N. S. (2012). Ferulic acid, a phenolic phytochemical, inhibits UVB-induced matrix metalloproteinases in mouse skin via posttranslational mechanisms. *Journal of Nutritional Biochemistry*, 23(5), 443–451.

Stanikunaite, R., Shabana I. Khan, Trappe, J. M., & Ross, S. A. (2009). Cyclooxygenase-2 Inhibitory and Antioxidant Compounds from the Truffle *Elaphomyces granulatus*. *Phytotherapy Research*, 23, 575–578.

Stern, R. (2004). Hyaluronan catabolism: A new metabolic pathway. *European Journal of Cell Biology*, 83(7), 317–325.

Stojković, D., Reis, F. S., Glamočlija, J., Ćirić, A., Barros, L., Van Griensven, L. J. L. D., Ferreira, I. C. F. R., & Soković, M. (2014a). Cultivated strains of *Agaricus bisporus* and *A. brasiliensis*: Chemical characterization and evaluation of antioxidant and antimicrobial properties for the final healthy product-natural preservatives in yoghurt. *Food and Function*, 5(7), 1602–1612.

Stojković, D. S., Barros, L., Calhelha, R. C., Glamočlija, J., Ćirić, A., van Griensven, L. J. L. D., Soković, M., & Ferreira, I. C. F. R. (2014b). A detailed comparative study between chemical and bioactive properties of *Ganoderma lucidum* from different origins. *International Journal of Food Sciences and Nutrition*, 65(1), 42–47.

Su, T. R., Lin, J. J., Tsai, C. C., Huang, T. K., Yang, Z. Y., Wu, M. O., Zheng, Y. Q., Su, C. C., & Wu, Y. J. (2013). Inhibition of melanogenesis by gallic acid: Possible involvement of the PI3K/Akt, MEK/ERK and Wnt/β-catenin signaling pathways in B16F10 cells. *International Journal of Molecular Sciences*, 14(10), 20443–20458.

Sui, Z. F., Yang, R., Liu, B., Gu, T. M., Zhao, Z. L., Shi, D. F., & Chang, D. Q. (2010). Chemical analysis of *Agaricus blazei* polysaccharides and effect of the polysaccharides on IL-1β mRNA expression in skin of burn wound-treated rats. *International Journal of Biological Macromolecules*, 47(2), 155–157.

Surber, C., & Kottner, J. (2017). Skin care products: What do they promise, what do they deliver. *Journal of Tissue Viability*, 26(1), 29–36.

Svobodová, A., Psotová, J., & Walterová, D. (2003). Natural phenolics in the prevention of UV-induced skin damage. A review. *Biomed Papers*, 147(2), 137–145.

Tachaprutinun, A., Meinke, M. C., Richter, H., Pan-In, P., Wanichwecharungruang, S., Knorr, F., Lademann, J., & Patzelt, A. (2014). Comparison of the skin penetration of *Garcinia mangostana* extract in particulate and non-particulate form. *European Journal of Pharmaceutics and Biopharmaceutics*, 86(2), 307–313.

Taieb, M., Gay, C., Sebban, S., & Secnazi, P. (2012). Hyaluronic acid plus mannitol treatment for improved skin hydration and elasticity. *Journal of Cosmetic Dermatology*, 11(2), 87–92.

Tamrakar, S., Nishida, M., Amen, Y., Tran, H. B., Suhara, H., Fukami, K., Parajuli, G. P., Shimizu, K. (2017). Antibacterial activity of Nepalese wild mushrooms against Staphylococcus aureus and *Propionibacterium acnes*. *Journal of Wood Science*, 63(4), 379–387.

Tang, S. C., & Yang, J. H. (2018). Dual effects of alpha-hydroxy acids on the skin. *Molecules*, 23(4), 1–12.

Taofiq, O., Heleno, S. A., Calhelha, R. C., Fernandes, I. P., Alves, M. J., Barros, L., González-Paramás, A. M., & Ferreira, I. C. F. R., & Barreiro, M. F. (2018). Mushroom-based

cosmeceutical ingredients: Microencapsulation and *in vitro* release profile. *Industrial Crops and Products*, 124, 44–52.

Taofiq, O., González-paramás, A. M., Barreiro, M. F., & Ferreira, I. C. F. R. (2017). Hydroxycinnamic Acids and Their Derivatives: Cosmeceutical Significance, Challenges and Future Perspectives, a Review. *Molecules*, 22, 1–24.

Taofiq, O., Heleno, S. A., Calhelha, R. C., Alves, M. J., Barros, L., González-Paramás, A. M., Barreiro, M. F., & Ferreira, I. C. F. R. (2017). The potential of Ganoderma lucidum extracts as bioactive ingredients in topical formulations, beyond its nutritional benefits. *Food and Chemical Toxicology*, 108, 139–147.

Taofiq, O., González-Paramás, A. M., Martins, A., Barreiro, M. F., & Ferreira, I. C. F. R. (2016). Mushrooms extracts and compounds in cosmetics, cosmeceuticals and nutricosmetics-A review. *Industrial Crops and Products*, 90, 38–48.

Taofiq, O., Heleno, S., Calhelha, R., Alves, M., Barros, L., Barreiro, M., González-Paramás, A. M., & Ferreira, I. C. F. R. (2016). Development of Mushroom-Based Cosmeceutical Formulations with Anti-Inflammatory, Anti-Tyrosinase, Antioxidant, and Antibacterial Properties. *Molecules*, 21(10), 1-12.

Taofiq, O., Martins, A., Barreiro, M. F., & Ferreira, I. C. F. R. (2016). Anti-inflammatory potential of mushroom extracts and isolated metabolites. *Trends in Food Science and Technology*, 50, 193–210.

Taofiq, O., Calhelha, R. C., Heleno, S., Barros, L., Martins, A., Santos-Buelga, C., Queiroz, M.J. R. P., & Ferreira, I. C. F. R. (2015). The contribution of phenolic acids to the anti-inflammatory activity of mushrooms: Screening in phenolic extracts, individual parent molecules and synthesized glucuronated and methylated derivatives. *Food Research International*, 76, 821–827.

Teodouro, G. R., Ellepola, K., Seneviratne, C. J., & Koga-Ito, C. Y. (2015). Potential use of phenolic acids as anti-Candida agents: A review. *Frontiers in Microbiology*, 6, 1–11.

Thabit, R. A. S., Cheng, X., Al-hajj, N. Q., Shi, H., Tang, X., & Le, G. (2014). Optimization of Extraction of Triterpense from *Geum japonicum* using Response Surface Methodology. *International Journal of Pharma Research & Review*, 3, 31–40.

Thangboonjit, W., Limsaeng-u-rai, S., & Panich, U. (2014). Comparative evaluation of antityrosinase and antioxidant activities of dietary phenolics and their activities in melanoma cells exposed to UVA. *Siriraj Medical Journal*, 66(1), 5–10.

Theocharis, A. D., Skandalis, S. S., Gialeli, C., & Karamanos, N. K. (2016). Extracellular matrix structure. *Advanced Drug Delivery Reviews*, 97, 4–27.

Thiele, J. J., & Ekanayake-Mudiyanselage, S. (2007). Vitamin E in human skin: Organ-specific physiology and considerations for its use in dermatology. *Molecular Aspects of Medicine*, 28, 646–667.

Thitilertdecha, P., Guy, R. H., & Rowan, M. G. (2014). Characterisation of polyphenolic compounds in *Clerodendrum petasites* S. Moore and their potential for topical delivery through the skin. *Journal of Ethnopharmacology*, 154(2), 400–407.

Tomšik, A., Pavlić, B., Vladić, J., Ramić, M., Brindza, J., & Vidović, S. (2016). Optimization of ultrasound-assisted extraction of bioactive compounds from wild garlic (*Allium ursinum* L.). *Ultrasonics Sonochemistry*, 29, 502–511.

Tse, T. W. (2010). Hydroquinone for skin lightening: Safety profile, duration of use and when should we stop? *Journal of Dermatological Treatment*, 21(5), 272–275.

Tuli, H. S., Sharma, A. K., Sandhu, S. S., & Kashyap, D. (2013). Cordycepin: A bioactive metabolite with therapeutic potential. *Life Sciences*, 93(23), 863–869.

Tung, N. T., Cuong, T. D., Hung, T. M., Lee, J. H., Woo, M. H., Choi, J. S., Kim, J., Ryu, R. H., & Min, B. S. (2013). Inhibitory effect on NO production of triterpenes from the fruiting bodies of Ganoderma lucidum. *Bioorganic and Medicinal Chemistry Letters*, 23(5), 1428–1432.

Uchida, R., Ishikawa, S., & Tomoda, H. (2014). Inhibition of tyrosinase activity and melanine pigmentation by 2-hydroxytyrosol. *Acta Pharmaceutica Sinica B*, 4(2), 141–145.

Uchida, T., Yakumaru, M., Nishioka, K., Higashi, Y., Sano, T., Todo, H., & Sugibayashi, K. (2016). Evaluation of a Silicone Membrane as an Alternative to Human Skin for Determining Skin Permeation Parameters of Chemical Compounds. *Chemical and Pharmaceutical Bulletin*, 64(64), 1338–1346.

Uchida, T., Kadhum, W. R., Kanai, S., Todo, H., Oshizaka, T., & Sugibayashi, K. (2015). Prediction of skin permeation by chemical compounds using the artificial membrane, Strat-MTM. *European Journal of Pharmaceutical Sciences*, 67, 113–118.

Ukawa, Y., Izumi, Y., Ohbuchi, T., Takahashi, T., Ikemizu, S., & Kojima, Y. (2007). Oral administration of the extract from Hatakeshimeji (*Lyophyllum decastes* sing.) mushroom inhibits the development of atopic dermatitis-like skin lesions in NC/Nga mice. *Journal of Nutritional Science and Vitaminology*, 53(3), 293–296.

Ullah, S., Kang, D., Lee, S., Ikram, M., Park, C., Park, Y., Yoon, S., Chun, P., & Moon, H. R. (2019). Synthesis of cinnamic amide derivatives and their anti-melanogenic effect in α-MSH-stimulated B16F10 melanoma cells. *European Journal of Medicinal Chemistry*, 161, 78–92.

Van Nguyen, T., Tung, N. T., Cuong, T. D., Hung, T. M., Kim, J. A., Woo, M. H., Choi J. S., Lee, J. H., & Min, B. S. (2015). Cytotoxic and anti-angiogenic effects of lanostane triterpenoids from *Ganoderma lucidum*. *Phytochemistry Letters*, 12, 69–74.

Vashisth, P., Kumar, N., Sharma, M., & Pruthi, V. (2015). Biomedical applications of ferulic acid encapsulated electrospun nanofibers. *Biotechnology Reports*, 8, 36–44.

Velegraki, T., Hapeshi, E., Fatta-Kassinos, D., & Poulios, I. (2015). Solar-induced heterogeneous photocatalytic degradation of methyl-paraben. *Applied Catalysis B: Environmental*, 178, 2–11.

Vieira da Silva, B., Barreira, J. C. M., & Oliveira, M. B. P. P. (2016). Natural phytochemicals and probiotics as bioactive ingredients for functional foods: Extraction, biochemistry and protected-delivery technologies. *Trends in Food Science and Technology*, 50, 144–158.

Vieira, V., Prieto, M. A., Barros, L., Coutinho, J. A. P., Ferreira, O., & Ferreira, I. C. F. R. (2017). Optimization and comparison of maceration and microwave extraction systems for the production of phenolic compounds from *Juglans regia* L. for the valorization of walnut leaves. *Industrial Crops and Products*, 107, 341–352.

Villares, A., Mateo-Vivaracho, L., & Guillamón, E. (2012). Structural Features and Healthy Properties of Polysaccharides Occurring in Mushrooms. *Agriculture*, 2(4), 452–471.

Vinardell, M. P., and Mitjans, M. (2017). Alternative Methods to Animal Testing for the Safety Evaluation of Cosmetic Ingredients: An Overview. *Cosmetics*, 4, 1–14.

Vincekovi, M., Viskic, M., Juric, S., Giacometti, J., Bursac Kovacevic, D., Putnik, P., Donsì F., Barba, F. J., & Jambrak, A. R. (2017). Innovative technologies for encapsulation of Mediterranean plants extracts. *Trends in Food Science & Technology*, 69, 1–12.

Wang, H. M. D., Chen, C. C., Huynh, P., & Chang, J. S. (2015). Exploring the potential of using algae in cosmetics. *Bioresource Technology*, 184, 355–362.

Wang, J., Luo, T., Li, S., & Zhao, J. (2012). The powerful applications of polyunsaturated fatty acids in improving the therapeutic efficacy of anticancer drugs. *Expert Opinion on Drug Delivery*, 9(1), 1–7.

Wang, L., & Weller, C. L. (2006). Recent advances in extraction of nutraceuticals from plants. *Trends in Food Science & Technology*, 17(6), 300–312.

Wang, S., Meckling, K. A., Marcone, M. F., Kakuda, Y., & Tsao, R. (2011). Synergistic, additive, and antagonistic effects of food mixtures on total antioxidant capacities. *Journal of Agricultural and Food Chemistry*, 59(3), 960–968.

Wangun, H. V. K., Berg, A., Hertel, W., Nkengfack, A. E., & Hertweck, C. (2004). Anti-inflammatory and anti-hyaluronate lyase activities of lanostanoids from *Piptoporus betulinus*. *The Journal of Antibiotics*, 57(11), 755–758.

Wei, L., Zhang, W., Yin, L., Yan, F., Xu, Y., & Chen, F. (2015). Extraction optimization of total triterpenoids from *Jatropha curcas* leaves using response surface methodology and evaluations of their antimicrobial and antioxidant capacities. *Electronic Journal of Biotechnology*, 18(2), 88–95.

Wen, L., Gao, Q., Ma, C. wah, Ge, Y., You, L., Liu, R. H., Fu, X., & Liu, D. (2016). Effect of polysaccharides from *Tremella fuciformis* on UV-induced photoaging. *Journal of Functional Foods*, 20, 400–410.

Wisitrassameewong, K., Karunarathna, S. C., Thongklang, N., Zhao, R., Callac, P., Moukha, S., Ferandon, C., Chukeatirote, E., Hyde, K. D. (2012). *Agaricus subrufescens*: A review. *Saudi Journal of Biological Sciences*, 19(2), 131–146.

Won, S. Y., & Park, E. H. (2005). Anti-inflammatory and related pharmacological activities of cultured mycelia and fruiting bodies of *Cordyceps militaris*. *Journal of Ethnopharmacology*, 96(3), 555–561.

Wong, W. H., Lee, W. X., Ramanan, R. N., Tee, L. H., Kong, K. W., Galanakis, C. M., Sun, J., & Prasad, K. N. (2015). Two level half factorial design for the extraction of phenolics,

flavonoids and antioxidants recovery from palm kernel by-product. *Industrial Crops and Products*, 63, 238–248.

Wu, M. D, Cheng, M. J., Wang, B. C., Yech, Y. J., Lai, J. T., Kuo, Y. H., Yuan, G. F., & Chen, I. S. (2008). Maleimide and maleic anhydride derivatives from the mycelia of *Antrodia cinnamomea* and their nitric oxide inhibitory activities in macrophages. *Journal of Natural Products*, 71(7), 1258–1261.

Wu, M. D, Cheng, M. J., Yech, Y. J., Yuan, G. F., & Chen, J. J. (2013). Inhibitory effects of maleimide derivatives from the mycelia of the fungus *Antrodia cinnamomea* BCRC 36799 on nitric oxide production in lipopolysaccharide (LPS)-activated RAW264.7 macrophages. *Chemistry and Biodiversity*, 10(3), 434–441.

Wu, S.-J., Lu, T.-M., Lai, M.-N., & Ng, L.-T. (2013). Immunomodulatory Activities of Medicinal Mushroom *Grifola frondosa* Extract and Its Bioactive Constituent. *The American Journal of Chinese Medicine*, 41(01), 131–144.

Wu, Y., Choi, M.-H., Li, J., Yang, H., & Shin, H.-J. (2016). Mushroom Cosmetics: The Present and Future. *Cosmetics*, 3(3), 22.

Xie, P. jun, Huang, L. xin, Zhang, C. hong, Ding, S., Deng, Y. jun, & Wang, X. jie. (2018). Skin-care effects of dandelion leaf extract and stem extract: Antioxidant properties, tyrosinase inhibitory and molecular docking simulations. *Industrial Crops and Products*, 111, 238–246.

Xu, X., Yasuda, M., Nakamura-Tsuruta, S., Mizuno, M., & Ashida, H. (2012). β-glucan from *Lentinus edodes* inhibits nitric oxide and tumor necrosis factor-α production and phosphorylation of mitogen-activated protein kinases in lipopolysaccharide-stimulated murine RAW 264.7 macrophages. *Journal of Biological Chemistry*, 287(2), 871–878.

Xu, Z., Yan, S., Bi, K., Han, J., Chen, Y., Wu, Z., & Liu, H. (2013). Isolation and identification of a new anti-inflammatory cyathane diterpenoid from the medicinal fungus *Cyathus hookeri* Berk. *Fitoterapia*, 86(1), 159–162.

Yahaya, E. S., Cordier, W., Steenkamp, P. A., & Steenkamp, V. (2018). Effect of ethnomedicinal extracts used for wound healing on cellular migration and intracellular reactive oxygen species release in SC-1 fibroblasts. *South African Journal of Botany*, 118, 11–17.

Yahaya, Y. A., & Don, M. M. (2012). Evaluation of *Trametes lactinea* extracts on the inhibition of hyaluronidase, lipoxygenase and xanthine oxidase activities *in Vitro*. *Journal of Physical Science*, 23(2), 1–15.

Yamamoto, K. A., Galhardi, L. C. F., Rincão, V. P., Soares, S. de A., Vieira, ícaro G. P., Ricardo, N. M. P. S., Nozawa, C., & Linhares, R. E. C. (2013). Antiherpetic activity of an *Agaricus brasiliensis* polysaccharide, its sulfated derivative and fractions. *International Journal of Biological Macromolecules*, 52(1), 9–13.

Yamamoto, K., & Kimura, T. (2013). Orally and Topically Administered *Sparassis crispa* (Hanabiratake) Improved Healing of Skin Wounds in Mice with Streptozotocin-Induced Diabetes. *Bioscience, Biotechnology, and Biochemistry*, 77(6), 1303–1305.

Yan, Z. F., Yang, Y., Tian, F. H., Mao, X. X., Li, Y., & Li, C. T. (2014). Inhibitory and acceleratory effects of *Inonotus obliquus* on tyrosinase activity and melanin formation in b16 melanoma cells. *Evidence-Based Complementary and Alternative Medicine*, 259836, 1–11.

Yang, M., Wang, X., Guan, S., Xia, J., Sun, J., Guo, H., & Guo, D. an. (2007). Analysis of Triterpenoids in *Ganoderma lucidum* Using Liquid Chromatography Coupled with Electrospray Ionization Mass Spectrometry. *Journal of the American Society for Mass Spectrometry*, 18(5), 927–939.

Yildiz, O., Can, Z., Laghari, A. Q., Şahin, H., & Malkoç, M. (2015). Wild edible mushrooms as a natural source of phenolics and antioxidants. *Journal of Food Biochemistry*, 39(2), 148–154.

Yoon, H. M., Jang, K. J., Han, M. S., Jeong, J. W., Kim, G. Y., Lee, J. H., & Choi, Y. H. (2013). *Ganoderma lucidum* ethanol extract inhibits the inflammatory response by suppressing the NF-κB and toll-like receptor pathways in lipopolysaccharide-stimulated BV2 microglial cells. *Experimental and Therapeutic Medicine*, 5(3), 957–963.

Yoon, K. N., Atom, N., Lee, J. S., Lee, K. R., & Lee, T. S. (2011). Antioxidant and Anti-tyrosinase Activities of Various Extracts from the Fruiting Bodies of *Lentinus lepideus*. *Molecules*, 16(10), 2334–2347.

Yoshikawa, K., Inoue, M., Matsumoto, Y., Sakakibara, C., Miyataka, H., Matsumoto, H., & Arihara, S. (2005). Lanostane Triterpenoids and Triterpene Glycosides from the Fruit Body of *Fomitopsis pinicola* and Their Inhibitory Activity against COX-1 and COX-2. *Journal of Natural Products*, 68(1), 69–73.

Yoshikawa, K., Koso, K., Shimomura, M., Tanaka, M., Yamamoto, H., Imagawa, H., Arihara, S., & Hashimoto, T. (2013). Yellow pigments, fomitellanols A and B, and drimane sesquiterpenoids, cryptoporic acids P and Q, from *Fomitella fraxinea* and their inhibitory activity against COX and 5-LO. *Molecules*, 18(4), 4181–4191.

Yue, L., Cui, H., Li, C., Lin, Y., Sun, Y., Niu, Y., Wen, X., & Liu, J. (2012). A polysaccharide from *Agaricus blazei* attenuates tumor cell adhesion via inhibiting E-selectin expression. *Carbohydrate Polymers*, 88(4), 1326–1333.

Zdařilová, A., Svobodová, A., Šimánek, V., & Ulrichová, J. (2009). *Prunella vulgaris* extract and rosmarinic acid suppress lipopolysaccharide-induced alteration in human gingival fibroblasts. *Toxicology in Vitro*, 23(3), 386–392.

Zhai, F. H., Wang, Q., & Han, J. R. (2015). Nutritional components and antioxidant properties of seven kinds of cereals fermented by the basidiomycete *Agaricus blazei*. *Journal of Cereal Science*, 65, 202–208.

Zhang, H., & Tsao, R. (2016). Dietary polyphenols, oxidative stress and antioxidant and anti-inflammatory effects. *Current Opinion in Food Science*, 8, 33–42.

Zhang, L. W., Al-Suwayeh, S. A., Hsieh, P. W., & Fang, J. Y. (2010). A comparison of skin delivery of ferulic acid and its derivatives: Evaluation of their efficacy and safety. *International Journal of Pharmaceutics*, 399, 44–51.

Zhang, Y., Mills, G. L., & Nair, M. G. (2002). Cyclooxygenase inhibitory and antioxidant compounds from the mycelia of the edible mushroom *Grifola frondosa*. *Journal of Agricultural and Food Chemistry*, 50(26), 7581–7585.

Zhang, Z. S., Wang, X. M., Han, Z. P., Zhao, M. X., & Yin, L. (2012). Purification, antioxidant and moisture-preserving activities of polysaccharides from papaya. *Carbohydrate Polymers*, 87(3), 2332–2337.

Zhao, H., Li, J., Zhang, J., Wang, X., Hao, L., & Jia, L. (2017). Purification, *in vitro* antioxidant and *in vivo* anti-aging activities of exopolysaccharides by *Agrocybe cylindracea*. *International Journal of Biological Macromolecules*, 102, 351–357.

Zhao, X. R., Zhang, B. J., Deng, S., Zhang, H. L., Huang, S. S., Huo, X. K., Wang, C., Liu, F., & Ma, X. C. (2016). Isolation and identification of oxygenated lanostane-type triterpenoids from the fungus *Ganoderma lucidum*. *Phytochemistry Letters*, 16, 87–91.

Zhou, Y., Chen, S., Ding, R., Yao, W., & Gao, X. (2014). Inflammatory modulation effect of Glycopeptide from *Ganoderma capense* (Lloyd) Teng. *Mediators of Inflammation*, 2014(691285), 1–8.

Zhu, Z., He, J., Liu, G., Barba, F. J., Koubaa, M., Ding, L., Bals, O., Grimi, N., & Vorobiev, E. (2016). Recent insights for the green recovery of inulin from plant food materials using non-conventional extraction technologies: A review. *Innovative Food Science and Emerging Technologies*, 33, 1–9.

Zi, Y., Zhang, B., Jiang, B., Yang, X., Liang, Z., Liu, W., He, C., & Liu, L. (2018). Antioxidant action and protective and reparative effects of lentinan on oxidative damage in HaCaT cells. Journal of Cosmetic Dermatology, 17, 1108-1114.

Žilius, M., Ramanauskiene, K., & Briedis, V. (2013). Release of propolis phenolic acids from semisolid formulations and their penetration into the human skin *in vitro*. *Evidence-Based Complementary and Alternative Medicine*, 2013(958717), 1–7.

Resistance profile of Gram- negative bacteria to different antibiotics; MIC values (µg/mL).

	Amoxicillin/ Clavulanic Acid	Ampicillin	Gentamicin	Cefuroxime	Ciprofloxacin	Fosfomycin	Nitrofurantoin	Norfloxacin
Gram negative								
E. coli	>8/4	>16	≤2	≤4	>2	≤16	≤32	>8
	S	R	R	S	R	S	S	R
P. mirabilis	≤ 8/4	≤8	na	≤4	>2	na	>64	na
	S	S		S	R		R	

S- Susceptible; R- Resistant: this classification was made according to the interpretative breakpoints suggested by Clinical and Laboratory Standards Institute (CLSI) and European Committee on Antimicrobial Susceptibility Testing (EUCAST); na- not applicable.

Resistance profile of Gram-positive bacteria and *C. albicans* to different antibiotics; MIC values (µg/mL; mg/mL, respectivelly).

	Ampicilin	Clindamycin	Erythromycin	Gentamicin	Levofloxacin	Linezolide	Oxacilin	Trimethoprim/ sulfamethoxazole	Vancomicin
Gram positive									
MRSA	na	≥ 8	≥ 8	**≥16**	4	2	≥4	≤10	2
		R	R	R	R	S	R	S	S
MSSA	na	<0,25	<0,25	≤1	na	2	<0,25	≤1/19	≤1
		S	S	S		S	S	S	S
E. faecalis	≤1	na	na	na	na	na	na	na	na
	S								

Yeast	Fluconazol								
C. albicans	0.06 mg/mL								

MSSA - methicillin-sensitive *Staphylococcus aureus*; MRSA - methicillin-resistant *Staphylococcus aureus*; S- Susceptible; I- Intermediate; R- Resistant: this classification was made according to the interpretative breakpoints suggested by Clinical and Laboratory Standards Institute (CLSI) and European Committee on Antimicrobial Susceptibility Testing (EUCAST); na- not applicable.